AWARD NUMBER: W81XWH-15-1-0600

TITLE: Adult Stem Cell-Based Enhancement of Nerve Conduit for Peripheral Nerve Repair

PRINCIPAL INVESTIGATOR: Peter G Alexander, PhD

CONTRACTING ORGANIZATION: University of Pittsburgh, Pittsburgh, PA

REPORT DATE: January 2022

TYPE OF REPORT: FINAL

PREPARED FOR: U.S. Army Medical Research and Development Command
Fort Detrick, Maryland 21702-5012

REPORT DOCUMENTATION PAGE		*Form Approved OMB No. 0704-0188*

1. REPORT DATE	**2. REPORT TYPE**	**3. DATES COVERED**
January 2022	Final	30Sep2015-29Sep2021

4. TITLE AND SUBTITLE

Adult Stem Cell-Based Enhancement of Nerve Conduit for Peripheral Nerve Repair

5a. CONTRACT NUMBER

5b. GRANT NUMBER
W81XWH-15-1-0600

5c. PROGRAM ELEMENT NUMBER

6. AUTHOR(S)

Peter G Alexander

E-Mail: pea9@pitt.edu

5d. PROJECT NUMBER

5e. TASK NUMBER

5f. WORK UNIT NUMBER

7. PERFORMING ORGANIZATION NAME(S) AND ADDRESS(ES)

University of Pittsburgh,
450 Technology Drive, Rm 219
Pittsburgh, PA, 15219

8. PERFORMING ORGANIZATION REPORT NUMBER

9. SPONSORING / MONITORING AGENCY NAME(S) AND ADDRESS(ES)

U.S. Army Medical Research and Development Command
Fort Detrick, Maryland 21702-5012

10. SPONSOR/MONITOR'S ACRONYM(S)

11. SPONSOR/MONITOR'S NUMBER(S)

12. DISTRIBUTION / AVAILABILITY STATEMENT

Approved for Public Release; Distribution Unlimited

13. SUPPLEMENTARY NOTES

14. ABSTRACT

Musculoskeletal trauma is frequently accompanied by injuries to peripheral nerves; if not repaired, the trauma can lead to significant dysfunction and disability. While nerves have the ability to regenerate and to reconnect across a limited gap, surgical intervention is often required to assist them in bridging a larger gap. Typically, surgeons will transplant a less important nerve from elsewhere in the body to the site of injury to provide a patch for the injured nerve. However, acceptable donor nerves are often not available for this purpose, particularly in patients suffering multiple extremity injuries or faced with traumatic amputations. Alternatives include the use of a blood vessel graft or a synthetic nerve guide, although these devices are only effective over distances less than 3 cm, mainly because of their lack of appropriate nerve-enhancing biological activities. In our current work, we have identified and isolated stem cells from the injured tissue site that have wound healing promoting activities. In this application, we propose to use these cells, which may be obtained autologously from the patient, in conjunction with a biodegradable scaffold tube to form bioactive nerve conduits that may be grafted to provide better guidance for the microstructure of the nerve to bridge the injury gap. Our Specific Aims are as follows: (1) optimize the neurotrophic bioactivity of stem cell-seeded nanofibrous scaffolds; (2) design and fabricate stem cell activated nerve conduits with optimal neurotrophic and neuroconductive activities that are compatible with point-of-care nerve repair; and (3) perform proof-of-concept functional tests of stem cell-activated nerve conduits in small animal models of nerve repair. Based on our previous and current findings, we expect that we will have positive outcomes from these studies, which will be used to develop testing in a large, clinically relevant animal model, as a basis for future clinical trial. Our long-term goal is to develop efficient and effective strategies to repair and restore function to peripheral nerve injuries resulting from battlefield trauma.

15. SUBJECT TERMS None listed.

16. SECURITY CLASSIFICATION OF:			**17. LIMITATION OF ABSTRACT**	**18. NUMBER OF PAGES**	**19a. NAME OF RESPONSIBLE PERSON** USAMRDC
a. REPORT	**b. ABSTRACT**	**c. THIS PAGE**			**19b. TELEPHONE NUMBER** *(include area code)*
Unclassified	Unclassified	Unclassified	Unclassified	88	

Standard Form 298 (Rev. 8-98)
Prescribed by ANSI Std.

TABLE OF CONTENTS

1. INTRODUCTION:

Peripheral nerve damage is a challenging complication of combat-related orthopaedic trauma. Given the severity of the orthopaedic injuries sustained during battlefield trauma, an acceptable donor nerve is often not available to serve as an autograft, particularly for patients with injuries in multiple extremities or traumatic amputations, and currently available nerve guide devices are often insufficient. We propose the use of a novel stem-cell activated nerve conduit graft with an aligned nanofiber scaffold and neurotrophic enhancement using cells clinically available at the site of surgery. Upon completion, these proposed studies will provide sufficient information to move to MPC-NC technology to testing in a large, clinically relevant animal model, which will be designed after consultation with the FDA. Favorable outcomes will form the basis for future clinical trials. The technologies described here are tailored for a "point-of-care" approach that could lead to improvements in overall functional recovery, minimized disability, and increased quality of life for our wounded warriors.

2. KEYWORDS:

Stem Cell, Nerve Conduit, Peripheral Nerve Regeneration, Nanofiber, Neurotrophic Factor, Tissue Engineering, Multifunctional

3. ACCOMPLISHMENTS:

What were the major goals of the project?

Aim 1: Optimization of the neurotrophic bioactivity of MPC-based nanofibrous scaffold

- Task 1: Produce nanofibrous scaffolds of controlled thickness comprised of laminated woven and aligned nanofibrous sheets
    - Milestone 1: Formation of bi-layered nanofibrous scaffolds (9/30/16, 100%)
- Task 2: Optimize the neurotrophic activity of MPC-seeded nanofibrous scaffolds
    - Milestone 2: Validation of a cell-seeded nanofibrous scaffold with neurotrophic activity in vitro (12/30/16, 100%)

Aim 2: Fabrication of MPC-impregnated nerve conduit (MPC-NC)

- Task 3: Construction of devices to assist in MPC-NC preparation
    - Milestone 3: Design and production of devices that aid in the preparation of MPC-NC that accommodate specific conduit dimensions (09/30/16, 100%)
- Task 4: Biomechanical and biological testing of final cell-laden MPC-NC
    - Milestone 4: An assembled cell-laden MPC-NC that promotes neurite outgrowth *in vitro* (5/30/17, 100%)

Aim 3: Perform proof-of-concept functional test of the MPC-NC constructs in small animal models (rat/rabbit) of sciatic nerve repair

- Task 5: Proof-of-concept functional test of the MPC-NC constructs in rats
    - Milestone 5: Demonstration of nerve repair *in vivo* using cell-laden MPC-NC (9/30/17, 80%)
- Task 6: Proof-of-concept functional test of the MPC-NC constructs in rabbits
    - Milestone 6: Demonstration of nerve repair *in vivo* using cell-laden MPC-NC prepared in a point-of-care single-step procedure (9/30/18, 40%)

What was accomplished under these goals?

Task 1: Produce nanofibrous scaffolds of controlled thickness comprised of laminated woven and aligned nanofibrous sheets (All objectives completed)

Specific objective 1: Purchase chemicals and polymeric materials for nanofibrous scaffold
Specific objective 2: Purchase electrospinner instrumentation with custom-designed specifications and components (**Figure 1**)
Specific objective 3: Fabricate sheath/tube constructs (months 4-8) of various PCL/PEO ratios
Specific objective 4: Mechanical testing of the nanofibrous constructs: Tensile testing and suture retention assays
Specific objective 5: Imaging of nanofibrous constructs (SEM): Ensure uniform alignment, fiber size, and porosity
Specific objective 6: Optimize the spinning conditions as needed.

Task 2: Optimize the neurotrophic activity of MPC-seeded nanofibrous scaffolds (All objectives completed)

Specific objective 7: Acquire MPCs, iMPs, iPSCs, ECs and MSCs (control cell type)
Specific objective 8: Generation and verification of neurotrophically activated cell types and conditioned media (via RT-PCR and ELISA of neurotrophic factors), followed by cell storage
Specific objective 9: Purchase reagents and materials for methacrylation of ECM hydrogel
Specific objective 10: Create photocrosslinkable hydrogel mixtures
Specific objective 11: Acquire embryonated chick eggs, dorsal root ganglia (DRG) and PC-12 cells.
Specific objective 12: Test the ability of the hydrogel-encapsulated MSCs adherent to the random fiber side of scaffold mats of different porosities to enhance neurite outgrowth on the aligned nanofibers in vitro.

- War-traumatized MPCs (Figures 2-4)
- iPSCs (Figures 5-7)
- Adipose-derived MSCs (Figures 8-13)

Specific objective 13: Test the effect of ECM coating, using clean or conditioned media as solvent, on neurite outgrowth (PC-12/DRG neurite extension assays) in 2D culture (using scaffold mats and ECM coating on the aligned fiber surface)
Specific objective 14: Test the effect of EC cell co-encapsulation with MPCs within hydrogels in clean or conditioned medium-fabricated hydrogels

Task 3: Construction of devices to assist in MPC-NC preparation (All objectives completed)

Specific objective 15: Design and fabricate device to assist in the formation of MPC-NC assembly
Specific objective 16: Test and optimize devices to assist in the formation of components of the MPC-NC assembly.
Specific objective 17: Optimize devices to assist in the formation of the full MPC-NC

Task 4: Biomechanical and biological testing of final cell-laden MPC-NC (All objectives completed)

Specific objective 18: Preparation of completed acellular and cell-laden MPC-NC

- Complete. **(Figure 8**).

Specific objective 19: Scanning electron microscopy to assess structural uniformity

- Complete. **(Figure 9).**

Specific objective 20: Tensile testing and suture retention assays

- Complete. **(Figure 10)**.

Specific objective 21: Assess biodegradation of the scaffold (mass and volume)

- Complete. **(Figure 11).**

Specific objective 22: Cell viability assay for biocompatibility

- Complete. **(Figure 12).**

Specific objective 23: Immunohistochemistry for biopermeability (with respect to neurotrophic factors)

- Complete. **(Figure 13)**.

Specific objective 24: Neurotrophic activity assay (PC-12/DRG neurite extension)

- Complete. (**Figure 14**)

Task 5: Proof-of-concept functional test of the MPC-NC constructs in rats (All objectives completed)

Specific objective 25: Local IRB/IACUC approval for rat model and ACURO approval.
Specific objective 26: Acquisition of Thy1-GFP rats. Non-transgenic Lewis rats were obtained.
Specific objective 27: Optimization of implant technique using cadaveric samples.
Specific objective 28: RFP Lenti-viral transduction of MPC. DiI labeling and use of transgenic GFP Lewis rat used instead of RFP Lenti-viral transduction.
Specific objective 29: Characterization of MPCs (**Figure 15**) and implantation of MPC-NC scaffold variants in sciatic nerve defects. (**Figure 16**)
Specific objective 30: Functional testing of nerve repair at experimental day 3 and the experimental end point
Specific objective 31: Harvest of samples. 6-week and 16-week time points
Specific objective 32: Testing and analysis of samples at 6 weeks for:

a. macroscopic (**Figure 17**)
b. Histological/immunohistochemistry (**Figure 18-23A**) and
c. functional assessment at 12 weeks only (**Figure 23b**)

Task 6: Proof-of-concept functional test of the MPC-NC construct in rabbits: (to be carried out in F
Specific objective 33: Local IRB/IACUC approval for rabbit model and ACURO approval.
New IACUC approved, currently under ACURO review
Specific objective 34: Optimization of implant technique using cadaveric samples **(Specific objective completed)**.
Specific objective 35: Implantation of nerve conduits in iatrogenic nerve defects (delayed due to protocol, renewal, animal facilities restrictions and COVID-19 pandemic)
Specific objective 36: Harvest of samples at 6 month time point.
Specific objective 37: Macroscopic, histological and immunohistochemical assessment of nerve repair. At the 6-month time point

3. Results and Figures:

Figure 1: IME Medical Electrospinning, is a leader in the field of electrospun nanofiber-based medical devices, tissue engineering products, and drug delivery solutions. Utilizing its fully automated MediSpin technology platform (depicted in GLP/GMP form), production of electrospun fibers is both consistent, reproducible and scalable. Importantly, the MediSpin platform, protected by seven patent families, meets the guidelines described in the first ASTM standard for fiber-based medical scaffolds (F3510-21), which IME Medical Electrospinning (now VIVOLTA) co-authored.

A. MPCs from war-traumatized muscle tissue enhances neurite outgrowth.

As reported in: Zupanc HRH, Alexander PG, Tuan RS. Neurotrophic support by traumatized muscle-derived multipotent progenitor cells: Role of endothelial cells and Vascular Endothelial Growth Factor-A. Stem Cell Res Ther. 2017 Oct 13;8(1):226. doi: 10.1186/s13287-017-0665-4. PMID: 29029631; PMCID: PMC5640955.

Adult mesenchymal stem cells (MSCs) have been shown to increase nerve regeneration in animal models of nerve injury. Traumatized muscle-derived multipotent progenitor cells (MPCs) share important characteristics with MSCs and are isolated from severely damaged muscle tissue following surgical debridement. Previous investigations have shown that MPCs may be induced to increase production of several neurotrophic factors, suggesting the possible utility of autologous MPCs in peripheral nerve regeneration following injury. Recent findings have also shown that components of the vascular niche, including endothelial cells (ECs) and vascular endothelial growth factor (VEGF)-A, regulate neural progenitor cells and sensory neurons. The results of this study suggested that the potential of MPCs to encourage nerve growth via a VEGF-A-dependent action, and the use of MPC-CM or a combination of MPC and CM from ECs for peripheral nerve repair in conjunction with NFs in a nerve guide conduit. Due to the ease of use, application of bioactive agents derived from cultured cells to enhance neurotrophic support presents a promising line of research into peripheral nerve repair.

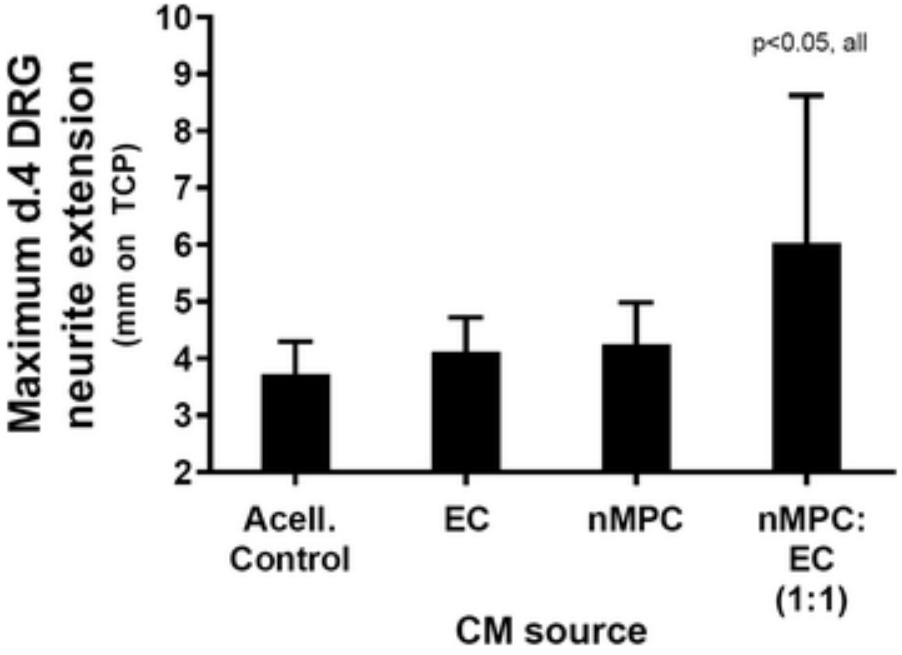

Figure 1: Neurite extension of dorsal root ganglia (DRGs) seeded on tissue culture plastic and cultured in the presence of conditioned medium (CM) from multipotent progenitor cells (MPCs) and/or endothelial cells (ECs). An increase in DRG neurite extension was detected as a synergistic effect of the mixed (1:1) CM derived from neurotrophically-induced MPCs (nMPC) and EC over the basal DRG media acellular control (Acell. control). n = 6; Tukey's. Indicated p value applies to that condition versus all other conditions

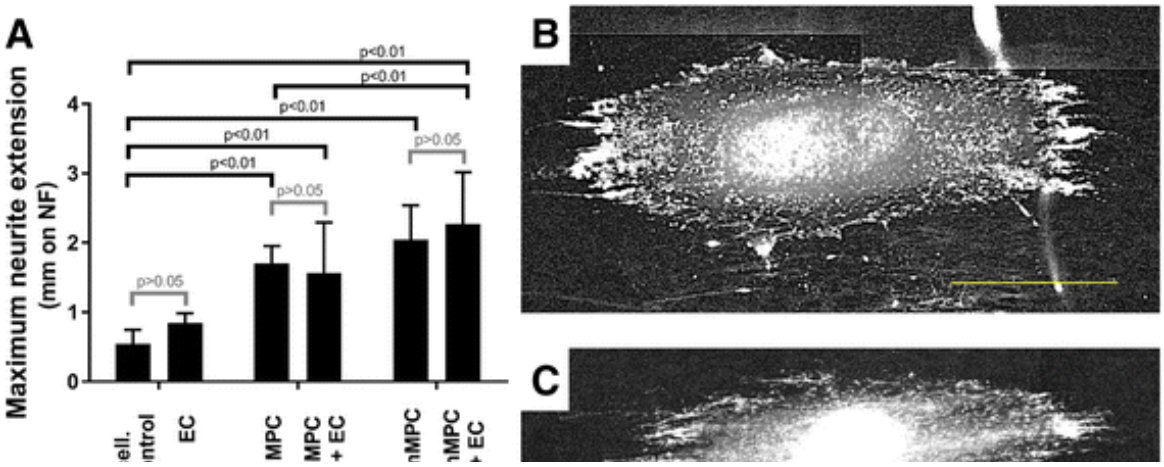

Figure 2: Neurite extensions of dorsal root ganglia (DRGs) seeded on nanofiber NF scaffold upon coculture with multipotent progenitor cells (MPCs) or combination of MPCs/endothelial cells (ECs) (1:1). The presence of MPCs, particularly after their neurotrophic induction, increased the length of DRG neurite extensions (a) over DRG control (acellular (Acell.) control/basal medium) cultures (b). EC coculture (c) slightly but not significantly increased DRG neurite extension length. MPC and neurotrophically-induced MPC (nMPC) coculture significantly increased neurite extension length when compared to the control. For xMPC-DRG coculture, EC coculture slightly but insignificantly increased neurite extension length. DRGs cocultured with both nMPC and EC (nMPC-EC-DRG cocultures; d) exhibited significantly longer neurite extensions than MPC-DRG or MPC-EC-DRG cocultures. a n = 4; Sidak's p values as indicated. b–d Scale bars= 400 μm for representative NEFH-stained images

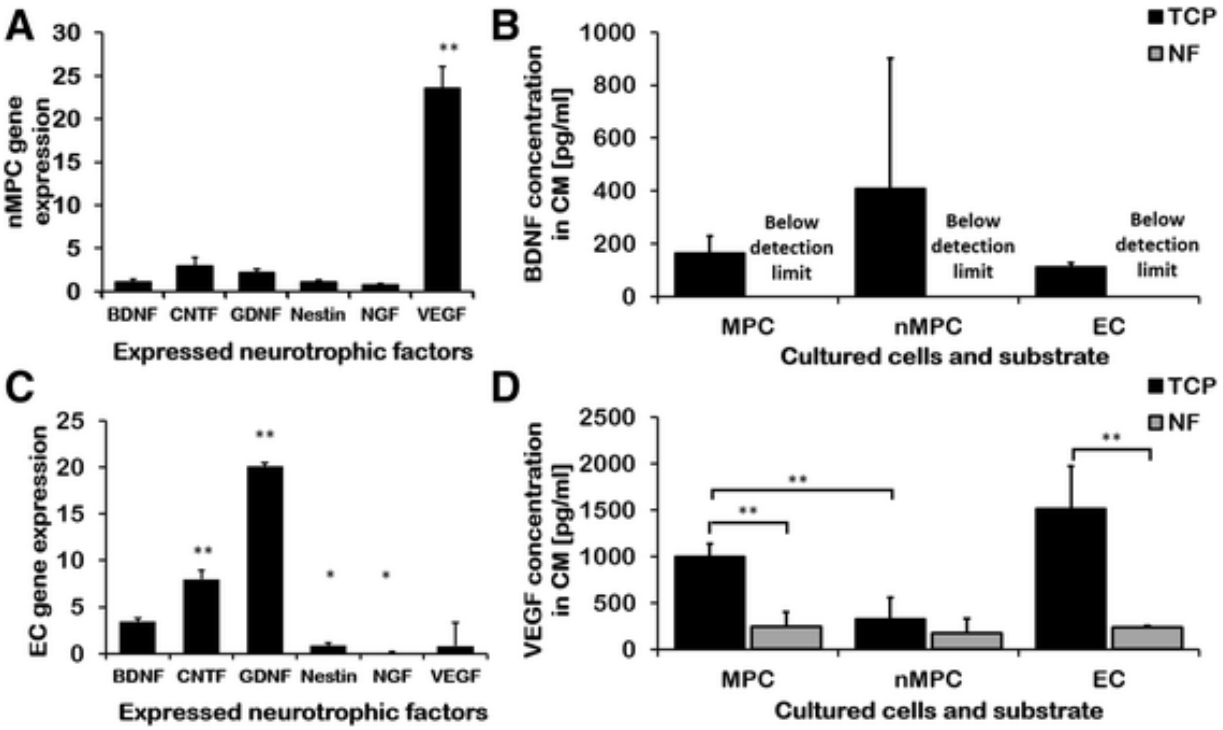

Figure 3: Expression and production of neurotrophically induced MPCs (nMPC) and endothelial cells (EC) cultured on tissue culture plastic (TCP) and nanofiber constructs (NF). a,c NF-cultured growth factor and neurotrophic marker gene expression, assayed by RT-PCR and normalized to TCP cultures: secreted brain-derived neurotrophic factor (BDNF) (b) or vascular endothelial growth factor (VEGF) (d) levels from cells seeded on TCP or NF as measured by ELISA. nMPC (a) and EC (c) neurotrophic gene expression was mildly or significantly increased by NF culture in almost all cases. CM from cultures on NF contained lower levels of secreted growth factors than conditioned medium (CM) from TCP-cultured cells (b,d). Noninduced multipotent progenitor cells (MPCs) secreted more VEGF than nMPCs (b,d). n = 6; Student's t test *$p < 0.05$, **$p < 0.01$, versus controls (a,c) or indicated groups (b,d). CNTF ciliary neurotrophic factor, GNDF glial cell-derived neurotrophic factor, NGF nerve growth factor

B. Neurotrophically induced mesenchymal progenitor cells derived from induced pluripotent stem cells enhance neuritogenesis

As reported in: Brick RM, Sun AX, Tuan RS. Neurotrophically Induced Mesenchymal Progenitor Cells Derived from Induced Pluripotent Stem Cells Enhance Neuritogenesis via Neurotrophin and Cytokine Production. Stem Cells Transl Med. 2018 Jan;7(1):45-58. doi: 10.1002/sctm.17-0108. Epub 2017 Dec 7. PMID: 29215199; PMCID: PMC5746147.

While neurotrophically induced-MSCs (NI-MSCs) are capable of producing many of the same neurotrophic factors (NTFs) as Schwann cells, they have finite expansion capacity, and require invasive techniques to acquire, for example, bone marrow aspiration. Induced pluripotent stem cells (iPSCs), derived by reprogramming adult somatic cells, including MSCs, that exhibit embryonic stem cell (ESC)-like pluripotency, represent a potential cell source that can overcome this drawback. iPSCs are produced by reprogramming with four transcription factors and have a virtually unlimited expansion capacity. We have shown that after expansion, the iPSCs can be differentiated into MSC-like cells, which we have termed induced mesenchymal progenitor cells (MiMPCs) [6]. In this manner, this technology has the potential to yield an almost unlimited supply of MiMPCs. In this study, we aim to test if these MiMPCs, originally derived from MSCs, have the same ability to support neuronal regeneration as the parent MSC. With this capacity, MiMPCs may represent a potentially infinitely renewable cell source for the support of nerve regeneration and cell therapy. Our results reported here show that MiMPCs can secrete NTFs after neuroinductive treatment, and can produce factors to improve neurite outgrowth in vitro in a chick embryonic dorsal root ganglion (DRG) model. These findings suggest that neurotrophically induced- MiMPCs (NI-MiMPCs) may be considered a suitable substitute cell type to support nerve growth.

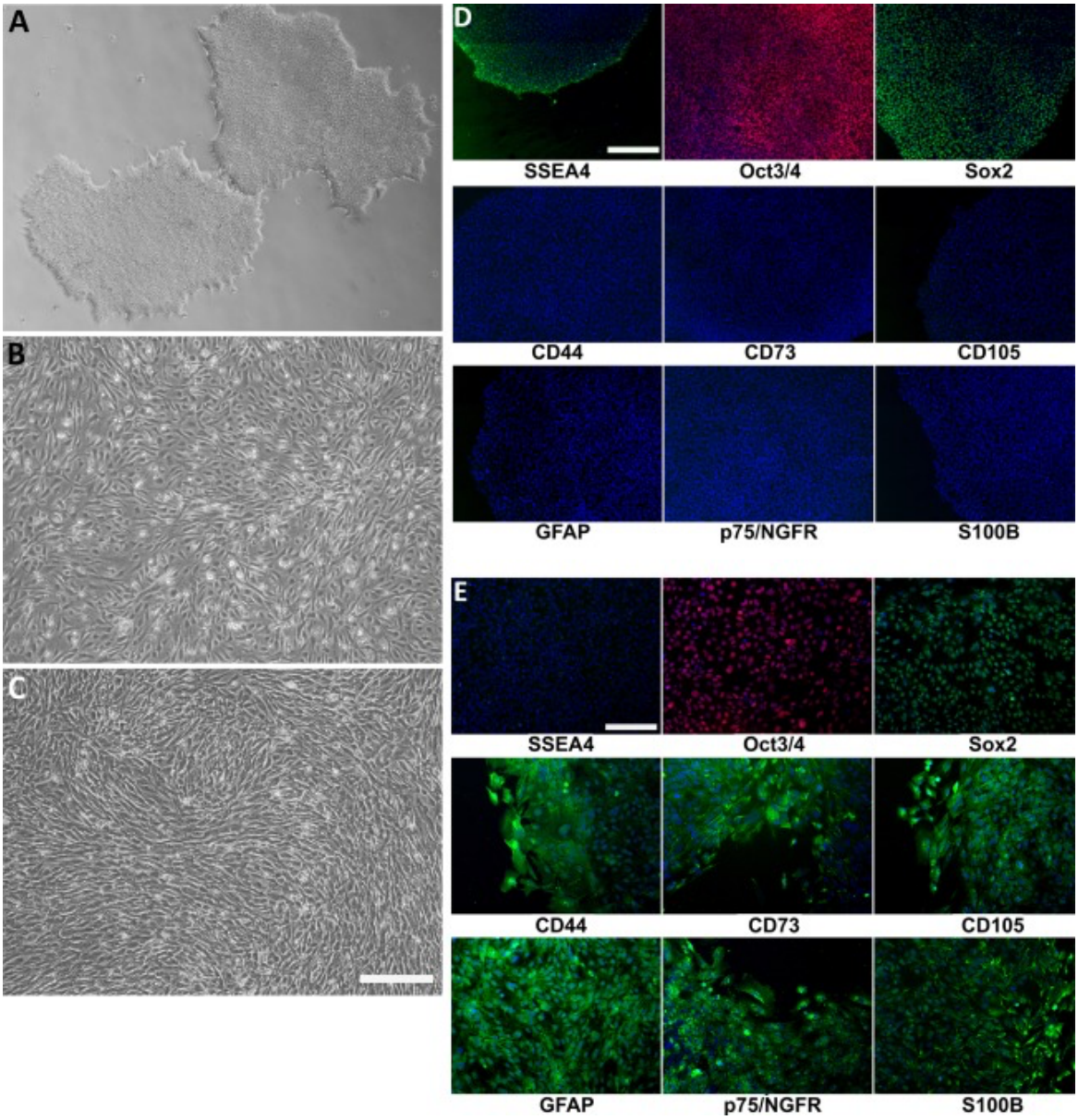

Figure 4: Morphology of induced mesenchymal progenitor cells (MiMPCs) and mesenchymal stem cells (MSCs) examined by phase contrast microscopy. (A): Undifferentiated colonies of human induced pluripotent stem cells (iPSCs) reprogrammed from human bone marrow MSCs [6]. Cells grew to confluent colonies on Matrigel, in feeder-free culture. (B): Confluent MiMPC cultures differentiated from iPSCs. All MiMPC cultures resembled MSCs in morphology, with no remaining iPSC morphology. (C): Confluent control MSCs isolated from human bone marrow (passage 5). Each cell type (n>5) was cultured over the course of all experiments performed in this study. Cells in (A–C) were imaged at 34 magnification (Bar5560 lm.) (D, E): MiMPCs were fixed and immunofluorescently stained on the third day of differentiation; colonies of confluent iPSCs served as controls. Cells were stained for MSC markers (CD44, CD73, and CD105), Schwann cell markers (GFAP, p75/NGFR, and S100B), and pluripotency stem cells markers (Sox2, SSEA4, and Oct3/4). All cells were counterstained with 40 ,6-diamidino-2-phenylindole dihydrochloride. (D) iPSCs were negative for MSC and Schwann cell markers, but stained positively for pluripotency markers, indicating the maintenance of stemness throughout culture and passaging. (E) MiMPCs cells were strongly positive for CD44 and CD105, and weakly positive for CD73. MiMPCs also stained positive for all Schwann cell markers, positive for Sox2, weakly positive for Oct3/4, and negative for SSEA4, showing their transition and demonstrating the need for long differentiation period. Cells in (D, E) were imaged at 310 magnification (Bar5220 lm). Abbreviation: GFAP, glial fibrillary acidic protein.

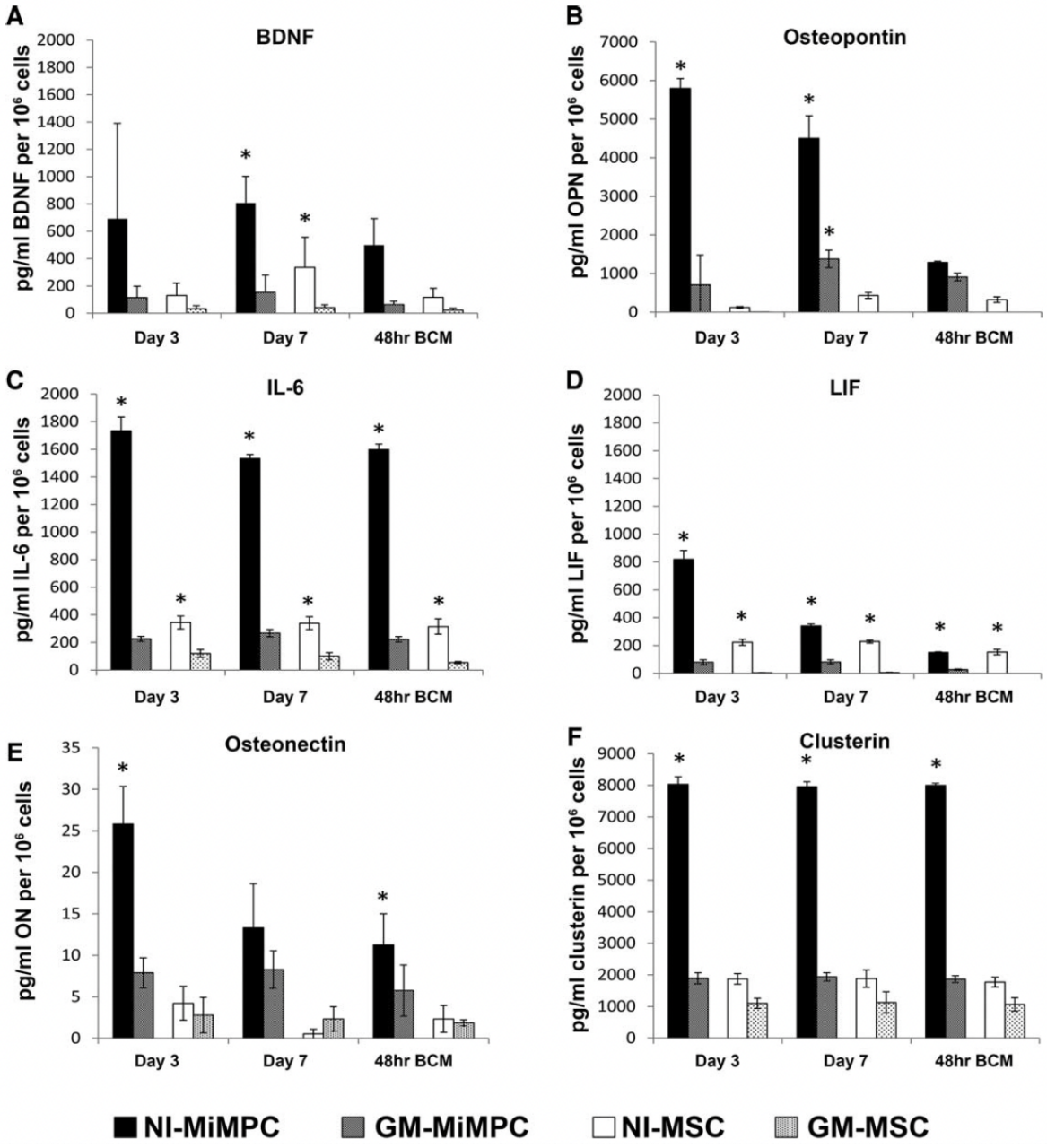

Figure 5: **Production of neurotrophic factors by NI-MiMPCs and MSCs, quantified via ELISA**. MiMPCs and MSCs were cultured in neurotrophic induction medium or growth medium. Conditioned media taken from days 3 and 7 of induction culture, and basal conditioned medium taken from cultures 48 hours post-induction (48-hour BCM). The conditioned media assayed include those from MiMPCs (induced, NIMiMPCs; uninduced, GM-MiMPCs), and from MSCs (induced, MI-MSCs; uninduced, GM-MSCs), as well as basal medium (controls). Medium was assayed for levels of (A) BDNF, (B) Osteopontin, (C) IL-6, (D) LIF, (E) osteonectin, and (F) clusterin. All ELISA results are expressed in pg/ml or ng/ml produced per million cells. Medium taken from NI-MiMPC cultures contained high levels of all assayed factors compared with GMMiMPCs, NI-MSCs, and GM-MSCs. BDNF, IL-6, osteonectin, and clusterin exhibited relatively constant secretion levels, while osteopontin and LIF showed decreased expression levels during induction treatment and the 48-hour post-induction period. *, $p<.05$, compared with GM controls, n 3 for all assays. Abbreviations: BDNF, brain-derived neurotrophic factor; ELISA, enzyme-linked immunosorbent assay; IL-6, interleukin-6; LIF, leukemia inhibitory factor; MSCs, mesenchymal stem cells; NI-MiMPCs, neurotrophically induced-MiMPCs.

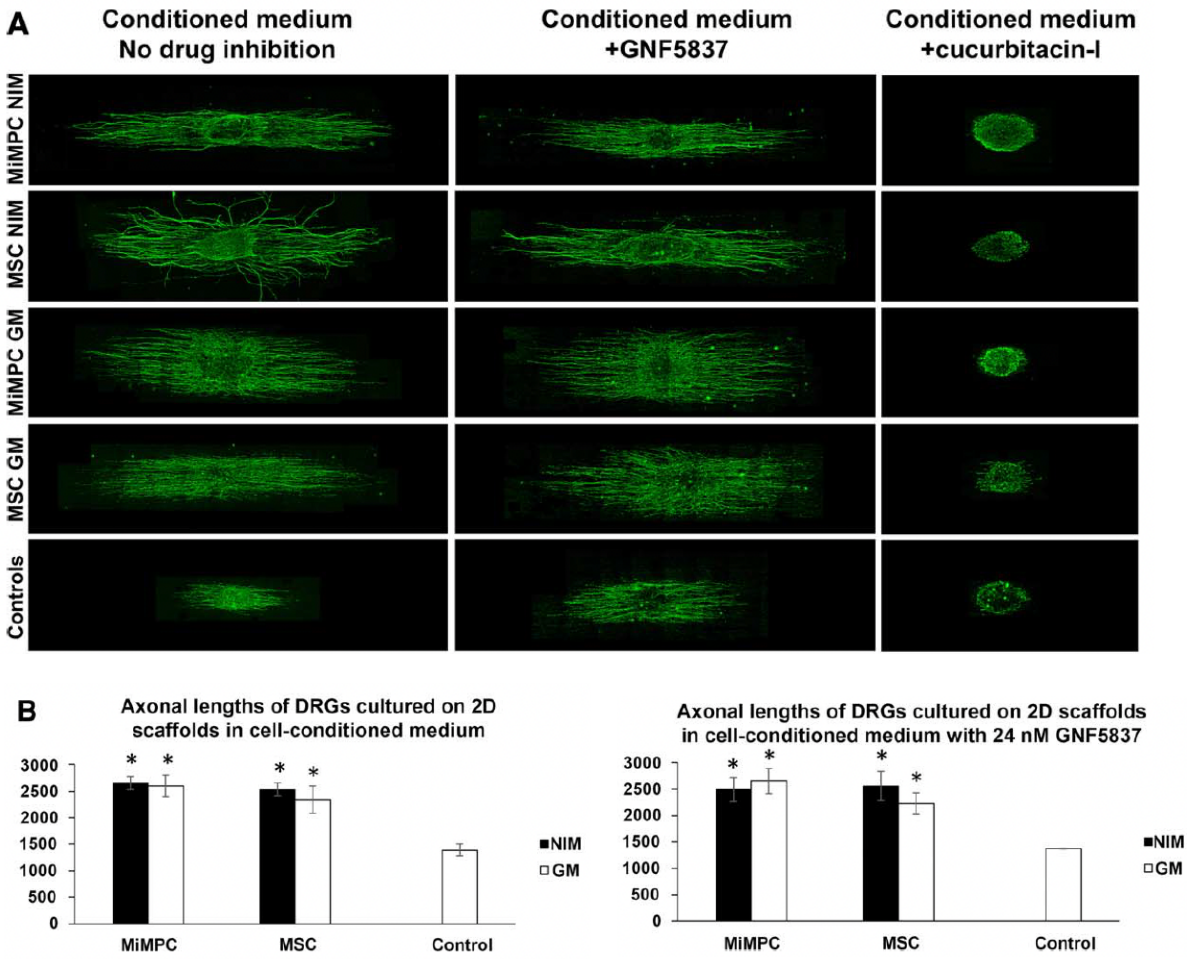

Figure 6. Morphological effect of MiMPCs and MSCs on neurite outgrowth in DRGs grown on electrospun nanofibrous scaffolds via image analysis and measurements by NIH ImageJ. (A): DRGs were cultured on aligned nanofibrous scaffolds prepared as described in Materials and Methods, using media conditioned by induced (NI) and noninduced (GM) MiMPCs and MSCs, with or without cotreatment with the pan Trkreceptor inhibitor, GNF5837 (24 nM), or the Jak/Stat inhibitor, cucurbitacin-I (60 nM). No observable difference in neurite extension lengths was seen, compared with cultures without GNF5837 cotreatment. On the other hand, cucurbitacin-I cotreatment resulted in substantial decrease in in neurite extension length, compared with controls or any other group. Neurite extension lengths were measured with ImageJ. Bar5800 lm. (B): Neurite extension outgrowth was traced using NIH ImageJ. DRGs were cultured on aligned scaffolds with conditioned media collected from NI- and GM-MiMPCs and MSCs. Results on neurite outgrowth lengths indicate that exposure to NI- and GM- MiMPC and MSC conditioned media improved neurite outgrowth compared with controls, and the addition of Trk-receptor inhibitor (1GNF5837) did not impede length of neurite extension. *, $p<.05$, denotes statistically significant difference compared with both controls. At least 10 axons were measured per group over an n53. Abbreviations: GM, growth medium; MiMPCs, induced mesenchymal progenitor cells; MSCs, mesenchymal stem cells; NIM, neurotrophic induction medium.

C: Adipose tissue-derived MSCs enhance neurite outgrowth and fundtional nerve repair in a rat sciatic nerve repair model.

As reported in: Sun AX, Prest TA, Fowler JR, Brick RM, Gloss KM, Li X, DeHart M, Shen H, Yang G, Brown BN, Alexander PG, Tuan RS. Conduits harnessing spatially controlled cell-secreted neurotrophic factors improve peripheral nerve regeneration. Biomaterials. 2019 May;203:86-95. doi: 10.1016/j.biomaterials.2019.01.038. Epub 2019 Feb 19. PMID: 30857644.

Peripheral nerve injury (PNI) affects over 300,000 people each year in the United States and is a significant cause of morbidity and lifelong disability despite surgical intervention. Through a variety of traumatic or disease-based mechanisms, such as high-speed motor vehicle collisions or schwannomas, peripheral nerves function is drastically altered or decreased. Warfighters, in particular, are exposed to higher incidences of PNI due to battlefield injuries, and PNI morbidity leads to reduced military preparedness, early discharge, poor reintegration into civilian life, and has been implicated in higher rates of depression and suicide among these veterans.

The best treatment option for nerve defects currently is tensionless end-to-end repair given its predictable positive outcomes, but many times this is not an option due to the various conditions that must be met: repair immediately after injury, minimal gap < 2.5mm in length, good blood supply and soft-tissue coverage, and exact alignment of the opposing ends. Alternative options such as autografting and allografting exist, but are limited by donor site morbidity (with a chance for neuroma formation at both sites), availability, and immune autografting. Another promising regenerative route, the use of a biomaterial nerve conduit, demonstrates potential due to reduced neuroma formation, lack of axonal escape, and lack of donor-site morbidity, but is constrained by range (≤3 cm) and low functional recovery rates Thus, the ability to provide an efficient and effective method towards bridging the gap in nerve regeneration would be a huge step forward in the care of peripheral nerve injuries.

In the pursuit of an effective nerve conduit, many physical and biological strategies have been employed during fabrication. On the physical side, electrospun nanofibers hold great promise due to their ability to be fabricated with aligned arrangements closely resembling native nerve ECM, and they have demonstrated the ability to guide neurite extensions. On the biological side, neurotrophic factors (NTFs), such as brain derived neurotrophic factor (BDNF) and vascular endothelial growth factor (VEGF), have been shown to play an important role in facilitating axonal growth, guidance, and survival. In addition, chemokine gradients are essential in driving Schwann cell migration into the regenerating nerve bridge and axon elongation. Current methods of sustained delivery of growth factors by microparticles, along with other technologies, have demonstrated utility in experimental models of nerve repair, but these technologies have not yet addressed the dynamic time course of growth factor production, the use of anti-inflammatory cytokines, or the capability to supply a multitude of growth factors simultaneously or separately.

A potential route toward addressing these issues lies in the use of stem cells. Adult mesenchymal stem cells (MSCs) are multipotent cells that have the ability to differentiate into many lineages, including neural-like lineages. Early transplantation experiments involving these stem cells demonstrated that they supported nerve regeneration (originally believed to be due to transdifferentiation to neural lineages but more recently thought to be through production of NTFs), and they have also been shown to possess immunoregulatory functions, which could potentially decrease scar tissue infiltration into conduits and neuroma formation. Studies utilizing nerve conduits seeded with MSCs reported both larger axons as well as greater amounts of myelination per axon. Additionally, studies including functional assays generally showed enhanced function compared to non-cellular controls, with some demonstrating function comparable to the gold standard autograft. Along with MSCs, other cell types such as neural stem cells, embryonic stem cells, and Schwann cells have also been applied to successfully support nerve regrowth with efficacies rivaling or exceeding those of MSCs.

While cell support demonstrates distinct benefits in conduit-mediated nerve regeneration, cell-seeding protocols typically either involve cell attachment in culture after fabrication, which can be lengthy (clinically undesirable) and potentially result in cell detachment in vivo, or injection into the lumen of the conduit, which is susceptible to leakage. In addition, these methods do not allow for precise control of cell seeding number or cellular distribution within the conduit due to the random nature of cell attachment and injection, and the seeded

cells are known to migrate out of the conduit, further confounding the dose- and location-dependent effect of the cells. There do exist gel-based systems that allow for encapsulation of cells within gels, which address the cell density challenges and immediate cell seeding, but they have not yet been effectively applied for cell distribution in conduits. Overall, these limitations have led to the inability to effectively produce and harness cell-secreted neurotrophic gradients.

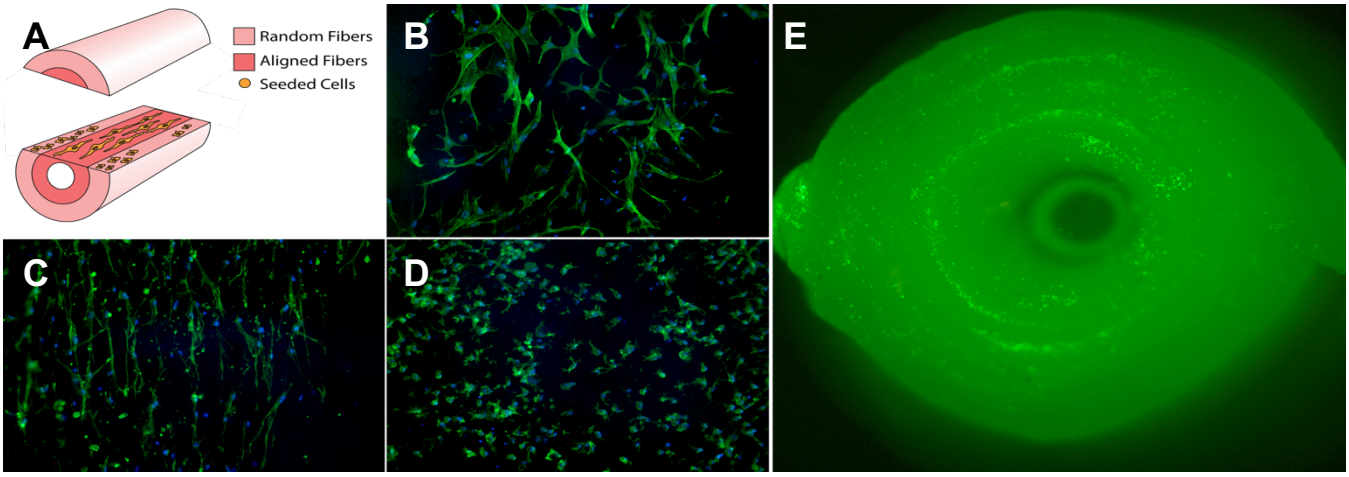

Figure 7 (2): Phalloidin and Calcein-AM staining of cells demonstrating morphology and distribution within scaffold. (A) Simplified view of constructed conduit without concentric layers showing location of aligned and randomly oriented cells. **(B-D)** Phalloidin/DAPI staining of cells within an unraveled conduit showing cells with randomly oriented processes, cells with aligned processes, and cells trapped in gelatin with retracted processes, respectively. **(E)** Calcein-AM live cell staining of cross-section of constructed scaffold demonstrating concentric distribution of cells.

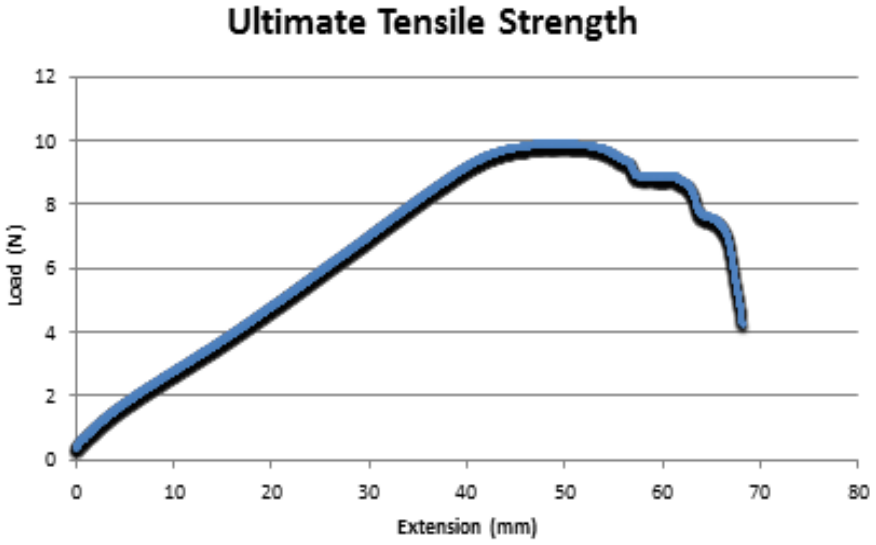

Figure 8 (3): Suture Retention and Tensile Strength. Nerve conduit withstood up to 10N of tensile force applied with suture before elongating and failing. This is well above the necessary force for the application of a nerve conduit.

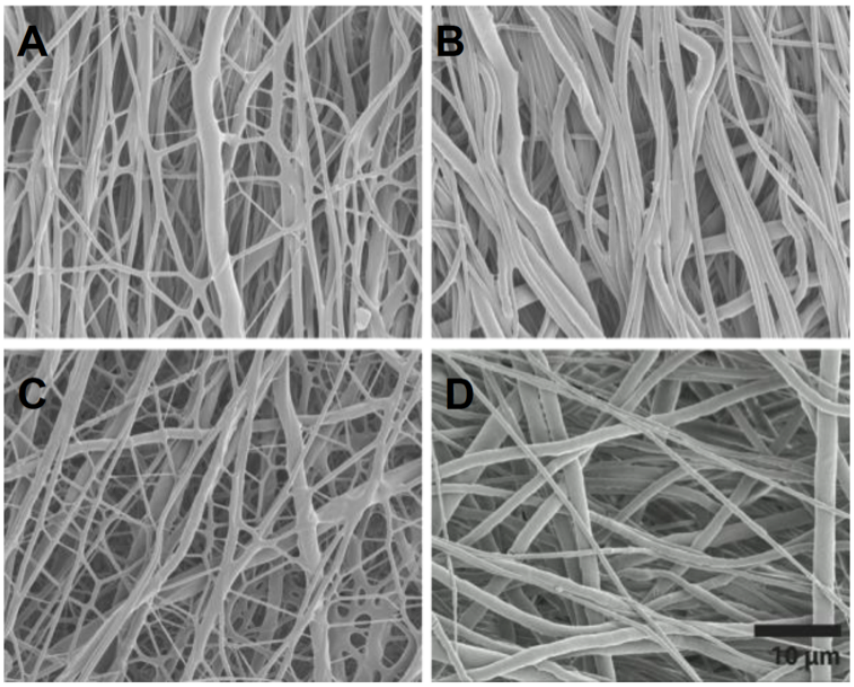

Figure 9 (4): SEM images of composite GelMA / PCL electrospun scaffolds. SEM images of **(A)** aligned composite scaffold, **(B)** aligned scaffold with GelMA removed, **(C)** random composite scaffold, and **(D)** random scaffold without GelMA.

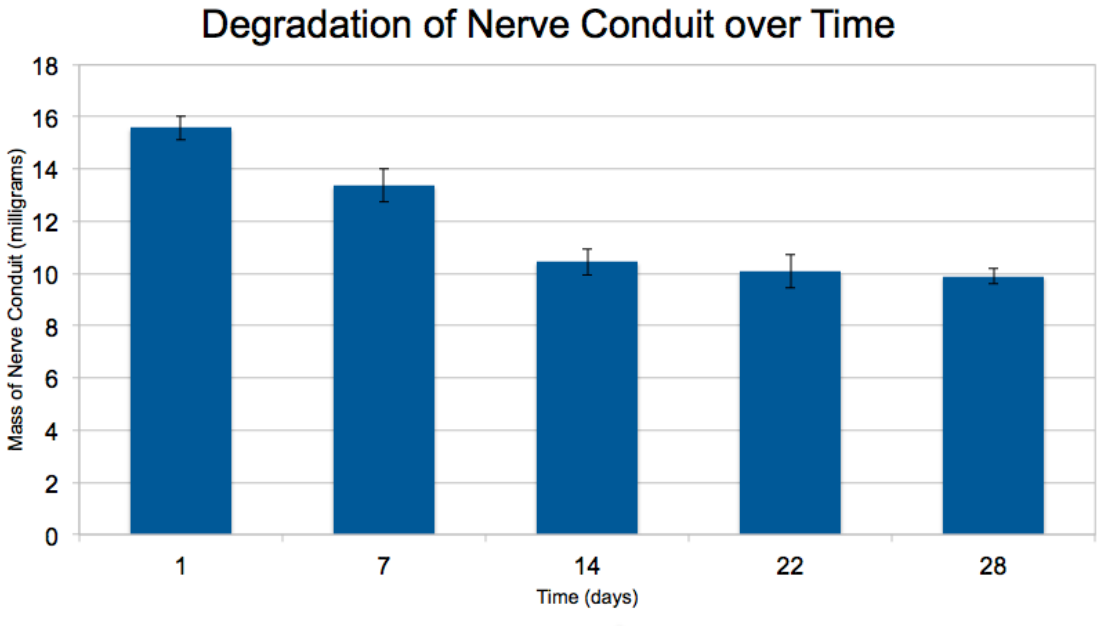

Figure 10 (5): Degradation of 3D nerve conduit over 28 days. Mass of conduit measured over a 28 day span. As expected, the gelatin component degrades relatively quickly with the hydrophobic polycaprolactone component remaining behind for structural stability. All conduits maintained structural stability over this period.

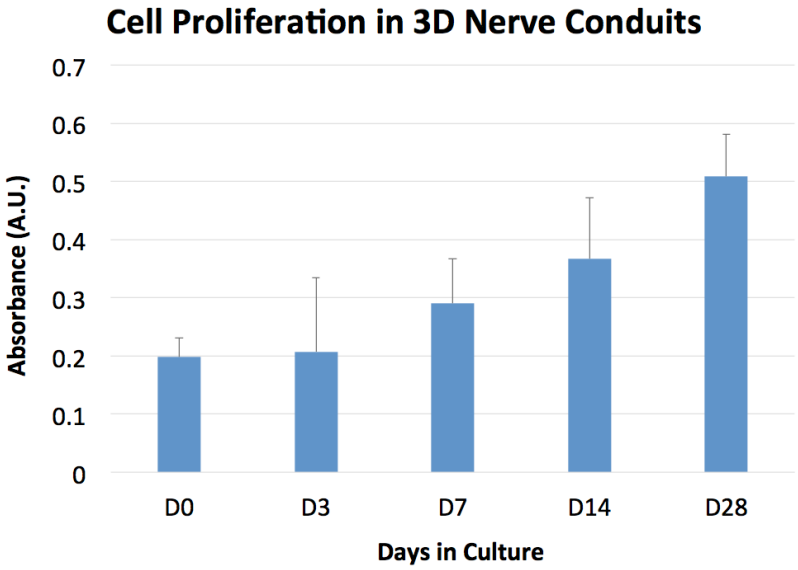

Figure 11 (6):. MTS assay for cellular metabolism within 3D nerve conduits over a 28 day period. Metabolism of cells within conduit significantly increases over a 28 day period, indicating cellular proliferation and biocompatibility of this nerve conduit system.

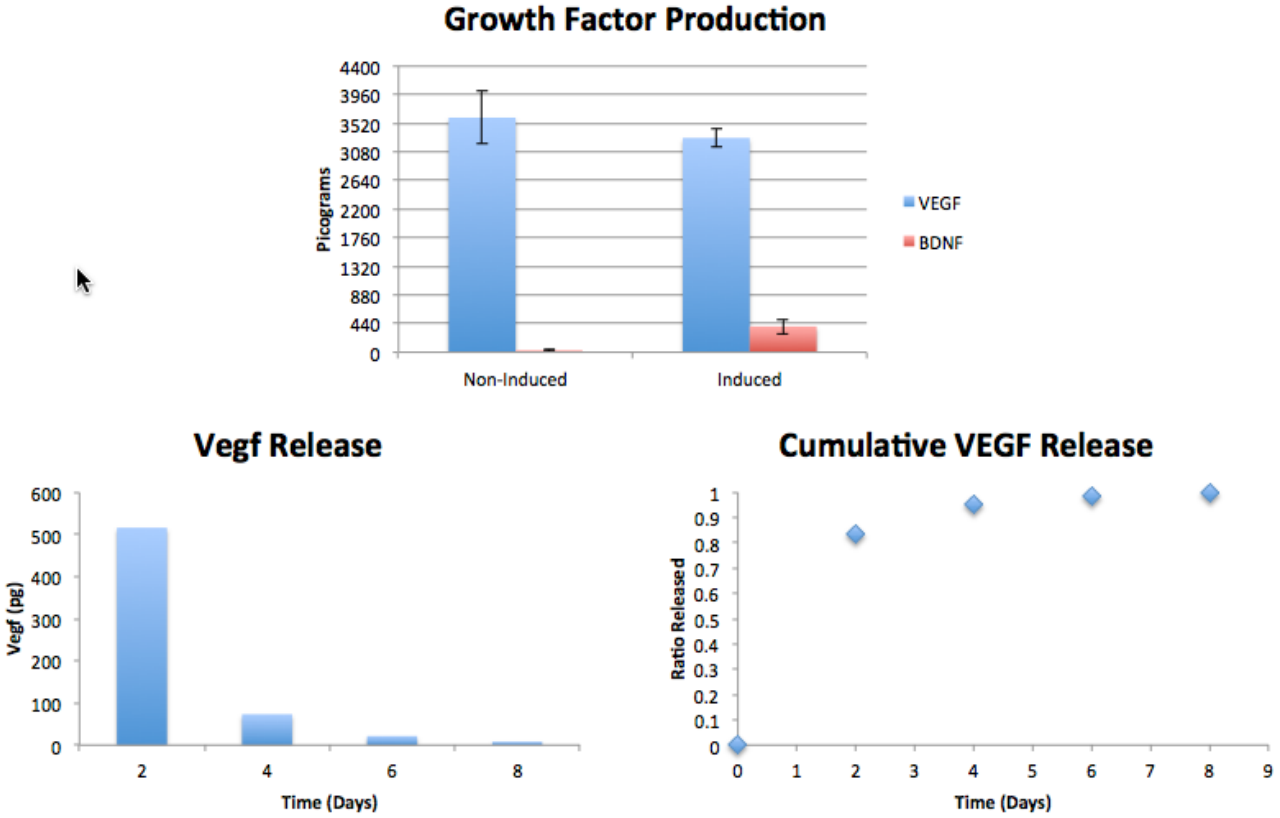

Figure 12 (7): Growth factor release from 3D nerve conduits. (Top) Secretion of BDNF and VEGF from non-induced and neurotrophically-induced MSCs seeded in 3D nerve conduits. **(Left)** VEGF measured in medium after bolus loading during conduit fabrication. **(Right)** Cumulative VEGF release from conduit over a 9 day period. Permeability of growth factors and slow release are observed, as expected due to the slow release capabilities of methacrylated gelatin.

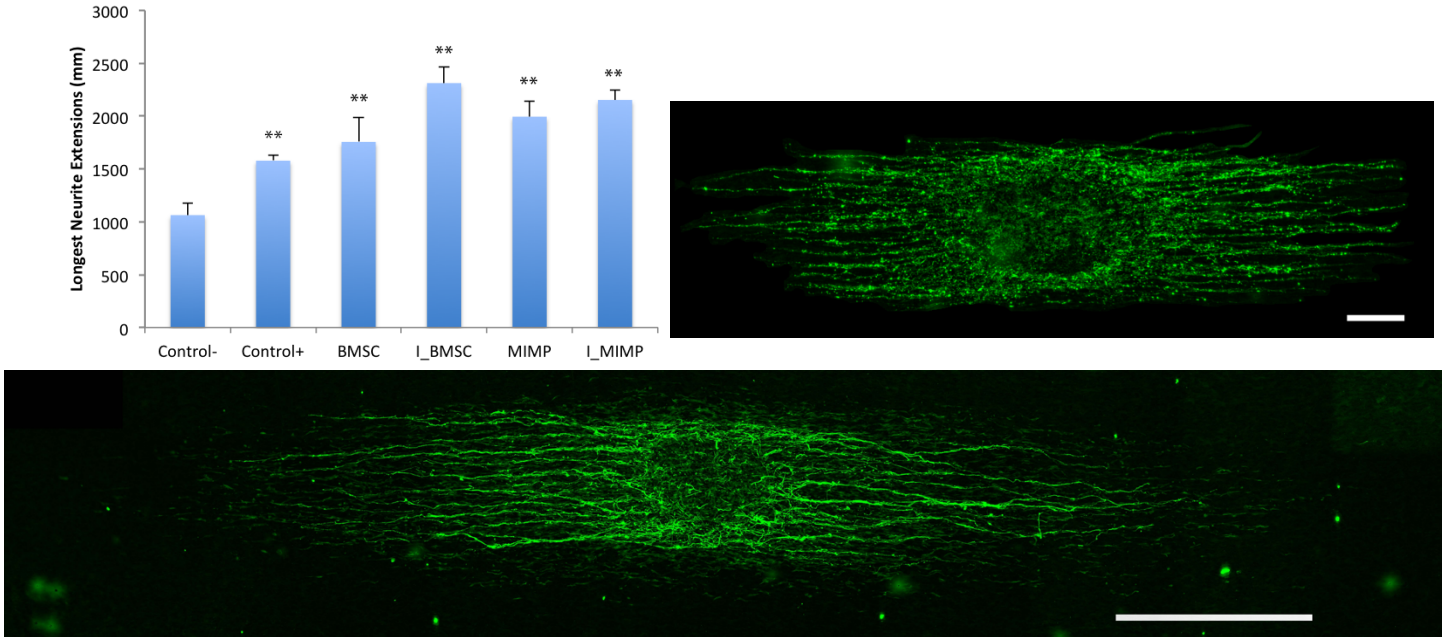

Figure 13 (8): Cell-seeded scaffolds significantly enhance nanofiber-guided neurite extensions from cultured Dorsal Root Ganglia (DRGs). (Top-Left) Average of 10 longest neurite extensions from 4 DRGs in each group. **(Top-Right)** Image of negative control - DRG on non-cell seeded scaffold. **(Bottom)** Image of DRG from I_BMSC group. Note remarkably increased neurite extension lengths in the cell-seeded groups. **, $p<0.001$ with respect to negative control. BMSC=Bone Marrow Stem Cell, MIMP = Induced Mesenchymal Progenitor, I_ = Neurotrophically Induced. Control- = Cultured on Non-Cell Seeded. Control+=10 ng/mL FGF, EGF, NGF supplementation. Top Scale Bar = 250 um. Bottom Scale Bar = 800 um.

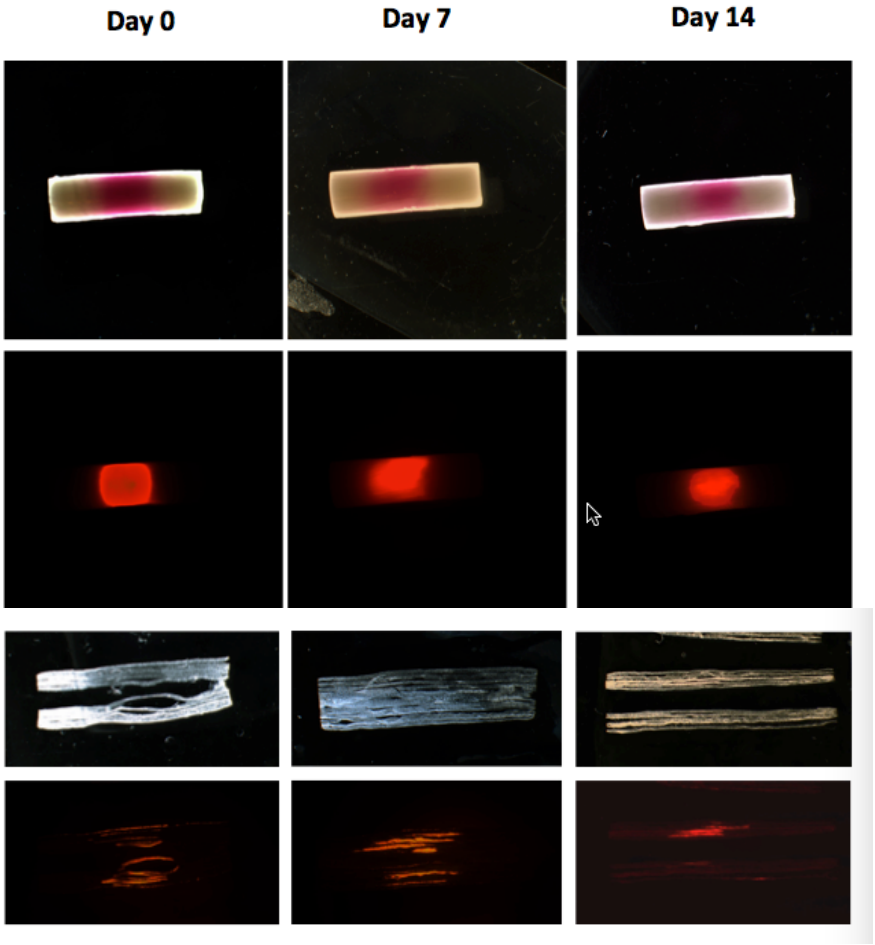

Figure 14 (9): DiI tracking of seeded cells within 3D nerve conduits. Day 0 **(left column),** day 7 **(middle column)**, and day 14 **(right column)** macroscopic and longitudinal sections of conduits with accompanying fluorescent images of DiI labeled cells. As seen from the images, cells that are encapsulated within the walls of the conduit tend to stay within the location they are seeded at day 0 over a 14 day course. This allows spatial control of cell seeding for *in vivo* conduits which utilize cells seeded in the middle of the conduit to provide a neurotrophic gradient for growing axons.

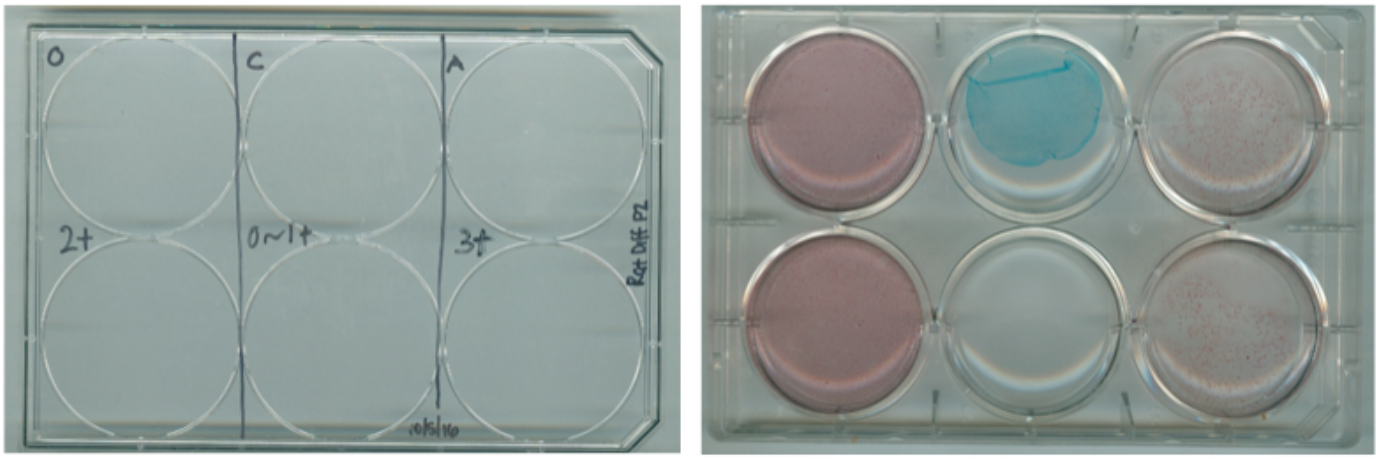

Figure 15 (10): Verification of multipotency of isolated rat MSCs. Rat adipose stem cells were isolated and underwent a differentiation protocol to demonstrate multipotency. Here, osteogenic, chondrogenic, and adipogenic differentiation are shown in the left, center, and right wells, respectively along with their corresponding scores (0-3+) on the left hand side.

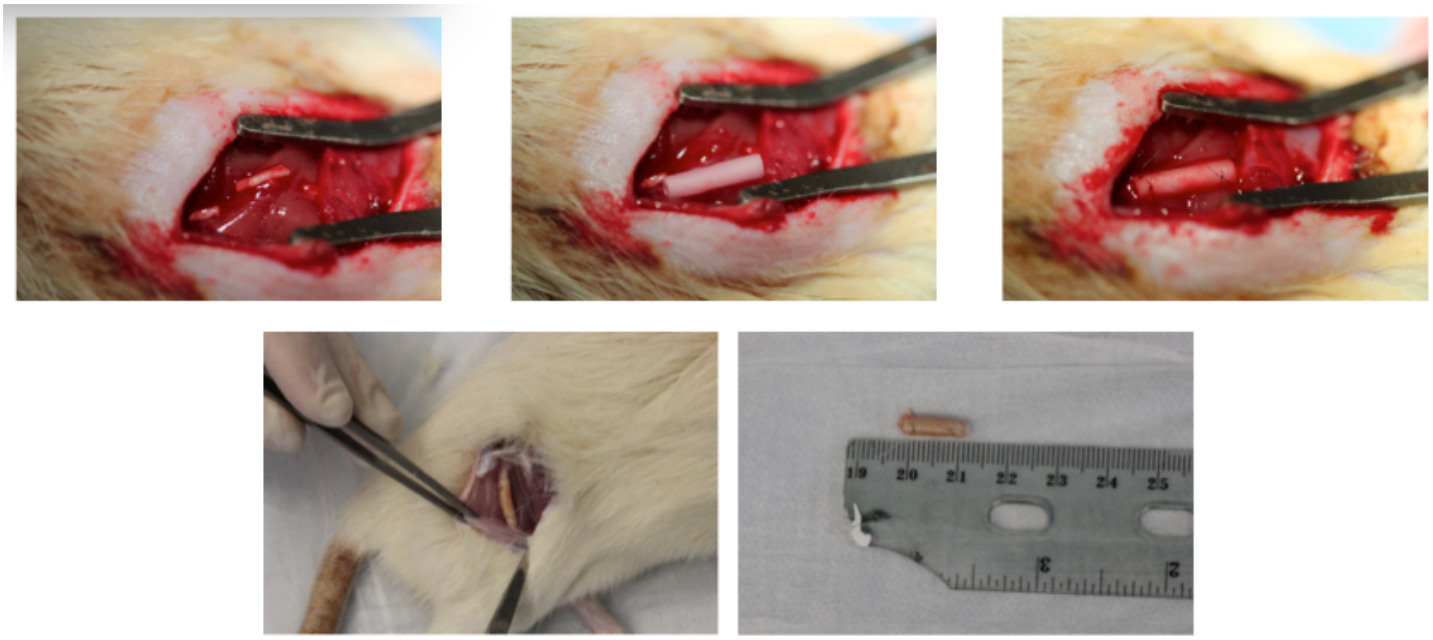

Figure 16 (11):. Surgical implantation of scaffold within rats and macroscopic conduit view after 6 weeks. Removal of 1cm sciatic nerve followed by implantation of scaffold into the defect site **(Top panels)**. Images of conduit during harvest after 6 weeks (**Bottom panels**). As seen from the conduits at harvest, structural integrity is maintained and there is no foreign body reaction to the conduit itself.

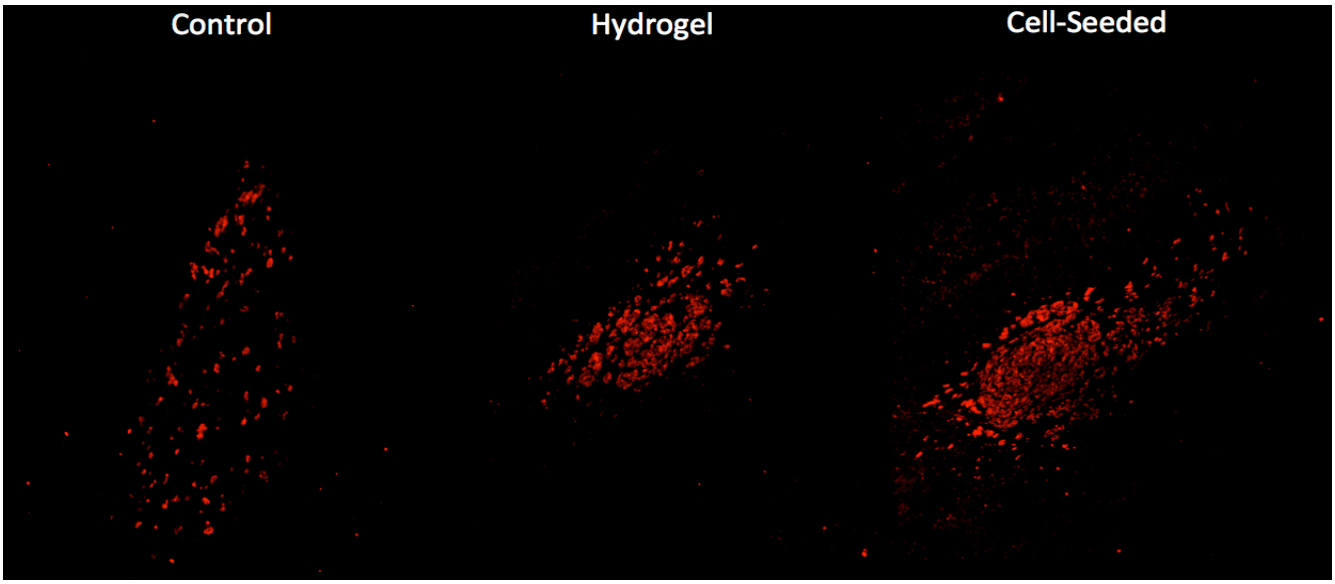

Figure 17 (12): S100 staining of tranverse sections at midpoint of conduit after 6 weeks. Immunohistochemistry for S100 schwann cell staining was used to observe schwann cell infiltration into the growing nerve. As seen from the staining, control conduits (with no encapsulated cells or hydrogel lumen filler) yielded spotty staining with little organization. In contrast, cell-seeded and hydrogel scaffolds displayed dense S100 staining with fascicular distribution – especially cell-seeded groups.

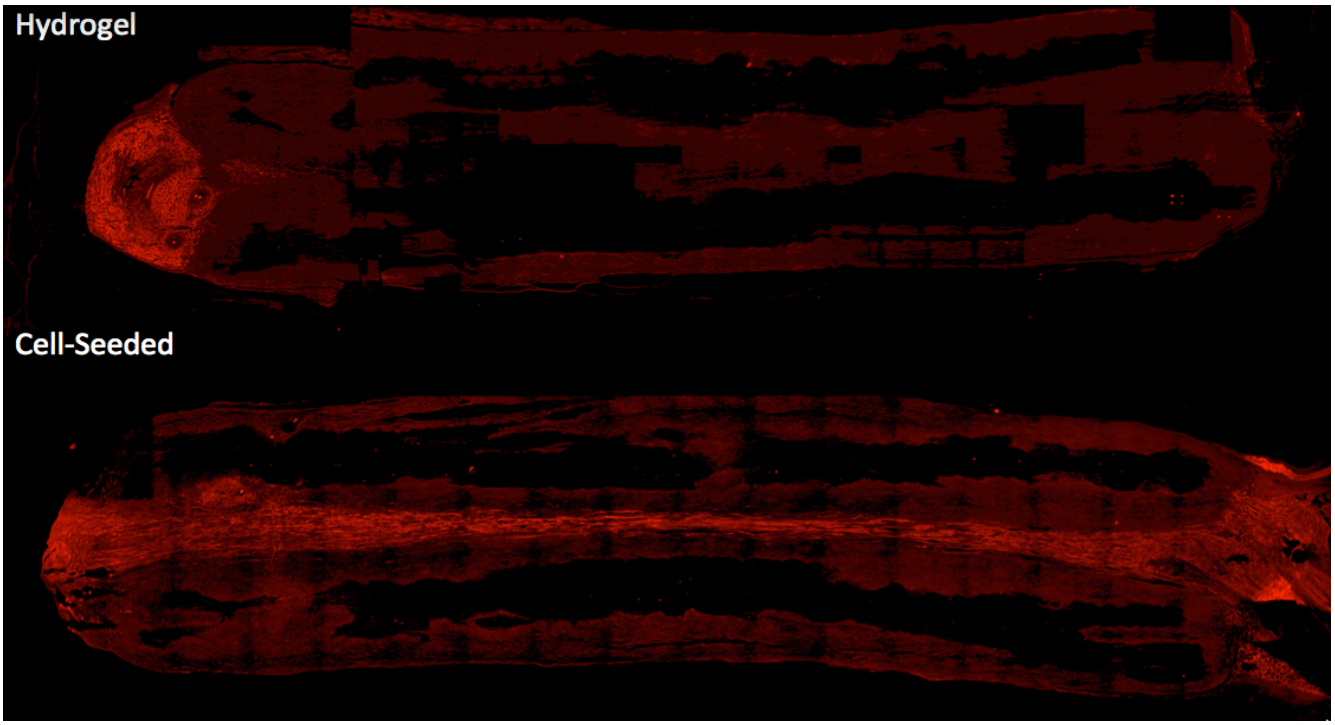

Figure 18 (13): Longitudinal S100 staining of conduit after 6 weeks. Immunohistochemistry for S100 schwann cell staining was used to observe schwann cell infiltration into the growing nerve. As seen from the staining, cell-seeded conduits exhibit a remarkable ability to allow for S100 schwann cell migration into the growing nerve with complete continuity after only 6 weeks. This was not observed in either hydrogel or control conduits (not shown due to imaging equipment malfunction).

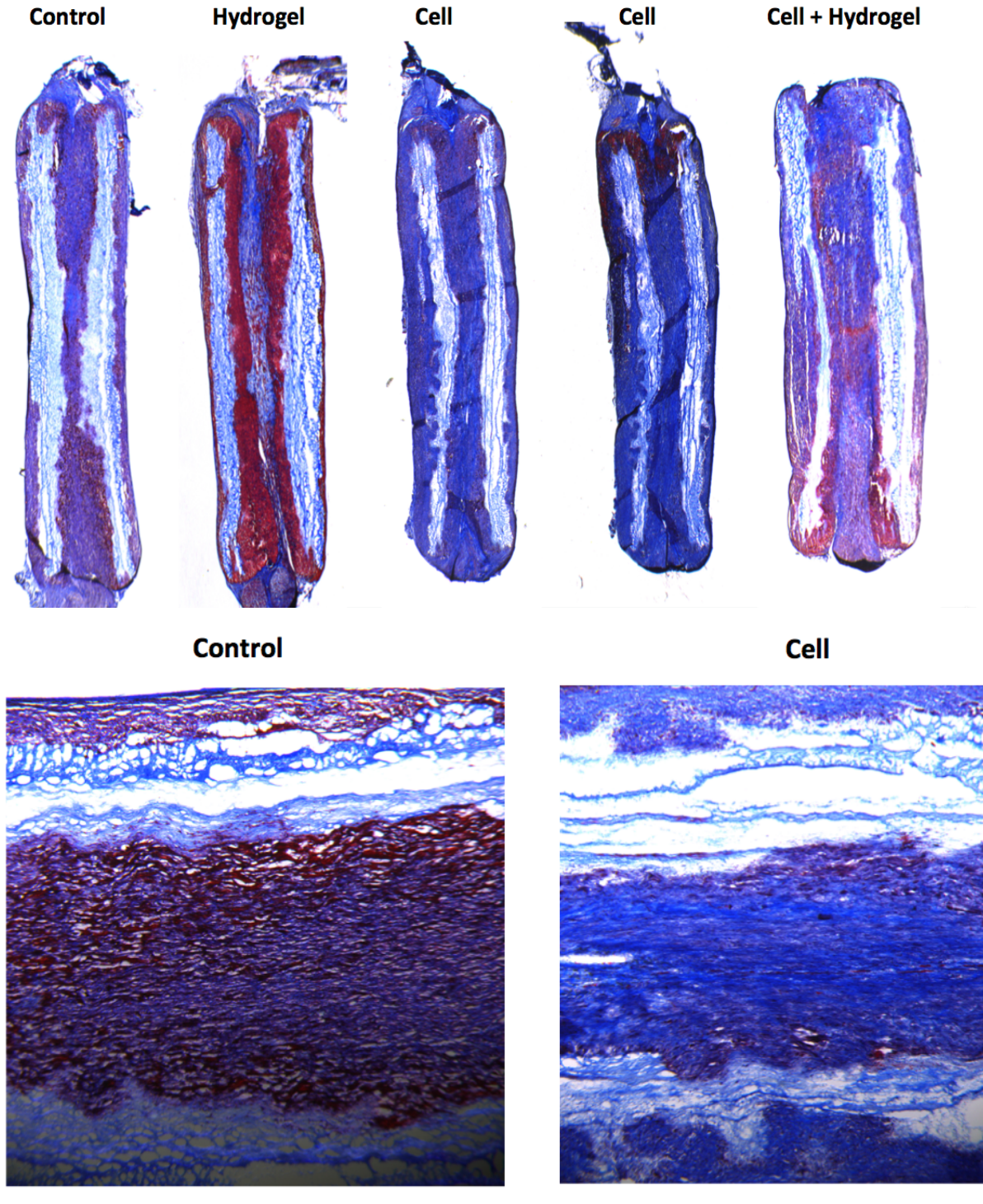

Figure 19 (14):. Longitudinal Masson Trichrome staining of conduit after 6 weeks. Masson trichrome staining was used to analyze longitudinal sections after 6 weeks growth (proximal oriented towards top and distal towards bottom). Pink is cellular cytoplasm while blue is presence of collagen. **(Top)** Strikingly, cell-seeded conduits display strong collagen staining (indicative of axon formation) in full continuity throughout the conduit – even at the distal end. This is in contrast to control and hydrogel-only conduits, which display weak staining at the distal portions. Hydrogel-only groups seem to promote cellular infiltration into the conduit without concurrent schwann cell migration or axon regrowth. In addition, blue staining is seen on the outer walls of the conduits, indicating cellular infiltration into only the random layers of the conduit while allowing nutrient perfusion through all layers as desired. **(Bottom)** Magnified view of distal portion of control and cell conduits demonstrating strong collagen staining in the cell group with weak blue staining in the control.

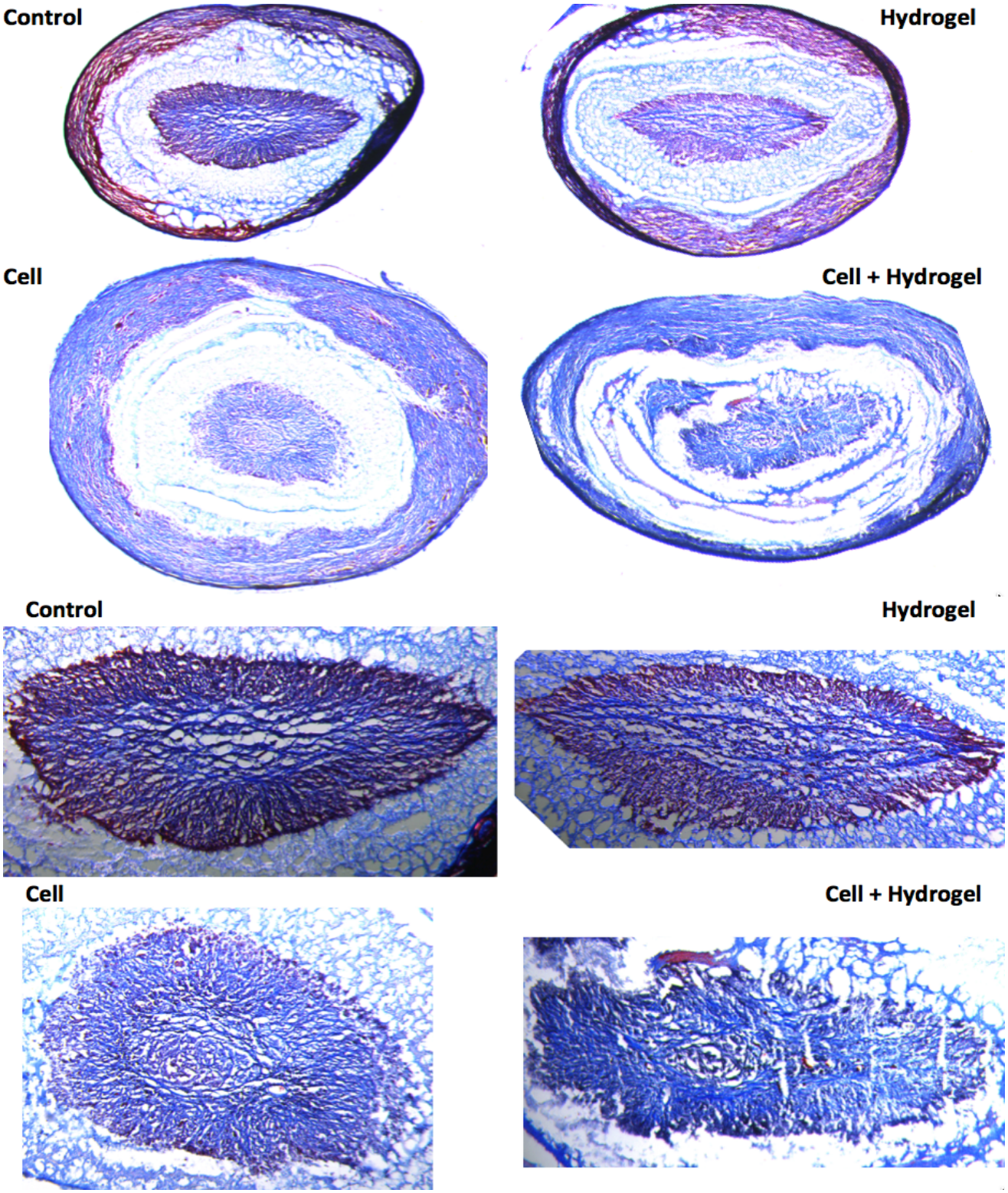

Figure 20 (15):. Transverse Masson Trichrome staining at midpoint of conduit after 6 weeks. Masson trichrome staining was used to analyze longitudinal sections after 6 weeks growth. Pink is cellular cytoplasm while blue is presence of collagen. **(Top)** The same observations hold true in these transverse sections as seen in the longitudinal sections in Figure 14. The cell-containing groups demonstrate dense collagenous stainin in the middle of the conduits (indicative of axon formation). In addition, cell-containing groups have much higher collagen deposition within the walls of the conduit – likely contributing to the structural stability of the conduit itself. **(Bottom)** Magnified views of the central portion of the conduits to better demonstrate the increased organization and collagen content in the cell based groups.

\

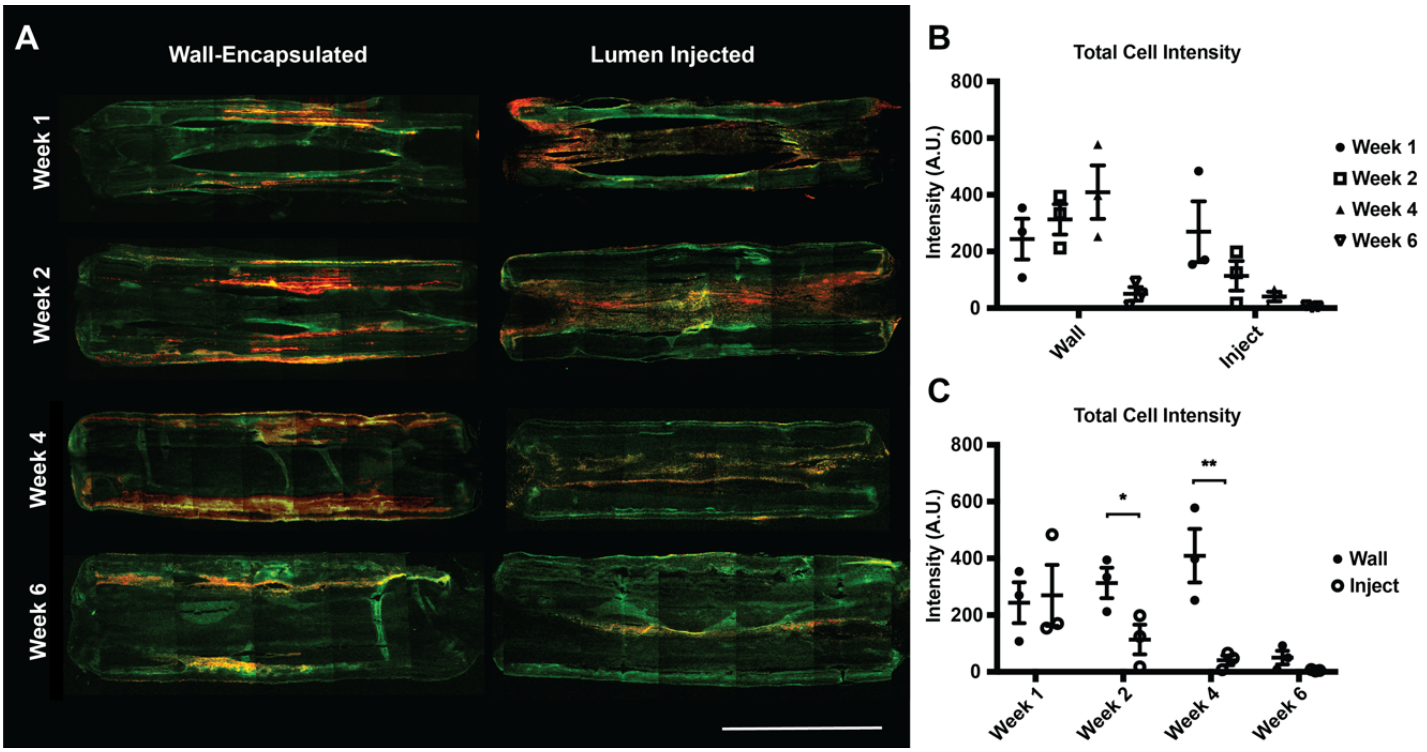

Figure 21 (16): Cells are retained longer *in vivo* with wall-encapsulation compared to lumen injection. (A) Representative images of DiI labeled cells in conduits over 6 weeks. Red channel is DiI label while green is scaffold autofluorescence. **(B)** Total DiI-labeled cell intensity across 6 weeks for wall-encapsulated vs. cell groups showing trends within groups. **(C)** Total DiI-labeled cell intensity across 6 weeks comparing between groups at each week. *, $p<0.05$. **, $p<0.005$. Scale bar = 5 mm.

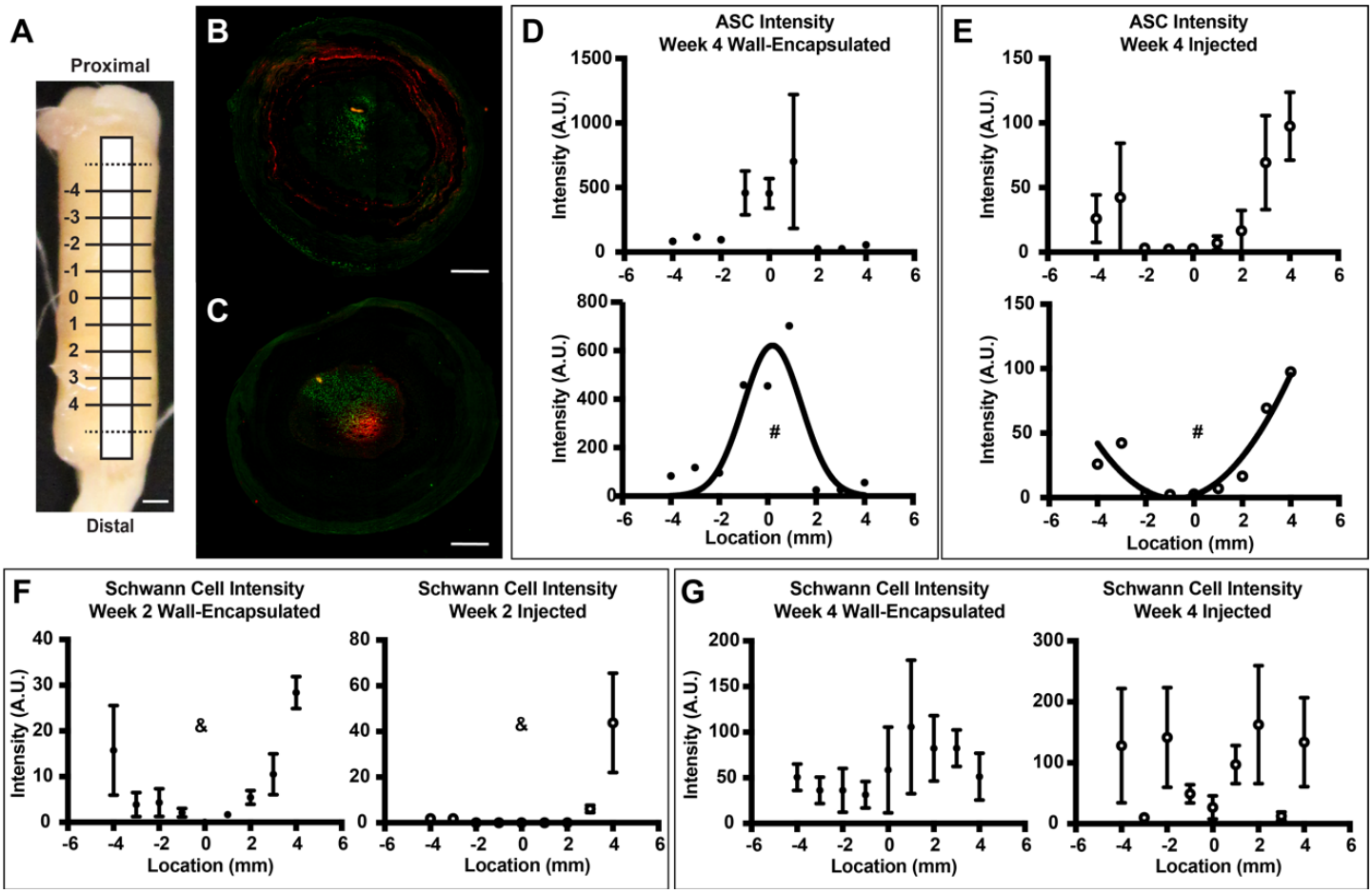

Figure 22 (17): Conduits with centrally located wall-encapsulated ASCs drive directional Schwann cell migration. (A) Schematic of locations sectioned along explanted nerve conduits (4 mm out from the center proximally and distally) from 1 cm rat sciatic nerve transection model. Scale bar = 1 mm. **(B,C)** Representative pictures of localization of Schwann cells and DiI-labeled wall-encapsulated or lumen-injected cells, respectively. Green channel equals Schwann cells while red channel equals ASCs. Scale bar = 500 μm. **(D,E)** ASC intensity along the length of explanted conduits in wall-encapsulation vs injection, respectively. Wall-encapsulated ASCs fit a Gaussian distribution while lumen-injected ASCs fit a quadratic distribution. **(F,G)** Schwann cell intensity along the length of the explanted conduit at two weeks and four weeks, respectively. Schwann cells possess a stronger inwards migration at two weeks in wall-encapsulation groups and by four weeks resemble a single peaked distribution near the center of the conduit as opposed to lumen injection, which possess no clear distribution pattern. #, $p<0.005$ between distributions (Gaussian, fit probability = 84.74% and $r^2 = 0.4463$. Quadratic, fit probability = 91.17% and $r^2 = 0.3280$). &, $p<0.05$ between distributions.

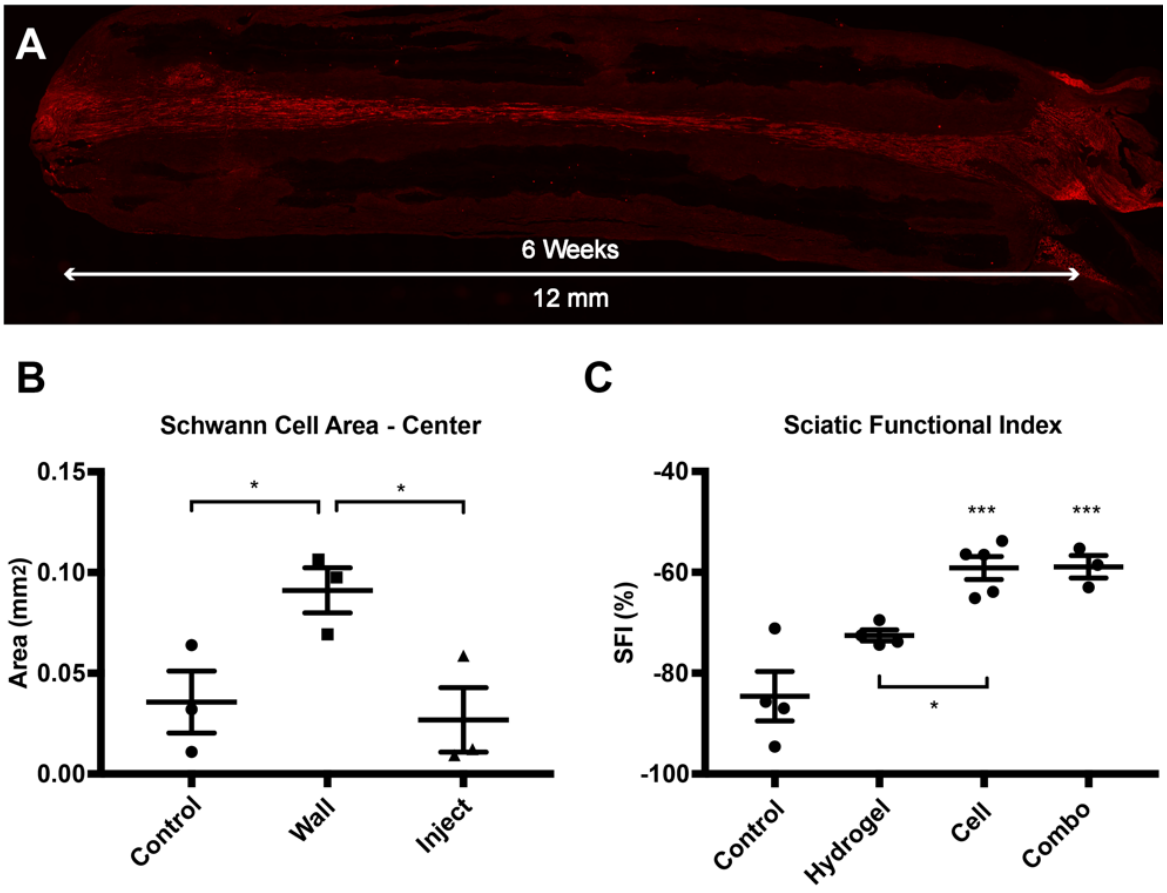

Figure 23 (18): Conduits with centrally located wall-encapsulated ASCs improve functional return. (A) Image of Schwann cells bridging the nerve conduit with wall-encapsulated ASCs at 6 weeks in a rat 1 cm sciatic nerve transection model. **(B)** Schwann cell-positive area in cross-section of center of conduits in cell-free control, wall-encapsulated and lumen injected cell groups. **(C)** Sciatic functional index at 16 weeks for cell-free control (control), nerve conduits with ECM hydrogel lumen filler (hydrogel), nerve conduit with wall-encapsulated cells (cell), or nerve conduit with wall-encapsulated cells plus ECM hydrogel lumen filler groups (combo). *, $p<0.05$. ***, $p<0.001$ compared to Control.

What opportunities for training and professional development has the project provided?

The following graduate students benefitted from the transfer of knowledge, skills and abilities in the course of this project:

1. Heidi Hofer
2. Kelsey Gloss
3. Rachel Brick
4. Aaron Sun

Other undergradutes with training opportunities:

1. Shannon Gorman
2. Michael DeHart
3. Xixuan Li

How were the results disseminated to communities of interest?

The work by Dr Hofer, Brick and Sun have been published in prestigious peer-reviewed journal:

1. Hofer HR, Tuan RS. Secreted trophic factors of mesenchymal stem cells support neurovascular and musculoskeletal therapies. Stem Cell Res Ther. 2016 Sep 9;7(1):131. doi: 10.1186/s13287-016-0394-0. PMID: 27612948; PMCID: PMC5016979.

2. Zupanc HRH, Alexander PG, Tuan RS. Neurotrophic support by traumatized muscle-derived multipotent progenitor cells: Role of endothelial cells and Vascular Endothelial Growth Factor-A. Stem Cell Res Ther. 2017 Oct 13;8(1):226. doi: 10.1186/s13287-017-0665-4. PMID: 29029631; PMCID: PMC5640955.

3. Brick RM, Sun AX, Tuan RS. Neurotrophically Induced Mesenchymal Progenitor Cells Derived from Induced Pluripotent Stem Cells Enhance Neuritogenesis via Neurotrophin and Cytokine Production. Stem Cells Transl Med. 2018 Jan;7(1):45-58. doi: 10.1002/sctm.17-0108. Epub 2017 Dec 7. PMID: 29215199; PMCID: PMC5746147.

4. Sun AX, Prest TA, Fowler JR, Brick RM, Gloss KM, Li X, DeHart M, Shen H, Yang G, Brown BN, Alexander PG, Tuan RS. Conduits harnessing spatially controlled cell-secreted neurotrophic factors improve peripheral nerve regeneration. Biomaterials. 2019 May;203:86-95. doi: 10.1016/j.biomaterials.2019.01.038. Epub 2019 Feb 19. PMID: 30857644.

The work was also presented at annual meetings of the Orthopaedic Rezearch Society, Military Health Sciences Research Symposium, the Biomedical Engineering Society and the International Society for Stem Cell Research, among others:

What do you plan to do during the next reporting period to accomplish the goals?

Final Report, Nothing to Report

4. IMPACT: This component is used to describe ways in which the work, findings, and specific products of the project have had an impact during this reporting period. Describe distinctive contributions, major accomplishments, innovations, successes, or any change in practice or behavior that has come about as a result of the project relative to:

- the development of the principal discipline(s) of the project;
- other disciplines;
- technology transfer; or
- society beyond science and technology.

What was the impact on the development of the principal discipline(s) of the project?

The biology of mesenchymal stomal (stem) cells: Adult mesenchymal stem cells (MSCs) remain a subject of intense experimental and biomedical interest. Among the growth factors we have shown produced by MSCs that contribute to nerve out-growth and tissue repair are: VEGF, CNTF, GDNF, TGF-β, interleukins (IL-1β, IL-6, and IL-8), and C-C ligands (CCL-2, CCL-5, and CCL-23), serving as paracrine control molecules secreted or packaged into extracellular vesicles, or exosomes. Further work has shown:

a. The importance of MSCs in both nerve outgrowth (recapitulating a function of the Bunger fibers) and
b. the formation and maintenance of blood vessels in early angiogenesis

The use of MSCs derived from wound margins:

Use of MSCs in Tissue engineering: Here were have contributed to use of MSCs in a novel neurotrophic nerve repair conduit: The neurotrophic abilities are largely mediated by secreted factors. The neurotrophic potential of MSCs to encourage nerve growth via a VEGF-A-dependent action is mediated by microparticles and as paracrine factors. These can be harnessed in conditioned medium, the use of the cells themselves or a

combination thereof. Due to the ease of use, application of bioactive agents derived from cultured cells to enhance neurotrophic support presents a promising line of research into peripheral nerve repair.

Use of photocrosslinked gelatin in a nerve repair conduit: The use of photopolymerized gelatin to encapsulate cells as a long-term, self-regulating source of neurotrophic factors. We have demonstrated the utility of the incorporation of MSCs and photopolymerizable gelatin within a novel nano-fibrous scaffold to support nerve repair in a rat model of sciatic nerve injury. Specifically we are demonstrating the capacity of MSCs to orchestrate repair via their secretome – a facility now being accepted by the MSCs community as a whole.

What was the impact on other disciplines?
The peer-reviewed publications have been cited a total of 24 times in the following fields:

a. Neuroscience: Schwann cell biology and engineering; use of the secretome in embryonic neural tube defect repair, adult CNS and spinal disease, and invitro brain model development.
b. Inflammation: Nerve repair and the control of inflammation and the extracellular environment (i.e. matrix) and MSC secretome characterization
c. Cell signaling (NGF, STAT 3 signaling)

What was the impact on technology transfer?

Nothing to Report. The University of Pittsburgh was unwilling to support a patent on the nerve assembly device

What was the impact on society beyond science and technology?

Nothing to report.

5. CHANGES/PROBLEMS:

Changes in approach and reasons for change

The neurotrophic abilities of MSCs derived from blast-traumatized muscle were initially used in the characterization of MSC neurotrophic capacities.

Endothelial cells were not used in co-culture with MSCs *in vitro* because culture conditions necessary for survival of ECs would confound the results of neurite extension given the vast number of growth factors necessary to sustain EC viability *in vitro*. In addition, from a point-of-care translatability aspect the use of two cell types – especially difficult to isolate ECs – would greatly reduce its applicability.

A 2D equivalent (mats) representative of the 3D conduit were used in neurite extension assays due to problems with imaging a DRG inside of the nerve conduit. We found that the results of this *in vitro* assay was still correlative with results demonstrated *in vivo*.

In the in vivo repair study, we made several changes:

1. We utilized allograft adipose tisseu-derived MSCs because they are (1) readily available and easy to isolate, (2) have immediate clinical translation. This change was approved.
2. Thy-1 GFP rats were not used due to cost and difficulty in obtaining them. In addition, from a scientific standpoint there are plenty of immunohistochemical labels that can identify host axons and nerves without needing a Thy-1 transgenic GFP rat.
3. Instead of using a Lenti-viral construct to label cells, we chose a higher efficiency labeling method (DiI). In addition, with this membrane label there is minimal concern of altering the secretome of the MSC that a lenti-viral approach might do.
4. Given the very promising results we saw *in vivo* at the 6 week mark, we chose to do earlier time points as well in order to track cells and parse out the activity of these cells in the early nerve regeneration response.
5. Functional testing was not completed at 8 weeks because full functional capacity after a sciatic nerve defect returns at 16 weeks. Thus, fcntional recovery was assessed at 4 months.

Actual or anticipated problems or delays and actions or plans to resolve them

1. We experienced several challenges/problems to completing the final Aim of this study. The initial problem was that space for the in vivo study of nerve repair in the rabbit was not immediately. A no-cost extension was requested and approved for that
2. Then, COVID19 pandemic severely restricted research activity. The impact of this cannot be overstated. The University and facilities experience shut-downs and/or severe restrictions. Most importantly, it inhibited travel between aEurope and the United States for extended periods of time. This prevented the repair of the electrospinner by experienced personnel. Work was postponed until the facility and University could support all functionality.
3. Although the rabbit study was not completed, We realized that gait analysis for rabbit is not established. Discussion with neurology department concluded in the request that electrophysiology replace gait analysis in the rabbit. This change was approved.

Changes that had a significant impact on expenditures

The inability to complete the rabbit study resulted in a remainder of $80,987 that is being return to the DoD.

Significant changes in use or care of human subjects, vertebrate animals, biohazards, and/or select agents

Nothing to report.

6. PRODUCTS:

- **Publications, conference papers, and presentations**

Journal publications.

5. Hofer HR, Tuan RS. Secreted trophic factors of mesenchymal stem cells support neurovascular and musculoskeletal therapies. Stem Cell Res Ther. 2016 Sep 9;7(1):131. doi: 10.1186/s13287-016-0394-0. PMID: 27612948; PMCID: PMC5016979.

6. Zupanc HRH, Alexander PG, Tuan RS. Neurotrophic support by traumatized muscle-derived multipotent progenitor cells: Role of endothelial cells and Vascular Endothelial Growth Factor-A. Stem Cell Res Ther. 2017 Oct 13;8(1):226. doi: 10.1186/s13287-017-0665-4. PMID: 29029631; PMCID: PMC5640955.

7. Brick RM, Sun AX, Tuan RS. Neurotrophically Induced Mesenchymal Progenitor Cells Derived from Induced Pluripotent Stem Cells Enhance Neuritogenesis via Neurotrophin and Cytokine Production. Stem Cells Transl Med. 2018 Jan;7(1):45-58. doi: 10.1002/sctm.17-0108. Epub 2017 Dec 7. PMID: 29215199; PMCID: PMC5746147.

8. Sun AX, Prest TA, Fowler JR, Brick RM, Gloss KM, Li X, DeHart M, Shen H, Yang G, Brown BN, Alexander PG, Tuan RS. Conduits harnessing spatially controlled cell-secreted neurotrophic factors improve peripheral nerve regeneration. Biomaterials. 2019 May;203:86-95. doi: 10.1016/j.biomaterials.2019.01.038. Epub 2019 Feb 19. PMID: 30857644.

- **Website(s) or other Internet site(s)**

  The results of this work were featured on the websites for CCME and the McGowan Institute for Regenerative Medicine

- **Technologies or techniques**

  The technique to create a stem cell-seeded nerve conduit that allows for immediate incorporation during fabrication as well as spatially controllable cell distribution within the walls of the conduit has been described in this reporting period. This technique will be disseminated to the research community through conferences and future publications. A JOVE article is inpreparation.

- **Inventions, patent applications, and/or licenses**

  Nothing to report.

- **Other Products**

  Nothing to report.

7. PARTICIPANTS & OTHER COLLABORATING ORGANIZATIONS

Nothing to Report

What individuals have worked on the project?

Name:	Peter Alexander
Project Role:	Principle Investigator
Researcher ID	University Employee ID# 124097
Nearest person month worked:	22% effort (2.5 Person Months)
Contribution to Project:	Dr. Alexander's responsibilities will include cell isolation, propagation, activation, biomaterial scaffold fabrication, histological, biochemical and histological analyses, and animal surgeries. He is also responsible for experimental design, data analysis, and the training of graduate students and residents. He will also be involved in data analysis, and presentation of research findings in manuscripts and at scientific meetings.
Funding Support:	N/A
Name:	Rocky S Tuan
Project Role:	Principle Investigator
Researcher ID	University Employee ID# 124200
Nearest person month worked:	5.0 % effort (0.6 Person Months)
Contribution to Project:	Dr. Tuan's responsibilities will include data analysis, and presentation of research findings in manuscripts and at scientific meetings.
Funding Support:	N/A

Name:	Jian Tan
Project Role:	Research Specialist
Research Identifier:	University Employee ID# 124708
Nearest person month worked:	25.0 % effort (3.0 Person Months)
Contribution to Project:	Jian will assist in the execution of the experiments in this project for all the proposed tasks. Jian will be trained by Dr. Alexander, and will be supervised directly by Dr. Tuan and Dr. Alexander in all of her research activities, including experimental design, assays, and data analyses. Jian will also be responsible for safety requirement, material acquisition, protocol development, and handle reporting duties according to Department of Defense protocols.
Funding Support:	N/A
Name:	John Fowler
Project Role:	Co-Investigator
Research Identifier:	University Employee ID# 150464
Nearest person month worked:	5% effort (0.60 Person Months)
Contribution to Project:	Dr. Fowler participates in the animal surgery aspects of this project, as well as in research design, outcome analysis, manuscript preparation, and preparation for future large animal trials.
Funding Support:	N/A
Name:	MaCalus Hogan
Project Role:	Co-Investigator
Research Identifier:	University Employee ID# 152173
Nearest person month worked:	5% effort (0.60 Person Months)
Contribution to Project:	Dr. Hogan participats in the animal surgery aspects of this project, as well as in research design, outcome analysis, manuscript preparation, and preparation for future large animal trials.
Funding Support:	N/A
Name:	Alessandro Pirosa
Project Role:	Postdoctoral Associate
Research Identifier:	University Employee ID# 160892
Nearest person month worked:	56% effort (6.72 Person Months)
Contribution to Project:	Alessandro responsibilities will include cell isolation and culture, nanofiber scaffold fabrication, histological and immunohistochemical evaluation of tissue and cell phenotype, ELISA, tissue imaging, and production of the MPC-NC constructs.
Funding Support:	N/A
Name:	Heidi Hofer
Project Role:	Graduate Student Researcher
Research Identifier:	University Employee ID# 138267
Nearest person month worked:	83.33% effort (10.00 Person Months – Left University on 8/1/17)
Contribution to Project:	Heidi's responsibilities included cell isolation and culture (of traumatized muscle-derived MSCs and chick dorsal root ganglia, histological and immunohistochemical evaluation of tissue and cell phenotype, gene expression analysis by RT-PCR, ELISA, tissue imaging, and in vitro functional testing of the MPC-seeded

	nanofibrous constructs. She was supervised by Dr Alexander and Dr Tuan (thesis advisor)
Funding Support:	N/A
Name:	Rachel Brick
Project Role:	Graduate Student Researcher
Researcher Identifier	University Employee ID# 138267
Nearest person month worked:	83.33% effort (10.00 Person Months – Left University on 8/1/17)
Contribution to Project:	Rachel's responsibilities included cell isolation and culture of induced peluripotent stem cells, histological and immunohistochemical evaluation of tissue and cell phenotype, gene expression analysis by RT-PCR, ELISA, tissue imaging, and in vitro functional testing of iPSC-seeded nanofibrous constructs. She was closely supervised by Dr. Tuan and Dr. Alexander.
Funding Support:	N/A
Name:	Aaron Sun
Project Role:	Graduate Student Researcher
Researcher Identifier	University Employee ID# 170453
Nearest person month worked:	83.33% effort (10.00 Person Months – Left University on 8/1/18)
Contribution to Project:	Rachel's responsibilities included cell isolation and culture of induced peluripotent stem cells, histological and immunohistochemical evaluation of tissue and cell phenotype, gene expression analysis by RT-PCR, ELISA, tissue imaging, and in vitro functional testing of iPSC-seeded nanofibrous constructs. She was closely supervised by Dr. Tuan and Dr. Alexander.
Funding Support:	N/A
Name:	Kelsey Gloss
Project Role:	Graduate Student Researcher
Researcher Identifier	University Employee ID# 171537
Nearest person month worked:	100% effort (12.00 Person Months – Left University on 10/1/16, employed for 4 months only)
Contribution to Project:	Kelsey's responsibilities will be involved in general laboratory protocol development and optimization, preparation of research reports, presentations and manuscripts. She will work under close supervision
Funding Support:	N/A

What other organizations were involved as partners?

Nothing to Report

8. SPECIAL REPORTING REQUIREMENTS:

QUAD CHARTS:

9. APPENDICES:

Appendix 1: Quad chart: QuadChart 15-1-0600 FINAL 12-17-2021

Appendix 2: Hofer HR, Tuan RS. Secreted trophic factors of mesenchymal stem cells support neurovascular and musculoskeletal therapies. Stem Cell Res Ther. 2016 Sep 9;7(1):131. doi: 10.1186/s13287-016-0394-0. PMID: 27612948; PMCID: PM
C5016979.

Appendix 3: Zupanc HRH, Alexander PG, Tuan RS. Neurotrophic support by traumatized muscle-derived multipotent progenitor cells: Role of endothelial cells and Vascular Endothelial Growth Factor-A. Stem Cell Res Ther. 2017 Oct 13;8(1):226. doi: 10.1186/s13287-017-0665-4. PMID: 29029631; PMCID: PMC5640955.

Appendix 4: Brick RM, Sun AX, Tuan RS. Neurotrophically Induced Mesenchymal Progenitor Cells Derived from Induced Pluripotent Stem Cells Enhance Neuritogenesis via Neurotrophin and Cytokine Production. Stem Cells Transl Med. 2018 Jan;7(1):45-58. doi: 10.1002/sctm.17-0108. Epub 2017 Dec 7. PMID: 29215199; PMCID: PMC5746147.

Appendix 5: Sun AX, Prest TA, Fowler JR, Brick RM, Gloss KM, Li X, DeHart M, Shen H, Yang G, Brown BN, Alexander PG, Tuan RS. Conduits harnessing spatially controlled cell-secreted neurotrophic factors improve peripheral nerve regeneration. Biomaterials. 2019 May;203:86-95. doi: 10.1016/j.biomaterials.2019.01.038. Epub 2019 Feb 19. PMID: 30857644.

Adult Stem Cell-Based Neurotrophic Conduit Enhancement of Peripheral Nerve Repair

Log Number: OR140390

Award Number: W81XWH-15-1-0600

PI: Peter G Alexander **Org:** University of Pittsburgh **Award Amount:** $1,557,090

Project Aims

The goal of this study is to develop a synthetic nerve conduit (NC) enhanced with bioactivated matrix and neuro-potentiating autologous stem cells (MPCs). The following aims are proposed:

1. Produce bi-layered nanofibrous scaffolds (NFS)
2. Optimize the neurotrophic (NT) activity of MPC-seeded NFS
3. Design and construct device for PoC NT-MPC-NC preparation
4. Biomechanical and biochemical testing of final NT-MPC-NC
5. Test NT-MPC-NC in small animal models (rat and rabbit)
6. Prepare and submit an IDE clinical trial protocol to FDA

Approach

A bilaminar scaffold comprised of (1) inner aligned nanofibers for contact-guidance axonal migration and (2) outer randomized fibers for tensile strength and suture retention filled with HA/gelatin or similar hydrogel (if efficacious) activated with conditioned medium from NT-MPCs conditioned medium and coated externally with MPCs to provide extended, physiologic release of neurotrophic, immuno-modulatory cytokines to enhance nerve regeneration.

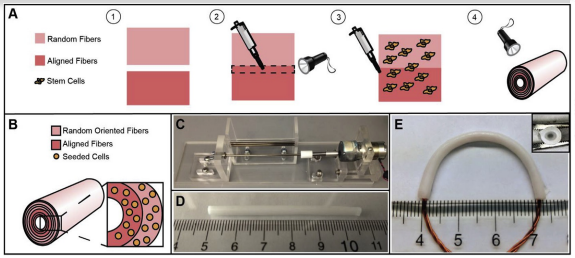

Fig. 1: (A) Step-wise production of the NFS-NC; (B) NFS layer schematic; (C) Conduit fabrication device; (D) Final Conduit; (E) Flexibility

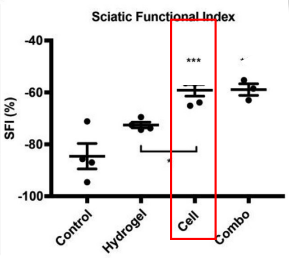

Fig. 2: SFI 12 wks after repair using empty, hydrogel lumen, cell-laden walls or combo product

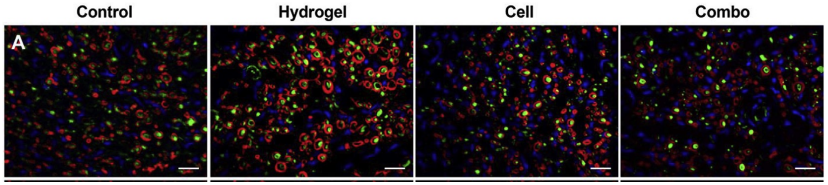

Fig. 3: IHC 12 wks after implant: NF-1 (green), myelin (red) and nuclei (blue)

Timeline and Cost

Activities FY	16	17	18	19	20	21
Produce bi-layered NFS.						
Optimize NT-MPC-seeded NFS.						
NT-MPC NFS-NC device.						
Biomech. biochem testing						
Test NT-MPC-NC in rat and rabbit						
Submit IDE clinical trial to FDA						
Expediture/budget ($K)	**311**	**585**	**344**	**76**	**87**	**60**

Updated: August 26, 2019; **Total Cost: $1,557K**

Past time-line; Projected time-line; ★ Completed; — Current status

Goals/Milestones

CY16 Goals

☑ Optimize biomaterial structure and composition of nerve conduit

CY17 Goals:

☑ Determine optimal neuroconductive ECM for nerve conduit.

☑ Construct device for point-of-care NT-MPC NC preparation

☑ Biomechanical and biological testing of MPC-NC.

CY18 Goals:

☑ Test biological activity of MPC-NC in a rat model

CY 20 Goals:

☐ Test surgical and regenerative activity of MPC-NC in a rabbit model

☐ Prepare and submit IDE protocol to the FDA

Comments/Challenges/Issues/Concerns: protocol resubmission asnd COVID-19 closure/precautions

Budget Expenditure to Date:

Projected Expenditure: $1,557,090; Actual Expenditure: $1,476,112.93

Hofer and Tuan *Stem Cell Research & Therapy* (2016) 7:131
DOI 10.1186/s13287-016-0394-0

Stem Cell Research & Therapy

REVIEW Open Access

Secreted trophic factors of mesenchymal stem cells support neurovascular and musculoskeletal therapies

Heidi R. Hofer and Rocky S. Tuan*

Abstract

Adult mesenchymal stem cells (MSCs) represent a subject of intense experimental and biomedical interest. Recently, trophic activities of MSCs have become the topic of a number of revealing studies that span both basic and clinical fields. In this review, we focus on recent investigations that have elucidated trophic mechanisms and shed light on MSC clinical efficacy relevant to musculoskeletal applications. Innate differences due to MSC sourcing may play a role in the clinical utility of isolated MSCs. Pain management, osteochondral, nerve, or blood vessel support by MSCs derived from both autologous and allogeneic sources have been examined. Recent mechanistic insights into the trophic activities of these cells point to ultimate regulation by nitric oxide, nuclear factor-kB, and indoleamine, among other signaling pathways. Classic growth factors and cytokines—such as VEGF, CNTF, GDNF, TGF-β, interleukins (IL-1β, IL-6, and IL-8), and C-C ligands (CCL-2, CCL-5, and CCL-23)—serve as paracrine control molecules secreted or packaged into extracellular vesicles, or exosomes, by MSCs. Recent studies have also implicated signaling by microRNAs contained in MSC-derived exosomes. The response of target cells is further regulated by their microenvironment, involving the extracellular matrix, which may be modified by MSC-produced matrix metalloproteinases (MMPs) and tissue inhibitor of MMPs. Trophic activities of MSCs, either resident or introduced exogenously, are thus intricately controlled, and may be further fine-tuned via implant material modifications. MSCs are actively being investigated for the repair and regeneration of both osteochondral and other musculoskeletal tissues, such as tendon/ligament and meniscus. Future rational and effective MSC-based musculoskeletal therapies will benefit from better mechanistic understanding of MSC trophic activities, for example using analytical "-omics" profiling approaches.

Keywords: Arthritis, Mesenchymal stem cells, Extracellular vesicles, Endothelial cells, Endothelial cell–mesenchymal stem cell interactions, Neurotrophic activity, Muscle-derived stem cells

Abbreviations: AD-MSC, Adipose-derived mesenchymal stem cell; AGN, Aggrecan; Ang, Angiopoietin; BDNF, Brain-derived neurotrophic factor; BM, Bone marrow; BMI, Body mass index; BMP, Bone morphogenetic protein; cAMP, Cyclic adenosine monophosphate; CCR/L, Chemokine (C-C) receptor/ligand; CD, Cluster of differentiation; CM, Conditioned medium; CNTF, Ciliary neurotrophic factor; COL, Collagen; COX, Cyclooxygenase; CPC, Chondrocyte progenitor cell; CSPC, Cartilage-derived stem/progenitor cell; CXCR/L, Chemokine (C-X-C) receptor/ligand; Cyr61, Cysteine-rich angiogenic inducer 61; Dkk, Dickkopf-related proteins; EC, Endothelial cell; ECM, Extracellular matrix; EF2, Eukaryotic elongation factor; ET, Endothelin; EV, Extracellular vesicle; FGF, Fibroblast growth factor; Foxp3, Forkhead box p3; GAG, Glycosaminoglycan; GARP, Glycoprotein A repetitions predomain; GDNF, Glial cell line-derived neurotrophic factor; GH-IGF, Growth hormone-insulin-like growth factor; GM-CSF, Granulocyte macrophage colony-stimulating factor;

(Continued on next page)

* Correspondence: rst13@pitt.edu
Center for Cellular and Molecular Engineering, Department of Orthopaedic Surgery, University of Pittsburgh School of Medicine, 450 Technology Drive, Room 221, Pittsburgh, PA 15219, USA

(Continued from previous page)
HA, Hyaluronan; HGF, Hepatocyte growth factor; HIF, Hypoxia inducible factor; HLA, Human leukocyte antigen; IDO, Indoleamine 2,3-dioxygenase; IFN, Interferon; IGF, Insulin-like growth factor; IL, Interleukin; iMSC, MSC generated from induced pluripotent stem cell (iPSC) lines via medium change; iNOS, Nitric oxide synthase; LIF, Leukemia inhibitory factor; LRRC32, Leucine-rich repeat containing-32; MDSC, Muscle-derived stem cell; MHC, Major histocompatibility complex; miRNA, MicroRNA; MMP, Matrix metalloproteinase; mRNA, Messenger RNA; MSC, Mesenchymal stem cell; NF-κB, Nuclear factor-kappa B; NGF, Nerve growth factor; NO, Nitric oxide; OA, Osteoarthritis; PCL, Polycaprolactone; PDGF, Platelet-derived growth factor; PE, Polyethylene; PEDF, Pigment epithelium-derived factor; PG, Prostaglandin; PLA, Poly-lactic acid; PLGF, Placental growth factor; PU, Polyurethane; RA, Rheumatoid arthritis; RANK, Receptor activator of nuclear factor-κB; Rgs, Regulator of G-protein signaling; SDF, Stromal-derived factor; SFRP, Secreted frizzled related protein; TGF, Transforming growth factor; TIMP, Tissue inhibitor of metalloproteinase; TNF, Tumor necrosis factor; TSG, Tumor necrosis factor-inducible gene; UCB, Umbilical cord blood; UV, Umbilical vein; VEGF, Vascular endothelial growth factor; WJ, Wharton's jelly; αSMA, Alpha smooth muscle actin

Background

From a research, medical, and business standpoint, mesenchymal stem cell (MSC)-based therapies are fascinating. Sales for stem cell products (e.g., as a subset of osteobiologics) were projected to top $600,000,000 by 2015 [1, 2], and a recent Scopus search for musculoskeletal and stem cells resulted in over 3000 documents, with more than a third being reviews. We have limited this review to highlighting noteworthy findings and concepts concerned with the understanding of and challenges with MSC musculoskeletal therapies.

MSCs were discovered in the 1960s [3], named in the early 1990s [4], and purportedly defined by the mid-2000s [5]. Despite the proposed criteria, the functional definition within the literature varies widely. MSCs can be defined by their ability to adhere to tissue culture plastic, their expression of several cell surface molecular epitopes—cluster of differentiation CD73, CD90, and CD105, and others—as well as their lack of several surface markers, including CD45 [6]. Some previously excluded markers are debated within certain circles, such as CD34 and CD146 [7–9]. MSCs can be isolated from a range of tissues, but the most commonly cited sources are bone marrow (BM), adipose tissue, muscle, bone, and perinatal tissues (e.g., Wharton's Jelly, umbilical vein/cord blood (UV/UCB), and amnion).

While they were originally utilized clinically in hopes of harnessing their differentiation and proliferation potential, MSCs are increasingly thought to also influence, in addition to participating in, tissue function [10, 11], especially within osteochondral spaces [12]. These MSC influences can range from relatively rare activities that require cell contact, such as mitochondrial transfer and cell fusion, to relatively common paracrine MSC actions through extracellular microvesicles or secreted factors. MSCs may modulate the immune response, angiogenesis, apoptosis, oxidation level, migration, and/or differentiation/stimulation of surrounding cells [13]. Because of this alternative use of MSCs, Caplan and Sorell [14] suggested a renaming of MSCs to medicinal signaling cells to suggest a new era of MSC clinical relevance due to their immunomodulatory properties. While acknowledging progress in the other areas mentioned, this work will focus on the current debates concerning sourcing, MSC alterations of angiogenesis, cell differentiation/stimulation, and strategies to improve MSC differentiation.

Sourcing

Sourcing of MSCs has become an area of debate due to well-recognized potential differences in differentiation abilities and trophic activities of the derived MSCs. Alternatively sourced MSCs may have different differentiation potentials as BM-MSCs, and they may require additional supplementation to achieve robust or similar differentiation. However, while relative abundance and ease of isolation of MSCs may allow their use for successful musculoskeletal interventions [15], there are concerns that diminished numbers of MSCs may be present in BM as patients age or succumb to disease [16]. One study found that mouse MSCs from four common sources (BM, adipose tissue, skeletal muscle, and myocardium) equally supported endothelial cell (EC) network formation in vitro and blood vessel formation in vivo [17]. Muscle-derived stem cells (MDSCs) and satellite cells are thought to contribute to repair of skeletal muscle and bone [18–20]. Although the exact mechanisms remain to be elucidated, cartilage and muscle health has been provocatively linked with changes in or lack of multipotent cell activity, including diseases such as osteoarthritis (OA, cartilage), sarcopenia (muscle), and related muscle and motor neuron diseases [21].

In one study attempting to address the most useful source of MSCs for angiogenesis through a hindlimb ischemia model, Bortolotti et al. examined adipose-derived MSCs (AD-MSCs) and BM-MSCs (along with a subpopulation of CD11-depleted BM-MSCs). They found, as have many others, that MSCs were not incorporated into the

healing wound but that wounds, particularly those in muscles, healed more rapidly when exposed to BM-MSCs (regardless of MSC sorting) [22]. Classic proangiogenic, chemotactic, and remodeling molecules were identified as being expressed by MSCs, with several factors appearing prominently in the also effective conditioned medium (CM) (platelet-derived growth factor-B (PDGFB), transforming growth factor beta (TGF-β), stromal-derived factor-1 (SDF1), angiopoietin-1 (Ang1), regulator of G-protein signaling-5 (Rgs5), matrix metalloproteinase-9 (MMP-9), chemokine (C-X-C) ligand-10 (CXCL10), chemokine (C-C) ligand (CCL5)) [22].

Work with 5–6-week-old human embryonic BM-MSCs and MDSCs suggests that MSCs have innate propensities for adipogenic and myogenic differentiation, respectively, which ultimately affects the organization of the engineered tissues [16, 23]. MSCs sourced from older tissue might overcome these propensities depending on the implantation culture environment [24]. Taking a cue from the successful use of stem cells from birth-associated tissues [25], one group recently investigated the angiogenic activity of endometrium/menstrual blood-sourced multipotent cells, showing that they support the recruitment of ECs, blood vessels, and, potentially, the proliferation of hematopoietic stem cells [26].

An encouraging finding is that the number of MSCs required to exert trophic action may be far less than originally calculated as necessary for tissue replacement, because a prospective study of BM-MSC vs mixed BM-MSC + lipoaspirate therapy for OA found no difference in patient-reported outcomes between the two groups [27]. Interestingly, increasing body mass index (BMI) appeared to correlate with patient-reported improvement of function, a link that should be explored in the future [28].

MSC musculoskeletal clinical use

Evidence for an altered view of MSC efficacy follows results from clinical trials, several of which have recently begun to yield data about long-term MSC efficacy in disease treatment. A large area of MSC-based musculoskeletal research has been directed towards the degenerative joint disease OA, which currently affects approximately 20 million Americans and is projected to affect 20 % of American adults by 2030 [29]. OA is characterized by the degeneration of articular cartilage and synovial inflammation, which alters associated soft tissue and subchondral bone, resulting in bony lesion and osteophyte formation. These degenerative events cause pain and loss of joint mobility and function. Because cartilage has a lower regenerative capacity than other, more vascularized tissues in the body, arthritis and joint degeneration are growing targets of MSC-based therapies.

Recent investigations into MSC treatment of OA have begun to include formal, controlled clinical trials [30] in addition to many uncontrolled trials by private entities. Several international companies, including Cartistem, Regenexx, Regeneus, BioHeart, and Mesoblast, are carrying out phase I and II clinical trials for the treatment of degenerative joint diseases with allogeneic or autologous, multipotent cell types that are capable of mesenchymal differentiation, usually derived from BM or adipose origin [15, 31, 32]. Several other companies have chosen to facilitate MSC isolation within the clinic by constructing machines that quickly sort stem cells from the mixed populations present in surgically isolated tissue [33]. Although published data have been relatively scarce for completed trials, adverse events such as tumors, infections, or premature trial closures have rarely been reported, suggesting safety of MSC-based therapies [34, 35]. The majority of reviewed studies utilize either dissociated cells injected into the joint space or cells delivered via seeding in various biocompatible and/or biodegradable materials.

A recent review details results of nine OA articular cartilage (knee) clinical trials which utilized cultured BM-MSCs, noncultured BM concentrate, peripheral blood-derived stem cells, or cells from the adipose stromal vascular fraction [36]. Some cells were immobilized with hyaluronan, collagen, platelet gel, and/or fibrin glue. Others were injected into the joint or at a defect using only saline. Regardless of cell origin, intra-articular injection of cells (vs hydrogel or flap immobilization through open surgery) resulted in improved clinical function over untreated controls in some studies as long as 5 years post treatment [36]. Pain relief with minor return of function was noted in most studies.

Noting the ameliorative effect of MSCs on joint pain, chronic lower back pain has recently become a target of MSC therapy. Autologous, scaffold-less BM-MSC injection into patients with spinal cord injury in a Brazilian clinical trial suggested clinically meaningful pain relief and possible improvement in cartilage structure after 6 months and as long as 2 years post treatment, although the high number of MSCs utilized coupled with the high cost of the procedure were identified as potential areas for improvement [37]. In a Spanish study, 7 of 12 patients showed mild return of function after 6 months when enrolled in a phase I safety and efficacy study for BM-MSC injection for long-term (>6 months) spinal cord injury [38]; although positive in terms of apparent MSC effect, the study faced almost immediate criticism from other researchers due to the small sample size and lack of appropriate controls [39]. A study by Mesoblast reported decreased lower back pain in 48 % of allogeneic BM-MSC-treated patients vs 13 % in placebo controls up to 2 years post injection [40].

A portion of these analgesic effects could be due to the anti-inflammatory activity of MSCs. Evidence that a decrease in granulocyte macrophage colony-stimulating factor (GM-CSF) resulted from MSC treatment and may decrease disease severity after 4 months comes from a rheumatoid arthritis (RA) clinical trial that used MOR103 antibodies to deplete serum GM-CSF [41]. In an excellent and very recent review of MSC applications to RA, De Bari described how immunomodulation could play a role in RA-specific joint degeneration. Immunoregulators, including interferon gamma (IFN-γ) and tumor necrosis factor alpha (TNF-α), which are regulated through indoleamine 2,3-dioxygenase (IDO) or nitric oxide (NO), and MSC effects on forkhead box $p3^+$ ($Foxp3^+$) Tregs or $CD4^+$ Th17 cells have been suggested [42]. Interestingly, the "transformation hypothesis" proposes that MSCs may become transformed by interplay with chronic inflammatory processes in the joint, resulting in a more aggressive cell type with abilities to either invade the articular cartilage and/or circulate, spreading arthritis to unaffected joints [43, 44]. UV-MSCs may help to relieve the severity of RA symptoms when combined with disease-modifying anti-rheumatic treatments [45].

Recent exploration of immunomodulation showed that AD-MSC surface-bound glycoprotein A repetitions predomain/leucine-rich repeat containing-32 (GARP/LRRC32), found on $CD4^+$/$Foxp3^+$ Tregs, megakaryocytes, and platelets, binds to membrane-bound TGF-β1, holding it in an inactivated but readily-accessible state. GARP silencing results in increased secretion and activation of TGF-β1 and impaired proliferation of AD-MSC as well as activation of T cells [46]. Immunosuppressive effects of membrane-bound TGF-β1, especially when bound to extracellular vesicles (EVs), have also been reported for other MSC types [47–49].

Mechanisms of MSC trophic activity

Insight into the mechanisms of MSC trophic activity is advancing across multiple fields (Table 1). Within the joint space, the MSC secretome is thought to influence the anabolic tendencies of chondrocytes, chondrocyte progenitor cells (CPCs), cartilage-derived stem/progenitor cells (CSPCs), synovium-resident multipotent progenitor cells, osteoblasts/osteoclasts/resident MSCs within the subchondral bone (especially after microfracture), and chondrogenic cells within the infrapatellar fat pad [36, 50, 51]. The MSC secretome can be modified through permanent or temporary alterations. Several studies have found that the exposure of MSCs to proinflammatory factors, sometimes for as little as a few hours, can alter the gene and protein expression of MSCs for days afterwards [52]. Factors known to be secreted or bound to MSC membranes with anti-inflammatory activities (activation of Tregs/tolerogenic dendritic cell phenotype; pro-resolving/M2 macrophage activation; inhibition or proapoptosis of T cells, B cells, NK cells, or dendritic cells; decreasing cytokine production) include: purines, bone morphogenetic proteins (BMPs, specifically BMP-4), CD274, CCL2, Connexin 43, cyclooxygenase (COX)/prostaglandin (PG), CD95/CD95 ligand, galectins, heme oxygenase-1, human leukocyte antigen-G (HLA-G), IDO/kynurenine, interleukin-6 (IL-6), leukemia inhibitory factor (LIF), NO, TGF-β, tumor necrosis factor-inducible gene-6 (TSG6), and vascular endothelial growth factor (VEGF) [53].

In addition to some of the classic chemotactic growth factors and molecules already mentioned (HGF, PDGF, and bFGF), MSCs are strongly influenced by the binding of CXCL12 (SDF1) to CXCR4 [54]. Embryonic muscle growth and adult muscle repair are thought to be heavily influenced by MMP-10-regulated CXCL12 stimulation of MSC migration [55, 56]. Additionally, MSCs express a variety of receptors, including various integrins and selectins, that allow extravasation at repair sites [57].

Clues to the mechanisms of MSC trophic activities (Fig. 1) can also be found in the extensive work done in other fields, particularly exploration of the stem cell secretome in the cardiac field [58]. Identified factors include adrenomedullin, angiogenin, fibroblast growth factor-2 (FGF2), CXCL12, cistatin C, cysteine-rich angiogenic inducer 61 (Cyr61), Dickkopf-related proteins (Dkk), hepatocyte growth factor (HGF), insulin-like growth factor (IGF), IL-1, IL-6, pigmented epithelium-derived factor (PEDF), placental growth factor (PLGF), SDF1, TSG6, VEGF, MMP-2, tissue inhibitor of metalloproteinase-1 (TIMP-1), TIMP-2, secreted frizzled related protein-2 (SFRP-2), thrombospondin-1, and tenascin C [58]. Belying their osseous origin, CM of BM-MSC appears enriched in molecules typically secreted by or influencing osteoblasts, including decorin, osteoprotegerin, Dkk-3, receptor activator of nuclear factor-kB (RANK), osteopontin, and CCL5; inflammatory factors maximally produced by BM-MSCs include CCL2, TIMP-2, IL-6, IL-7, IL-3, MMP-7, chemokine (C-X-C) receptor-16 (CXCR16), and MMP-10. CCL2 and CCL7 produced by BM-MSCs appear to strongly influence nascent bone formation [59, 60]. Recent work also suggests that AD-MSC, BM-MSC, and dental pulp stem cell-secreted CXCL14 and CCL2 help to recruit $CXCR4^+$ cells and chemokine (C-C) receptor-2^+ ($CCR2^+$) vessel-associated cells, without inducing proliferation [61]. Besides these influential but potentially short-lived proteins, some MSCs secrete EVs which may contain any number of influential molecules, protected from systemic degradation by virtue of their natural, membrane-bound packaging [62–65].

In many cell types, EVs of varying sizes, including ectosomes/exosomes and microvesicles/microparticles, were derived from either cytoplasmic protrusions or

Table 1 MSC trophic activities relevant to musculoskeletal therapy: mechanistic insights from in-vitro and host tissue studies

System and reference	In vitro/ host	Cell sources	Observed trophic activity	Mechanistic insights
Angiogenesis [84]	IV	Human BM-MSCs; UCB-ECs	MSCs encouraged EC migration, proliferation, and tubule formation	GHK (osteonectin peptide) induces MSC-VEGF secretion
Angiogenesis [81]	IV	Human BM-MSCs (commercial); microvascular ECs	MSC culture on stiff, fibronectin-coated surfaces encouraged EC spreading/tubule formation	Actomyosin contractility increased MSC expression of proangiogenic factors (angiogenin, VEGF, and IGF)
Angiogenesis [105]	IV	Human BM-MSCs (commercial); UV-ECs	EC-MSC coculture increased MSC-myogenic and EC-PLAU, EC-FGF, and EC-NF-kB-regulated gene expression	• MSC IL-1β and IL-6 regulate EC NF-kB target genes, including P-selectin, CCL23, and CXCL2/3 • EC TGF-β1/3 may regulate MSC myogenic differentiation
Angiogenesis [107]	IV/mouse	Human BM-MSCs (commercial); UV-ECs	• IV: EC-MSC (vs EC) cultures on degradable scaffolds expressed higher perivascular markers • Host angiogenic and perivascular markers, except vessel diameter and density, were equivalent between EC/MSC-EC implants	IV: cocultures upregulated VEGF and ANG1 while downregulating ANG2
Angiogenesis [73]	IV/mouse	Human iMSCs (medium change of iPSCs); UV-ECs	• iMSC exosomes promoted EC migration, proliferation, and dose-dependent tubule formation (IV) • Exosome treatment correlated with modest functional improvement, better perfusion and tissue damage scores, increased CD31/CD34^{+} cells	iMSCs induced EC expression of proangiogenic molecules, including VEGF, TGF-β1, and ANG1
Angiogenesis (hindlimb ischemia) [22]	Mouse	Mouse AD-MSCs (plastic adherence); BM-MSCs (plastic adherence); BM-iMSCs (immunodepletion)	• BM-MSCs maximally decreased inflammatory cell invasion • MSCs were associated with smaller lesions, more mature neovascularization, and increased perfusion	IV: BM-MSCs expressed the highest levels of tested chemokines, vessel stabilizing, and matrix-remodeling factors
Neurovascular system (fibrin conduit, resection) [116]	Rat	Human AD-MSCs (plastic adherence); DRG; UV-EC	• Medium cocktail-stimulated MSCs enhanced DRG neurite extension and EC-tubule formation • Stimulated and unstimulated MSCs encouraged neurite extension	Stimulated MSCs produced increased VEGF, ANG1, NGF, BDNF, and GDNF
Neurogenesis [167]	IV	Rat BM-MSCs (plastic adherence)	Spinal cord tissue–MSC coculture supported neurite outgrowth	Cocultured MSCs produced NGF, BDNF, and GDNF, maximally supporting neurite extension
Neurogenesis (spinal nerve ligation) [123]	Rat	Rat BM-MSCs (commercial)	MSC-treated rats displayed decreased hyperalgesia and increased pain threshold	TUBB3^{-}, GFAP^{-}, and αSMA^{-} and STRO1^{+} MSCs engrafted into DRGs
Neurogenesis (sciatic crush) [124]	Mouse	Human AD-MSCs and AM-MSCs (commercial)	• AM-MSC-treated groups exhibited higher recovery, coordination, and perfusion scores (4 weeks) • MSCs localized in the epineurium and perivascular area	Nerves injected with AM-MSCs versus AD-MSCs or PBS produced more ANG1, FGF1, IGF1, and VEGFA
Distraction Osteogenesis (DO) [59]	Mouse	Human BM-MSCs (commercial)	• MSC and MSC-CM accelerated DO healing • MSC-CM recruited more vessels	• IV: IL-3/IL-6/CCL5/SDF1 recruited mononuclear cells, contributed to enhanced mineralization • MCP1/MCP3 but not SDF1 were critical for SC-CM osteogenic activity
Osteogenesis [168]	Mouse	Human AD-MSCs and BM-MSCs; UCB-ECs	• MSC-EC cotransplantation increased MSC engraftment • Cotransplantation restricted MSC multipotency, enhanced MSC source-related differentiation abilities, and maintained MSC proliferation capacity	PDGFBB/PDGFRβ receptor activity regulates MSC engraftment and differentiation in the presence of ECs

Table 1 MSC trophic activities relevant to musculoskeletal therapy: mechanistic insights from in-vitro and host tissue studies *(Continued)*

Osteoporosis (lupus associated) [60]	Mouse	Human BM-MSCs and DP-MSCs	• MSC injections improved osteoporosis-related bone scores • MSCs lowered osteoclast differentiation (IV)	IL-17 removal following MSC injection maintains osteoclast immaturity
Osteogenesis [169]	Rat	Rat BM-MSCs (centrifugation and plastic adherence)	Fibrin-loaded MSC recruited host macrophages to fill long bone defect by 4 weeks	Implanted MSCs increased early expression of VEGF and decreased later expression of CD45, IL-6, IL-1β, TNF-α, and IL-10
Osteogenesis, chondrogenesis, angiogenesis [170]	IV	Human BM-MSCs (density gradient) and human embryonic stem cell MSCs (medium/substrate changes); human aortic ECs	MSC-EC cocultures proliferated and exhibited higher expression of mesenchymal differentiation transcription factors	EC-produced ET1 activates MSC AKT, driving osteogenic and chondrogenic capacities
Chondrogenesis [95]	IV	Human BM-MSCs (density gradient)	• MSCs and/or chondrocytes in fibrin gels exhibited superior mechanical properties to those cultured with OA cartilage explants • COLI/II/III production reduced in OA cartilage–MSC or chondrocyte–MSC cocultures	IL-1β and IL-6 decreased COL production versus control cultures, except in chondrogenic cultures at longer culture times (4 weeks)
Chondrogenesis [93]	IV	Human BM-MSCs; Human OA primary chondrocytes; bovine primary chondrocytes	FGF1 caused chondrocyte proliferation	• FGF1 was concentrated in places where MSCs contacted chondrocytes
Tenogenesis (enzymatic lesion) [152]	Horse	Horse AD-MSCs	Lesions were smaller, more vascularized, and less cellular when treated with platelet concentrate-injected MSCs	• Greater amount of RNA was recovered from the MSC-treated group • No difference in anabolic and tendon-specific gene expression observed
Musculogenesis (dystrophin/utrophin) [135]	IV	Mouse quickly and slowly adhering MSCs (non-myogenic nmMSCs and MPCs), dKO)	• dKO-MPC-dKO-nmMSC co-culture decreased global myogenic markers • dKO vs. WT-nmMSCs differentiated more efficiently along osteogenic and adipogenic lines with donor age	Soluble frizzled-related protein-1 and active β-catenin encouraged nonmyogenic differentiation of dKO-nmMSCs in gastrocnemius tissues
Musculogenesis (myofibroblast proliferation) [138]	IV	Human AD-MSCs and BM-MSCs (commercial); Dupuytren's disease-derived myofibroblast (DDMF)	• AD-MSCs (similar to normal skin-derived fibroblasts) decreased while BM-MSCs increased DDMF co-culture contractility • AD-/BM-MSCs inhibited myofibroblast proliferation • AD-MSC effects were strongest with direct or indirect contact	AD-MSC/myofibroblast cocultures exhibited decreased COLI and αSMA
Musculogenesis (dystrophin) [160]	Mouse	Human (STRO1^{+}) DP-MSCs; human (c-Kit^{+}) amniotic fluid MSCs	• MSCs differentiated in the presence of C2C12-formed myotubes (IV) • MSCs differentiated most efficiently with C2C12-CM • All differentiated MSCs engrafted and improved muscle histology	Demethylation was critical for IV myogenic differentiation
Musculogenesis [137]	IV	Mouse BM-MSCs (centrifugation and plastic adherence)	MSC-CM stimulated myoblast and satellite cell proliferation and migration, activated satellite cells, inhibited myofibroblast differentiation	MSC MMP-2/9 and TIMP-1/2 support myogenic differentiation

AD, adipose-derived, *AM* amniotic membrane, *BM*, bone marrow, *CM* conditioned medium, *dKO* double knockout, *DP* dental pulp, *DRG* dorsal root ganglia, *EC* endothelial cell, *iMSCs* MSCs generated from induced pluripotent stem cell (*iPSC*) lines via medium change, *IV* in vitro, *MMP* matrix metalloproteinase, *MPC* multipotent cell, *MSC* mesenchymal stem cell, *SC* stem cell, *TIMP* tissue inhibitor of metalloproteinase, *UCB* umbilical cord blood, *UV* umbilical vein

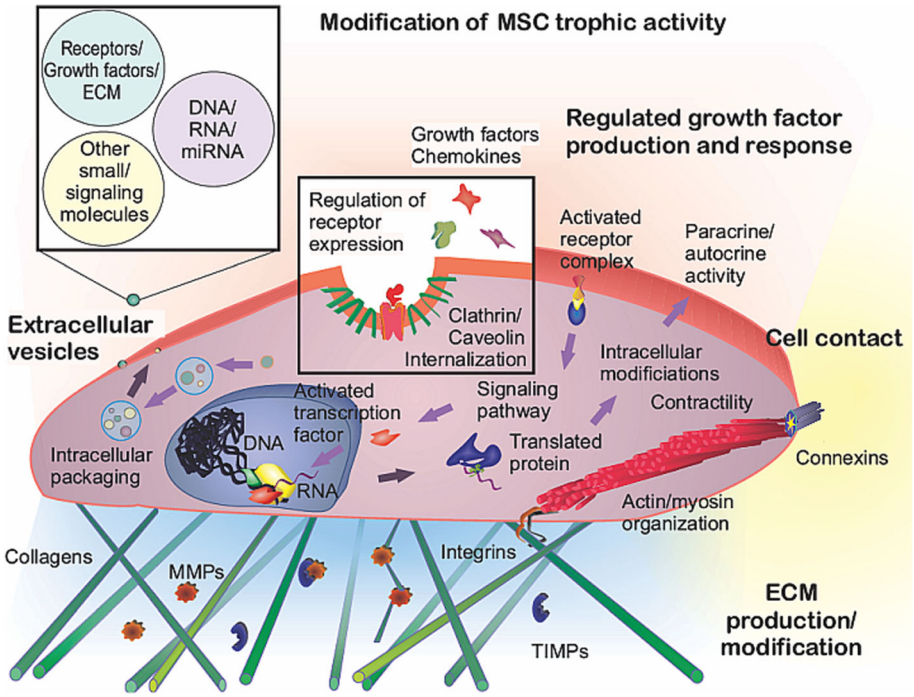

Fig. 1 MSC trophic mechanisms depend on MSC interactions with and modification of the local environment. MSC trophic functions can be both achieved and altered through dynamic ECM–cytoskeletal interactions, cell–cell contacts, and soluble and transcription factor signaling. *ECM* extracellular matrix, *miRNA* microRNA, *MMP* matrix metalloproteinase, *MSC* mesenchymal stem cell, *TIMP* tissue inhibitor of metalloproteinase

lipid raft internalization and subsequent endosomal fusion with the plasma membrane [66–69]. These 30 nm–1 μm vesicles may be studded with multiple proteins, usually tetraspanins, and filled with a combination of proteins, lipids, and copious amounts of mRNA and microRNA (miRNA), particularly miR22 and miR-19a [58]. EC and cancer cell-derived microparticles may potently increase MSC NF-kB activity, stimulating local trophic support [70]. Gap junctions, formed via connexins, are another avenue allowing direct cell–cell communication, with strong evidence for membrane and (to a lesser extent) cytoplasmic exchange between MSCs and ECs [71].

Likely mediated through EC-stimulated VEGF production, CXCR4-enriched exosomes derived from MSCs generated from induced pluripotent stem cell (iPSC) lines via medium change (iMSCs) improved recovery from myocardial infarction [72]. In work addressing hindlimb ischemia in mice, iMSC exosomes were associated with a higher number of $CD31^+$ and $CD34^+$ cells in damaged muscle tissue as well as increased EC secretion of VEGF, TGF-β1, and angiogenin, suggesting enhanced vascular recruitment by vesicles alone [73]. Another group generated iMSCs through TGF-β-pathway inhibition and medium changes; those iMSCs, surprisingly, did less to promote cancer than BM-MSCs, appearing to express and produce lower amounts of several of the inflammatory and differentiation factors (particularly TGF-β receptor-2 and, interestingly, hyaluronan (HA)) when cultured with various types of cancer cells [74].

In a recent study, Baglio et al. [75] characterized the RNA contents of exosomes obtained through ultracentrifugation, and found that exosomes were enriched for tRNA, in particular tRNA CTC. Their work further suggested that the differentiation state of a MSC might be deduced by the content of its exosomes, particularly the presence of full-length tRNA and tRNA long fragments, consistent with a stem-like state of the cells [76]. miRNA loading within vesicles is not random, as dexamethasone treatment of both C2C12 cells and diabetic rats increased the concentration of miR-23a and miR-182 in collected microvesicles and urine, respectively [77], thus providing MSCs with a dynamic way to influence and respond to their microenvironment. Microvesicles may also suppress the infiltration of macrophages into damaged tissues [75]. However, the relevance of vesicles/microvesicles to classical and clinically approved MSCs is questionable, because a different group noted that MSCs produced much fewer vesicles than immortalized ESC-derived MSCs [78]. The group offered an immortalization strategy that would maximize the yield of MSC-produced vesicles, should they prove effective in the clinic.

Altering MSC activity prior to bone or cartilage implantation

Because "plain" MSC implantation has faced such varied success in the clinic, the next generation of MSC-based strategies seeks to harness and direct MSC trophic activities. It was observed that substrate composition and stiffness, sensed through various integrins, could influence the expression of myogenic factors [79]. Substrate stiffness, known to affect the differentiation of MSCs, acting possibly through regulation of alpha-smooth muscle actin (αSMA), could also play a role in the eventual differentiation capacity of culture-expanded MSCs [80]. Substrate stiffness, in turn, affects MSC trophic properties; stiff (40 kPA) polyacrylamide gels coated with fibronectin induced proangiogenic factor secretion by BM-MSCs [81]. Through internalization and recycling of focal adhesions and receptors, caveolins play an intriguing role in MSC sensing of both substrate stiffness and surrounding soluble signals, particularly in vascular, muscular, and osteogenic settings [82]. Alternatively, hydrogels made from autologous plasma may also help to temporarily concentrate either AD-MSCs or AD-MSC-CM at the injury site [83].

The ability of MSCs to self-generate abundant collagenous extracellular matrix (ECM) may partially explain some of the positive effects witnessed in some joint degeneration trials involving MSCs [27]. Medium supplements or additional modifications to the substrate to mimic other ECM molecules or bioactive factors, such as osteonectin, may further increase MSC secretion of bioactive molecules (FGF2, CCL5, and VEGF), supporting native cell migration and differentiation [84].

The milieu present in culture serum appears to strongly influence the fate of cultured cells, more so than any single exogenous supplement [85]. One method to both encourage MSC trophic activity as well as ease immunological concerns in the clinic could be to utilize autologously derived cell culture supplements such as platelet lysate for autologous MSC expansion and culture [86]. Platelet-rich plasma, for example, may protect cartilage from injury by enhancing collagen II (COLII)/aggrecan (AGN) expression and suppressing MMP-3, COX2, iNOS, and associated NO and PGE2 production [87]. Once established in vitro, however, the role of serum becomes less clear; while serum content affects MSC gene expression and growth rate, inherent multipotency and stem cell marker surface expression do not appear to be affected by the absence of serum [88]. For that reason, MSC-CM concentration and injection may sidestep issues of autophagy [89] or apoptosis of MSCs upon in-vitro expansion [13].

Culture under hypoxia is another attractive method to increase initial MSC production of trophic factors. Under hypoxia, hypoxia inducible factor-1 alpha (HIF1α) expression increases, driving VEGF and other proangiogenic, antiapoptotic, and antioxidant molecules [90]. Under certain circumstances, hypoxic MSCs may serve to prevent harmful fibrosis through HGF production, TGF-β1/COLII, and IL-1β downregulation, and fibronectin expression [91]. Work in vitro with chondrocytes has specifically identified HGF as an antifibrotic agent released by AD-MSCs [92]. Furthermore, FGF1 secreted by MSCs in contact with chondrocytes may stimulate the proliferation of and help to preserve the function of chondrocytes [93, 94].

In-vitro evidence suggests that the addition of BM-MSCs to OA cartilage may initially increase IL-1β and IL-8 production but ultimately reduce the amount of soluble glycosaminoglycan (GAG) released by the cartilage over time, making the exact influence of MSCs on cartilage structure unclear [95].

Reported pain relief associated with the introduction of MSCs may be the result of immunomodulation but was by no means universal [36]. In-vitro studies suggest that exposure of MSCs to chondrocytes may induce expression of MSC major histocompatibility complex (MHC) I/II and other costimulatory molecules [96].

Pretreatment of MSCs, especially with IFN-γ to prime their immunosuppressive activity, may result in decreased MSC-associated tissue degradation [97]. Possibly in response to IL-1α, MSCs exposed to platelet lysate have the capacity to encourage a proinflammatory/M1 or proresolving/M2 macrophage phenotype through GM-CSF and PGE2 activity, respectively [53, 98]. Growing evidence suggests that the native, inflamed cartilage environment may both trigger the release and limit the effectiveness of MSC-anti-inflammatory PGE2 [99]. MSCs may recruit $CD4^+$ T cells, which can also play a role in increasing local osteogenic activity [100]. Care must be taken with extensive culture, because MSCs may gain genetic abnormalities and lose some ability to differentiate, promoting senescence [88].

Vascular/inflammation regulation

Several key targets of regenerative medicine therapies, including restored nerve and muscle function and the previously discussed bone repair, rely heavily on the influence of vascular cells [101]. Consequently, MSC effects on blood vessel cells have long fascinated researchers. Recent work has begun to elucidate mechanisms by which MSCs may affect blood vessel morphology and function. Chen et al. [102] reported that MSC-produced HGF, upon interaction with ECs in coculture and, to a lesser extent, via paracrine signaling, caused an increase in EC cadherin and F-actin remodeling, thereby decreasing EC permeability [90, 103, 104]. This and earlier work with ECs suggests that MSC–EC interactions may temporarily restrict both the physical clearance of MSCs and the

invasion of inflammatory cells. Once in the bloodstream, MSC inhibition of NF-kB, perhaps through IL-10 or other factors, may decrease the binding of monocytes to the endothelium, further decreasing inflammation at wound/MSC injection sites [45]. This temporary pause in the battle with chronic inflammation may explain some of the positive results seen with MSCs.

Following a more classical approach focused on EC motility and activity, VEGF, ANG, and NF-kB pathways have all been implicated in regulating angiogenesis. Recent work suggests that, in the short term, the NF-kB pathway may control EC response through BM-MSC-produced IL-6 and IL-1β; following this NF-kB activation, ECs activate P-selectin, producing CCL23, CXCL2, and CXCL3. In turn, MSCs showed signs of early differentiation towards a smooth muscle phenotype in coculture, influenced by TGF-β1 and TGF-β3 [105]. BM-MSC production of VEGF may be stimulated by IL-8, either through paracrine or autocrine mechanisms [106]. In turn, BM-MSCs may stabilize ECs by upregulating ANG1, thereby downregulating EC proliferation [107]. Conversely, the interaction of MSCs with ECs, particularly through endothelin 1 (ET1) and PDGFB, may prime cells to survive transplantation and differentiate more easily upon reimplantation [108].

Neural support

MSCs have long been known to support nerve growth through the support of Schwann cells, secretion of neurovascular factors (including FGF2 and VEGF-A), and, possibly, transdifferentiation into Schwann-like cells. Combined with varying types of biocompatible and bioactive materials, such as poly-lactic acid (PLA), polycaprolactone (PCL), polyurethane (PU), polyethylene (PE), and silicone (for strength) and COLI, HA, and so forth (for bioactivity), several groups have observed enhanced nerve extension and functional improvements in a range of animal models [109, 110]. The most recent work refines previous findings that guidance fibers of particular spacing and architecture may aid MSCs in further accelerating the nerve healing process [111–113]. AD-MSCs, at sufficient density, secrete brain-derived neurotrophic factor (BDNF) in response to autocrine IFN-β [114]. Stimulating cocktails that increase cyclic-adenosine monophosphate (cAMP) and include retinoic acid (pretreatment), FGF2, PDGFAA, and different forms of neuregulin have been shown to increase neurite outgrowth in vitro and nerve extension after injury in vivo [115]. In addition to neurotrophic BDNF, nerve growth factor (NGF), and glial cell line-derived neurotrophic factor (GDNF), as well as angiogenic VEGF and ANG1 identified in many other experiments, recent work identified the antiapoptotic activity of AD-MSCs, possibly by decreasing neuronal c-jun [116]. As mentioned in previous sections, such pretreatment is relatively common in nonclinical work, and may become de rigeur as new progenitor cell sources are explored for musculoskeletal therapies [117]. Crucially, it appears that MSCs should not be directly injected intrathecally for early spinal cord repair, as the subsequent inflammation seemed to prevent MSC migration to neuronal injury sites [118]; later injection may prove beneficial [119].

Ciliary neurotrophic factor (CNTF) is a particularly well known neuroprotective factor produced by MSCs. While the factor has potent therapeutic effects on nerve apoptosis, neuroinflammation, and neuronal proliferation, it has been linked with altered metabolism (due to neurogenesis in the hypothalamus as well as direct action on adipocytes) when administered systemically and may negatively affect osteoblast differentiation and mineralization [120–122]. GDNF, another potent neurotrophic molecule often produced by MSCs, may help to ease allodynia and hyperalgesia experienced in dorsal root ganglia sensory nerves [123]. Amniotic membrane-derived MSCs expressed more ANG1, FGF1, IGF1, and VEGFA (but not FGF2) than AD-MSCs in a mouse sciatic nerve injury trial [124].

While CM from cells treated under hypoxic and normoxic conditions both increased the observed number of differentiating neurons in vitro, hypoxia-cultured Wharton's Jelly (WJ)-derived MSCs upregulated thymosin B and eukaryotic elongation factor (EF2) and may have contributed to a slight increase in total neuron maturity [125]. WJ-MSCs under normoxic conditions were shown to produce PDGFAA, HGF, TGF-β2, IL-6, IL-8, IL-1ra, CCL5, CCL2, and CXCL10 at much larger concentrations than BM-MSCs and AD-MSCs [126]. Whatever the mechanism for neural support, tissue response to neurological directives is critical to the ultimate utility of the repaired nerve.

Muscles and miscellany

Intriguing results suggest that MSCs derived from less traditional sources could one day be utilized therapeutically. One readily available source for MSCs could be skeletal muscles. Our research group has worked extensively with blast-traumatized muscle-derived multipotent cells [127–129]. This particular type of muscle-derived multipotent cells is especially attractive therapeutically due to its relative abundance and ease of isolation [130] as well as neurotrophic activity [131]. MDSCs should be used cautiously when attempting to rebuild musculoskeletal tissues, because several groups have identified populations that seem predisposed to mineralize ectopically [132–134], especially in the presence of muscular genetic abnormalities [135]. Growth factor coinjection might attenuate this ectopic bone formation, as growth hormone–insulin-like growth factor-1 (GH-IGF1) activity

promotes muscle cell proliferation, regulates muscle fiber size and type, controls osteoblast proliferation and differentiation, inhibits osteoclast activity, stimulates renal conversion of 25-OH-vitamin D_3, and controls phosphate reabsorption [136]. By contrast, this matrix-modifying MSC activity may help to attenuate disease severity and ultimately contribute to useful muscle mass [137]. Harmful proliferation and contraction of myofibroblasts, as occurs in Dupuytren's contracture, may be attenuated in the presence of the CM of both AD-MSCs or BM-MSCs as well as the physical presence of AD-MSCs (but not BM-MSCs) [138]. BM-MSCs appear to contribute to pathological myofibroblast proliferation while AD-MSCs appear to inhibit the activity slightly [138]. MMP-2 and MMP-9 are required for efficient skeletal muscle regeneration and are enhanced by mouse BM-MSCs/MSC-CM along with reduced TIMP-1/2 levels. Muscle cell motility may also be encouraged by BM-MSC-secreted MMP-2 [139].

Aside from their ECM-modifying properties, the immunomodulatory properties of MSCs are intriguing from a therapeutic standpoint but must be used carefully, because MSC treatment, concurrent with a *Staphylococcus aureus* infection, was shown to increase the severity of bone loss, despite increased MSC proinflammatory cytokine expression, in an osteomyelitis model [140]. Conversely, encouraging results were recently published from a small idiopathic osteonecrosis trial in Japan, where BM-MSCs were isolated, cultured for 2 weeks, and returned to osteonecrotic patients along with tricalcium phosphate chips (Osferion) and tricortical iliac crest bone [141]; after a 12-week rehabilitation program, all patients reported reduced pain and increased physical function with no serious adverse events reported in the study [142]. The likelihood of MSC engraftment being the cause for the recovery is low, however, as MSCs have been found to migrate towards apoptotic cells, via HGF signaling, but not HGF produced in the presence of necrotic cells [143].

Evidence of MSC trophic efficacy has generated intense excitement in clinically focused research. This excitement is evident in the increasing number of reviews examining MSC trophic properties. Marked therapeutic successes will likely hinge on technological and computational advancements that allow dynamic, high-resolution, and quantitative observation of MSC–ECM, MSC–paracrine, and MSC–cellular interactions to better define the appropriate perspective on the true activity of MSCs.

Conclusions

The application of allogeneic and autologous MSC therapies for the treatment of diseases and dysfunctions of multiple musculoskeletal tissues has received increasing attention. Exciting in-vitro and in-vivo investigations on tendon [117, 144, 145], meniscus [146–148], and ligaments [149, 150] have been reported, along with the use of autologous products such as platelet-rich plasma/plasma lysate [151]. Studies using larger, clinically relevant animal models are both underway and necessary before human clinical trials can be developed [152].

This review has primarily explored secreted trophic factors produced by MSCs. A whole host of therapies are dedicated to engineering or modifying the physical environment and ECM of MSCs to affect their therapeutic potential. A recently developed approach attempts to anchor cells to the collagenous tissue matrix by engineering collagen anchors [153], to promote local action of MSCs and minimize their systemic loss to the lungs, liver, and spleen. Changes in substrate composition (especially the presence of collagen) and stiffness may expand the potential applications of MSC therapies to include muscle volume loss through stimulation of muscle-resident progenitor cells [134, 154, 155]. Local ECM modifications are known to affect MSC differentiation potential [156, 157] and are beyond the scope of this review. Through continuing advancements in genetic engineering, MSCs may eventually be used to treat genetic musculoskeletal conditions, including osteogenesis imperfect [158] and Duchenne's muscular dystrophy [159, 160]. Careful selection of the therapeutic cells, taking into account subtle tissue source-related differences, may be the key to successful clinical dystrophy therapies [35]. To prove their efficacy in the clinic, these potential treatments will need to be tested in well-controlled studies to assess physical functions for an extended period of time [27].

New or more precise modes of MSC trophic activity may be discovered by adopting contemporary analytical technologies to evaluate and compare genomic, transcriptomic, proteomic, metabolomic, and secretomic profiles, exemplified by the great strides that have been made in genetic and metabolic diseases [161–164]. Lessons learned from previous iterations of MSC therapies and clinical drug trials should overcome some of the regulatory and therapeutic hurdles to MSC use [2, 32, 33]. It is also noteworthy that while genetic engineering of iPSCs may hold the answer to unlimited numbers of perfectly-tuned stem cells, managing the safety concerns of iPSCs and negotiating the patent landscape of this saturated market will be highly challenging [165]. Another major challenge is the uncertainty in terms of biological responsiveness of the diseased tissue, because evidence in several fields suggests that ischemic tissue may be incapable of responding to MSCs [166]. Finally, each of these avenues should be explored while juggling the needs for rigorous science, proven therapeutic efficacy, regulatory approval (e.g., by the Food and Drug Agency) (and thus reproducibility) of a final therapy, and cost/benefit for the patient.

Acknowledgements
This work is supported in part by the Commonwealth of Pennsylvania Department of Health (SAP 4100050913), NIH (5U18 TR000532), and US Department of Defense (W81XWH-08-2-0032, W81XWH-14-2-0003). A portion of the predoctoral training of HRH was supported by a Training Grant funded by the National Institute of Biomedical Imaging and Bioengineering, NIH (T32EB0010216). HRH acknowledges the faculty, staff, and students of CCME, where HRH served as a Research Fellow during a portion of the time required to draft and edit this document.

Authors' contributions
HRH created the figure and tables, and researched, drafted, and arranged the document. RST suggested the content, edited the document, and was the invited, corresponding author. Both authors read and approved the final manuscript.

Competing interests
The authors declare that they have no competing interests.

Published online: 09 September 2016

References

1. Wei C, Lin AB, Hung S. Mesenchymal stem cells in regenerative medicine for musculoskeletal diseases: bench, bedside, and industry. Cell Transplant. 2014;23:505–12.
2. Heathman TR, Nienow AW, McCall MJ, Coopman K, Kara B, Hewitt CJ. The translation of cell-based therapies: clinical landscape and manufacturing challenges. Regen Med. 2015;10:49–64.
3. Friedenstein AJ, Piatetzky-Shapiro II, Petrakova KV. Osteogenesis in transplants of bone marrow cells. J Embryol Exp Morphol. 1966;16:381–90.
4. Caplan AI. Mesenchymal stem cells. J Orthop Res. 1991;9:641–50.
5. Dominici M, Le Blanc K, Mueller I, Slaper-Cortenbach I, Marini F, Krause D, et al. Minimal criteria for defining multipotent mesenchymal stromal cells The International Society for Cellular Therapy position statement. Cytotherapy. 2006;8:315–7.
6. Salem HK, Thiemermann C. Mesenchymal stromal cells: current understanding and clinical status. Stem Cells. 2010;28:585–96.
7. Dmitrieva RI, Minullina R, Bilibina AA, Tarasova OV, Anisimov SV, Zaritskey AY. Bone marrow- and subcutaneous adipose tissue-derived mesenchymal stem cells: differences and similarities. Cell Cycle. 2012;11:377–83.
8. Sidney LE, Branch MJ, Dunphy SE, Dua HS, Hopkinson A. Evidence for CD34 as a common marker for diverse progenitors. Stem Cells. 2014;32:1380–9.
9. Lv F-J, Tuan RS, Cheung KMC, Leung VYL. The surface markers and identity of human mesenchymal stem cells. Stem Cells. 2014;32:1408–19.
10. Caplan AI, Correa D. The MSC: an injury drugstore. Cell Stem Cell. 2011;9:11–5.
11. Vonk LA, de Windt TS, Slaper-Cortenbach ICM, Saris DBF. Autologous, allogeneic, induced pluripotent stem cell or a combination stem cell therapy? Where are we headed in cartilage repair and why: a concise review. Stem Cell Res Ther. 2015;6:1–11.
12. Ruetze M, Richter W. Adipose-derived stromal cells for osteoarticular repair: trophic function versus stem cell activity. Expert Rev Mol Med. 2014;16:e9.
13. Liang X, Ding Y, Zhang Y, Tse H, Lian Q. Paracrine mechanisms of mesenchymal stem cell-based therapy: current status and perspectives. Cell Transplant. 2014;23:1045–59.
14. Caplan AI, Sorrell JM. The MSC curtain that stops the immune system. Immunol Lett. 2015;168:136–9.
15. Diederichs S, Shine KM, Tuan RS. The promise and challenges of stem cell-based therapies for skeletal diseases. Bioessays. 2013;35:220–30.
16. Hass R, Kasper C, Böhm S, Jacobs R. Different populations and sources of human mesenchymal stem cells (MSC): a comparison of adult and neonatal tissue-derived MSC. Cell Commun Signal. 2011;9:1–14.
17. Mahdi NS, Rahbarghazi R. Interactions of mesenchymal stem cells with endothelial cells. Stem Cells Dev. 2014;23:319–32.
18. Tamaki T, Okada Y, Uchiyama Y, Tono K, Masuda M, Wada M, et al. Clonal multipotency of skeletal muscle-derived stem cells between mesodermal and ectodermal lineage. Stem Cells. 2007;25:2283–90.
19. Zou J, Yuan C, Wu C, Cao C, Shi Q, Yang H. Isolation and osteogenic differentiation of skeletal muscle-derived stem cells for bone tissue engineering. Mol Med Rep. 2013;9:185–91.
20. Meszaros LB, Usas A, Cooper GM, Huard J. Effect of host sex and sex hormones on muscle-derived stem cell-mediated bone formation and defect healing. Tissue Eng Part A. 2012;18:1751–9.
21. De Ceuninck F, Fradin A, Pastoureau P. Bearing arms against osteoarthritis and sarcopenia: when cartilage and skeletal muscle find common interest in talking together. Drug Discov Today. 2014;19:305–11.
22. Bortolotti F, Ukovich L, Razban V, Martinelli V, Ruozi G, Pelos B, et al. In vivo therapeutic potential of mesenchymal stromal cells depends on the source and the isolation procedure. Stem Cell Reports. 2015;4:332–9.
23. Krylova TA, Musorina AS, Zenin VV, Yakovleva TK, Poljanskaya GG. A comparative analysis of mesenchymal stem-cell lines derived from bone marrow and limb muscle of early human embryos. Cell Tissue Biol. 2014;8:441–53.
24. Baker N, Boyette LB, Tuan RS. Characterization of bone marrow-derived mesenchymal stem cells in aging. Bone. 2015;70:37–47.
25. Verdi J, Tan A, Shoae-Hassani A, Seifalian AM. Endometrial stem cells in regenerative medicine. J Biol Eng. 2014;8:20.
26. Alcayaga-Miranda F, Cuenca J, Luz-Crawford P, Aguila-Díaz C, Fernandez A, Figueroa FE, et al. Characterization of menstrual stem cells: angiogenic effect, migration and hematopoietic stem cell support in comparison with bone marrow mesenchymal stem cells. Stem Cell Res Ther. 2015;6:1–14.
27. Grässel S, Lorenz J. Tissue-engineering strategies to repair chondral and osteochondral tissue in osteoarthritis: use of mesenchymal stem cells. Curr Rheumatol Rep. 2014;16:1–16.
28. Centeno C, Pitts J, Al-Sayegh H, Freeman M. Efficacy of autologous bone marrow concentrate for knee osteoarthritis with and without adipose graft. Biomed Res Int. 2014;2014:370621.
29. Mobasheri A, Kalamegam G, Musumeci G, Batt ME. Chondrocyte and mesenchymal stem cell-based therapies for cartilage repair in osteoarthritis and related orthopaedic conditions. Maturitas. 2014;78:188–98.
30. Baugé C, Boumédiene K. Use of adult stem cells for cartilage tissue engineering: current status and future developments. Stem Cells Int. 2015;2015:438026.
31. Boregowda SV, Phinney DG. Therapeutic applications of mesenchymal stem cells: current outlook. BioDrugs. 2012;26:201–8.
32. Sharma RR, Pollock K, Hubel A, McKenna D. Mesenchymal stem or stromal cells: a review of clinical applications and manufacturing practices. Transfusion. 2014;54:1418–37.
33. Srijaya TC, Ramasamy TS, Kasim NHA. Advancing stem cell therapy from bench to bedside: lessons from drug therapies. J Transl Med. 2014;12:243.
34. Wang R, Rao MS. Application of mesenchymal stem cells in joint diseases. OA Musculoskelet Med. 2013;1:26.
35. Farini A, Sitzia C, Erratico S, Meregalli M, Torrente Y. Clinical applications of mesenchymal stem cells in chronic diseases. Stem Cells Int. 2014;2014:306573.
36. Counsel PD, Bates D, Boyd R, Connell DA. Cell therapy in joint disorders. Sports Health. 2014;7:27–37.
37. Mendonça MV, Larocca T, de Freitas SB, Villarreal C, Silva LF, Matos A, et al. Safety and neurological assessments after autologous transplantation of bone marrow mesenchymal stem cells in subjects with chronic spinal cord injury. Stem Cell Res Ther. 2014;5:126.
38. Orozco L, Soler R, Morera C, Alberca M, Sánchez A, García-Sancho J. Intervertebral disc repair by autologous mesenchymal bone marrow cells: a pilot study. Transplantation. 2011;92:822–8.
39. Kovacs FM, Abraira V, Gérvas J, Arana E, Peul WC, Schoene ML, et al. Overenthusiastic interpretations of a nonetheless promising study. Transplantation. 2012;93:e6–7.
40. Itescu S. Mesoblast—a global leader in cell based medicines. In: 34th Annual J.P. Morgan Healthcare Conference; San Francisco, CA; January 2016.
41. Behrens F, Tak PP, Ostergaard M, Stoilov R, Wiland P, Huizinga TW, et al. MOR103, a human monoclonal antibody to granulocyte-macrophage colony-stimulating factor, in the treatment of patients with moderate rheumatoid arthritis: results of a phase Ib/IIa randomised, double-blind, placebo-controlled, dose-escalation trial. Ann Rheum Dis. 2014;74:1058–64.
42. De Bari C. Are mesenchymal stem cells in rheumatoid arthritis the good or bad guys? Arthritis Res Ther. 2015;17:113.
43. Lefèvre S, Knedla A, Tennie C, Kampmann A, Wunrau C, Dinser R, et al. Synovial fibroblasts spread rheumatoid arthritis to unaffected joints. Nat Med. 2009;15:1414–20.
44. El-Jawhari JJ, El-Sherbiny YM, Jones EA, McGonagle D. Mesenchymal stem cells, autoimmunity and rheumatoid arthritis. QJM. 2014;107:505–14.

45. Letourneau PA, Menge TD, Wataha KA, Wade CE, S Cox C, Holcomb JB, et al. Human bone marrow derived mesenchymal stem cells regulate leukocyte-endothelial interactions and activation of transcription factor NF-kappa B. J Tissue Sci Eng. 2011;Suppl 3:001.
46. Carrillo-Galvez AB, Cobo M, Cuevas-Ocaña S, Gutiérrez-Guerrero A, Sánchez-Gilabert A, Bongarzone P, et al. Mesenchymal stromal cells express GARP/LRRC32 on their surface: effects on their biology and immunomodulatory capacity. Stem Cells. 2015;33:183–95.
47. Maumus M, Jorgensen C, Noël D. Mesenchymal stem cells in regenerative medicine applied to rheumatic diseases: role of secretome and exosomes. Biochimie. 2013;95:2229–34.
48. Mokarizadeh A, Delirezh N, Morshedi A, Mosayebi G, Farshid AA, Mardani K. Microvesicles derived from mesenchymal stem cells: potent organelles for induction of tolerogenic signaling. Immunol Lett. 2012;147:47–54.
49. Ottoboni L, De Feo D, Merlini A, Martino G. Commonalities in immune modulation between mesenchymal stem cells (MSCs) and neural stem/precursor cells (NPCs). Immunol Lett. 2015;168:228–39.
50. Jiang Y, Tuan RS. Origin and function of cartilage stem/progenitor cells in osteoarthritis. Nat Rev Rheumatol. 2014;11:206–12.
51. Uth K, Trifonov D. Stem cell application for osteoarthritis in the knee joint: a minireview. World J Stem Cells. 2014;6:629–36.
52. Czekanska EM, Czekanska EM, Ralphs JR, Alini M, Stoddart MJ. Enhancing inflammatory and chemotactic signals to regulate bone regeneration. Eur Cells Mater. 2014;28:320–34.
53. Ulivi V, Tasso R, Cancedda R, Descalzi F. Mesenchymal stem cell paracrine activity is modulated by platelet lysate: induction of an inflammatory response and secretion of factors maintaining macrophages in a proinflammatory phenotype. Stem Cells Dev. 2014;23:1858–69.
54. Maijenburg MW, van der Schoot CE, Voermans C. Mesenchymal stromal cell migration: possibilities to improve cellular therapy. Stem Cells Dev. 2012;21:19–29.
55. Gomez-Rodriguez V, Orbe J, Martinez-Aguilar E, Rodriguez JA, Fernandez-Alonso L, Serneels J, et al. Functional MMP-10 is required for efficient tissue repair after experimental hind limb ischemia. FASEB J. 2015;29:960–72.
56. Bobadilla M, Sainz N, Abizanda G, Orbe J, Rodriguez JA, Páramo JA, et al. The CXCR4/SDF1 axis improves muscle regeneration through MMP-10 activity. Stem Cells Dev. 2014;23:1417-27.
57. Chamberlain G, Fox J, Ashton B, Middleton J. Concise review: mesenchymal stem cells: their phenotype, differentiation capacity, immunological features, and potential for homing. Stem Cells. 2007;25:2739–49.
58. Gallina C, Turinetto V, Giachino C. A new paradigm in cardiac regeneration: the mesenchymal stem cell secretome. Stem Cells Int. 2015;2015:765846.
59. Ando Y, Matsubara K, Ishikawa J, Fujio M, Shohara R, Hibi H, et al. Stem cell-conditioned medium accelerates distraction osteogenesis through multiple regenerative mechanisms. Bone. 2014;61:82–90.
60. Ma L, Aijima R, Hoshino Y, Yamaza H, Tomoda E, Tanaka Y, et al. Transplantation of mesenchymal stem cells ameliorates secondary osteoporosis through interleukin-17-impaired functions of recipient bone marrow mesenchymal stem cells in MRL/lpr mice. Stem Cell Res Ther. 2015;6:104.
61. Hayashi Y, Murakami M, Kawamura R, Ishizaka R, Fukuta O, Nakashima M. CXCL14 and MCP1 are potent trophic factors associated with cell migration and angiogenesis leading to higher regenerative potential of dental pulp side population cells. Stem Cell Res Ther. 2015;6:111.
62. Koga Y, Yasunaga M, Moriya Y, Akasu T, Fujita S, Yamamoto S, et al. Exosome can prevent RNase from degrading microRNA in feces. J Gastrointest Oncol. 2011;2:215–22.
63. Subra C, Grand D, Laulagnier K, Stella A, Lambeau G, Paillasse M, et al. Exosomes account for vesicle-mediated transcellular transport of activatable phospholipases and prostaglandins. J Lipid Res. 2010;51:2105–20.
64. Borges FT, Reis LA, Schor N. Extracellular vesicles: structure, function, and potential clinical uses in renal diseases. Braz J Med Biol Res. 2013;46:824–30.
65. Katsuda T, Kosaka N, Takeshita F, Ochiya T. The therapeutic potential of mesenchymal stem cell-derived extracellular vesicles. Proteomics. 2013;13:1637–53.
66. Cocucci E, Meldolesi J. Ectosomes and exosomes: shedding the confusion between extracellular vesicles. Trends Cell Biol. 2015;25:364–72.
67. Raposo G, Stoorvogel W. Extracellular vesicles: exosomes, microvesicles, and friends. J Cell Biol. 2013;200:373–83.
68. György B, Szabó TG, Pásztói M, Pál Z, Misják P, Aradi B, et al. Membrane vesicles, current state-of-the-art: emerging role of extracellular vesicles. Cell Mol Life Sci. 2011;68:2667–88.
69. Tan SS, Yin Y, Lee T, Lai RC, Yeo RWY, Zhang B, et al. Therapeutic MSC exosomes are derived from lipid raft microdomains in the plasma membrane. J Extracell Vesicles. 2013;2:22614.
70. Lozito TP, Tuan RS. Endothelial and cancer cells interact with mesenchymal stem cells via both microparticles and secreted factors. J Cell Mol Med. 2014;18:2372–84.
71. Boomsma RA, Geenen DL. Evidence for transfer of membranes from mesenchymal stem cells to HL-1 cardiac cells. Stem Cells Int. 2014;2014:653734.
72. Kang K, Ma R, Cai W, Huang W, Paul C, Liang J, et al. Exosomes secreted from CXCR4 overexpressing mesenchymal stem cells promote cardioprotection via Akt signaling pathway following myocardial infarction. Stem Cells Int. 2015. doi:10.1155/2015/659890.
73. Hu G, Li Q, Niu X, Hu B, Liu J, Zhou S, et al. Exosomes secreted by human-induced pluripotent stem cell-derived mesenchymal stem cells attenuate limb ischemia by promoting angiogenesis in mice. Stem Cell Res Ther. 2015;6:10.
74. Zhao Q, Gregory CA, Lee RH, Reger RL, Qin L, Hai B, et al. MSCs derived from iPSCs with a modified protocol are tumor-tropic but have much less potential to promote tumors than bone marrow MSCs. Proc Natl Acad Sci U S A. 2015;112:530–5.
75. Baglio SR, Rooijers K, Koppers-Lalic D, Verweij FJ, Pérez Lanzón M, Zini N, et al. Human bone marrow- and adipose-mesenchymal stem cells secrete exosomes enriched in distinctive miRNA and tRNA species. Stem Cell Res Ther. 2015. doi:10.1186/s13287-015-0116-z.
76. Hudson M, Woodworth-Hobbs M, Rahnert J, Zheng B, Price S. Glucocorticoids reduce muscle atrophy-related microRNAs via exosomal microRNA packaging (11634). FASEB J. 2014;28 Suppl 1:1163.4.
77. Müller G. Microvesicles/exosomes as potential novel biomarkers of metabolic diseases. Diabetes Metab Syndr Obes. 2012;5:247–82.
78. Chen TS, Arslan F, Yin Y, Tan SS, Lai RC, Choo ABH, et al. Enabling a robust scalable manufacturing process for therapeutic exosomes through oncogenic immortalization of human ESC-derived MSCs. J Transl Med. 2011;9:47.
79. Lv H, Li L, Sun M, Zhang Y, Chen L, Rong Y, et al. Mechanism of regulation of stem cell differentiation by matrix stiffness. Stem Cell Res Ther. 2015;6:103.
80. Talele NP, Fradette J, Davies JE, Kapus A, Hinz B. Expression of α-smooth muscle actin determines the fate of mesenchymal stromal cells. Stem Cell Reports. 2015;4:1016–30.
81. Abdeen AA, Weiss JB, Lee J, Kilian KA. Matrix composition and mechanics direct proangiogenic signaling from mesenchymal stem cells. Tissue Eng Part A. 2014;20:2737–45.
82. Baker N, Tuan RS. The less-often-traveled surface of stem cells: caveolin-1 and caveolae in stem cells, tissue repair and regeneration. Stem Cell Res Ther. 2013;4:90.
83. Linero I, Chaparro O. Paracrine effect of mesenchymal stem cells derived from human adipose tissue in bone regeneration. PLoS One. 2014;9:e107001.
84. Jose S, Hughbanks ML, Binder BYK, Ingavle GC, Leach JK. Enhanced trophic factor secretion by mesenchymal stem/stromal cells with Glycine-Histidine-Lysine (GHK)-modified alginate hydrogels. Acta Biomater. 2014;10:1955–64.
85. Tratwal J, Mathiasen AB, Juhl M, Brorsen SK, Kastrup J, Ekblond A. Influence of vascular endothelial growth factor stimulation and serum deprivation on gene activation patterns of human adipose tissue-derived stromal cells. Stem Cell Res Ther. 2015;6:62.
86. Li C, Wu X, Tong J, Yang X, Zhao J, Zheng Q, et al. Comparative analysis of human mesenchymal stem cells from bone marrow and adipose tissue under xeno-free conditions for cell therapy. Stem Cell Res Ther. 2015;6:55.
87. Xie X, Ulici V, Alexander PG, Jiang Y, Zhang C, Tuan RS. Platelet-rich plasma inhibits mechanically induced injury in chondrocytes. Arthrosc J Arthrosc Relat Surg. 2015;31:1142–50.
88. Bellayr IH, Catalano JG, Lababidi S, Yang AX, Lo Surdo JL, Bauer SR, et al. Gene markers of cellular aging in human multipotent stromal cells in culture. Stem Cell Res Ther. 2014;5:59.
89. Nuschke A, Rodrigues M, Stolz DB, Chu CT, Griffith L, Wells A. Human mesenchymal stem cells/multipotent stromal cells consume accumulated autophagosomes early in differentiation. Stem Cell Res Ther. 2014;5:140.

90. Liew A, O'Brien T. Therapeutic potential for mesenchymal stem cell transplantation in critical limb ischemia. Stem Cell Res Ther. 2012;3:28.
91. Lan YW, Choo KB, Chen CM, Hung TH, Chen YB, Hsieh CH, et al. Hypoxia-preconditioned mesenchymal stem cells attenuate bleomycin-induced pulmonary fibrosis. Stem Cell Res Ther. 2015;6:97.
92. Maumus M, Manferdini C, Toupet K, Peyrafitte JA, Ferreira R, Facchini A, et al. Adipose mesenchymal stem cells protect chondrocytes from degeneration associated with osteoarthritis. Stem Cell Res. 2013;11:834–44.
93. Wu L, Leijten J, van Blitterswijk CA, Karperien M. Fibroblast growth factor-1 is a mesenchymal stromal cell-secreted factor stimulating proliferation of osteoarthritic chondrocytes in co-culture. Stem Cells Dev. 2013;22:2356–67.
94. Song X, Xie Y, Liu Y, Shao M, Wang W. Beneficial effects of coculturing synovial derived mesenchymal stem cells with meniscus fibrochondrocytes are mediated by fibroblast growth factor 1: increased proliferation and collagen synthesis. Stem Cells Int. 2015;2015:926325.
95. Leyh M, Seitz A, Dürselen L, Springorum HR, Angele P, Ignatius A, et al. Osteoarthritic cartilage explants affect extracellular matrix production and composition in cocultured bone marrow-derived mesenchymal stem cells and articular chondrocytes. Stem Cell Res Ther. 2014;5:77.
96. Lohan P, Coleman CM, Murphy JM, Griffin MD, Ritter T, Ryan AE. Changes in immunological profile of allogeneic mesenchymal stem cells after differentiation: should we be concerned? Stem Cell Res Ther. 2014;5:99.
97. Crop MJ, Baan CC, Korevaar SS, IJzermans JNM, Pescatori M, Stubbs AP, et al. Inflammatory conditions affect gene expression and function of human adipose tissue-derived mesenchymal stem cells. Clin Exp Immunol. 2010;162(I):474–86.
98. Waterman RS, Tomchuck SL, Henkle SL, Betancourt AM. A new mesenchymal stem cell (MSC) paradigm: polarization into a pro-inflammatory MSC1 or an immunosuppressive MSC2 phenotype. PLoS One. 2010;5:e10088.
99. Manferdini C, Maumus M, Gabusi E, Piacentini A, Filardo G, Peyrafitte JA, et al. Adipose-derived mesenchymal stem cells exert antiinflammatory effects on chondrocytes and synoviocytes from osteoarthritis patients through prostaglandin E2. Arthritis Rheum. 2013;65:1271–81.
100. Grassi F, Cattini L, Gambari L, Manferdini C, Piacentini A, Gabusi E, et al. T cell subsets differently regulate osteogenic differentiation of human mesenchymal stromal cells in vitro. J Tissue Eng Regen Med. 2016;10:305–14.
101. Faroni A, Mobasseri SA, Kingham PJ, Reid AJ. Peripheral nerve regeneration: experimental strategies and future perspectives. Adv Drug Deliv Rev. 2014. doi:10.1016/j.addr.2014.11.010.
102. Chen QH, Liu AR, Qiu HB, Yang Y. Interaction between mesenchymal stem cells and endothelial cells restores endothelial permeability via paracrine hepatocyte growth factor in vitro. Stem Cell Res Ther. 2015;6:44.
103. Bronckaers A, Hilkens P, Martens W, Gervois P, Ratajczak J, Struys T, et al. Mesenchymal stem/stromal cells as a pharmacological and therapeutic approach to accelerate angiogenesis. Pharmacol Ther. 2014;143:181–96.
104. Pati S, Khakoo AY, Zhao J, Jimenez F, Gerber MH, Harting M, et al. Human mesenchymal stem cells inhibit vascular permeability by modulating vascular endothelial cadherin/β-catenin signaling. Stem Cells Dev. 2011;20:89–101.
105. Li J, Ma Y, Teng R, Guan Q, Lang J, Fang J, et al. Transcriptional profiling reveals crosstalk between mesenchymal stem cells and endothelial cells promoting prevascularization by reciprocal mechanisms. Stem Cells Dev. 2015;24:610–23.
106. Hou Y, Ryu CH, Jun JA, Kim SM, Jeong CH, Jeun SS. IL-8 enhances the angiogenic potential of human bone marrow mesenchymal stem cells by increasing vascular endothelial growth factor. Cell Biol Int. 2014;38:1050–9.
107. Pedersen TO, Blois AL, Xue Y, Xing Z, Sun Y, Finne-Wistrand A, et al. Mesenchymal stem cells induce endothelial cell quiescence and promote capillary formation. Stem Cell Res Ther. 2014;5:23.
108. Lin RZ, Moreno-Luna R, Zhou B, Pu WT, Melero-Martin JM. Equal modulation of endothelial cell function by four distinct tissue-specific mesenchymal stem cells. Angiogenesis. 2012;15:443–55.
109. Kehoe S, Zhang XF, Boyd D. FDA approved guidance conduits and wraps for peripheral nerve injury: a review of materials and efficacy. Injury. 2012;43:553–72.
110. Tamaki T. Bridging long gap peripheral nerve injury using skeletal muscle-derived multipotent stem cells. Neural Regen Res. 2014;9:1333–6.
111. Oliveira JT, Bittencourt-Navarrete RE, de Almeida FM, Tonda-Turo C, Martinez AMB, Franca JG. Enhancement of median nerve regeneration by mesenchymal stem cells engraftment in an absorbable conduit: improvement of peripheral nerve morphology with enlargement of somatosensory cortical representation. Front Neuroanat. 2014;8:111.
112. Frattini F, Pereira Lopes FR, Almeida FM, Rodrigues RF, Boldrini LC, Tomaz MA, et al. Mesenchymal stem cells in a polycaprolactone conduit promote sciatic nerve regeneration and sensory neuron survival after nerve injury. Tissue Eng Part A. 2012;18:2030–9.
113. Carrier-Ruiz A, Evaristo-Mendonça F, Mendez-Otero R, Ribeiro-Resende V. Biological behavior of mesenchymal stem cells on poly-epsilon-caprolactone filaments and a strategy for tissue engineering of segments of the peripheral nerves. Stem Cell Res Ther. 2015;6:128.
114. Ryu H, Oh JE, Rhee KJ, Baik SK, Kim J, Kang SJ, et al. Adipose tissue-derived mesenchymal stem cells cultured at high density express IFN-β and suppress the growth of MCF-7 human breast cancer cells. Cancer Lett. 2015;37:213–21.
115. Maltman DJ, Hardy SA, Przyborski SA. Role of mesenchymal stem cells in neurogenesis and nervous system repair. Neurochem Int. 2011;59:347–56.
116. Kingham PJ, Kolar MK, Novikova LN, Novikov LN, Wiberg M. Stimulating the neurotrophic and angiogenic properties of human adipose-derived stem cells enhances nerve repair. Stem Cells Dev. 2014;23:741–54.
117. Bashir J, Sherman A, Lee H, Kaplan L, Hare JM. Mesenchymal stem cell therapies in the treatment of musculoskeletal diseases. PM R. 2014;6:61–9.
118. Schäfer S, Berger JV, Deumens R, Goursaud S, Hanisch UK, Hermans E. Influence of intrathecal delivery of bone marrow-derived mesenchymal stem cells on spinal inflammation and pain hypersensitivity in a rat model of peripheral nerve injury. J Neuroinflammation. 2014;11:157.
119. Jones J, Estirado A, Redondo C, Pacheco-Torres J, Sirerol-Piquer MS, Garcia-Verdugo JM, et al. Mesenchymal stem cells improve motor functions and decrease neurodegeneration in ataxic mice. Mol Ther. 2014;23:130–8.
120. Fargali S, Sadahiro M, Jiang C, Frick AL, Indall T, Cogliani V, et al. Role of neurotrophins in the development and function of neural circuits that regulate energy homeostasis. J Mol Neurosci. 2012;48:654–9.
121. McGregor NE, Poulton IJ, Walker EC, Pompolo S, Quinn JMW, Martin TJ, et al. Ciliary neurotrophic factor inhibits bone formation and plays a sex-specific role in bone growth and remodeling. Calcif Tissue Int. 2010;86:261–70.
122. Pasquin S, Sharma M, Gauchat JF. Ciliary neurotrophic factor (CNTF): new facets of an old molecule for treating neurodegenerative and metabolic syndrome pathologies. Cytokine Growth Factor Rev. 2015. doi:10.1016/j.cytogfr.2015.07.007.
123. Yu H, Fischer G, Ebert AD, Wu HE, Bai X, Hogan QH. Analgesia for neuropathic pain by dorsal root ganglion transplantation of genetically engineered mesenchymal stem cells: initial results. Mol Pain. 2015;11:1–13.
124. Li Y, Guo L, Ahn HS, Kim MH, Kim SW. Amniotic mesenchymal stem cells display neurovascular tropism and aid in the recovery of injured peripheral nerves. J Cell Mol Med. 2014;18:1028–34.
125. Teixeira FG, Panchalingam KM, Anjo SI, Manadas B, Pereira R, Sousa N, et al. Do hypoxia/normoxia culturing conditions change the neuroregulatory profile of Wharton Jelly mesenchymal stem cell secretome? Stem Cell Res Ther. 2015;6:133.
126. Amable PR, Teixeira MV, Carias RB, Granjeiro JM, Borojevic R. Protein synthesis and secretion in human mesenchymal cells derived from bone marrow, adipose tissue and Wharton's jelly. Stem Cell Res Ther. 2014;5:53.
127. Jackson WM, Nesti LJ, Tuan RS. Potential therapeutic applications of muscle-derived mesenchymal stem and progenitor cells. Expert Opin Biol Ther. 2010;10:505–17.
128. Jackson WM, Aragon AB, Bulken-Hoover JD, Nesti LJ, Tuan RS. Putative heterotopic ossification progenitor cells derived from traumatized muscle. J Orthop Res. 2009;27:1645–51.
129. Jackson WM, Lozito TP, Djouad F, Kuhn NZ, Nesti LJ, Tuan RS. Differentiation and regeneration potential of mesenchymal progenitor cells derived from traumatized muscle tissue. J Cell Mol Med. 2011;15:2377–88.
130. Jackson WM, Aragon AB, Djouad F, Song Y, Koehler SM, Nesti LJ, et al. Mesenchymal progenitor cells derived from traumatized human muscle. J Tissue Eng Regen Med. 2009;3:129–38.
131. Jackson WM, Alexander PG, Bulken-Hoover JD, Vogler JA, Ji Y, McKay P, et al. Mesenchymal progenitor cells derived from traumatized muscle enhance neurite growth. J Tissue Eng Regen Med. 2013;7:443–51.
132. Jackson WM, Aragon AB, Onodera J, Koehler SM, Ji Y, Bulken-Hoover JD, et al. Cytokine expression in muscle following traumatic injury. J Orthop Res. 2011;29:1613–20.

133. Kluk MW, Ji Y, Shin EH, Amrani O, Onodera J, Jackson WM, et al. Fibroregulation of mesenchymal progenitor cells by BMP-4 after traumatic muscle injury. J Orthop Trauma. 2012;26:693–8.
134. Smith LR. Influencing the secretion of myogenic factors from mesenchymal stem cells. Stem Cell Res Ther. 2014;5:96.
135. Sohn J, Lu A, Tang Y, Wang B, Huard J. Activation of non-myogenic mesenchymal stem cells during the disease progression in dystrophic dystrophin/utrophin knockout mice. Hum Mol Genet. 2015;24:3814–29.
136. Gurgis C, Mokbel N, DiGirolamo DJ. Therapies for musculoskeletal disease: can we treat two birds with one stone? Curr Osteoporos Rep. 2014;12:142–53.
137. Sassoli C, Nosi D, Tani A, Chellini F, Mazzanti B, Quercioli F, et al. Defining the role of mesenchymal stromal cells on the regulation of matrix metalloproteinases in skeletal muscle cells. Exp Cell Res. 2014;323:297–313.
138. Verhoekx JSN, Mudera V, Walbeehm ET, Hovius SER. Adipose-derived stem cells inhibit the contractile myofibroblast in Dupuytren's disease. Plast Reconstr Surg. 2013;132:1139–48.
139. Brew K, Nagase H. The tissue inhibitors of metalloproteinases (TIMPs): an ancient family with structural and functional diversity. Biochim Biophys Acta Mol Cell Res. 2010;1803:55–71.
140. Seebach E, Holschbach J, Buchta N, Bitsch RG, Kleinschmidt K, Richter W. Mesenchymal stromal cell implantation for stimulation of long bone healing aggravates Staphylococcus aureus induced osteomyelitis. Acta Biomater. 2015;21:165–77.
141. Aoyama T, Goto K, Kakinoki R, Ikeguchi R, Ueda M, Kasai Y, et al. An exploratory clinical trial for idiopathic osteonecrosis of femoral head by cultured autologous multipotent mesenchymal stromal cells augmented with vascularized bone grafts. Tissue Eng Part B Rev. 2014;20:233–42.
142. Aoyama T, Fujita Y, Madoba K, Nankaku M, Yamada M, Tomita M, et al. Rehabilitation program after mesenchymal stromal cell transplantation augmented by vascularized bone grafts for idiopathic osteonecrosis of the femoral head: a preliminary study. Arch Phys Med Rehabil. 2015;96:532–9.
143. Vogel S, Börger V, Peters C, Förster M, Liebfried P, Metzger K, et al. Necrotic cell-derived high mobility group box 1 attracts antigen-presenting cells but inhibits hepatocyte growth factor-mediated tropism of mesenchymal stem cells for apoptotic cell death. Cell Death Differ. 2015;22:1219–30.
144. Docheva D, Müller SA, Majewski M, Evans CH. Biologics for tendon repair. Adv Drug Deliv Rev. 2014;84:222–39.
145. Gaspar D, Holladay C, Pandit A, Zeugolis D. Progress in cell based therapies for tendon repair. Trends Biotechnol. 2015;84:240–56.
146. Angele P, Kujat R, Koch M, Zellner J. Role of mesenchymal stem cells in meniscal repair. J Exp Orthop. 2014;1:12.
147. Zellner J, Taeger CD, Schaffer M, Roldan JC, Loibl M, Mueller MB, et al. Are applied growth factors able to mimic the positive effects of mesenchymal stem cells on the regeneration of meniscus in the avascular zone? Biomed Res Int. 2014. doi:10.1155/2014/537686.
148. Ding Z, Huang H. Mesenchymal stem cells in rabbit meniscus and bone marrow exhibit a similar feature but a heterogeneous multi-differentiation potential: superiority of meniscus as a cell source for meniscus repair. BMC Musculoskelet Disord. 2015;16:65.
149. Centeno CJ, Pitts J, Al-sayegh H, Freeman MD. Anterior cruciate ligament tears treated with percutaneous injection of autologous bone marrow nucleated cells: a case series. J Pain Res. 2015;8:437–47.
150. Takayama K, Kawakami Y, Mifune Y, Matsumoto T, Tang Y, Cummins JH, et al. The effect of blocking angiogenesis on anterior cruciate ligament healing following stem cell transplantation. Biomaterials. 2015;60:9–19.
151. Hogan MV, Walker GN, Cui LR, Fu FH, Huard J. The role of stem cells and tissue engineering in orthopaedic sports medicine: current evidence and future directions. Arthrosc J Arthrosc Relat Surg. 2015;31:1017–21.
152. Carvalho ADM, Badial PR, Alvarez LEC, Yamada ALM, Borges AS, Deffune E, et al. Equine tendonitis therapy using mesenchymal stem cells and platelet concentrates: a randomized controlled trial. Stem Cell Res Ther. 2013;4:85.
153. Steplewski A, Fertala J, Beredjiklian P, Wang ML, Fertala A. Matrix-specific anchors: a new concept for targeted delivery and retention of therapeutic cells. Tissue Eng Part A. 2015;21:1207–16.
154. De Lisio M, Jensen T, Sukiennik RA, Huntsman HD, Boppart M. Substrate and strain alter the muscle-derived mesenchymal stem cell secretome to promote myogenesis. Stem Cell Res Ther. 2014;5:74.
155. Meleshko A, Prakharenia I, Kletski S, Isaikina Y. Chimerism of allogeneic mesenchymal cells in bone marrow, liver, and spleen after mesenchymal stem cells infusion. Pediatr Transplant. 2013;17:189–94.
156. Lozito TP, Taboas JM, Kuo CK, Tuan RS. Mesenchymal stem cell modification of endothelial matrix regulates their vascular differentiation. J Cell Biochem. 2009;107:706–13.
157. Lozito TP, Kuo CK, Taboas JM, Tuan RS. Human mesenchymal stem cells express vascular cell phenotypes upon interaction with endothelial cell matrix. J Cell Biochem. 2009;107:714–22.
158. Titorencu I, Pruna V, Jinga VV, Simionescu M. Osteoblast ontogeny and implications for bone pathology: an overview. Cell Tissue Res. 2014;355:23–33.
159. Chen WCW, Péault B, Huard J. Regenerative translation of human blood-vessel-derived MSC precursors. Stem Cells Int. 2015;2015:11.
160. Pisciotta A, Riccio M, Carnevale G, Lu A, De Biasi S, Gibellini L, et al. Stem cells isolated from human dental pulp and amniotic fluid improve skeletal muscle histopathology in mdx/SCID mice. Stem Cell Res Ther. 2015;6:156.
161. Mukherjee P, Mani S. Methodologies to decipher the cell secretome. Biochim Biophys Acta Proteins Proteomics. 2013;1834:2226–32.
162. Kupcova Skalnikova H. Proteomic techniques for characterisation of mesenchymal stem cell secretome. Biochimie. 2013;95:2196–211.
163. Caccia D, Dugo M, Callari M, Bongarzone I. Bioinformatics tools for secretome analysis. Biochim Biophys Acta Proteins Proteomics. 2013;1834:2442–53.
164. Brown KJ, Seol H, Pillai DK, Sankoorikal BJ, Formolo CA, Mac J, et al. The human secretome atlas initiative: implications in health and disease conditions. Biochim Biophys Acta Proteins Proteomics. 2013;1834:2454–61.
165. Roberts M, Wall IB, Bingham I, Icely D, Reeve B, Bure K, et al. The global intellectual property landscape of induced pluripotent stem cell technologies. Nat Biotechnol. 2014;32:742–8.
166. Sanz-Nogués C, O'Brien T. MSCs isolated from patients with ischemic vascular disease have normal angiogenic potential. Mol Ther. 2014;22:1888–9.
167. Lin W, Li M, Li Y, Sun X, Li X, Yang F, et al. Bone marrow stromal cells promote neurite outgrowth of spinal motor neurons by means of neurotrophic factors in vitro. Neurol Sci. 2014;35:449–57.
168. Lin R-Z, Moreno-Luna R, Li D, Jaminet SC, Greene AK, Melero-Martin JM. Human endothelial colony-forming cells serve as trophic mediators for mesenchymal stem cell engraftment via paracrine signaling. Proc Natl Acad Sci U S A. 2014;111:10137–42.
169. Seebach E, Freischmidt H, Holschbach J, Fellenberg J, Richter W. Mesenchymal stroma cells trigger early attraction of M1 macrophages and endothelial cells into fibrin hydrogels, stimulating long bone healing without long-term engraftment. Acta Biomater. 2014;10:4730–41.
170. Tsai TL, Wang B, Squire MW, Guo LW, Li WJ. Endothelial cells direct human mesenchymal stem cells for osteo- and chondro-lineage differentiation through endothelin-1 and AKT signaling. Stem Cell Res Ther. 2015;6:88.

Hofer and Tuan *Stem Cell Research & Therapy* (2016) 7:131
DOI 10.1186/s13287-016-0394-0

Stem Cell Research & Therapy

REVIEW Open Access

Secreted trophic factors of mesenchymal stem cells support neurovascular and musculoskeletal therapies

Heidi R. Hofer and Rocky S. Tuan*

Abstract

Adult mesenchymal stem cells (MSCs) represent a subject of intense experimental and biomedical interest. Recently, trophic activities of MSCs have become the topic of a number of revealing studies that span both basic and clinical fields. In this review, we focus on recent investigations that have elucidated trophic mechanisms and shed light on MSC clinical efficacy relevant to musculoskeletal applications. Innate differences due to MSC sourcing may play a role in the clinical utility of isolated MSCs. Pain management, osteochondral, nerve, or blood vessel support by MSCs derived from both autologous and allogeneic sources have been examined. Recent mechanistic insights into the trophic activities of these cells point to ultimate regulation by nitric oxide, nuclear factor-kB, and indoleamine, among other signaling pathways. Classic growth factors and cytokines—such as VEGF, CNTF, GDNF, TGF-β, interleukins (IL-1β, IL-6, and IL-8), and C-C ligands (CCL-2, CCL-5, and CCL-23)—serve as paracrine control molecules secreted or packaged into extracellular vesicles, or exosomes, by MSCs. Recent studies have also implicated signaling by microRNAs contained in MSC-derived exosomes. The response of target cells is further regulated by their microenvironment, involving the extracellular matrix, which may be modified by MSC-produced matrix metalloproteinases (MMPs) and tissue inhibitor of MMPs. Trophic activities of MSCs, either resident or introduced exogenously, are thus intricately controlled, and may be further fine-tuned via implant material modifications. MSCs are actively being investigated for the repair and regeneration of both osteochondral and other musculoskeletal tissues, such as tendon/ligament and meniscus. Future rational and effective MSC-based musculoskeletal therapies will benefit from better mechanistic understanding of MSC trophic activities, for example using analytical "-omics" profiling approaches.

Keywords: Arthritis, Mesenchymal stem cells, Extracellular vesicles, Endothelial cells, Endothelial cell–mesenchymal stem cell interactions, Neurotrophic activity, Muscle-derived stem cells

Abbreviations: AD-MSC, Adipose-derived mesenchymal stem cell; AGN, Aggrecan; Ang, Angiopoietin; BDNF, Brain-derived neurotrophic factor; BM, Bone marrow; BMI, Body mass index; BMP, Bone morphogenetic protein; cAMP, Cyclic adenosine monophosphate; CCR/L, Chemokine (C-C) receptor/ligand; CD, Cluster of differentiation; CM, Conditioned medium; CNTF, Ciliary neurotrophic factor; COL, Collagen; COX, Cyclooxygenase; CPC, Chondrocyte progenitor cell; CSPC, Cartilage-derived stem/progenitor cell; CXCR/L, Chemokine (C-X-C) receptor/ligand; Cyr61, Cysteine-rich angiogenic inducer 61; Dkk, Dickkopf-related proteins; EC, Endothelial cell; ECM, Extracellular matrix; EF2, Eukaryotic elongation factor; ET, Endothelin; EV, Extracellular vesicle; FGF, Fibroblast growth factor; Foxp3, Forkhead box p3; GAG, Glycosaminoglycan; GARP, Glycoprotein A repetitions predomain; GDNF, Glial cell line-derived neurotrophic factor; GH-IGF, Growth hormone-insulin-like growth factor; GM-CSF, Granulocyte macrophage colony-stimulating factor;

(Continued on next page)

* Correspondence: rst13@pitt.edu
Center for Cellular and Molecular Engineering, Department of Orthopaedic Surgery, University of Pittsburgh School of Medicine, 450 Technology Drive, Room 221, Pittsburgh, PA 15219, USA

(Continued from previous page)
HA, Hyaluronan; HGF, Hepatocyte growth factor; HIF, Hypoxia inducible factor; HLA, Human leukocyte antigen; IDO, Indoleamine 2,3-dioxygenase; IFN, Interferon; IGF, Insulin-like growth factor; IL, Interleukin; iMSC, MSC generated from induced pluripotent stem cell (iPSC) lines via medium change; iNOS, Nitric oxide synthase; LIF, Leukemia inhibitory factor; LRRC32, Leucine-rich repeat containing-32; MDSC, Muscle-derived stem cell; MHC, Major histocompatibility complex; miRNA, MicroRNA; MMP, Matrix metalloproteinase; mRNA, Messenger RNA; MSC, Mesenchymal stem cell; NF-κB, Nuclear factor-kappa B; NGF, Nerve growth factor; NO, Nitric oxide; OA, Osteoarthritis; PCL, Polycaprolactone; PDGF, Platelet-derived growth factor; PE, Polyethylene; PEDF, Pigment epithelium-derived factor; PG, Prostaglandin; PLA, Poly-lactic acid; PLGF, Placental growth factor; PU, Polyurethane; RA, Rheumatoid arthritis; RANK, Receptor activator of nuclear factor-κB; Rgs, Regulator of G-protein signaling; SDF, Stromal-derived factor; SFRP, Secreted frizzled related protein; TGF, Transforming growth factor; TIMP, Tissue inhibitor of metalloproteinase; TNF, Tumor necrosis factor; TSG, Tumor necrosis factor-inducible gene; UCB, Umbilical cord blood; UV, Umbilical vein; VEGF, Vascular endothelial growth factor; WJ, Wharton's jelly; αSMA, Alpha smooth muscle actin

Background

From a research, medical, and business standpoint, mesenchymal stem cell (MSC)-based therapies are fascinating. Sales for stem cell products (e.g., as a subset of osteobiologics) were projected to top $600,000,000 by 2015 [1, 2], and a recent Scopus search for musculoskeletal and stem cells resulted in over 3000 documents, with more than a third being reviews. We have limited this review to highlighting noteworthy findings and concepts concerned with the understanding of and challenges with MSC musculoskeletal therapies.

MSCs were discovered in the 1960s [3], named in the early 1990s [4], and purportedly defined by the mid-2000s [5]. Despite the proposed criteria, the functional definition within the literature varies widely. MSCs can be defined by their ability to adhere to tissue culture plastic, their expression of several cell surface molecular epitopes—cluster of differentiation CD73, CD90, and CD105, and others—as well as their lack of several surface markers, including CD45 [6]. Some previously excluded markers are debated within certain circles, such as CD34 and CD146 [7–9]. MSCs can be isolated from a range of tissues, but the most commonly cited sources are bone marrow (BM), adipose tissue, muscle, bone, and perinatal tissues (e.g., Wharton's Jelly, umbilical vein/cord blood (UV/UCB), and amnion).

While they were originally utilized clinically in hopes of harnessing their differentiation and proliferation potential, MSCs are increasingly thought to also influence, in addition to participating in, tissue function [10, 11], especially within osteochondral spaces [12]. These MSC influences can range from relatively rare activities that require cell contact, such as mitochondrial transfer and cell fusion, to relatively common paracrine MSC actions through extracellular microvesicles or secreted factors. MSCs may modulate the immune response, angiogenesis, apoptosis, oxidation level, migration, and/or differentiation/stimulation of surrounding cells [13]. Because of this alternative use of MSCs, Caplan and Sorell [14] suggested a renaming of MSCs to medicinal signaling cells to suggest a new era of MSC clinical relevance due to their immunomodulatory properties. While acknowledging progress in the other areas mentioned, this work will focus on the current debates concerning sourcing, MSC alterations of angiogenesis, cell differentiation/stimulation, and strategies to improve MSC differentiation.

Sourcing

Sourcing of MSCs has become an area of debate due to well-recognized potential differences in differentiation abilities and trophic activities of the derived MSCs. Alternatively sourced MSCs may have different differentiation potentials as BM-MSCs, and they may require additional supplementation to achieve robust or similar differentiation. However, while relative abundance and ease of isolation of MSCs may allow their use for successful musculoskeletal interventions [15], there are concerns that diminished numbers of MSCs may be present in BM as patients age or succumb to disease [16]. One study found that mouse MSCs from four common sources (BM, adipose tissue, skeletal muscle, and myocardium) equally supported endothelial cell (EC) network formation in vitro and blood vessel formation in vivo [17]. Muscle-derived stem cells (MDSCs) and satellite cells are thought to contribute to repair of skeletal muscle and bone [18–20]. Although the exact mechanisms remain to be elucidated, cartilage and muscle health has been provocatively linked with changes in or lack of multipotent cell activity, including diseases such as osteoarthritis (OA, cartilage), sarcopenia (muscle), and related muscle and motor neuron diseases [21].

In one study attempting to address the most useful source of MSCs for angiogenesis through a hindlimb ischemia model, Bortolotti et al. examined adipose-derived MSCs (AD-MSCs) and BM-MSCs (along with a subpopulation of CD11-depleted BM-MSCs). They found, as have many others, that MSCs were not incorporated into the

healing wound but that wounds, particularly those in muscles, healed more rapidly when exposed to BM-MSCs (regardless of MSC sorting) [22]. Classic proangiogenic, chemotactic, and remodeling molecules were identified as being expressed by MSCs, with several factors appearing prominently in the also effective conditioned medium (CM) (platelet-derived growth factor-B (PDGFB), transforming growth factor beta (TGF-β), stromal-derived factor-1 (SDF1), angiopoietin-1 (Ang1), regulator of G-protein signaling-5 (Rgs5), matrix metalloproteinase-9 (MMP-9), chemokine (C-X-C) ligand-10 (CXCL10), chemokine (C-C) ligand (CCL5)) [22].

Work with 5–6-week-old human embryonic BM-MSCs and MDSCs suggests that MSCs have innate propensities for adipogenic and myogenic differentiation, respectively, which ultimately affects the organization of the engineered tissues [16, 23]. MSCs sourced from older tissue might overcome these propensities depending on the implantation culture environment [24]. Taking a cue from the successful use of stem cells from birth-associated tissues [25], one group recently investigated the angiogenic activity of endometrium/menstrual blood-sourced multipotent cells, showing that they support the recruitment of ECs, blood vessels, and, potentially, the proliferation of hematopoietic stem cells [26].

An encouraging finding is that the number of MSCs required to exert trophic action may be far less than originally calculated as necessary for tissue replacement, because a prospective study of BM-MSC vs mixed BM-MSC + lipoaspirate therapy for OA found no difference in patient-reported outcomes between the two groups [27]. Interestingly, increasing body mass index (BMI) appeared to correlate with patient-reported improvement of function, a link that should be explored in the future [28].

MSC musculoskeletal clinical use

Evidence for an altered view of MSC efficacy follows results from clinical trials, several of which have recently begun to yield data about long-term MSC efficacy in disease treatment. A large area of MSC-based musculoskeletal research has been directed towards the degenerative joint disease OA, which currently affects approximately 20 million Americans and is projected to affect 20 % of American adults by 2030 [29]. OA is characterized by the degeneration of articular cartilage and synovial inflammation, which alters associated soft tissue and subchondral bone, resulting in bony lesion and osteophyte formation. These degenerative events cause pain and loss of joint mobility and function. Because cartilage has a lower regenerative capacity than other, more vascularized tissues in the body, arthritis and joint degeneration are growing targets of MSC-based therapies.

Recent investigations into MSC treatment of OA have begun to include formal, controlled clinical trials [30] in addition to many uncontrolled trials by private entities. Several international companies, including Cartistem, Regenexx, Regeneus, BioHeart, and Mesoblast, are carrying out phase I and II clinical trials for the treatment of degenerative joint diseases with allogeneic or autologous, multipotent cell types that are capable of mesenchymal differentiation, usually derived from BM or adipose origin [15, 31, 32]. Several other companies have chosen to facilitate MSC isolation within the clinic by constructing machines that quickly sort stem cells from the mixed populations present in surgically isolated tissue [33]. Although published data have been relatively scarce for completed trials, adverse events such as tumors, infections, or premature trial closures have rarely been reported, suggesting safety of MSC-based therapies [34, 35]. The majority of reviewed studies utilize either dissociated cells injected into the joint space or cells delivered via seeding in various biocompatible and/or biodegradable materials.

A recent review details results of nine OA articular cartilage (knee) clinical trials which utilized cultured BM-MSCs, noncultured BM concentrate, peripheral blood-derived stem cells, or cells from the adipose stromal vascular fraction [36]. Some cells were immobilized with hyaluronan, collagen, platelet gel, and/or fibrin glue. Others were injected into the joint or at a defect using only saline. Regardless of cell origin, intra-articular injection of cells (vs hydrogel or flap immobilization through open surgery) resulted in improved clinical function over untreated controls in some studies as long as 5 years post treatment [36]. Pain relief with minor return of function was noted in most studies.

Noting the ameliorative effect of MSCs on joint pain, chronic lower back pain has recently become a target of MSC therapy. Autologous, scaffold-less BM-MSC injection into patients with spinal cord injury in a Brazilian clinical trial suggested clinically meaningful pain relief and possible improvement in cartilage structure after 6 months and as long as 2 years post treatment, although the high number of MSCs utilized coupled with the high cost of the procedure were identified as potential areas for improvement [37]. In a Spanish study, 7 of 12 patients showed mild return of function after 6 months when enrolled in a phase I safety and efficacy study for BM-MSC injection for long-term (>6 months) spinal cord injury [38]; although positive in terms of apparent MSC effect, the study faced almost immediate criticism from other researchers due to the small sample size and lack of appropriate controls [39]. A study by Mesoblast reported decreased lower back pain in 48 % of allogeneic BM-MSC-treated patients vs 13 % in placebo controls up to 2 years post injection [40].

A portion of these analgesic effects could be due to the anti-inflammatory activity of MSCs. Evidence that a decrease in granulocyte macrophage colony-stimulating factor (GM-CSF) resulted from MSC treatment and may decrease disease severity after 4 months comes from a rheumatoid arthritis (RA) clinical trial that used MOR103 antibodies to deplete serum GM-CSF [41]. In an excellent and very recent review of MSC applications to RA, De Bari described how immunomodulation could play a role in RA-specific joint degeneration. Immunoregulators, including interferon gamma (IFN-γ) and tumor necrosis factor alpha (TNF-α), which are regulated through indoleamine 2,3-dioxygenase (IDO) or nitric oxide (NO), and MSC effects on forkhead box $p3^+$ ($Foxp3^+$) Tregs or $CD4^+$ Th17 cells have been suggested [42]. Interestingly, the "transformation hypothesis" proposes that MSCs may become transformed by interplay with chronic inflammatory processes in the joint, resulting in a more aggressive cell type with abilities to either invade the articular cartilage and/or circulate, spreading arthritis to unaffected joints [43, 44]. UV-MSCs may help to relieve the severity of RA symptoms when combined with disease-modifying anti-rheumatic treatments [45].

Recent exploration of immunomodulation showed that AD-MSC surface-bound glycoprotein A repetitions predomain/leucine-rich repeat containing-32 (GARP/LRRC32), found on $CD4^+$/$Foxp3^+$ Tregs, megakaryocytes, and platelets, binds to membrane-bound TGF-β1, holding it in an inactivated but readily-accessible state. GARP silencing results in increased secretion and activation of TGF-β1 and impaired proliferation of AD-MSC as well as activation of T cells [46]. Immunosuppressive effects of membrane-bound TGF-β1, especially when bound to extracellular vesicles (EVs), have also been reported for other MSC types [47–49].

Mechanisms of MSC trophic activity

Insight into the mechanisms of MSC trophic activity is advancing across multiple fields (Table 1). Within the joint space, the MSC secretome is thought to influence the anabolic tendencies of chondrocytes, chondrocyte progenitor cells (CPCs), cartilage-derived stem/progenitor cells (CSPCs), synovium-resident multipotent progenitor cells, osteoblasts/osteoclasts/resident MSCs within the subchondral bone (especially after microfracture), and chondrogenic cells within the infrapatellar fat pad [36, 50, 51]. The MSC secretome can be modified through permanent or temporary alterations. Several studies have found that the exposure of MSCs to proinflammatory factors, sometimes for as little as a few hours, can alter the gene and protein expression of MSCs for days afterwards [52]. Factors known to be secreted or bound to MSC membranes with anti-inflammatory activities (activation of Tregs/tolerogenic dendritic cell phenotype; pro-resolving/M2 macrophage activation; inhibition or proapoptosis of T cells, B cells, NK cells, or dendritic cells; decreasing cytokine production) include: purines, bone morphogenetic proteins (BMPs, specifically BMP-4), CD274, CCL2, Connexin 43, cyclooxygenase (COX)/prostaglandin (PG), CD95/CD95 ligand, galectins, heme oxygenase-1, human leukocyte antigen-G (HLA-G), IDO/kynurenine, interleukin-6 (IL-6), leukemia inhibitory factor (LIF), NO, TGF-β, tumor necrosis factor-inducible gene-6 (TSG6), and vascular endothelial growth factor (VEGF) [53].

In addition to some of the classic chemotactic growth factors and molecules already mentioned (HGF, PDGF, and bFGF), MSCs are strongly influenced by the binding of CXCL12 (SDF1) to CXCR4 [54]. Embryonic muscle growth and adult muscle repair are thought to be heavily influenced by MMP-10-regulated CXCL12 stimulation of MSC migration [55, 56]. Additionally, MSCs express a variety of receptors, including various integrins and selectins, that allow extravasation at repair sites [57].

Clues to the mechanisms of MSC trophic activities (Fig. 1) can also be found in the extensive work done in other fields, particularly exploration of the stem cell secretome in the cardiac field [58]. Identified factors include adrenomedullin, angiogenin, fibroblast growth factor-2 (FGF2), CXCL12, cistatin C, cysteine-rich angiogenic inducer 61 (Cyr61), Dickkopf-related proteins (Dkk), hepatocyte growth factor (HGF), insulin-like growth factor (IGF), IL-1, IL-6, pigmented epithelium-derived factor (PEDF), placental growth factor (PLGF), SDF1, TSG6, VEGF, MMP-2, tissue inhibitor of metalloproteinase-1 (TIMP-1), TIMP-2, secreted frizzled related protein-2 (SFRP-2), thrombospondin-1, and tenascin C [58]. Belying their osseous origin, CM of BM-MSC appears enriched in molecules typically secreted by or influencing osteoblasts, including decorin, osteoprotegerin, Dkk-3, receptor activator of nuclear factor-kB (RANK), osteopontin, and CCL5; inflammatory factors maximally produced by BM-MSCs include CCL2, TIMP-2, IL-6, IL-7, IL-3, MMP-7, chemokine (C-X-C) receptor-16 (CXCR16), and MMP-10. CCL2 and CCL7 produced by BM-MSCs appear to strongly influence nascent bone formation [59, 60]. Recent work also suggests that AD-MSC, BM-MSC, and dental pulp stem cell-secreted CXCL14 and CCL2 help to recruit $CXCR4^+$ cells and chemokine (C-C) receptor-2^+ ($CCR2^+$) vessel-associated cells, without inducing proliferation [61]. Besides these influential but potentially short-lived proteins, some MSCs secrete EVs which may contain any number of influential molecules, protected from systemic degradation by virtue of their natural, membrane-bound packaging [62–65].

In many cell types, EVs of varying sizes, including ectosomes/exosomes and microvesicles/microparticles, were derived from either cytoplasmic protrusions or

Table 1 MSC trophic activities relevant to musculoskeletal therapy: mechanistic insights from in-vitro and host tissue studies

System and reference	In vitro/ host	Cell sources	Observed trophic activity	Mechanistic insights
Angiogenesis [84]	IV	Human BM-MSCs; UCB-ECs	MSCs encouraged EC migration, proliferation, and tubule formation	GHK (osteonectin peptide) induces MSC-VEGF secretion
Angiogenesis [81]	IV	Human BM-MSCs (commercial); microvascular ECs	MSC culture on stiff, fibronectin-coated surfaces encouraged EC spreading/tubule formation	Actomyosin contractility increased MSC expression of proangiogenic factors (angiogenin, VEGF, and IGF)
Angiogenesis [105]	IV	Human BM-MSCs (commercial); UV-ECs	EC-MSC coculture increased MSC-myogenic and EC-PLAU, EC-FGF, and EC-NF-kB-regulated gene expression	• MSC IL-1β and IL-6 regulate EC NF-kB target genes, including P-selectin, CCL23, and CXCL2/3 • EC TGF-β1/3 may regulate MSC myogenic differentiation
Angiogenesis [107]	IV/mouse	Human BM-MSCs (commercial); UV-ECs	• IV: EC-MSC (vs EC) cultures on degradable scaffolds expressed higher perivascular markers • Host angiogenic and perivascular markers, except vessel diameter and density, were equivalent between EC/MSC-EC implants	IV: cocultures upregulated VEGF and ANG1 while downregulating ANG2
Angiogenesis [73]	IV/mouse	Human iMSCs (medium change of iPSCs); UV-ECs	• iMSC exosomes promoted EC migration, proliferation, and dose-dependent tubule formation (IV) • Exosome treatment correlated with modest functional improvement, better perfusion and tissue damage scores, increased CD31/CD34^{+} cells	iMSCs induced EC expression of proangiogenic molecules, including VEGF, TGF-β1, and ANG1
Angiogenesis (hindlimb ischemia) [22]	Mouse	Mouse AD-MSCs (plastic adherence); BM-MSCs (plastic adherence); BM-iMSCs (immunodepletion)	• BM-MSCs maximally decreased inflammatory cell invasion • MSCs were associated with smaller lesions, more mature neovascularization, and increased perfusion	IV: BM-MSCs expressed the highest levels of tested chemokines, vessel stabilizing, and matrix-remodeling factors
Neurovascular system (fibrin conduit, resection) [116]	Rat	Human AD-MSCs (plastic adherence); DRG; UV-EC	• Medium cocktail-stimulated MSCs enhanced DRG neurite extension and EC-tubule formation • Stimulated and unstimulated MSCs encouraged neurite extension	Stimulated MSCs produced increased VEGF, ANG1, NGF, BDNF, and GDNF
Neurogenesis [167]	IV	Rat BM-MSCs (plastic adherence)	Spinal cord tissue–MSC coculture supported neurite outgrowth	Cocultured MSCs produced NGF, BDNF, and GDNF, maximally supporting neurite extension
Neurogenesis (spinal nerve ligation) [123]	Rat	Rat BM-MSCs (commercial)	MSC-treated rats displayed decreased hyperalgesia and increased pain threshold	TUBB3^{-}, GFAP^{-}, and αSMA^{-} and STRO1^{+} MSCs engrafted into DRGs
Neurogenesis (sciatic crush) [124]	Mouse	Human AD-MSCs and AM-MSCs (commercial)	• AM-MSC-treated groups exhibited higher recovery, coordination, and perfusion scores (4 weeks) • MSCs localized in the epineurium and perivascular area	Nerves injected with AM-MSCs versus AD-MSCs or PBS produced more ANG1, FGF1, IGF1, and VEGFA
Distraction Osteogenesis (DO) [59]	Mouse	Human BM-MSCs (commercial)	• MSC and MSC-CM accelerated DO healing • MSC-CM recruited more vessels	• IV: IL-3/IL-6/CCL5/SDF1 recruited mononuclear cells, contributed to enhanced mineralization • MCP1/MCP3 but not SDF1 were critical for SC-CM osteogenic activity
Osteogenesis [168]	Mouse	Human AD-MSCs and BM-MSCs; UCB-ECs	• MSC-EC cotransplantation increased MSC engraftment • Cotransplantation restricted MSC multipotency, enhanced MSC source-related differentiation abilities, and maintained MSC proliferation capacity	PDGFBB/PDGFRβ receptor activity regulates MSC engraftment and differentiation in the presence of ECs

Table 1 MSC trophic activities relevant to musculoskeletal therapy: mechanistic insights from in-vitro and host tissue studies *(Continued)*

Osteoporosis (lupus associated) [60]	Mouse	Human BM-MSCs and DP-MSCs	• MSC injections improved osteoporosis-related bone scores • MSCs lowered osteoclast differentiation (IV)	IL-17 removal following MSC injection maintains osteoclast immaturity
Osteogenesis [169]	Rat	Rat BM-MSCs (centrifugation and plastic adherence)	Fibrin-loaded MSC recruited host macrophages to fill long bone defect by 4 weeks	Implanted MSCs increased early expression of VEGF and decreased later expression of CD45, IL-6, IL-1β, TNF-α, and IL-10
Osteogenesis, chondrogenesis, angiogenesis [170]	IV	Human BM-MSCs (density gradient) and human embryonic stem cell MSCs (medium/substrate changes); human aortic ECs	MSC-EC cocultures proliferated and exhibited higher expression of mesenchymal differentiation transcription factors	EC-produced ET1 activates MSC AKT, driving osteogenic and chondrogenic capacities
Chondrogenesis [95]	IV	Human BM-MSCs (density gradient)	• MSCs and/or chondrocytes in fibrin gels exhibited superior mechanical properties to those cultured with OA cartilage explants • COLI/II/III production reduced in OA cartilage–MSC or chondrocyte–MSC cocultures	IL-1β and IL-6 decreased COL production versus control cultures, except in chondrogenic cultures at longer culture times (4 weeks)
Chondrogenesis [93]	IV	Human BM-MSCs; Human OA primary chondrocytes; bovine primary chondrocytes	FGF1 caused chondrocyte proliferation	• FGF1 was concentrated in places where MSCs contacted chondrocytes
Tenogenesis (enzymatic lesion) [152]	Horse	Horse AD-MSCs	Lesions were smaller, more vascularized, and less cellular when treated with platelet concentrate-injected MSCs	• Greater amount of RNA was recovered from the MSC-treated group • No difference in anabolic and tendon-specific gene expression observed
Musculogenesis (dystrophin/utrophin) [135]	IV	Mouse quickly and slowly adhering MSCs (non-myogenic nmMSCs and MPCs), dKO)	• dKO-MPC-dKO-nmMSC co-culture decreased global myogenic markers • dKO vs. WT-nmMSCs differentiated more efficiently along osteogenic and adipogenic lines with donor age	Soluble frizzled-related protein-1 and active β-catenin encouraged nonmyogenic differentiation of dKO-nmMSCs in gastrocnemius tissues
Musculogenesis (myofibroblast proliferation) [138]	IV	Human AD-MSCs and BM-MSCs (commercial); Dupuytren's disease-derived myofibroblast (DDMF)	• AD-MSCs (similar to normal skin-derived fibroblasts) decreased while BM-MSCs increased DDMF co-culture contractility • AD-/BM-MSCs inhibited myofibroblast proliferation • AD-MSC effects were strongest with direct or indirect contact	AD-MSC/myofibroblast cocultures exhibited decreased COLI and αSMA
Musculogenesis (dystrophin) [160]	Mouse	Human (STRO1^{+}) DP-MSCs; human (c-Kit^{+}) amniotic fluid MSCs	• MSCs differentiated in the presence of C2C12-formed myotubes (IV) • MSCs differentiated most efficiently with C2C12-CM • All differentiated MSCs engrafted and improved muscle histology	Demethylation was critical for IV myogenic differentiation
Musculogenesis [137]	IV	Mouse BM-MSCs (centrifugation and plastic adherence)	MSC-CM stimulated myoblast and satellite cell proliferation and migration, activated satellite cells, inhibited myofibroblast differentiation	MSC MMP-2/9 and TIMP-1/2 support myogenic differentiation

AD, adipose-derived, *AM* amniotic membrane, *BM*, bone marrow, *CM* conditioned medium, *dKO* double knockout, *DP* dental pulp, *DRG* dorsal root ganglia, *EC* endothelial cell, *iMSCs* MSCs generated from induced pluripotent stem cell (*iPSC*) lines via medium change, *IV* in vitro, *MMP* matrix metalloproteinase, *MPC* multipotent cell, *MSC* mesenchymal stem cell, *SC* stem cell, *TIMP* tissue inhibitor of metalloproteinase, *UCB* umbilical cord blood, *UV* umbilical vein

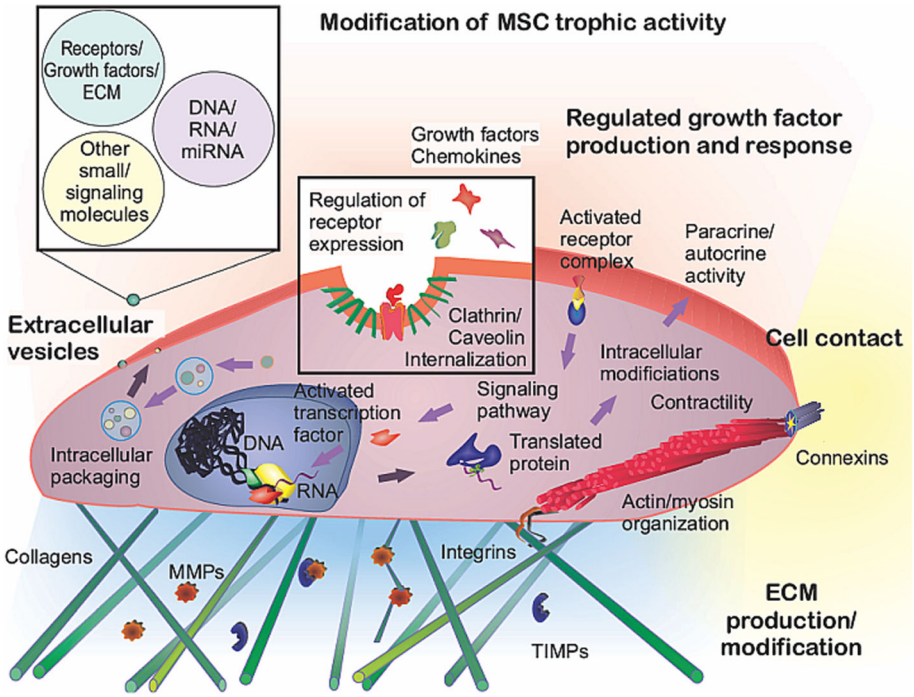

Fig. 1 MSC trophic mechanisms depend on MSC interactions with and modification of the local environment. MSC trophic functions can be both achieved and altered through dynamic ECM–cytoskeletal interactions, cell–cell contacts, and soluble and transcription factor signaling. *ECM* extracellular matrix, *miRNA* microRNA, *MMP* matrix metalloproteinase, *MSC* mesenchymal stem cell, *TIMP* tissue inhibitor of metalloproteinase

lipid raft internalization and subsequent endosomal fusion with the plasma membrane [66–69]. These 30 nm–1 μm vesicles may be studded with multiple proteins, usually tetraspanins, and filled with a combination of proteins, lipids, and copious amounts of mRNA and microRNA (miRNA), particularly miR22 and miR-19a [58]. EC and cancer cell-derived microparticles may potently increase MSC NF-kB activity, stimulating local trophic support [70]. Gap junctions, formed via connexins, are another avenue allowing direct cell–cell communication, with strong evidence for membrane and (to a lesser extent) cytoplasmic exchange between MSCs and ECs [71].

Likely mediated through EC-stimulated VEGF production, CXCR4-enriched exosomes derived from MSCs generated from induced pluripotent stem cell (iPSC) lines via medium change (iMSCs) improved recovery from myocardial infarction [72]. In work addressing hindlimb ischemia in mice, iMSC exosomes were associated with a higher number of $CD31^+$ and $CD34^+$ cells in damaged muscle tissue as well as increased EC secretion of VEGF, TGF-β1, and angiogenin, suggesting enhanced vascular recruitment by vesicles alone [73]. Another group generated iMSCs through TGF-β-pathway inhibition and medium changes; those iMSCs, surprisingly, did less to promote cancer than BM-MSCs, appearing to express and produce lower amounts of several of the inflammatory and differentiation factors (particularly TGF-β receptor-2 and, interestingly, hyaluronan (HA)) when cultured with various types of cancer cells [74].

In a recent study, Baglio et al. [75] characterized the RNA contents of exosomes obtained through ultracentrifugation, and found that exosomes were enriched for tRNA, in particular tRNA CTC. Their work further suggested that the differentiation state of a MSC might be deduced by the content of its exosomes, particularly the presence of full-length tRNA and tRNA long fragments, consistent with a stem-like state of the cells [76]. miRNA loading within vesicles is not random, as dexamethasone treatment of both C2C12 cells and diabetic rats increased the concentration of miR-23a and miR-182 in collected microvesicles and urine, respectively [77], thus providing MSCs with a dynamic way to influence and respond to their microenvironment. Microvesicles may also suppress the infiltration of macrophages into damaged tissues [75]. However, the relevance of vesicles/microvesicles to classical and clinically approved MSCs is questionable, because a different group noted that MSCs produced much fewer vesicles than immortalized ESC-derived MSCs [78]. The group offered an immortalization strategy that would maximize the yield of MSC-produced vesicles, should they prove effective in the clinic.

Altering MSC activity prior to bone or cartilage implantation

Because "plain" MSC implantation has faced such varied success in the clinic, the next generation of MSC-based strategies seeks to harness and direct MSC trophic activities. It was observed that substrate composition and stiffness, sensed through various integrins, could influence the expression of myogenic factors [79]. Substrate stiffness, known to affect the differentiation of MSCs, acting possibly through regulation of alpha-smooth muscle actin (αSMA), could also play a role in the eventual differentiation capacity of culture-expanded MSCs [80]. Substrate stiffness, in turn, affects MSC trophic properties; stiff (40 kPA) polyacrylamide gels coated with fibronectin induced proangiogenic factor secretion by BM-MSCs [81]. Through internalization and recycling of focal adhesions and receptors, caveolins play an intriguing role in MSC sensing of both substrate stiffness and surrounding soluble signals, particularly in vascular, muscular, and osteogenic settings [82]. Alternatively, hydrogels made from autologous plasma may also help to temporarily concentrate either AD-MSCs or AD-MSC-CM at the injury site [83].

The ability of MSCs to self-generate abundant collagenous extracellular matrix (ECM) may partially explain some of the positive effects witnessed in some joint degeneration trials involving MSCs [27]. Medium supplements or additional modifications to the substrate to mimic other ECM molecules or bioactive factors, such as osteonectin, may further increase MSC secretion of bioactive molecules (FGF2, CCL5, and VEGF), supporting native cell migration and differentiation [84].

The milieu present in culture serum appears to strongly influence the fate of cultured cells, more so than any single exogenous supplement [85]. One method to both encourage MSC trophic activity as well as ease immunological concerns in the clinic could be to utilize autologously derived cell culture supplements such as platelet lysate for autologous MSC expansion and culture [86]. Platelet-rich plasma, for example, may protect cartilage from injury by enhancing collagen II (COLII)/aggrecan (AGN) expression and suppressing MMP-3, COX2, iNOS, and associated NO and PGE2 production [87]. Once established in vitro, however, the role of serum becomes less clear; while serum content affects MSC gene expression and growth rate, inherent multipotency and stem cell marker surface expression do not appear to be affected by the absence of serum [88]. For that reason, MSC-CM concentration and injection may sidestep issues of autophagy [89] or apoptosis of MSCs upon in-vitro expansion [13].

Culture under hypoxia is another attractive method to increase initial MSC production of trophic factors. Under hypoxia, hypoxia inducible factor-1 alpha (HIF1α) expression increases, driving VEGF and other proangiogenic, antiapoptotic, and antioxidant molecules [90]. Under certain circumstances, hypoxic MSCs may serve to prevent harmful fibrosis through HGF production, TGF-β1/COLII, and IL-1β downregulation, and fibronectin expression [91]. Work in vitro with chondrocytes has specifically identified HGF as an antifibrotic agent released by AD-MSCs [92]. Furthermore, FGF1 secreted by MSCs in contact with chondrocytes may stimulate the proliferation of and help to preserve the function of chondrocytes [93, 94].

In-vitro evidence suggests that the addition of BM-MSCs to OA cartilage may initially increase IL-1β and IL-8 production but ultimately reduce the amount of soluble glycosaminoglycan (GAG) released by the cartilage over time, making the exact influence of MSCs on cartilage structure unclear [95].

Reported pain relief associated with the introduction of MSCs may be the result of immunomodulation but was by no means universal [36]. In-vitro studies suggest that exposure of MSCs to chondrocytes may induce expression of MSC major histocompatibility complex (MHC) I/II and other costimulatory molecules [96].

Pretreatment of MSCs, especially with IFN-γ to prime their immunosuppressive activity, may result in decreased MSC-associated tissue degradation [97]. Possibly in response to IL-1α, MSCs exposed to platelet lysate have the capacity to encourage a proinflammatory/M1 or proresolving/M2 macrophage phenotype through GM-CSF and PGE2 activity, respectively [53, 98]. Growing evidence suggests that the native, inflamed cartilage environment may both trigger the release and limit the effectiveness of MSC-anti-inflammatory PGE2 [99]. MSCs may recruit $CD4^+$ T cells, which can also play a role in increasing local osteogenic activity [100]. Care must be taken with extensive culture, because MSCs may gain genetic abnormalities and lose some ability to differentiate, promoting senescence [88].

Vascular/inflammation regulation

Several key targets of regenerative medicine therapies, including restored nerve and muscle function and the previously discussed bone repair, rely heavily on the influence of vascular cells [101]. Consequently, MSC effects on blood vessel cells have long fascinated researchers. Recent work has begun to elucidate mechanisms by which MSCs may affect blood vessel morphology and function. Chen et al. [102] reported that MSC-produced HGF, upon interaction with ECs in coculture and, to a lesser extent, via paracrine signaling, caused an increase in EC cadherin and F-actin remodeling, thereby decreasing EC permeability [90, 103, 104]. This and earlier work with ECs suggests that MSC–EC interactions may temporarily restrict both the physical clearance of MSCs and the

invasion of inflammatory cells. Once in the bloodstream, MSC inhibition of NF-kB, perhaps through IL-10 or other factors, may decrease the binding of monocytes to the endothelium, further decreasing inflammation at wound/MSC injection sites [45]. This temporary pause in the battle with chronic inflammation may explain some of the positive results seen with MSCs.

Following a more classical approach focused on EC motility and activity, VEGF, ANG, and NF-kB pathways have all been implicated in regulating angiogenesis. Recent work suggests that, in the short term, the NF-kB pathway may control EC response through BM-MSC-produced IL-6 and IL-1β; following this NF-kB activation, ECs activate P-selectin, producing CCL23, CXCL2, and CXCL3. In turn, MSCs showed signs of early differentiation towards a smooth muscle phenotype in coculture, influenced by TGF-β1 and TGF-β3 [105]. BM-MSC production of VEGF may be stimulated by IL-8, either through paracrine or autocrine mechanisms [106]. In turn, BM-MSCs may stabilize ECs by upregulating ANG1, thereby downregulating EC proliferation [107]. Conversely, the interaction of MSCs with ECs, particularly through endothelin 1 (ET1) and PDGFB, may prime cells to survive transplantation and differentiate more easily upon reimplantation [108].

Neural support

MSCs have long been known to support nerve growth through the support of Schwann cells, secretion of neurovascular factors (including FGF2 and VEGF-A), and, possibly, transdifferentiation into Schwann-like cells. Combined with varying types of biocompatible and bioactive materials, such as poly-lactic acid (PLA), polycaprolactone (PCL), polyurethane (PU), polyethylene (PE), and silicone (for strength) and COLI, HA, and so forth (for bioactivity), several groups have observed enhanced nerve extension and functional improvements in a range of animal models [109, 110]. The most recent work refines previous findings that guidance fibers of particular spacing and architecture may aid MSCs in further accelerating the nerve healing process [111–113]. AD-MSCs, at sufficient density, secrete brain-derived neurotrophic factor (BDNF) in response to autocrine IFN-β [114]. Stimulating cocktails that increase cyclic-adenosine monophosphate (cAMP) and include retinoic acid (pretreatment), FGF2, PDGFAA, and different forms of neuregulin have been shown to increase neurite outgrowth in vitro and nerve extension after injury in vivo [115]. In addition to neurotrophic BDNF, nerve growth factor (NGF), and glial cell line-derived neurotrophic factor (GDNF), as well as angiogenic VEGF and ANG1 identified in many other experiments, recent work identified the antiapoptotic activity of AD-MSCs, possibly by decreasing neuronal c-jun [116]. As mentioned in previous sections, such pretreatment is relatively common in nonclinical work, and may become de rigeur as new progenitor cell sources are explored for musculoskeletal therapies [117]. Crucially, it appears that MSCs should not be directly injected intrathecally for early spinal cord repair, as the subsequent inflammation seemed to prevent MSC migration to neuronal injury sites [118]; later injection may prove beneficial [119].

Ciliary neurotrophic factor (CNTF) is a particularly well known neuroprotective factor produced by MSCs. While the factor has potent therapeutic effects on nerve apoptosis, neuroinflammation, and neuronal proliferation, it has been linked with altered metabolism (due to neurogenesis in the hypothalamus as well as direct action on adipocytes) when administered systemically and may negatively affect osteoblast differentiation and mineralization [120–122]. GDNF, another potent neurotrophic molecule often produced by MSCs, may help to ease allodynia and hyperalgesia experienced in dorsal root ganglia sensory nerves [123]. Amniotic membrane-derived MSCs expressed more ANG1, FGF1, IGF1, and VEGFA (but not FGF2) than AD-MSCs in a mouse sciatic nerve injury trial [124].

While CM from cells treated under hypoxic and normoxic conditions both increased the observed number of differentiating neurons in vitro, hypoxia-cultured Wharton's Jelly (WJ)-derived MSCs upregulated thymosin B and eukaryotic elongation factor (EF2) and may have contributed to a slight increase in total neuron maturity [125]. WJ-MSCs under normoxic conditions were shown to produce PDGFAA, HGF, TGF-β2, IL-6, IL-8, IL-1ra, CCL5, CCL2, and CXCL10 at much larger concentrations than BM-MSCs and AD-MSCs [126]. Whatever the mechanism for neural support, tissue response to neurological directives is critical to the ultimate utility of the repaired nerve.

Muscles and miscellany

Intriguing results suggest that MSCs derived from less traditional sources could one day be utilized therapeutically. One readily available source for MSCs could be skeletal muscles. Our research group has worked extensively with blast-traumatized muscle-derived multipotent cells [127–129]. This particular type of muscle-derived multipotent cells is especially attractive therapeutically due to its relative abundance and ease of isolation [130] as well as neurotrophic activity [131]. MDSCs should be used cautiously when attempting to rebuild musculoskeletal tissues, because several groups have identified populations that seem predisposed to mineralize ectopically [132–134], especially in the presence of muscular genetic abnormalities [135]. Growth factor coinjection might attenuate this ectopic bone formation, as growth hormone–insulin-like growth factor-1 (GH-IGF1) activity

promotes muscle cell proliferation, regulates muscle fiber size and type, controls osteoblast proliferation and differentiation, inhibits osteoclast activity, stimulates renal conversion of 25-OH-vitamin D_3, and controls phosphate reabsorption [136]. By contrast, this matrix-modifying MSC activity may help to attenuate disease severity and ultimately contribute to useful muscle mass [137]. Harmful proliferation and contraction of myofibroblasts, as occurs in Dupuytren's contracture, may be attenuated in the presence of the CM of both AD-MSCs or BM-MSCs as well as the physical presence of AD-MSCs (but not BM-MSCs) [138]. BM-MSCs appear to contribute to pathological myofibroblast proliferation while AD-MSCs appear to inhibit the activity slightly [138]. MMP-2 and MMP-9 are required for efficient skeletal muscle regeneration and are enhanced by mouse BM-MSCs/MSC-CM along with reduced TIMP-1/2 levels. Muscle cell motility may also be encouraged by BM-MSC-secreted MMP-2 [139].

Aside from their ECM-modifying properties, the immunomodulatory properties of MSCs are intriguing from a therapeutic standpoint but must be used carefully, because MSC treatment, concurrent with a *Staphylococcus aureus* infection, was shown to increase the severity of bone loss, despite increased MSC proinflammatory cytokine expression, in an osteomyelitis model [140]. Conversely, encouraging results were recently published from a small idiopathic osteonecrosis trial in Japan, where BM-MSCs were isolated, cultured for 2 weeks, and returned to osteonecrotic patients along with tricalcium phosphate chips (Osferion) and tricortical iliac crest bone [141]; after a 12-week rehabilitation program, all patients reported reduced pain and increased physical function with no serious adverse events reported in the study [142]. The likelihood of MSC engraftment being the cause for the recovery is low, however, as MSCs have been found to migrate towards apoptotic cells, via HGF signaling, but not HGF produced in the presence of necrotic cells [143].

Evidence of MSC trophic efficacy has generated intense excitement in clinically focused research. This excitement is evident in the increasing number of reviews examining MSC trophic properties. Marked therapeutic successes will likely hinge on technological and computational advancements that allow dynamic, high-resolution, and quantitative observation of MSC–ECM, MSC–paracrine, and MSC–cellular interactions to better define the appropriate perspective on the true activity of MSCs.

Conclusions

The application of allogeneic and autologous MSC therapies for the treatment of diseases and dysfunctions of multiple musculoskeletal tissues has received increasing attention. Exciting in-vitro and in-vivo investigations on tendon [117, 144, 145], meniscus [146–148], and ligaments [149, 150] have been reported, along with the use of autologous products such as platelet-rich plasma/plasma lysate [151]. Studies using larger, clinically relevant animal models are both underway and necessary before human clinical trials can be developed [152].

This review has primarily explored secreted trophic factors produced by MSCs. A whole host of therapies are dedicated to engineering or modifying the physical environment and ECM of MSCs to affect their therapeutic potential. A recently developed approach attempts to anchor cells to the collagenous tissue matrix by engineering collagen anchors [153], to promote local action of MSCs and minimize their systemic loss to the lungs, liver, and spleen. Changes in substrate composition (especially the presence of collagen) and stiffness may expand the potential applications of MSC therapies to include muscle volume loss through stimulation of muscle-resident progenitor cells [134, 154, 155]. Local ECM modifications are known to affect MSC differentiation potential [156, 157] and are beyond the scope of this review. Through continuing advancements in genetic engineering, MSCs may eventually be used to treat genetic musculoskeletal conditions, including osteogenesis imperfect [158] and Duchenne's muscular dystrophy [159, 160]. Careful selection of the therapeutic cells, taking into account subtle tissue source-related differences, may be the key to successful clinical dystrophy therapies [35]. To prove their efficacy in the clinic, these potential treatments will need to be tested in well-controlled studies to assess physical functions for an extended period of time [27].

New or more precise modes of MSC trophic activity may be discovered by adopting contemporary analytical technologies to evaluate and compare genomic, transcriptomic, proteomic, metabolomic, and secretomic profiles, exemplified by the great strides that have been made in genetic and metabolic diseases [161–164]. Lessons learned from previous iterations of MSC therapies and clinical drug trials should overcome some of the regulatory and therapeutic hurdles to MSC use [2, 32, 33]. It is also noteworthy that while genetic engineering of iPSCs may hold the answer to unlimited numbers of perfectly-tuned stem cells, managing the safety concerns of iPSCs and negotiating the patent landscape of this saturated market will be highly challenging [165]. Another major challenge is the uncertainty in terms of biological responsiveness of the diseased tissue, because evidence in several fields suggests that ischemic tissue may be incapable of responding to MSCs [166]. Finally, each of these avenues should be explored while juggling the needs for rigorous science, proven therapeutic efficacy, regulatory approval (e.g., by the Food and Drug Agency) (and thus reproducibility) of a final therapy, and cost/benefit for the patient.

Acknowledgements
This work is supported in part by the Commonwealth of Pennsylvania Department of Health (SAP 4100050913), NIH (5U18 TR000532), and US Department of Defense (W81XWH-08-2-0032, W81XWH-14-2-0003). A portion of the predoctoral training of HRH was supported by a Training Grant funded by the National Institute of Biomedical Imaging and Bioengineering, NIH (T32EB0010216). HRH acknowledges the faculty, staff, and students of CCME, where HRH served as a Research Fellow during a portion of the time required to draft and edit this document.

Authors' contributions
HRH created the figure and tables, and researched, drafted, and arranged the document. RST suggested the content, edited the document, and was the invited, corresponding author. Both authors read and approved the final manuscript.

Competing interests
The authors declare that they have no competing interests.

Published online: 09 September 2016

References

1. Wei C, Lin AB, Hung S. Mesenchymal stem cells in regenerative medicine for musculoskeletal diseases: bench, bedside, and industry. Cell Transplant. 2014;23:505–12.
2. Heathman TR, Nienow AW, McCall MJ, Coopman K, Kara B, Hewitt CJ. The translation of cell-based therapies: clinical landscape and manufacturing challenges. Regen Med. 2015;10:49–64.
3. Friedenstein AJ, Piatetzky-Shapiro II, Petrakova KV. Osteogenesis in transplants of bone marrow cells. J Embryol Exp Morphol. 1966;16:381–90.
4. Caplan AI. Mesenchymal stem cells. J Orthop Res. 1991;9:641–50.
5. Dominici M, Le Blanc K, Mueller I, Slaper-Cortenbach I, Marini F, Krause D, et al. Minimal criteria for defining multipotent mesenchymal stromal cells The International Society for Cellular Therapy position statement. Cytotherapy. 2006;8:315–7.
6. Salem HK, Thiemermann C. Mesenchymal stromal cells: current understanding and clinical status. Stem Cells. 2010;28:585–96.
7. Dmitrieva RI, Minullina R, Bilibina AA, Tarasova OV, Anisimov SV, Zaritskey AY. Bone marrow- and subcutaneous adipose tissue-derived mesenchymal stem cells: differences and similarities. Cell Cycle. 2012;11:377–83.
8. Sidney LE, Branch MJ, Dunphy SE, Dua HS, Hopkinson A. Evidence for CD34 as a common marker for diverse progenitors. Stem Cells. 2014;32:1380–9.
9. Lv F-J, Tuan RS, Cheung KMC, Leung VYL. The surface markers and identity of human mesenchymal stem cells. Stem Cells. 2014;32:1408–19.
10. Caplan AI, Correa D. The MSC: an injury drugstore. Cell Stem Cell. 2011;9:11–5.
11. Vonk LA, de Windt TS, Slaper-Cortenbach ICM, Saris DBF. Autologous, allogeneic, induced pluripotent stem cell or a combination stem cell therapy? Where are we headed in cartilage repair and why: a concise review. Stem Cell Res Ther. 2015;6:1–11.
12. Ruetze M, Richter W. Adipose-derived stromal cells for osteoarticular repair: trophic function versus stem cell activity. Expert Rev Mol Med. 2014;16:e9.
13. Liang X, Ding Y, Zhang Y, Tse H, Lian Q. Paracrine mechanisms of mesenchymal stem cell-based therapy: current status and perspectives. Cell Transplant. 2014;23:1045–59.
14. Caplan AI, Sorrell JM. The MSC curtain that stops the immune system. Immunol Lett. 2015;168:136–9.
15. Diederichs S, Shine KM, Tuan RS. The promise and challenges of stem cell-based therapies for skeletal diseases. Bioessays. 2013;35:220–30.
16. Hass R, Kasper C, Böhm S, Jacobs R. Different populations and sources of human mesenchymal stem cells (MSC): a comparison of adult and neonatal tissue-derived MSC. Cell Commun Signal. 2011;9:1–14.
17. Mahdi NS, Rahbarghazi R. Interactions of mesenchymal stem cells with endothelial cells. Stem Cells Dev. 2014;23:319–32.
18. Tamaki T, Okada Y, Uchiyama Y, Tono K, Masuda M, Wada M, et al. Clonal multipotency of skeletal muscle-derived stem cells between mesodermal and ectodermal lineage. Stem Cells. 2007;25:2283–90.
19. Zou J, Yuan C, Wu C, Cao C, Shi Q, Yang H. Isolation and osteogenic differentiation of skeletal muscle-derived stem cells for bone tissue engineering. Mol Med Rep. 2013;9:185–91.
20. Meszaros LB, Usas A, Cooper GM, Huard J. Effect of host sex and sex hormones on muscle-derived stem cell-mediated bone formation and defect healing. Tissue Eng Part A. 2012;18:1751–9.
21. De Ceuninck F, Fradin A, Pastoureau P. Bearing arms against osteoarthritis and sarcopenia: when cartilage and skeletal muscle find common interest in talking together. Drug Discov Today. 2014;19:305–11.
22. Bortolotti F, Ukovich L, Razban V, Martinelli V, Ruozi G, Pelos B, et al. In vivo therapeutic potential of mesenchymal stromal cells depends on the source and the isolation procedure. Stem Cell Reports. 2015;4:332–9.
23. Krylova TA, Musorina AS, Zenin VV, Yakovleva TK, Poljanskaya GG. A comparative analysis of mesenchymal stem-cell lines derived from bone marrow and limb muscle of early human embryos. Cell Tissue Biol. 2014;8:441–53.
24. Baker N, Boyette LB, Tuan RS. Characterization of bone marrow-derived mesenchymal stem cells in aging. Bone. 2015;70:37–47.
25. Verdi J, Tan A, Shoae-Hassani A, Seifalian AM. Endometrial stem cells in regenerative medicine. J Biol Eng. 2014;8:20.
26. Alcayaga-Miranda F, Cuenca J, Luz-Crawford P, Aguila-Díaz C, Fernandez A, Figueroa FE, et al. Characterization of menstrual stem cells: angiogenic effect, migration and hematopoietic stem cell support in comparison with bone marrow mesenchymal stem cells. Stem Cell Res Ther. 2015;6:1–14.
27. Grässel S, Lorenz J. Tissue-engineering strategies to repair chondral and osteochondral tissue in osteoarthritis: use of mesenchymal stem cells. Curr Rheumatol Rep. 2014;16:1–16.
28. Centeno C, Pitts J, Al-Sayegh H, Freeman M. Efficacy of autologous bone marrow concentrate for knee osteoarthritis with and without adipose graft. Biomed Res Int. 2014;2014:370621.
29. Mobasheri A, Kalamegam G, Musumeci G, Batt ME. Chondrocyte and mesenchymal stem cell-based therapies for cartilage repair in osteoarthritis and related orthopaedic conditions. Maturitas. 2014;78:188–98.
30. Baugé C, Boumédiene K. Use of adult stem cells for cartilage tissue engineering: current status and future developments. Stem Cells Int. 2015;2015:438026.
31. Boregowda SV, Phinney DG. Therapeutic applications of mesenchymal stem cells: current outlook. BioDrugs. 2012;26:201–8.
32. Sharma RR, Pollock K, Hubel A, McKenna D. Mesenchymal stem or stromal cells: a review of clinical applications and manufacturing practices. Transfusion. 2014;54:1418–37.
33. Srijaya TC, Ramasamy TS, Kasim NHA. Advancing stem cell therapy from bench to bedside: lessons from drug therapies. J Transl Med. 2014;12:243.
34. Wang R, Rao MS. Application of mesenchymal stem cells in joint diseases. OA Musculoskelet Med. 2013;1:26.
35. Farini A, Sitzia C, Erratico S, Meregalli M, Torrente Y. Clinical applications of mesenchymal stem cells in chronic diseases. Stem Cells Int. 2014;2014:306573.
36. Counsel PD, Bates D, Boyd R, Connell DA. Cell therapy in joint disorders. Sports Health. 2014;7:27–37.
37. Mendonça MV, Larocca T, de Freitas SB, Villarreal C, Silva LF, Matos A, et al. Safety and neurological assessments after autologous transplantation of bone marrow mesenchymal stem cells in subjects with chronic spinal cord injury. Stem Cell Res Ther. 2014;5:126.
38. Orozco L, Soler R, Morera C, Alberca M, Sánchez A, García-Sancho J. Intervertebral disc repair by autologous mesenchymal bone marrow cells: a pilot study. Transplantation. 2011;92:822–8.
39. Kovacs FM, Abraira V, Gérvas J, Arana E, Peul WC, Schoene ML, et al. Overenthusiastic interpretations of a nonetheless promising study. Transplantation. 2012;93:e6–7.
40. Itescu S. Mesoblast—a global leader in cell based medicines. In: 34th Annual J.P. Morgan Healthcare Conference; San Francisco, CA; January 2016.
41. Behrens F, Tak PP, Ostergaard M, Stoilov R, Wiland P, Huizinga TW, et al. MOR103, a human monoclonal antibody to granulocyte-macrophage colony-stimulating factor, in the treatment of patients with moderate rheumatoid arthritis: results of a phase Ib/IIa randomised, double-blind, placebo-controlled, dose-escalation trial. Ann Rheum Dis. 2014;74:1058–64.
42. De Bari C. Are mesenchymal stem cells in rheumatoid arthritis the good or bad guys? Arthritis Res Ther. 2015;17:113.
43. Lefèvre S, Knedla A, Tennie C, Kampmann A, Wunrau C, Dinser R, et al. Synovial fibroblasts spread rheumatoid arthritis to unaffected joints. Nat Med. 2009;15:1414–20.
44. El-Jawhari JJ, El-Sherbiny YM, Jones EA, McGonagle D. Mesenchymal stem cells, autoimmunity and rheumatoid arthritis. QJM. 2014;107:505–14.

45. Letourneau PA, Menge TD, Wataha KA, Wade CE, S Cox C, Holcomb JB, et al. Human bone marrow derived mesenchymal stem cells regulate leukocyte-endothelial interactions and activation of transcription factor NF-kappa B. J Tissue Sci Eng. 2011;Suppl 3:001.
46. Carrillo-Galvez AB, Cobo M, Cuevas-Ocaña S, Gutiérrez-Guerrero A, Sánchez-Gilabert A, Bongarzone P, et al. Mesenchymal stromal cells express GARP/LRRC32 on their surface: effects on their biology and immunomodulatory capacity. Stem Cells. 2015;33:183–95.
47. Maumus M, Jorgensen C, Noël D. Mesenchymal stem cells in regenerative medicine applied to rheumatic diseases: role of secretome and exosomes. Biochimie. 2013;95:2229–34.
48. Mokarizadeh A, Delirezh N, Morshedi A, Mosayebi G, Farshid AA, Mardani K. Microvesicles derived from mesenchymal stem cells: potent organelles for induction of tolerogenic signaling. Immunol Lett. 2012;147:47–54.
49. Ottoboni L, De Feo D, Merlini A, Martino G. Commonalities in immune modulation between mesenchymal stem cells (MSCs) and neural stem/precursor cells (NPCs). Immunol Lett. 2015;168:228–39.
50. Jiang Y, Tuan RS. Origin and function of cartilage stem/progenitor cells in osteoarthritis. Nat Rev Rheumatol. 2014;11:206–12.
51. Uth K, Trifonov D. Stem cell application for osteoarthritis in the knee joint: a minireview. World J Stem Cells. 2014;6:629–36.
52. Czekanska EM, Czekanska EM, Ralphs JR, Alini M, Stoddart MJ. Enhancing inflammatory and chemotactic signals to regulate bone regeneration. Eur Cells Mater. 2014;28:320–34.
53. Ulivi V, Tasso R, Cancedda R, Descalzi F. Mesenchymal stem cell paracrine activity is modulated by platelet lysate: induction of an inflammatory response and secretion of factors maintaining macrophages in a proinflammatory phenotype. Stem Cells Dev. 2014;23:1858–69.
54. Maijenburg MW, van der Schoot CE, Voermans C. Mesenchymal stromal cell migration: possibilities to improve cellular therapy. Stem Cells Dev. 2012;21:19–29.
55. Gomez-Rodriguez V, Orbe J, Martinez-Aguilar E, Rodriguez JA, Fernandez-Alonso L, Serneels J, et al. Functional MMP-10 is required for efficient tissue repair after experimental hind limb ischemia. FASEB J. 2015;29:960–72.
56. Bobadilla M, Sainz N, Abizanda G, Orbe J, Rodriguez JA, Páramo JA, et al. The CXCR4/SDF1 axis improves muscle regeneration through MMP-10 activity. Stem Cells Dev. 2014;23:1417-27.
57. Chamberlain G, Fox J, Ashton B, Middleton J. Concise review: mesenchymal stem cells: their phenotype, differentiation capacity, immunological features, and potential for homing. Stem Cells. 2007;25:2739–49.
58. Gallina C, Turinetto V, Giachino C. A new paradigm in cardiac regeneration: the mesenchymal stem cell secretome. Stem Cells Int. 2015;2015:765846.
59. Ando Y, Matsubara K, Ishikawa J, Fujio M, Shohara R, Hibi H, et al. Stem cell-conditioned medium accelerates distraction osteogenesis through multiple regenerative mechanisms. Bone. 2014;61:82–90.
60. Ma L, Aijima R, Hoshino Y, Yamaza H, Tomoda E, Tanaka Y, et al. Transplantation of mesenchymal stem cells ameliorates secondary osteoporosis through interleukin-17-impaired functions of recipient bone marrow mesenchymal stem cells in MRL/lpr mice. Stem Cell Res Ther. 2015;6:104.
61. Hayashi Y, Murakami M, Kawamura R, Ishizaka R, Fukuta O, Nakashima M. CXCL14 and MCP1 are potent trophic factors associated with cell migration and angiogenesis leading to higher regenerative potential of dental pulp side population cells. Stem Cell Res Ther. 2015;6:111.
62. Koga Y, Yasunaga M, Moriya Y, Akasu T, Fujita S, Yamamoto S, et al. Exosome can prevent RNase from degrading microRNA in feces. J Gastrointest Oncol. 2011;2:215–22.
63. Subra C, Grand D, Laulagnier K, Stella A, Lambeau G, Paillasse M, et al. Exosomes account for vesicle-mediated transcellular transport of activatable phospholipases and prostaglandins. J Lipid Res. 2010;51:2105–20.
64. Borges FT, Reis LA, Schor N. Extracellular vesicles: structure, function, and potential clinical uses in renal diseases. Braz J Med Biol Res. 2013;46:824–30.
65. Katsuda T, Kosaka N, Takeshita F, Ochiya T. The therapeutic potential of mesenchymal stem cell-derived extracellular vesicles. Proteomics. 2013;13:1637–53.
66. Cocucci E, Meldolesi J. Ectosomes and exosomes: shedding the confusion between extracellular vesicles. Trends Cell Biol. 2015;25:364–72.
67. Raposo G, Stoorvogel W. Extracellular vesicles: exosomes, microvesicles, and friends. J Cell Biol. 2013;200:373–83.
68. György B, Szabó TG, Pásztói M, Pál Z, Misják P, Aradi B, et al. Membrane vesicles, current state-of-the-art: emerging role of extracellular vesicles. Cell Mol Life Sci. 2011;68:2667–88.
69. Tan SS, Yin Y, Lee T, Lai RC, Yeo RWY, Zhang B, et al. Therapeutic MSC exosomes are derived from lipid raft microdomains in the plasma membrane. J Extracell Vesicles. 2013;2:22614.
70. Lozito TP, Tuan RS. Endothelial and cancer cells interact with mesenchymal stem cells via both microparticles and secreted factors. J Cell Mol Med. 2014;18:2372–84.
71. Boomsma RA, Geenen DL. Evidence for transfer of membranes from mesenchymal stem cells to HL-1 cardiac cells. Stem Cells Int. 2014;2014:653734.
72. Kang K, Ma R, Cai W, Huang W, Paul C, Liang J, et al. Exosomes secreted from CXCR4 overexpressing mesenchymal stem cells promote cardioprotection via Akt signaling pathway following myocardial infarction. Stem Cells Int. 2015. doi:10.1155/2015/659890.
73. Hu G, Li Q, Niu X, Hu B, Liu J, Zhou S, et al. Exosomes secreted by human-induced pluripotent stem cell-derived mesenchymal stem cells attenuate limb ischemia by promoting angiogenesis in mice. Stem Cell Res Ther. 2015;6:10.
74. Zhao Q, Gregory CA, Lee RH, Reger RL, Qin L, Hai B, et al. MSCs derived from iPSCs with a modified protocol are tumor-tropic but have much less potential to promote tumors than bone marrow MSCs. Proc Natl Acad Sci U S A. 2015;112:530–5.
75. Baglio SR, Rooijers K, Koppers-Lalic D, Verweij FJ, Pérez Lanzón M, Zini N, et al. Human bone marrow- and adipose-mesenchymal stem cells secrete exosomes enriched in distinctive miRNA and tRNA species. Stem Cell Res Ther. 2015. doi:10.1186/s13287-015-0116-z.
76. Hudson M, Woodworth-Hobbs M, Rahnert J, Zheng B, Price S. Glucocorticoids reduce muscle atrophy-related microRNAs via exosomal microRNA packaging (11634). FASEB J. 2014;28 Suppl 1:1163.4.
77. Müller G. Microvesicles/exosomes as potential novel biomarkers of metabolic diseases. Diabetes Metab Syndr Obes. 2012;5:247–82.
78. Chen TS, Arslan F, Yin Y, Tan SS, Lai RC, Choo ABH, et al. Enabling a robust scalable manufacturing process for therapeutic exosomes through oncogenic immortalization of human ESC-derived MSCs. J Transl Med. 2011;9:47.
79. Lv H, Li L, Sun M, Zhang Y, Chen L, Rong Y, et al. Mechanism of regulation of stem cell differentiation by matrix stiffness. Stem Cell Res Ther. 2015;6:103.
80. Talele NP, Fradette J, Davies JE, Kapus A, Hinz B. Expression of α-smooth muscle actin determines the fate of mesenchymal stromal cells. Stem Cell Reports. 2015;4:1016–30.
81. Abdeen AA, Weiss JB, Lee J, Kilian KA. Matrix composition and mechanics direct proangiogenic signaling from mesenchymal stem cells. Tissue Eng Part A. 2014;20:2737–45.
82. Baker N, Tuan RS. The less-often-traveled surface of stem cells: caveolin-1 and caveolae in stem cells, tissue repair and regeneration. Stem Cell Res Ther. 2013;4:90.
83. Linero I, Chaparro O. Paracrine effect of mesenchymal stem cells derived from human adipose tissue in bone regeneration. PLoS One. 2014;9:e107001.
84. Jose S, Hughbanks ML, Binder BYK, Ingavle GC, Leach JK. Enhanced trophic factor secretion by mesenchymal stem/stromal cells with Glycine-Histidine-Lysine (GHK)-modified alginate hydrogels. Acta Biomater. 2014;10:1955–64.
85. Tratwal J, Mathiasen AB, Juhl M, Brorsen SK, Kastrup J, Ekblond A. Influence of vascular endothelial growth factor stimulation and serum deprivation on gene activation patterns of human adipose tissue-derived stromal cells. Stem Cell Res Ther. 2015;6:62.
86. Li C, Wu X, Tong J, Yang X, Zhao J, Zheng Q, et al. Comparative analysis of human mesenchymal stem cells from bone marrow and adipose tissue under xeno-free conditions for cell therapy. Stem Cell Res Ther. 2015;6:55.
87. Xie X, Ulici V, Alexander PG, Jiang Y, Zhang C, Tuan RS. Platelet-rich plasma inhibits mechanically induced injury in chondrocytes. Arthrosc J Arthrosc Relat Surg. 2015;31:1142–50.
88. Bellayr IH, Catalano JG, Lababidi S, Yang AX, Lo Surdo JL, Bauer SR, et al. Gene markers of cellular aging in human multipotent stromal cells in culture. Stem Cell Res Ther. 2014;5:59.
89. Nuschke A, Rodrigues M, Stolz DB, Chu CT, Griffith L, Wells A. Human mesenchymal stem cells/multipotent stromal cells consume accumulated autophagosomes early in differentiation. Stem Cell Res Ther. 2014;5:140.

90. Liew A, O'Brien T. Therapeutic potential for mesenchymal stem cell transplantation in critical limb ischemia. Stem Cell Res Ther. 2012;3:28.
91. Lan YW, Choo KB, Chen CM, Hung TH, Chen YB, Hsieh CH, et al. Hypoxia-preconditioned mesenchymal stem cells attenuate bleomycin-induced pulmonary fibrosis. Stem Cell Res Ther. 2015;6:97.
92. Maumus M, Manferdini C, Toupet K, Peyrafitte JA, Ferreira R, Facchini A, et al. Adipose mesenchymal stem cells protect chondrocytes from degeneration associated with osteoarthritis. Stem Cell Res. 2013;11:834–44.
93. Wu L, Leijten J, van Blitterswijk CA, Karperien M. Fibroblast growth factor-1 is a mesenchymal stromal cell-secreted factor stimulating proliferation of osteoarthritic chondrocytes in co-culture. Stem Cells Dev. 2013;22:2356–67.
94. Song X, Xie Y, Liu Y, Shao M, Wang W. Beneficial effects of coculturing synovial derived mesenchymal stem cells with meniscus fibrochondrocytes are mediated by fibroblast growth factor 1: increased proliferation and collagen synthesis. Stem Cells Int. 2015;2015:926325.
95. Leyh M, Seitz A, Dürselen L, Springorum HR, Angele P, Ignatius A, et al. Osteoarthritic cartilage explants affect extracellular matrix production and composition in cocultured bone marrow-derived mesenchymal stem cells and articular chondrocytes. Stem Cell Res Ther. 2014;5:77.
96. Lohan P, Coleman CM, Murphy JM, Griffin MD, Ritter T, Ryan AE. Changes in immunological profile of allogeneic mesenchymal stem cells after differentiation: should we be concerned? Stem Cell Res Ther. 2014;5:99.
97. Crop MJ, Baan CC, Korevaar SS, IJzermans JNM, Pescatori M, Stubbs AP, et al. Inflammatory conditions affect gene expression and function of human adipose tissue-derived mesenchymal stem cells. Clin Exp Immunol. 2010;162(I):474–86.
98. Waterman RS, Tomchuck SL, Henkle SL, Betancourt AM. A new mesenchymal stem cell (MSC) paradigm: polarization into a pro-inflammatory MSC1 or an immunosuppressive MSC2 phenotype. PLoS One. 2010;5:e10088.
99. Manferdini C, Maumus M, Gabusi E, Piacentini A, Filardo G, Peyrafitte JA, et al. Adipose-derived mesenchymal stem cells exert antiinflammatory effects on chondrocytes and synoviocytes from osteoarthritis patients through prostaglandin E2. Arthritis Rheum. 2013;65:1271–81.
100. Grassi F, Cattini L, Gambari L, Manferdini C, Piacentini A, Gabusi E, et al. T cell subsets differently regulate osteogenic differentiation of human mesenchymal stromal cells in vitro. J Tissue Eng Regen Med. 2016;10:305–14.
101. Faroni A, Mobasseri SA, Kingham PJ, Reid AJ. Peripheral nerve regeneration: experimental strategies and future perspectives. Adv Drug Deliv Rev. 2014. doi:10.1016/j.addr.2014.11.010.
102. Chen QH, Liu AR, Qiu HB, Yang Y. Interaction between mesenchymal stem cells and endothelial cells restores endothelial permeability via paracrine hepatocyte growth factor in vitro. Stem Cell Res Ther. 2015;6:44.
103. Bronckaers A, Hilkens P, Martens W, Gervois P, Ratajczak J, Struys T, et al. Mesenchymal stem/stromal cells as a pharmacological and therapeutic approach to accelerate angiogenesis. Pharmacol Ther. 2014;143:181–96.
104. Pati S, Khakoo AY, Zhao J, Jimenez F, Gerber MH, Harting M, et al. Human mesenchymal stem cells inhibit vascular permeability by modulating vascular endothelial cadherin/β-catenin signaling. Stem Cells Dev. 2011;20:89–101.
105. Li J, Ma Y, Teng R, Guan Q, Lang J, Fang J, et al. Transcriptional profiling reveals crosstalk between mesenchymal stem cells and endothelial cells promoting prevascularization by reciprocal mechanisms. Stem Cells Dev. 2015;24:610–23.
106. Hou Y, Ryu CH, Jun JA, Kim SM, Jeong CH, Jeun SS. IL-8 enhances the angiogenic potential of human bone marrow mesenchymal stem cells by increasing vascular endothelial growth factor. Cell Biol Int. 2014;38:1050–9.
107. Pedersen TO, Blois AL, Xue Y, Xing Z, Sun Y, Finne-Wistrand A, et al. Mesenchymal stem cells induce endothelial cell quiescence and promote capillary formation. Stem Cell Res Ther. 2014;5:23.
108. Lin RZ, Moreno-Luna R, Zhou B, Pu WT, Melero-Martin JM. Equal modulation of endothelial cell function by four distinct tissue-specific mesenchymal stem cells. Angiogenesis. 2012;15:443–55.
109. Kehoe S, Zhang XF, Boyd D. FDA approved guidance conduits and wraps for peripheral nerve injury: a review of materials and efficacy. Injury. 2012;43:553–72.
110. Tamaki T. Bridging long gap peripheral nerve injury using skeletal muscle-derived multipotent stem cells. Neural Regen Res. 2014;9:1333–6.
111. Oliveira JT, Bittencourt-Navarrete RE, de Almeida FM, Tonda-Turo C, Martinez AMB, Franca JG. Enhancement of median nerve regeneration by mesenchymal stem cells engraftment in an absorbable conduit: improvement of peripheral nerve morphology with enlargement of somatosensory cortical representation. Front Neuroanat. 2014;8:111.
112. Frattini F, Pereira Lopes FR, Almeida FM, Rodrigues RF, Boldrini LC, Tomaz MA, et al. Mesenchymal stem cells in a polycaprolactone conduit promote sciatic nerve regeneration and sensory neuron survival after nerve injury. Tissue Eng Part A. 2012;18:2030–9.
113. Carrier-Ruiz A, Evaristo-Mendonça F, Mendez-Otero R, Ribeiro-Resende V. Biological behavior of mesenchymal stem cells on poly-epsilon-caprolactone filaments and a strategy for tissue engineering of segments of the peripheral nerves. Stem Cell Res Ther. 2015;6:128.
114. Ryu H, Oh JE, Rhee KJ, Baik SK, Kim J, Kang SJ, et al. Adipose tissue-derived mesenchymal stem cells cultured at high density express IFN-β and suppress the growth of MCF-7 human breast cancer cells. Cancer Lett. 2015;37:213–21.
115. Maltman DJ, Hardy SA, Przyborski SA. Role of mesenchymal stem cells in neurogenesis and nervous system repair. Neurochem Int. 2011;59:347–56.
116. Kingham PJ, Kolar MK, Novikova LN, Novikov LN, Wiberg M. Stimulating the neurotrophic and angiogenic properties of human adipose-derived stem cells enhances nerve repair. Stem Cells Dev. 2014;23:741–54.
117. Bashir J, Sherman A, Lee H, Kaplan L, Hare JM. Mesenchymal stem cell therapies in the treatment of musculoskeletal diseases. PM R. 2014;6:61–9.
118. Schäfer S, Berger JV, Deumens R, Goursaud S, Hanisch UK, Hermans E. Influence of intrathecal delivery of bone marrow-derived mesenchymal stem cells on spinal inflammation and pain hypersensitivity in a rat model of peripheral nerve injury. J Neuroinflammation. 2014;11:157.
119. Jones J, Estirado A, Redondo C, Pacheco-Torres J, Sirerol-Piquer MS, Garcia-Verdugo JM, et al. Mesenchymal stem cells improve motor functions and decrease neurodegeneration in ataxic mice. Mol Ther. 2014;23:130–8.
120. Fargali S, Sadahiro M, Jiang C, Frick AL, Indall T, Cogliani V, et al. Role of neurotrophins in the development and function of neural circuits that regulate energy homeostasis. J Mol Neurosci. 2012;48:654–9.
121. McGregor NE, Poulton IJ, Walker EC, Pompolo S, Quinn JMW, Martin TJ, et al. Ciliary neurotrophic factor inhibits bone formation and plays a sex-specific role in bone growth and remodeling. Calcif Tissue Int. 2010;86:261–70.
122. Pasquin S, Sharma M, Gauchat JF. Ciliary neurotrophic factor (CNTF): new facets of an old molecule for treating neurodegenerative and metabolic syndrome pathologies. Cytokine Growth Factor Rev. 2015. doi:10.1016/j.cytogfr.2015.07.007.
123. Yu H, Fischer G, Ebert AD, Wu HE, Bai X, Hogan QH. Analgesia for neuropathic pain by dorsal root ganglion transplantation of genetically engineered mesenchymal stem cells: initial results. Mol Pain. 2015;11:1–13.
124. Li Y, Guo L, Ahn HS, Kim MH, Kim SW. Amniotic mesenchymal stem cells display neurovascular tropism and aid in the recovery of injured peripheral nerves. J Cell Mol Med. 2014;18:1028–34.
125. Teixeira FG, Panchalingam KM, Anjo SI, Manadas B, Pereira R, Sousa N, et al. Do hypoxia/normoxia culturing conditions change the neuroregulatory profile of Wharton Jelly mesenchymal stem cell secretome? Stem Cell Res Ther. 2015;6:133.
126. Amable PR, Teixeira MV, Carias RB, Granjeiro JM, Borojevic R. Protein synthesis and secretion in human mesenchymal cells derived from bone marrow, adipose tissue and Wharton's jelly. Stem Cell Res Ther. 2014;5:53.
127. Jackson WM, Nesti LJ, Tuan RS. Potential therapeutic applications of muscle-derived mesenchymal stem and progenitor cells. Expert Opin Biol Ther. 2010;10:505–17.
128. Jackson WM, Aragon AB, Bulken-Hoover JD, Nesti LJ, Tuan RS. Putative heterotopic ossification progenitor cells derived from traumatized muscle. J Orthop Res. 2009;27:1645–51.
129. Jackson WM, Lozito TP, Djouad F, Kuhn NZ, Nesti LJ, Tuan RS. Differentiation and regeneration potential of mesenchymal progenitor cells derived from traumatized muscle tissue. J Cell Mol Med. 2011;15:2377–88.
130. Jackson WM, Aragon AB, Djouad F, Song Y, Koehler SM, Nesti LJ, et al. Mesenchymal progenitor cells derived from traumatized human muscle. J Tissue Eng Regen Med. 2009;3:129–38.
131. Jackson WM, Alexander PG, Bulken-Hoover JD, Vogler JA, Ji Y, McKay P, et al. Mesenchymal progenitor cells derived from traumatized muscle enhance neurite growth. J Tissue Eng Regen Med. 2013;7:443–51.
132. Jackson WM, Aragon AB, Onodera J, Koehler SM, Ji Y, Bulken-Hoover JD, et al. Cytokine expression in muscle following traumatic injury. J Orthop Res. 2011;29:1613–20.

133. Kluk MW, Ji Y, Shin EH, Amrani O, Onodera J, Jackson WM, et al. Fibroregulation of mesenchymal progenitor cells by BMP-4 after traumatic muscle injury. J Orthop Trauma. 2012;26:693–8.
134. Smith LR. Influencing the secretion of myogenic factors from mesenchymal stem cells. Stem Cell Res Ther. 2014;5:96.
135. Sohn J, Lu A, Tang Y, Wang B, Huard J. Activation of non-myogenic mesenchymal stem cells during the disease progression in dystrophic dystrophin/utrophin knockout mice. Hum Mol Genet. 2015;24:3814–29.
136. Gurgis C, Mokbel N, DiGirolamo DJ. Therapies for musculoskeletal disease: can we treat two birds with one stone? Curr Osteoporos Rep. 2014;12:142–53.
137. Sassoli C, Nosi D, Tani A, Chellini F, Mazzanti B, Quercioli F, et al. Defining the role of mesenchymal stromal cells on the regulation of matrix metalloproteinases in skeletal muscle cells. Exp Cell Res. 2014;323:297–313.
138. Verhoekx JSN, Mudera V, Walbeehm ET, Hovius SER. Adipose-derived stem cells inhibit the contractile myofibroblast in Dupuytren's disease. Plast Reconstr Surg. 2013;132:1139–48.
139. Brew K, Nagase H. The tissue inhibitors of metalloproteinases (TIMPs): an ancient family with structural and functional diversity. Biochim Biophys Acta Mol Cell Res. 2010;1803:55–71.
140. Seebach E, Holschbach J, Buchta N, Bitsch RG, Kleinschmidt K, Richter W. Mesenchymal stromal cell implantation for stimulation of long bone healing aggravates Staphylococcus aureus induced osteomyelitis. Acta Biomater. 2015;21:165–77.
141. Aoyama T, Goto K, Kakinoki R, Ikeguchi R, Ueda M, Kasai Y, et al. An exploratory clinical trial for idiopathic osteonecrosis of femoral head by cultured autologous multipotent mesenchymal stromal cells augmented with vascularized bone grafts. Tissue Eng Part B Rev. 2014;20:233–42.
142. Aoyama T, Fujita Y, Madoba K, Nankaku M, Yamada M, Tomita M, et al. Rehabilitation program after mesenchymal stromal cell transplantation augmented by vascularized bone grafts for idiopathic osteonecrosis of the femoral head: a preliminary study. Arch Phys Med Rehabil. 2015;96:532–9.
143. Vogel S, Börger V, Peters C, Förster M, Liebfried P, Metzger K, et al. Necrotic cell-derived high mobility group box 1 attracts antigen-presenting cells but inhibits hepatocyte growth factor-mediated tropism of mesenchymal stem cells for apoptotic cell death. Cell Death Differ. 2015;22:1219–30.
144. Docheva D, Müller SA, Majewski M, Evans CH. Biologics for tendon repair. Adv Drug Deliv Rev. 2014;84:222–39.
145. Gaspar D, Holladay C, Pandit A, Zeugolis D. Progress in cell based therapies for tendon repair. Trends Biotechnol. 2015;84:240–56.
146. Angele P, Kujat R, Koch M, Zellner J. Role of mesenchymal stem cells in meniscal repair. J Exp Orthop. 2014;1:12.
147. Zellner J, Taeger CD, Schaffer M, Roldan JC, Loibl M, Mueller MB, et al. Are applied growth factors able to mimic the positive effects of mesenchymal stem cells on the regeneration of meniscus in the avascular zone? Biomed Res Int. 2014. doi:10.1155/2014/537686.
148. Ding Z, Huang H. Mesenchymal stem cells in rabbit meniscus and bone marrow exhibit a similar feature but a heterogeneous multi-differentiation potential: superiority of meniscus as a cell source for meniscus repair. BMC Musculoskelet Disord. 2015;16:65.
149. Centeno CJ, Pitts J, Al-sayegh H, Freeman MD. Anterior cruciate ligament tears treated with percutaneous injection of autologous bone marrow nucleated cells: a case series. J Pain Res. 2015;8:437–47.
150. Takayama K, Kawakami Y, Mifune Y, Matsumoto T, Tang Y, Cummins JH, et al. The effect of blocking angiogenesis on anterior cruciate ligament healing following stem cell transplantation. Biomaterials. 2015;60:9–19.
151. Hogan MV, Walker GN, Cui LR, Fu FH, Huard J. The role of stem cells and tissue engineering in orthopaedic sports medicine: current evidence and future directions. Arthrosc J Arthrosc Relat Surg. 2015;31:1017–21.
152. Carvalho ADM, Badial PR, Alvarez LEC, Yamada ALM, Borges AS, Deffune E, et al. Equine tendonitis therapy using mesenchymal stem cells and platelet concentrates: a randomized controlled trial. Stem Cell Res Ther. 2013;4:85.
153. Steplewski A, Fertala J, Beredjiklian P, Wang ML, Fertala A. Matrix-specific anchors: a new concept for targeted delivery and retention of therapeutic cells. Tissue Eng Part A. 2015;21:1207–16.
154. De Lisio M, Jensen T, Sukiennik RA, Huntsman HD, Boppart M. Substrate and strain alter the muscle-derived mesenchymal stem cell secretome to promote myogenesis. Stem Cell Res Ther. 2014;5:74.
155. Meleshko A, Prakharenia I, Kletski S, Isaikina Y. Chimerism of allogeneic mesenchymal cells in bone marrow, liver, and spleen after mesenchymal stem cells infusion. Pediatr Transplant. 2013;17:189–94.
156. Lozito TP, Taboas JM, Kuo CK, Tuan RS. Mesenchymal stem cell modification of endothelial matrix regulates their vascular differentiation. J Cell Biochem. 2009;107:706–13.
157. Lozito TP, Kuo CK, Taboas JM, Tuan RS. Human mesenchymal stem cells express vascular cell phenotypes upon interaction with endothelial cell matrix. J Cell Biochem. 2009;107:714–22.
158. Titorencu I, Pruna V, Jinga VV, Simionescu M. Osteoblast ontogeny and implications for bone pathology: an overview. Cell Tissue Res. 2014;355:23–33.
159. Chen WCW, Péault B, Huard J. Regenerative translation of human blood-vessel-derived MSC precursors. Stem Cells Int. 2015;2015:11.
160. Pisciotta A, Riccio M, Carnevale G, Lu A, De Biasi S, Gibellini L, et al. Stem cells isolated from human dental pulp and amniotic fluid improve skeletal muscle histopathology in mdx/SCID mice. Stem Cell Res Ther. 2015;6:156.
161. Mukherjee P, Mani S. Methodologies to decipher the cell secretome. Biochim Biophys Acta Proteins Proteomics. 2013;1834:2226–32.
162. Kupcova Skalnikova H. Proteomic techniques for characterisation of mesenchymal stem cell secretome. Biochimie. 2013;95:2196–211.
163. Caccia D, Dugo M, Callari M, Bongarzone I. Bioinformatics tools for secretome analysis. Biochim Biophys Acta Proteins Proteomics. 2013;1834:2442–53.
164. Brown KJ, Seol H, Pillai DK, Sankoorikal BJ, Formolo CA, Mac J, et al. The human secretome atlas initiative: implications in health and disease conditions. Biochim Biophys Acta Proteins Proteomics. 2013;1834:2454–61.
165. Roberts M, Wall IB, Bingham I, Icely D, Reeve B, Bure K, et al. The global intellectual property landscape of induced pluripotent stem cell technologies. Nat Biotechnol. 2014;32:742–8.
166. Sanz-Nogués C, O'Brien T. MSCs isolated from patients with ischemic vascular disease have normal angiogenic potential. Mol Ther. 2014;22:1888–9.
167. Lin W, Li M, Li Y, Sun X, Li X, Yang F, et al. Bone marrow stromal cells promote neurite outgrowth of spinal motor neurons by means of neurotrophic factors in vitro. Neurol Sci. 2014;35:449–57.
168. Lin R-Z, Moreno-Luna R, Li D, Jaminet SC, Greene AK, Melero-Martin JM. Human endothelial colony-forming cells serve as trophic mediators for mesenchymal stem cell engraftment via paracrine signaling. Proc Natl Acad Sci U S A. 2014;111:10137–42.
169. Seebach E, Freischmidt H, Holschbach J, Fellenberg J, Richter W. Mesenchymal stroma cells trigger early attraction of M1 macrophages and endothelial cells into fibrin hydrogels, stimulating long bone healing without long-term engraftment. Acta Biomater. 2014;10:4730–41.
170. Tsai TL, Wang B, Squire MW, Guo LW, Li WJ. Endothelial cells direct human mesenchymal stem cells for osteo- and chondro-lineage differentiation through endothelin-1 and AKT signaling. Stem Cell Res Ther. 2015;6:88.

STEM CELLS TRANSLATIONAL MEDICINE®

PLURIPOTENT STEM CELLS

Neurotrophically Induced Mesenchymal Progenitor Cells Derived from Induced Pluripotent Stem Cells Enhance Neuritogenesis via Neurotrophin and Cytokine Production

RACHEL M. BRICK,[a,b] AARON X. SUN,[a,c] ROCKY S. TUAN [a,b,c]

Key Words. Mesenchymal stem cells • Induced pluripotent stem cells • Nerve growth • Sholl analysis • Nanofiber scaffold • Neurotrophins • Cytokines • Nerve repair • Regenerative medicine • Tissue engineering

[a]Center for Cellular and Molecular Engineering, Department of Orthopaedic Surgery, University of Pittsburgh School of Medicine, Pittsburgh, Pennsylvania, USA; [b]Department of Pathology, University of Pittsburgh School of Medicine, Pittsburgh, Pennsylvania, USA; [c]Department of Bioengineering, University of Pittsburgh Swanson School of Engineering, Pittsburgh, Pennsylvania, USA

Correspondence: Rocky S. Tuan, Ph.D., Center for Cellular and Molecular Engineering, Department of Orthopaedic Surgery, University of Pittsburgh School of Medicine, 450 Technology Drive, Room 221, Pittsburgh, Pennsylvania 15219, USA. Telephone: 1 4126482603; e-mail: rst13@pitt.edu

Received April 27, 2017; accepted for publication November 6, 2017; first published December 7, 2017.

http://dx.doi.org/10.1002/sctm.17-0108

ABSTRACT

Adult tissue-derived mesenchymal stem cells (MSCs) are known to produce a number of bioactive factors, including neurotrophic growth factors, capable of supporting and improving nerve regeneration. However, with a finite culture expansion capacity, MSCs are inherently limited in their lifespan and use. We examined here the potential utility of an alternative, mesenchymal-like cell source, derived from induced pluripotent stem cells, termed induced mesenchymal progenitor cells (MiMPCs). We found that several genes were upregulated and proteins were produced in MiMPCs that matched those previously reported for MSCs. Like MSCs, the MiMPCs secreted various neurotrophic and neuroprotective factors, including brain-derived neurotrophic factor (BDNF), interleukin-6 (IL-6), leukemia inhibitory factor (LIF), osteopontin, and osteonectin, and promoted neurite outgrowth in chick embryonic dorsal root ganglia (DRG) cultures compared with control cultures. Cotreatment with a pharmacological Trk-receptor inhibitor did not result in significant decrease in MiMPC-induced neurite outgrowth, which was however inhibited upon Jak/STAT3 blockade. These findings suggest that the MiMPC induction of DRG neurite outgrowth is unlikely to be solely dependent on BDNF, but instead Jak/STAT3 activation by IL-6 and/or LIF is likely to be critical neurotrophic signaling pathways of the MiMPC secretome. Taken together, these findings suggest MiMPCs as a renewable, candidate source of therapeutic cells and a potential alternative to MSCs for peripheral nerve repair, in view of their ability to promote nerve growth by producing many of the same growth factors and cytokines as Schwann cells and signaling through critical neurotrophic pathways. STEM CELLS TRANSLATIONAL MEDICINE *2018;7:45–58*

SIGNIFICANCE STATEMENT

Using human induced pluripotent stem cells, progenitor cells that resemble adult tissue-derived mesenchymal stem cells, which are currently considered to be a promising cell type for regenerative therapies, have been derived. In addition to exhibiting similar surface markers and morphology, these cells secrete factors into their conditioned medium that are capable of promoting neurite sprouting and axon elongation in an embryonic dorsal root ganglion explant culture model. Given the indefinite life span of induced pluripotent stem cells, the findings of this study strongly suggest their utility as a source of neurotrophic cells that may be applied for nerve regeneration and repair.

INTRODUCTION

Peripheral nerve damage often accompanies and complicates limb injuries. Proper healing of nerve damage can be quite challenging, especially as the success of nerve regeneration is dependent upon the rate and quality of axon growth and myelination to bridge the gap across the injured area. Regeneration is mediated by Schwann cells, which secrete neurotrophic factors and migrate to form Bands of Büngner, a longitudinal tunnel that both guides the regenerating neuron toward its target and secretes neurotrophic factors to encourage nerve regrowth. However, this process is error-prone, and can often result in formation of painful neuromas. Currently, the gold standard treatment for peripheral nerve repair is a direct end-to-end suture. In the case of longer gaps where tension-less end-to-end sutures cannot be achieved, autologous nerve graft surgery at the sacrifice of other nerves from a donor site deemed less important is carried out [1]. However, the best treatment is

still limited, that is, even with multiple surgeries and meticulous care to align fascicles and match graft and host nerve sizes, complete motor function is often never fully regained, and may also leave the donor site at least partially deinnervated [2].

An alternative to the autologous nerve graft is an autologous Schwann cell transplant to the injured site. While this method does not sacrifice a healthy nerve, it still risks damage to the nerve at the Schwann cell donor site. The patient thus risks similar donor site morbidities as those seen in autologous nerve grafts. Allogeneic Schwann cell transplants have also been attempted, but due to the immunogenic nature of Schwann cells, these transplants are quickly rejected by the host [3]. Because of these limitations, a more practical approach is needed. To address this need, several studies have shown that bone marrow-derived mesenchymal stem cells (MSCs) have the ability to act as Schwann-like cells, given the proper induction environment, and can support nerve regeneration by secreting neurotrophic factors (NTFs) [4, 5].

While neurotrophically induced-MSCs (NI-MSCs) are capable of producing many of the same NTFs as Schwann cells, they have finite expansion capacity, and require invasive techniques to acquire, for example, bone marrow aspiration. Induced pluripotent stem cells (iPSCs), derived by reprogramming adult somatic cells, including MSCs, that exhibit embryonic stem cell (ESC)-like pluripotency, represent a potential cell source that can overcome this drawback. iPSCs are produced by reprogramming with four transcription factors and have a virtually unlimited expansion capacity. We have shown that after expansion, the iPSCs can be differentiated into MSC-like cells, which we have termed induced mesenchymal progenitor cells (MiMPCs) [6]. In this manner, this technology has the potential to yield an almost unlimited supply of MiMPCs. In this study, we aim to test if these MiMPCs, originally derived from MSCs, have the same ability to support neuronal regeneration as the parent MSC. With this capacity, MiMPCs may represent a potentially infinitely renewable cell source for the support of nerve regeneration and cell therapy. Our results reported here show that MiMPCs can secrete NTFs after neuroinductive treatment, and can produce factors to improve neurite outgrowth in vitro in a chick embryonic dorsal root ganglion (DRG) model. These findings suggest that neurotrophically induced-MiMPCs (NI-MiMPCs) may be considered a suitable substitute cell type to support nerve growth.

Materials and Methods

Generation of MiMPCs from iPSCs

A previously reported human iPSC line derived from reprogramming of human adult bone marrow MSCs was used [6]. Feeder-free, undifferentiated iPSCs colonies were grown to confluency in six-well plates coated with Matrigel (Corning, Corning, NY), using mTesR1 media (Stem Cell Technologies, Vancouver, Canada). Confluent iPSC colonies are switched from mTeSR1 media to MSC growth medium (GM), consisting of α-MEM (ThermoFisher, Waltham, MA), supplemented with 10% fetal bovine serum (FBS; ThermoFisher), 1 ng/ml fibroblast growth factor-2 (FGF2; RayBiotech, Norcross, GA), and antibiotic-antimycotic (penicillin-streptomycin/fungizone [PSF]; ThermoFisher). The iPSCs are maintained in the MSC growth medium for 7 days with medium changes every 2 to 3 days. After 1 week, cells are trypsinized and seeded into gelatin (Stem Cell Technologies, Vancouver, Canada) coated flasks for continued culture.

Neurotrophic Induction and Preparation of Conditioned Media

MiMPCs and control MSCs were plated at approximately 3,000 cells per cm^2 on gelatin-coated flasks and maintained in MSC GM until the cultures reached 70% confluency. Prior to culture in neurotrophic induction medium (NIM), cells were pretreated for a total of 72 hours: the first 24 hours with pretreatment medium consisting of α-MEM supplemented with 10% FBS, 1 mM β-mercaptoethanol (Sigma-Aldrich, St. Louis, MO), and PSF, and the following 48 hours of pretreatment included 35 ng/ml retinoic acid (RA; Sigma-Aldrich) in the pretreatment medium. For 7 days following pretreatment, MiMPCs and control MSCs were treated with NIM, consisting of Dulbecco's MEM (DMEM)/Ham's F-12 medium (ThermoFisher) supplemented with 5% FBS, 0.5 mM 3-isobutyl-1-methylxanthine (Sigma-Aldrich), 5 ng/ml platelet-derived growth factor (Peprotech, Rocky Hill, NJ), 50 ng/ml recombinant human neuregulin (hNRG1; R&D Systems, Minneapolis, MN), 10 ng/ml FGF2, 20 ng/ml epidermal growth factor (EGF; Peprotech), 6 μg/ml RA, 10 ng/ml IL-1β, and 2% vol/vol B-27 Supplement (ThermoFisher). The MiMPCs and MSCs remained in NIM medium for 7 days, with one intermittent medium change after 3 days in culture. After the 7-day induction in NIM, the MiMPCs and MSCs were cultured in a basal medium (DMEM-F12, 5% FBS, insulin-transferrin-selenium-X [ITS-X], penicillin-streptomycin [PS]; all reagents obtained from ThermoFisher) for 48 hours, at which point the medium samples were collected, filtered, and designated as 48-hour basal conditioned medium (48 hours BCM) for use in functional bioassay DRG culture experiments (see below).

Immunofluorescence Labeling

The culture medium was aspirated from the MiMPC, MSC, and Schwann cell control cultures (cell line sFN92.6, obtained from ATCC, Manassas, VA), and cells were washed with phosphate buffered saline (ThermoFisher). Cells were fixed with 4% paraformaldehyde (Electron Microscopy Sciences, Hatfield, PA) for 20 minutes, washed, and treated for 1 hour with hot 10 mm sodium citrate (Sigma-Aldrich) in 10% ethanol for antigen retrieval. After blocking with 5% FBS for at least 1 hour at room temperature, the cultures were incubated with primary antibodies for at least 4 hours at room temperature, or overnight at 4°C. Immunofluorescence was carried out to localize the following cell markers on MiMPC, MSC, and Schwann cell cultures both before and after neurotrophic induction treatment: Schwann markers—glial fibrillary acidic protein (GFAP) (chicken IgY; cat. ab4674), P75/NGFR (rabbit IgG; cat. ab8874), S100B (rabbit monoclonal IgG; cat. ab52642); pluripotency markers—Sox2 (rabbit IgG; cat. ab97959), SSEA4 (mouse IgG; cat. 560307), and Oct3/4 (mouse IgG; cat. 560308); and MSC markers—CD44 (mouse monoclonal IgG; cat. MAB7045), CD73 (mouse monoclonal IgG; cat. ab81720), and CD105 (goat IgG; cat. AF1097). Primary antibodies were diluted in block buffer per manufacturer's instructions. Samples were incubated with secondary antibodies, diluted in block buffer per manufacturer's instructions, for 1 hour at room temperature. All cells were nuclear-counterstained with 4′,6-diamidino-2-phenylindole dihydrochloride (DAPI; ThermoFisher) for approximately 1 minute. SSEA4 and Oct3/4 antibodies were obtained from BD Biosciences (Franklin Lakes, NJ). CD44 and CD105 antibodies were obtained from R&D Systems. All other antibodies were purchased from abcam (Cambridge, MA). Secondary antibodies used were AlexaFluor 488 conjugates from ThermoFisher (rabbit anti-goat IgG

[cat. A27012], goat anti-mouse IgG [A10680], goat anti-chicken IgY [A11039], donkey anti-rabbit IgG [A21206]).

ELISA

Neurotrophic induction was performed on MiMPC cultures as described above. After induction treatment, conditioned media were collected from the cultures and concentrations of brain-derived neurotrophic factor (BDNF), ciliary NTFs (CNTF), glial cell-derived neurotrophic factor, (GDNF), neurotrophin-3 (NT-3), and nerve growth factor (NGF) were assayed via DuoSet ELISA kits (R&D Systems) according to the manufacturer's protocols.

Additional ELISAs for non-neurotrophins were also performed on conditioned media, including interleukin-6 (IL-6), leukemia inhibitory factor (LIF), tumor growth factor-β (TGF-β), interleukin-10, neuregulin (NRG), and fibroblast growth factor 9 (DuoSet ELISA kits from R&D Systems).

Gene Expression Assay

RNA was isolated from induced MiMPCs using RNeasy Plus Mini Kit (Qiagen, Valencia, CA) according to manufacturer's protocol. cDNA was synthesized using Invitrogen's SuperScript III First-Strand kit (ThermoFisher). Real-time polymerase chain reaction (RT-PCR) was performed using SYBR Green PCR Master Mix from Life Technologies (ThermoFisher) and a StepOnePlus Real Time PCR machine (ThermoFisher). All gene expression levels were normalized to that of 18S rRNA as the control housekeeping gene. Primers for BDNF, GDNF, CNTF, and 18S rRNA were obtained from Qiagen, and the primer for NGF was obtained from Integrated DNA Technologies (Coralville, IA).

RT^2 Profiler PCR Arrays (Qiagen) were used to assay for expression of human neurotrophins and receptors, and inflammatory cytokines and receptors. Arrays were run using RT^2 SYBR Green ROX qPCR Mastermix (Qiagen) as per manufacturer's protocols. PCR data analysis and heat map generation were done via Qiagen's online RT^2 Profiler PCR Array Data Analysis (version 3.5; http://pcrdataanalysis.sabiosciences.com/pcr/arrayanalysis.php).

Dorsal Root Ganglia /MiMPC Coculture Assay

DRGs were harvested from day 9 chick embryos, using a previously described protocol [7]. The isolated DRGs were plated one per well of a 12-well plate coated with poly-D-lysine and laminin (both supplied by Sigma-Aldrich). Poly-D-lysine solution (100 ng/ml) was prepared and dispensed into each well of a 12-well plate, allowed to coat the plate for 3 days at 4°C with gentle rocking. Laminin (10 μg/ml) was prepared and applied as a supplemental coating in the same manner as poly-D-lysine.

The DRGs were allowed to adhere to the substrate in medium consisting of DMEM-F12 and 5% FBS, further supplemented with 10 ng/ml each of basic FGF-2, epithelial growth factor (EGF), and NGF. After a 3-day settlement period, medium on DRGs was exchanged for 48-hour basal conditioned medium (48-hour BCM) collected from: (a) NI-MiMPCs, (b) GM-MiMPCs, (c) NI-MSCs, or (d) GM-MSCs. Control DRGs were cultured in cell-free unconditioned basal medium consisting of DMEM-F12, 5% FBS, ITS-X, and pen-strep. All DRGs were cultured for 5 days. Cultures were then immunostained as outlined previously. Briefly, DRGs were fixed with 4% paraformaldehyde, incubated in hot sodium citrate for antigen retrieval, blocked in 5% FBS and incubated with chicken IgY anti-heavy neurofilament primary antibody (abcam; cat. ab4680) diluted to 1:10,000 overnight at 4°C. AlexaFluor 488 conjugated secondary antibody (ThermoFisher; cat. A11039) was allowed to incubate for 1 hour at room temperature at a 1:300 dilution with blocking buffer. Neurite outgrowth was quantitatively assessed (see below).

Trk Signaling Inhibition

To assess the involvement of Trk receptor-mediated neurotrophin signaling, the Pan-Trk inhibitor, GNF-5837 (Sigma-Aldrich), was used at a concentration of 24 nM, which exceeded IC_{50} values (7–11 nM for TrkA, TrkB, and TrkC) reported in the literature [8]. GNF-5837 was supplemented to 48-hours BCM from neurotrophically induced MiMPCs (NI-MiMPCs) and control MiMPCs (GM-MiMPCs), and neurotrophically induced MSCs (NI-MSCs) and control MSCs (GM-MSCs), which were subsequently used to culture chick DRGs for 5 days. Cultures were paraformaldehyde-fixed and immunostained for heavy neurofilament, and branching complexity of neurite outgrowth was assessed (see below).

JAK/STAT3 Inhibition

To assess the involvement of JAK/STAT3-mediated signaling, cucurbitacin I (Sigma-Aldrich), a selective inhibitor of the JAK/STAT3 signaling pathway that suppresses the levels of tyrosine phosphorylated STAT3 [9], was used at a concentration of 60 nM. Cucurbitacin was supplemented to 48-hours BCM from NI-MiMPCs and control MiMPCs, and NI-MSCs and control MSCs, which were subsequently used to culture chick DRGs for 5 days. Cultures were paraformaldehyde-fixed and immunostained for heavy neurofilament, and branching complexity of neurite outgrowth was assessed (see below).

Immunofluorescence Staining of DRG

DRG cultures were fixed in buffered 4% paraformaldehyde and permeabilized for antigen retrieval with hot 10 mM sodium citrate for 1 hour, blocked with 5% FBS, and incubated with mouse anti-human heavy neurofilament (1:500; abcam) in block buffer overnight at 4°C. After rinsing, cultures were then incubated with fluorescently labeled secondary antibodies (1:300; AlexaFluor 488 goat IgY [cat. A11039]; Invitrogen, Carlsbad, CA) for 1 hour at room temperature.

Quantitation of Neurite Extension

Fluorescent DRG image tiles were processed with MetaMorph (Molecular Devices, Sunnyvale, CA), and digitally stitched together using open source software Fiji/NIH ImageJ [10]. All grayscale images were thresholded to create binary bitmap images. Neurite extension densities were measured using the Sholl analysis plugin function within Fiji. The algorithm automatically retrieves data from two-dimensional (2D) or three-dimensional (3D) images to perform a regression analysis and generate the metrics for Sholl-based dendrite arborization [11]. All images were taken at ×4 magnification using an inverted microscope (Olympus IX81) with a motorized stage controlled through MetaMorph, and the scale used was 620 px = 1 mm.

Neurite extension lengths were quantified based on images of DRGs cultured on 2D aligned nanofibrous poly-ε-caprolactone (PCL) scaffolds prepared by electrospinning (see below). All images for scaffold cultures were taken at ×10 using the inverted Olympus scope (IX81). Tracings were converted from pixel length into μm measurements using the scale of 1245 px = 800 μm.

Preparation and Photocrosslinking of Methacrylated Gelatin (mGelatin)

mGelatin was prepared by reacting gelatin (type B) (Sigma-Aldrich) with methacrylic anhydride using our recently published

protocol [12]. Photocrosslinking was initiated using the visible-light sensitive initiator lithium phenyl-2,4,6-trimethylbenzoylphosphinate (LAP) [13].

Fabrication of Electrospun Scaffolds

A PCL-mGelatin composite scaffold was prepared using a modification of our recently published procedure [14]. Two separate solutions were prepared: (a) 14.0% wt/vol PCL (80 kDa; Sigma-Aldrich) in 2,2,2-trifluoroethanol (Sigma-Aldrich); and (b) 18% methacrylated-gelatin (mGelatin) in 95% 2,2,2-triflurorethanol in water to generate a mGelatin:PCL (40:60) composite nanofibrous scaffold. Two 10-ml syringes were separately filled with the PCL and mGelatin electrospinning solution, and they were fitted with a stainless steel 22G blunt-ended needle that served as a charged spinneret, and directed at a single central rotating mandrel (surface velocity of 10 m/s) in a custom-designed electrospinning apparatus. The speed of the mandrel was sufficiently fast to align the collected fibers in a single direction. A flow rate of 2 ml/hour was maintained with a syringe pump (Harvard Apparatus, Holliston, MA). A power supply (Gamma High Voltage Research, Inc., Ormond Beach, FL) applied a +15–20 kV potential difference between the needles and grounded mandrel to obtain a Taylor cone for mGelatin and a +7–10 kV potential difference for PCL. Additionally, two aluminum shields charged to +5kV were placed perpendicular to and on either side of the mandrel to better direct the electrospun fibers toward the grounded mandrel. The distance between the mandrel and the needle was 15 cm for mGelatin fibers and 15 cm for the PCL fibers. The composite electrospun scaffold was generated to a final thickness of 100 μm. The procedure was the same for creating randomly aligned scaffolds, except that the mandrel surface velocity was 0.75 m/s.

Preparation of Aligned Scaffolds and Seeding of DRGs

A 8% wt/vol mGelatin solution in HBSS (480 mg in 6 ml) was prepared, to which 1.8 mg of photoinitiator LAP was added to achieve a 0.3% wt/vol concentration of the photoinitiator. A 3.0 × 5.5 cm sheet of composite scaffold consisting of either aligned or random fibers prepared as described above was wetted with 540 μl of the mGelatin solution. Following this, each scaffold was folded lengthwise (along the 5.5 cm side) into thirds. The remaining 60 μl of the mGelatin solution was then evenly applied on top of the folded random scaffold, on top of which the folded aligned scaffold was placed. The six-layered construct was then exposed to visible light for 3 minutes (1.5 minutes on each side) to photopolymerize the construct. After construction of the completed multilayer scaffold, five cylinders of 8 mm diameter were punched out with a punch biopsy.

All scaffolds were prepared on the same day as DRG isolations and kept in basal medium (DMEM-F12, 5% FBS, ITS-X, and penstrep) until needed. DRGs were seeded as follows: (a) upon isolation from the chick embryo, DRGs were individually pipetted, and pipette tips were held above the scaffold and below the level of medium in the well; and (b) to ensure more accurate placement on the scaffolds, DRGs were allowed to descend out of the pipette via gravity, rather than being actively pipetted.

Statistical Analysis

All data were expressed as mean ± standard deviation. Statistical analysis was performed using one-way analysis of variance (ANOVA) followed by Games-Howell post hoc testing for all experiments except DRG neurite extensions, where Tukey's HSD post hoc was used. A threshold of $p < .05$ was used to determine statistical significance.

Results

iPSCs Can Be Differentiated into Cells with Neural Cell Phenotype

The iPSCs used in this study were obtained by lentiviral reprogramming of adult human bone marrow MSCs as described previously [6]. Morphological examination and immunofluorescence staining confirmed that these cells grew in colonies of small, undifferentiated cells, and that through their usage and numerous passages, they retained expression of pluripotency markers SSEA4, Oct3/4, and Sox2 (Fig. 1A–1D).

Feeder-free iPSCs were subsequently grown to confluency and differentiated into mesenchymal-lineage MiMPCs. On the third day of the differentiation period, a group of MiMPCs were set aside, paraformaldehyde-fixed and stained for mesenchymal, Schwann, and pluripotency markers in order to chart their transition. On day 3, it was shown that MiMPCs expressed mesenchymal markers CD44 and CD105, but was only weakly positive for CD73. MiMPCs were positive for all Schwann cell markers, and were positive for Sox2, faintly positive for Oct3/4, and negative for SSEA4 (Fig. 1E). This prompted us to extend the differentiation period in the protocol out to 7 days total, in order to give the cells more time to fully differentiate into a mesenchymal-like cell. With a 7-day differentiation protocol, cells were strongly positive for all mesenchymal markers, and negative for all pluripotency markers (Fig. 2).

These cells have been shown to be a distinct population of cells that express mesenchymal cell markers, such as CD44, CD73 and CD105, and are capable of behaving similarly to MSCs in that they can be differentiated along osteogenic, as well as adipogenic and chondrogenic lineages [6]. Phase contrast microscopy showed morphological changes examined indicating that while feeder-free iPSCs grew in undifferentiated colonies (Fig. 1A), after differentiation, MiMPCs (Fig. 1B) were morphologically similar to control MSCs (Fig. 1C). Immunohistochemistry also showed that MiMPCs, like MSCs and Schwann cell controls, expressed mesenchymal markers (CD44, CD105, and CD73) and neurologically relevant cell markers (GFAP, S100B, and p75-NGFR), the expression of which was not affected upon neuroinductive treatment (NI-MiMPCs and NI-MSCs). Similarly, noninduced MiMPCs and MSCs grown in growth medium (GM-MiMPCs and GM-MSCs) were also positive for mesenchymal and Schwann cell markers (Fig. 2).

MiMPCs and MSCs Maintain p75/NGFR and GFAP Expression

MSCs and MiMPCs expressed glial fibrillary acidic protein (GFAP) and low affinity p75 NGF receptor (p75/NGFR) both before and after neuroinductive (NI) treatment (Fig. 2). GFAP is an intermediate filament and is a major component of the astrocyte cytoskeleton, and may also play a role in maintenance of myelination [15]. p75/NGFR is important for axonal growth and Schwann cell migration during development, with severe peripheral neuronal defects resulting from its absence [16]. Presence of these neural markers suggested that both MSCs and MiMPCs phenotypically resembled Schwann cells regardless of whether or not the cells were treated with NI medium.

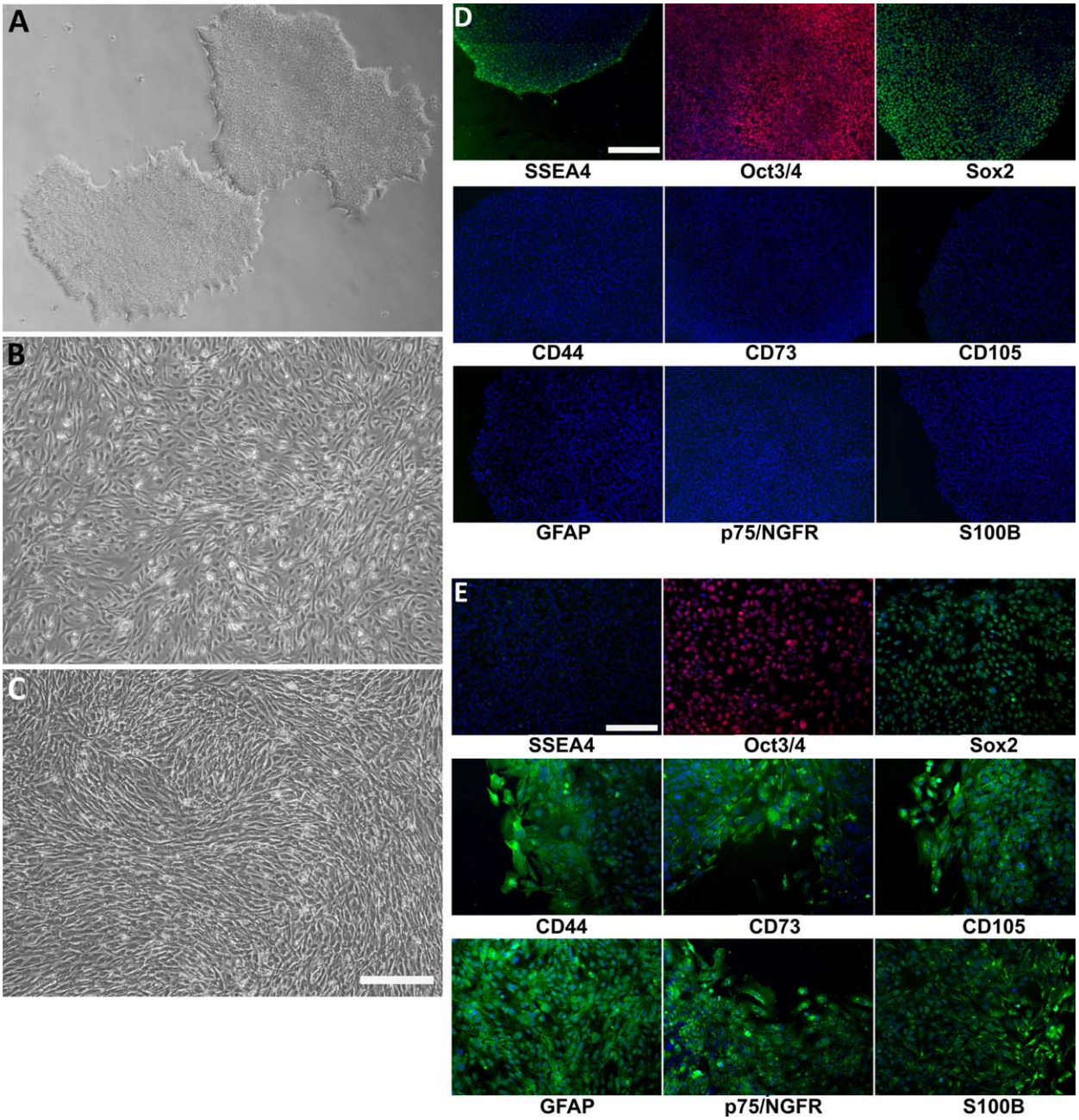

Figure 1. Morphology of induced mesenchymal progenitor cells (MiMPCs) and mesenchymal stem cells (MSCs) examined by phase contrast microscopy. **(A):** Undifferentiated colonies of human induced pluripotent stem cells (iPSCs) reprogrammed from human bone marrow MSCs [6]. Cells grew to confluent colonies on Matrigel, in feeder-free culture. **(B):** Confluent MiMPC cultures differentiated from iPSCs. All MiMPC cultures resembled MSCs in morphology, with no remaining iPSC morphology. **(C):** Confluent control MSCs isolated from human bone marrow (passage 5). Each cell type ($n > 5$) was cultured over the course of all experiments performed in this study. Cells in (A–C) were imaged at $\times 4$ magnification (Bar = 560 μm.) **(D, E):** MiMPCs were fixed and immunofluorescently stained on the third day of differentiation; colonies of confluent iPSCs served as controls. Cells were stained for MSC markers (CD44, CD73, and CD105), Schwann cell markers (GFAP, p75/NGFR, and S100B), and pluripotency stem cells markers (Sox2, SSEA4, and Oct3/4). All cells were counterstained with 4′,6-diamidino-2-phenylindole dihydrochloride. (D) iPSCs were negative for MSC and Schwann cell markers, but stained positively for pluripotency markers, indicating the maintenance of stemness throughout culture and passaging. (E) MiMPCs cells were strongly positive for CD44 and CD105, and weakly positive for CD73. MiMPCs also stained positive for all Schwann cell markers, positive for Sox2, weakly positive for Oct3/4, and negative for SSEA4, showing their transition and demonstrating the need for long differentiation period. Cells in (D, E) were imaged at $\times 10$ magnification (Bar = 220 μm). Abbreviation: GFAP, glial fibrillary acidic protein.

MiMPCs Produce BDNF as Well as Other Non-Neurotrophic Factors After Neurotrophic Induction

Analysis of gene expression using PCR array panels for neurotrophins and inflammatory cytokines showed an upregulation in genes relevant to nerve regeneration, including IL-6, LIF, IL-1B, and osteopontin (SPP1) in NI-MiMPCs, compared with GM-MiMPCs and to MSC groups (Supporting Information Fig. 1). ELISA results confirmed that the upregulated genes correlated with increased,

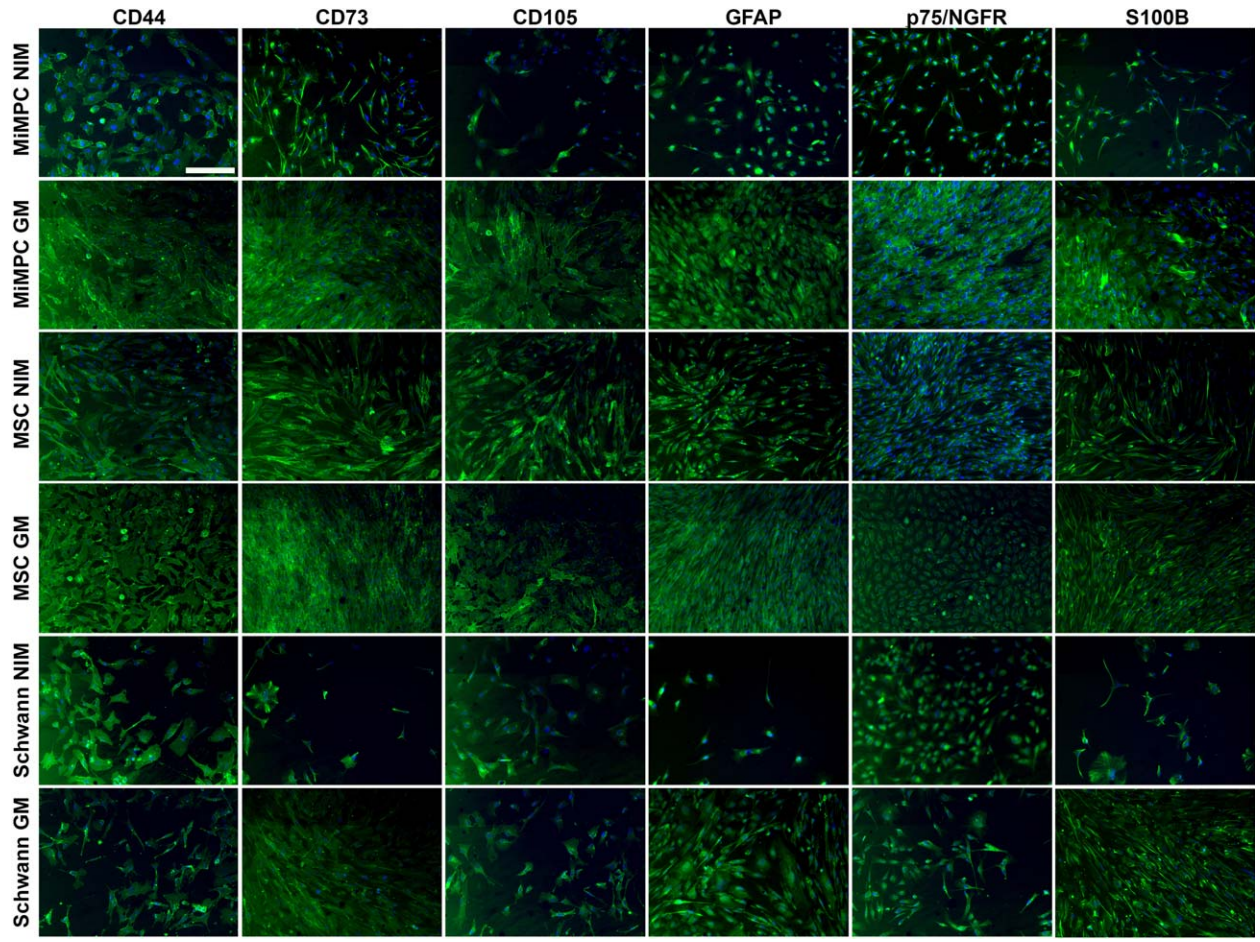

Figure 2. Expression of neurological and mesenchymal cell markers in MiMPCs and MSCs during neurotrophic induction examined by immunofluorescence. MiMPCs and MSCs were cultured in NIM or growth medium (GM). Neurotrophically induced MiMPCs and MSCs were fixed and stained with antibodies against MSC markers (CD44, CD73, CD105) and Schwann cell markers (GFAP, p75/NGFR, and S100B). Neurotrophically induced and noninduced MiMPC and MSC cultures stained positive for all MSC and Schwann cell markers. Schwann cells were stained as a control, and were positive for all markers. All cells were counterstained with 4′,6-diamidino-2-phenylindole dihydrochloride. All images were taken at $\times 10$ magnification and are representative of all fields. Bar = 220 μm, $n = 2$. Abbreviations: GFAP, glial fibrillary acidic protein; GM, growth medium; MiMPCs, induced mesenchymal progenitor cells; MSCs, mesenchymal stem cells; NIM, neurotrophic induction medium.

corresponding protein levels in cell culture supernatant. We did not conduct an ELISA to detect IL-1B, as 10 ng/ml of IL-1β was included in the NI medium.

As there was only approximately a 40% correlation between mRNA upregulation and protein production [17–19], we performed ELISAs to confirm the production of each of the aforementioned factors. Our ELISA data show that under normal growth medium conditions, control MSCs produced low levels of BDNF. Following neurotrophic induction, NI-MSCs produced significantly higher levels of BDNF. Although MiMPCs exhibited many of the same characteristics seen in MSCs, our results showed that GM-MiMPCs were able to produce small amounts of BDNF; in fact, BDNF production levels from GM-MiMPCs were comparable to those seen from induced MSCs. However, our ELISAs detected significantly higher BDNF production from MiMPCs after treatment with NI medium (Fig. 3).

BDNF production by MiMPCs was further enhanced when 10 ng/ml IL-1β was added to the NI medium. Conditioned medium assayed by ELISA during and after the induction period showed a consistent increase in BDNF concentrations compared with both normal NI medium and growth controls. The most marked increase in BDNF production by MiMPCs when IL-1β was present occurred at day 7, with an approximately fivefold increase in BDNF levels compared with that in MiMPCs cultured in NI-medium without IL-1β. Although this enhanced production of BDNF tapered off after the inductive medium was removed, conditioned medium collected 48-hours after induction still showed a twofold increase in BDNF concentration. While MSCs also showed a significant increase in BDNF production at Day 7, the total concentration was well below the levels detected in the MiMPC conditioned medium. The significant increase in BDNF production did not persist in conditioned medium taken from either MiMPCs or MSCs 48 hours after induction. However, at this time point, BDNF concentration from MiMPCs induced with NI-medium supplemented with IL-1B still remained higher than MiMPCs induced with normal NI-medium (Fig. 3). For this reason, we continued supplementing our NI-medium with 10 ng/ml IL-1β.

Other cytokines have been shown previously to improve nerve regeneration after injury, among them IL-6 [20, 21], LIF [22, 23], osteopontin, clusterin [24], and osteonectin [25–27].

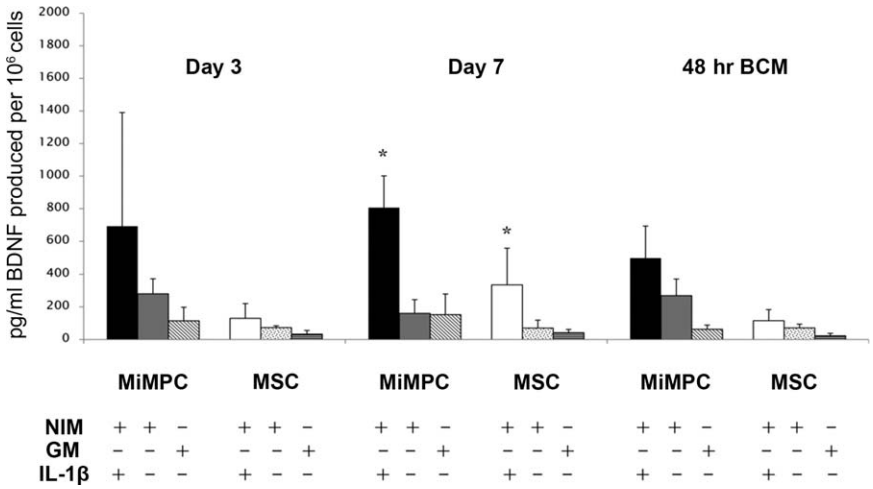

Figure 3. Effect of IL-1β on BDNF production in MiMPCs and MSCs. MiMPCs and MSCs were cultured in NIM, GM, or NIM including 10 ng/ml interleukin-1β (IL-1β). The presence (+) or absence (–) of NIM, GM, and/or IL-1β is as indicated. BDNF ELISA results showed that the presence of IL-1β in NIM significantly enhanced BDNF production by MiMPCs, particularly on day 7 (∼5-fold increase). This effect was less pronounced at 48-hours post-induction, although the level of BDNF in MiMPCs induced with NIM + IL-1β was still ∼2-fold higher than in NIM alone. *, $p < .05$ compared with GM controls, $n > 3$. Abbreviations: 48-hours BCM, 48-hour basal conditioned medium; BDNF, brain-derived neurotrophic factor; ELISA, enzyme-linked immunosorbent assay; NIM, neurotrophic induction medium; GM, growth medium; IL-1β, interleukin-1β; MiMPCs, induced mesenchymal progenitor cells; MSCs, mesenchymal stem cells.

Interestingly, the cytokine ELISA results on medium samples conditioned by NI-MiMPCs and NI-MSCs also demonstrated marked increases in the concentration of these factors (Fig. 4).

We assayed conditioned medium collected at days 3 and 7 of the NI medium treatment, as well as basal medium conditioned for 48-hours after the NI treatment period was over. The ELISA data in Figure 4 show that BDNF, IL-6, and osteonectin production remained relatively constant throughout and after the induction period (Fig. 4A, 4C, 4E), but there was a significant decrease in osteopontin and LIF production during and after the NI treatment period (Fig. 4B, 4D). Since osteopontin and LIF concentration levels were low in the NI-MiMPC conditioned basal medium, we focused on BDNF, IL-6, and osteonectin for our next set of experiments on the effects of MiMPCs and MSCs of neurite extension in DRG cultures.

Neurotrophically Induced MiMPCs Enhance Dorsal Root Ganglia Neurite Extension Complexity

We evaluated the effect of neurotrophically induced cells on nerve growth by culturing DRGs with conditioned medium from NI-MiMPCs and NI-MSCs (Fig. 5). All DRGs were dissected from 9-day-old chick embryos.

DRG neurite extension complexity was evaluated by Sholl analysis [28] using ImageJ. A morphological examination of immunofluorescence staining showed that DRGs cultured with both conditioned medium from NI- and GM-MiMPCs appeared to have significantly improved neurite outgrowth, compared with either control cultures or those cultured with conditioned media from NI-MSCs. DRGs cultured in conditioned medium from GM-MSCs also exhibited significantly enhanced neurite outgrowth. This demonstrated that MSCs and MiMPCs, particularly the latter, were producing factors that enhanced nerve growth.

Our first objective was to determine if BDNF production by these cells played a role in this improvement. The involvement of BDNF was tested by examining the effect of inhibiting the action of the neurotrophin Trk-receptor on DRG neurite outgrowth. The pan-Trk receptor inhibitor drug, GNF5837 (24 nM), was co-administered to the MiMPC conditioned medium treated DRGs. As shown in Figure 5A, DRG growth appeared to be only slightly reduced in complexity and size. The Sholl analysis results showed that, upon GNF5837 cotreatment, all conditioned medium treated groups, except for medium collected from NI-MiMPCs, experienced a marked decrease in neurite extension density such that they were no longer significantly different from controls, with average number of intersections decreasing from 319 to 139 [GM-MiMPC], 313 to 170 [GM-MSC], and increasing minimally from 173 to 215 [NI-MSC], as opposed to only a 10% decrease in measured branching density in cultures containing NI-MiMPC conditioned medium (286–257) (Fig. 5B). Furthermore, as our cells did not produce detectable levels of the neurotrophins, NGF, NT-3, CNTF, or GDNF, with the latter two not acting through the Trk receptors, this observation suggested that additional non-NTFs were likely being produced by NI-MiMPCs that were capable of initiating neurite extensions, acting independently of the Trk-receptors.

As many published investigations have suggested a role for IL-6 in nerve regeneration [20, 21, 29], and as our results suggested that BDNF was unlikely to be the only factor involved in enhancing neurite extension density, we sought to block the effects of IL-6 to determine if neurite density would be affected. As IL-6 signals through the Jak/STAT pathway, we targeted the inhibition of this pathway with a pharmacological blocker, cucurbitacin-I [9]. Results from the Sholl analysis showed that treatment with cucurbitacin-I decreased neurite complexity to the extent that the effects of the conditioned medium from noninduced cells was no longer significantly different from that seen in control cultures, with average numbers of intersections decreasing from 319 to 274 (GM-MiMPC), and 313 to 241 (GM-MSC). Although the average number of intersections increased slightly upon the addition of cucurbitacin-I in the NI-MiMPCs (286–425) and NI-MSCs (173–230) groups, the extent of standard deviation prevented the data from achieving statistical significance. However, conditioned medium from NI-MSCs still enhanced complexity of DRG neurite extensions compared with controls (Fig. 5B). The more pronounced effect of

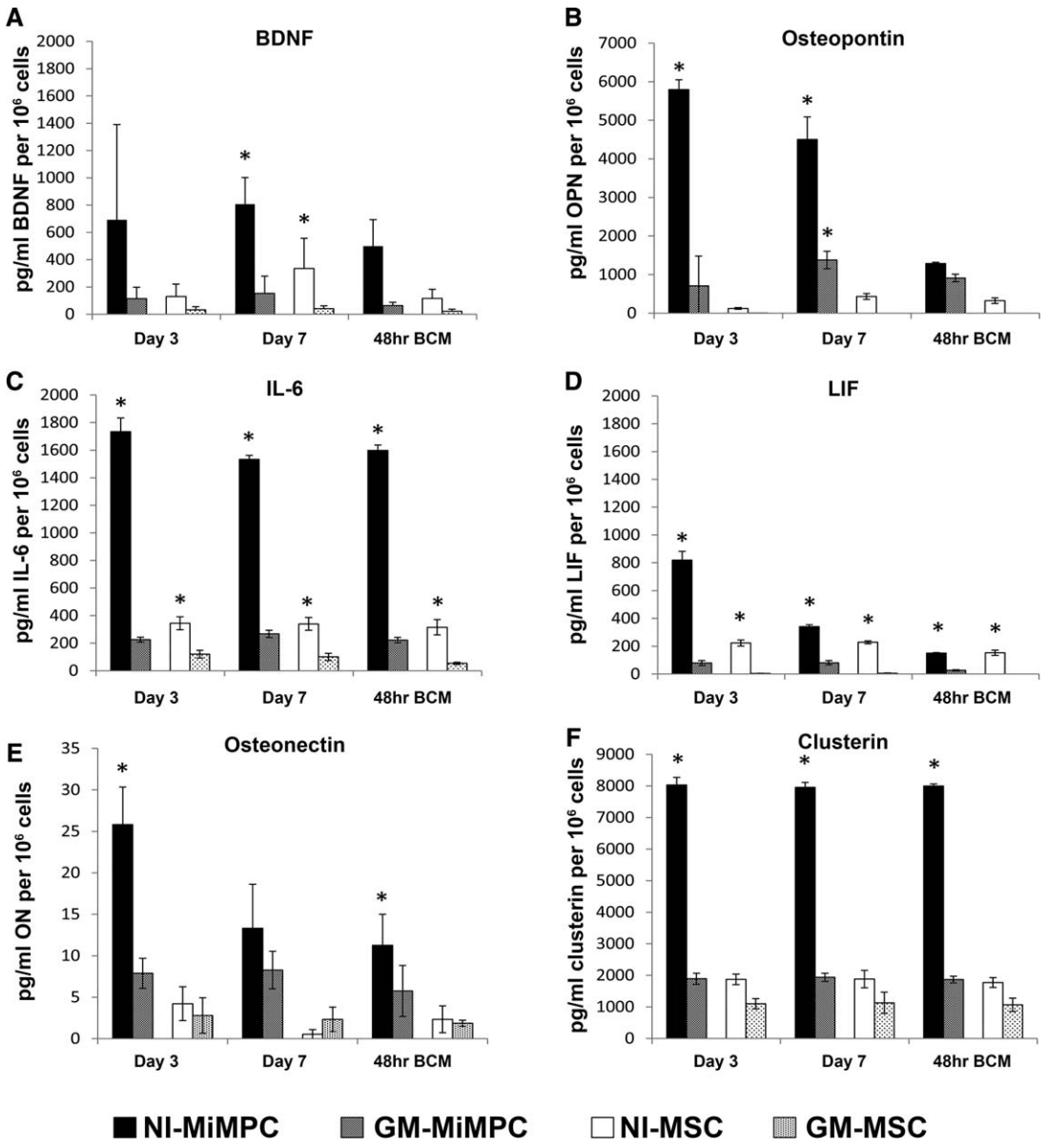

Figure 4. Production of neurotrophic factors by NI-MiMPCs and MSCs, quantified via ELISA. MiMPCs and MSCs were cultured in neurotrophic induction medium or growth medium. Conditioned media taken from days 3 and 7 of induction culture, and basal conditioned medium taken from cultures 48 hours post-induction (48-hour BCM). The conditioned media assayed include those from MiMPCs (induced, NI-MiMPCs; uninduced, GM-MiMPCs), and from MSCs (induced, MI-MSCs; uninduced, GM-MSCs), as well as basal medium (controls). Medium was assayed for levels of **(A)** BDNF, **(B)** Osteopontin, **(C)** IL-6, **(D)** LIF, **(E)** osteonectin, and **(F)** clusterin. All ELISA results are expressed in pg/ml or ng/ml produced per million cells. Medium taken from NI-MiMPC cultures contained high levels of all assayed factors compared with GM-MiMPCs, NI-MSCs, and GM-MSCs. BDNF, IL-6, osteonectin, and clusterin exhibited relatively constant secretion levels, while osteopontin and LIF showed decreased expression levels during induction treatment and the 48-hour post-induction period. *, $p < .05$, compared with GM controls, $n \geq 3$ for all assays. Abbreviations: BDNF, brain-derived neurotrophic factor; ELISA, enzyme-linked immunosorbent assay; IL-6, interleukin-6; LIF, leukemia inhibitory factor; MSCs, mesenchymal stem cells; NI-MiMPCs, neurotrophically induced-MiMPCs.

the addition of cucurbitacin-I to the DRG cultures, however, was the decrease in extension length (see below).

Neurotrophically Induced MiMPCs Enhance Dorsal Root Ganglia Neurite Extension Lengths

We next determined the influence of NI-MiMPCs on DRG neurite length. This was carried out using embryonic chicken DRGs cultured on electrospun 2D aligned nanofibrous PCL/gelatin scaffolds, which afforded more consistent and reliable measurements of neurite length (Fig. 6), as the aligned fibers helped to better organize neurite outgrowth, and allowed visualization and more precise measurements of axonal distance covered.

In doing so, we found that culturing DRGs in conditioned medium from any cell group significantly increased the length of neurite extensions compared with controls, although there was no difference between conditioned medium taken from any cell group (maximum length achieved with conditioned medium was 2,650 μm, while control lengths averaged 1,389 μm, an increase of 47.6%). There was no difference in lengths measured between induced and noninduced cells, or MiMPC and MSC groups (Fig. 6B).

Again, we co-administered 24 nM of GNF5837 to determine if any factor acting through the Trk receptors played a role in altering length of the extensions. It has been reported that BDNF, acting through TrkB, is capable of activating STAT3, which is essential in axon extension [30, 31]. However, the addition of the pharmacological blocker did not result in a difference in neurite extension lengths (Fig. 6B). This led us to conclude that, as with neurite initiation, BDNF was unlikely to be the sole factor produced by the NI- or GM-MiMPCs that contributed to neurite extension length, suggesting the action of other signaling pathway(s).

IL-6 Produced by MiMPCs Contribute to DRG Neurite Extension Length

Our results showed that GNF5837 inhibition of the Trk receptors did not affect the enhancement of neurite extension length by MiMPCs, as there was no observable or measurable difference in lengths between cultures where GNF5837 was absent or present (Fig. 6B). In view of the apparent difference in neurite extension density between exposure to NI-MiMPCs and GM-MiMPCs in the presence of the Trk-receptor inhibitor, we postulated that the induced MiMPCs must produce some factors, besides BDNF, to drive increased neurite extension density through non-Trk receptor mediated signaling, particularly the Jak/STAT pathway. Therefore, we looked to the presence of other secreted non-neurotrophin factors. Our PCR and ELISA data confirmed that NI-MiMPCs produced and maintained a high level of IL-6 compared with uninduced cells (see Supporting Information Figs. 1, 4), so our next set of experiments focused on the possible involvement of IL-6 on neuritogenesis and neurite extension length.

Cytokines in the IL-6 cytokine superfamily signal through the gp130 receptor to activate the Jak/STAT3 pathway, which has been shown to be important in the growth of neurite extensions and nerve regeneration [32, 33]. Our ELISA results (Fig. 4) showed that NI-MiMPCs were able of producing some cytokines in this family, including IL-6 and LIF, but not others, such as oncostatin-M and ciliary NTFs (CNTF) (data not shown). We postulated that these pro-inflammatory cytokines secreted into the conditioned medium from NI-MiMPCs could act through the Jak/STAT3 pathway to maintain improved neurite outgrowth, even when Trk-receptors were blocked.

To test this possibility, we chose the drug cucurbitacin-I to inhibit the Jak/STAT3 pathway [9]. Upon administration of cucurbitacin-I (60 nM) to the conditioned media, a dramatic decrease in neurite extension length and size of DRG cultures was observed (Fig. 6A). DRGs treated with cucurbitacin-I appeared to have stunted extension length while maintaining comparable number of neurite extensions. Sholl analysis confirmed that neuritogenesis, and therefore, density of neurite extensions, appeared unaffected (Fig. 6B). This indicated that while the actions of the Jak/STAT3 pathway and, by implication, the action of IL-6, was critical to neurite length, it did not play a crucial role in neuritogenesis.

To better measure neurite extension lengths in the presence of a Jak/STAT3 pharmacological inhibitor, DRGs were cultured on 2D nanofiber scaffolds, and treated with conditioned media containing 60 nM of cucurbitacin-I. We found that these DRG cultures on 2D nanofibrous scaffolds did not produce neurite extensions at all when grown in the presence of cucurbitacin-I, contrary to what was observed in cultures maintained on tissue culture plastic. Physical topography of cell culture substrate surfaces is well known to influence cell growth [34–36]. Our observations suggested that cucurbitacin-I could have affected the ability of the outgrowing neurites in interacting with different substrate surfaces, that is, tissue culture plastic versus nanofibers. Since there were no observable extensions from the cucurbitacin-I treated group, these measurements were not included in Figure 6B. As the complex, aligned topography is likely to be more relevant to tissue architecture in vivo, these results are consistent with an important role of IL-6 signaling through the Jak/STAT pathway in mediating the improvement of the length and complexity of neurite extensions by the MSC/MiMPC conditioned media.

Discussion

In this study, we have shown that MiMPCs are capable of supporting and enhancing neuritogenesis and axon length in DRG cultures. Their neurotrophic effects are similar to those of MSCs, and are enhanced with NI-medium treatment, although the latter exhibit effective neurotrophic support even without NI-medium treatment.

The goal of this study was to determine if NI-MiMPCs, which are generated from iPSCs and are thus available without additional, invasive cell harvesting, are capable of providing the support necessary for nerve regeneration. Our ultimate objective is to identify a candidate therapeutic cell type to support nerve growth akin to that seen by Schwann cells or induced MSCs. Our results suggest that MiMPCs may indeed be applicable for cell therapy for nerve injuries as nerve outgrowth in the DRG is enhanced by treatment with conditioned medium taken from MiMPC cultures.

MiMPCs generated from iPSCs morphologically resemble typical MSCs, and differ substantially from the parent iPSCs. iPSC colonies are negative for all mesenchymal and Schwann cell markers, but are instead positive for the pluripotency markers, SSEA4, Sox2, and Oct3/4. Our previous study demonstrated the pluripotency nature of the bone marrow MSC-derived iPSC line used here [6]. In contrast, characterization of MiMPCs showed positive staining for many of the same cell surface markers as both MSCs and Schwann cells, including CD44, CD73, CD105, GFAP, S100B, and P75/NGFR.

It is noteworthy that MiMPCs show expression of p75/NGFR. A study by Bentley and Lee [16] showed that the lack of p75/NGFR was linked to a deficit in Schwann cell migration and coverage, as well as a substantial reduction in nerve bundle and axon formation. Interestingly, there have also been reports stating the negative effects of p75 after injury, and that it may have a role in axon apoptosis and death signaling pathways [37, 38]. However, the literature related to p75 is insufficient to confirm whether or not the presence of p75 is helpful or harmful in terms of axon regeneration after injury, though some data suggest that a p75 antagonist can have neuro-protective effects on retinal ganglion [39]. In our study, MiMPC-conditioned medium was used to treat DRG cultures. The functional involvement of p75/NGFR will be tested in future studies by examining the effect of treatment with p75/NGFR inhibitors, for example, EVT901 [40], on neuritogenesis.

Our ELISA results show that NI-MiMPCs and NI-MSCs express BDNF, detectable in the conditioned media, although NI-MiMPCs are able to produce much higher levels of BDNF than NI-MSCs. However, conditioned media from MiMPCs and MSCs show comparable ability to encourage DRG neurite extension growth. Neurite extensions are denser when DRGs are cultured with

conditioned media taken from NI-MiMPCs and GM-MiMPCs, as well as GM-MSCs, as shown by Sholl analysis. Our initial thought was that the enhanced neurite growth resulted from the action of the NTFs, particularly the well-characterized BDNF, produced by the cells. We briefly investigated the effect of supplementing 20 ng/ml BDNF to basal medium and observed that the addition of BDNF improved neurite extension lengths compared with controls (data not shown). However, when the actions of BDNF were blocked via the pan-Trk receptor inhibition drug GNF5837, neurite extension outgrowth was not completely abolished, and in the case of NI-MiMPC conditioned medium, were still significantly denser than those found in DRG control growth cultures. This

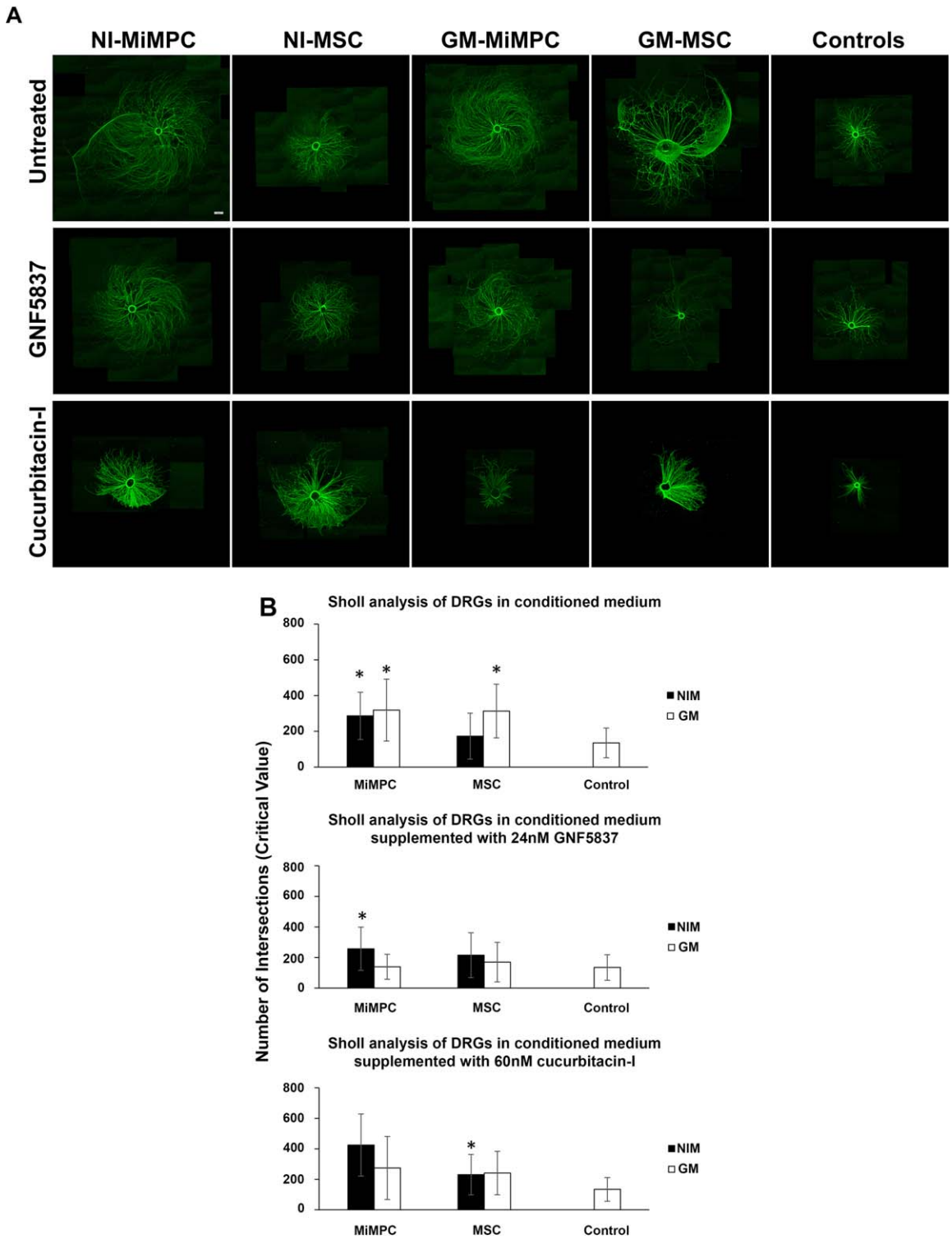

Figure 5.

finding strongly suggests that there may be another factor(s) present in the secretome of the induced MiMPCs and MSCs that aids neurite regeneration.

This unexpected result prompted us to investigate what other factors are produced by the cells that could be mediating the neurotrophic effect. Literature has shown that a varied host of cytokines and growth factors appear to have a positive effect on nerve regeneration [21, 24, 26, 27, 29, 41]. Our PCR array results show upregulation of the expression of a number of relevant cytokines, including IL-6, LIF, and osteopontin, the production of which is confirmed with ELISA performed on the cell-conditioned medium. We believe that aside from BDNF, these other cytokines may be responsible for the MiMPC and MSC mediated improvement of neurite growth observed in DRG cultures.

Osteonectin is a secreted matricellular protein that plays a role in bone mineralization by binding calcium to collagen [42]. Previous studies have shown that osteonectin can also play a role in promoting neural cell survival and initiating extension outgrowth [25, 26]. It has also been suggested that osteonectin and BDNF may work synergistically to promote neurite outgrowth. Although there is evidence to suggest that a specific receptor may exist, mediating osteonectin binding to cell surfaces in other tissues, such as smooth muscle cells and endothelial cells [25, 43, 44], this receptor has not yet been identified, and there is evidence to suggest that osteonectin only partially functions through the Trk receptors [27]. However, while both the MiMPCs and MSCs are capable of producing BDNF and osteonectin whether or not they have gone through neurotrophic induction, it seems that the positive effects of cell-conditioned medium on DRG outgrowth can be lessened, but not completely abolished, with the addition of GNF5837, a potent Trk-receptor inhibitor, for all conditioned medium groups except NI-MiMPCs. It is possible that dosage of both BDNF and osteonectin are important, or that osteonectin is operating through a yet unknown receptor pathway, which is likely as a major osteonectin-mediated signaling pathway has not yet been found [27]. Taking all this information together, it is likely that osteonectin production by the NI-MiMPCs is responsible for the increased neuritogenesis, and therefore, higher neurite extension density compared with controls, even in the presence of GNF5837. In our next studies, we plan to deplete osteonectin from the conditioned medium to assess whether osteonectin plays a synergistic role with BDNF in enhancing DRG neurite growth.

Osteopontin, a cell adhesion molecule that is expressed in a wide variety of cell types, has been implicated in cell survival and inflammatory regulation [45, 46]. A limited number of studies have suggested that osteopontin also plays a role in nerve regeneration, although the association is more likely to be with motor neuron outgrowth rather than sensory DRG neuron outgrowth [24, 46]. Clusterin is another commonly expressed glycoprotein found in most tissues, and various functional roles for clusterin have been implicated, including pathogenesis of Alzheimer's, and alleviation of peripheral neuropathy in rats [47, 48]. Interestingly, mRNA levels of clusterin were reported to increase after peripheral nerve injury, and as clusterin is involved in lipid recycling, it was suggested that the presence of this molecule at the site of injury aids Wallerian degeneration and Schwann cell proliferation [49, 50]. Meanwhile, clusterin may also signal through the megalin receptor, a pathway which has been shown in the DRG to selectively promote sensory neuron outgrowth [50, 51]. Although only sensory neurite outgrowth is assayed in the in vitro DRG model used here, the fact that the MiMPCs are capable of producing osteopontin as well as clusterin, suggests the potential application of MiMPCS for motor nerve injuries, further enhancing their clinical relevance.

It is well established that cytokines found in the IL-6 superfamily activate the Jak/STAT3 pathway, which is an important signaling pathway in neurite axon extension [33, 52]. We observed that upon pharmacologic blocking of Jak/STAT3 pathway activation, using cucurbitacin-I, the MiMPC/MSC-conditioned medium could not rescue the length of neurite extension, regardless of whether the conditioned medium was taken from induced cells or not. That only certain growth factors and cytokines, including IL-6, but not LIF, maintained their higher concentrations during and after the neuroinductive treatment period suggests that enhancement of neurite extensions found in conditioned medium cultures is a result of these cytokines, particularly IL-6, produced by the cells, by activating STAT3. Naturally, the possibility exists that LIF, also a potent cytokine, may exert a similar effect as IL-6 at a lower concentration [53]. However, as the equimolar potency of LIF versus IL-6 has been compared only on microvascular and endothelial cells [53], whether the two cytokines have similar effects on nerve regeneration remains to be assessed.

Topographical cues have long been found to affect cell adhesion, growth and differentiation [36, 54–56]. Multiple studies have shown the advantages of culturing DRGs on aligned surfaces, with improved adherence and axon elongation [34, 35, 56]. Therefore,

Figure 5. Immunofluorescent images and Sholl analysis of DRG neurite outgrowth upon treatment with conditioned media derived from neurotrophically induced MiMPCs and MSCs. **(A)**: Chick embryonic DRGs were cultured for 5 days in basal medium previously conditioned for 48 hours by NI-MiMPCs, NI-MSC, GM-MiMPCs, or GM-MSCs, or cultured in unconditioned basal medium (controls). For pan-Trk receptor inhibition, the inhibitor GNF5837 (24 nM final concentration) was added to each conditioned medium group and used to culture DRGs. Jak/STAT3 inhibition was achieved by the addition of the Jak/STAT3 inhibitor, cucurbitacin-I, at a final concentration of 60 nM, to each conditioned medium group and used to culture DRGs. Cultures exposed to conditioned media show substantial increase in size and complexity of neurite outgrowth compared with control groups. Cotreatment with GNF5837 did not result in apparent changes in neurite extension lengths. Cucurbitacin-I treatment drastically decreased the neurite extension lengths. Bar = 560 μm. **(B)**: Conditioned media from MiMPCs and MSCs are derived from (left) uninduced cells, and (right) induced cells. Sholl analysis measures the highest value of number of intersections where neurite branching is most dense (critical value). Controls consisted of basal medium alone that was not unconditioned by cells. Sholl analysis was carried out on DRG cultures exposed to conditioned media alone (top row), or conditioned media in the presence of the pan-Trk inhibitor, GNF5837 (24 nM final concentration) (middle row), or the Jak/STAT3 inhibitor, cucurbitacin-I (60 nM final concentration). Sholl analysis showed that conditioned medium from uninduced MiMPCs and MSCs significantly increased DRG neurite branching complexity compared with controls. Conditioned medium from NI-MiMPCs significantly increased DRG neurite branching complexity even in the presence of GNF5837. Conditioned medium from induced MSCs were unable to enhance branching complexity, and could not rescue neuritogenesis in the presence of GNF5837. The presence of cucurbitacin-I in conditioned medium decreased the number of neurite extensions in all conditioned medium except for that collected from induced MSCs. *, $p < .05$, indicating significant differences in complexity, compared via Games-Howell tests. At least 10 images per group were quantified via Sholl analysis. Abbreviations: DRG, dorsal root ganglia; GM-MiMPCs, control MiMPCs; GM-MSCs, control MSCs; NI-MSCs, neurotrophically induced-MSCs; NI-MiMPCs, neurotrophically induced-MiMPCs.

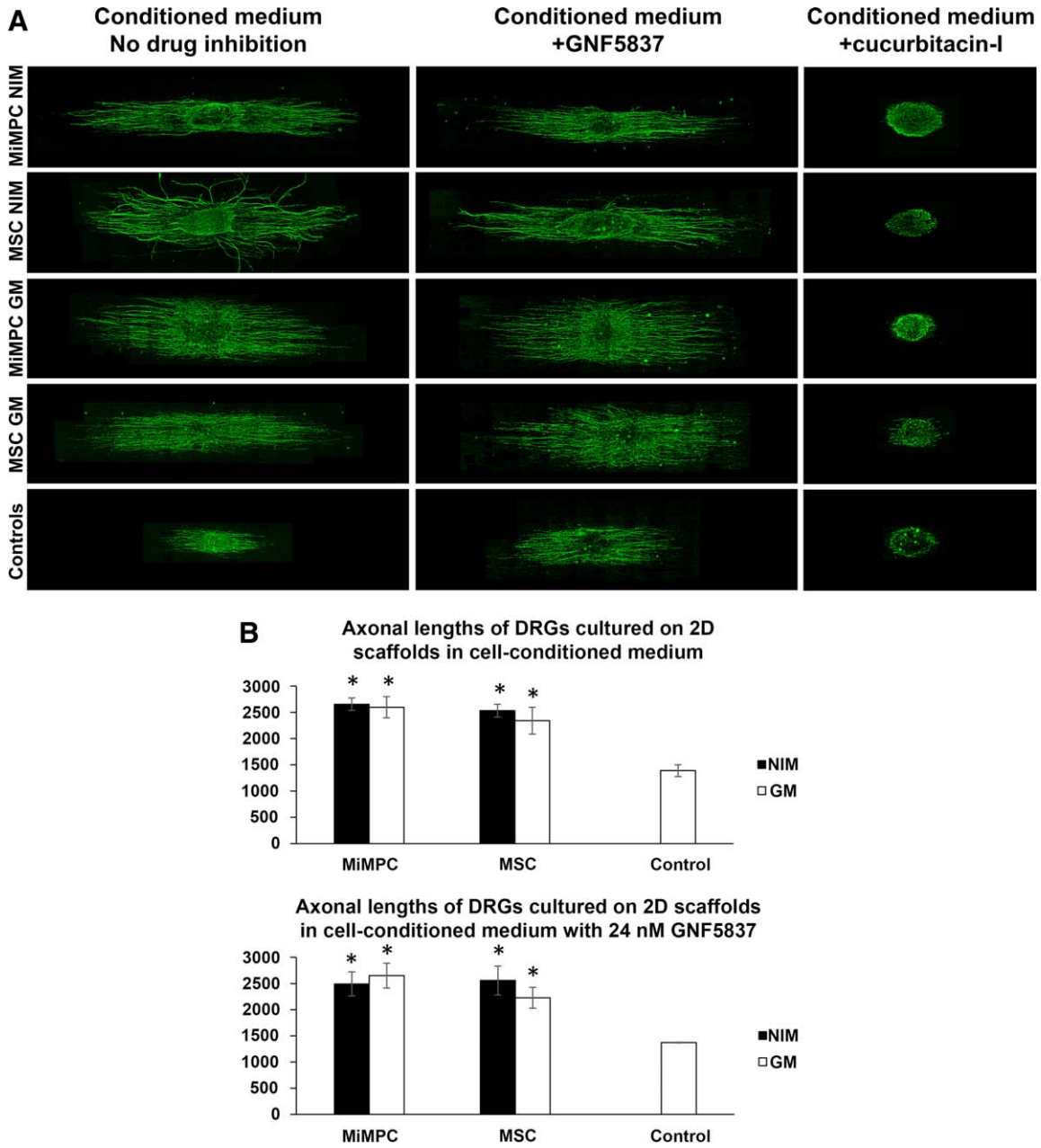

Figure 6. Morphological effect of MiMPCs and MSCs on neurite outgrowth in DRGs grown on electrospun nanofibrous scaffolds via image analysis and measurements by NIH ImageJ. **(A)**: DRGs were cultured on aligned nanofibrous scaffolds prepared as described in Materials and Methods, using media conditioned by induced (NI) and noninduced (GM) MiMPCs and MSCs, with or without cotreatment with the pan Trk-receptor inhibitor, GNF5837 (24 nM), or the Jak/Stat inhibitor, cucurbitacin-I (60 nM). No observable difference in neurite extension lengths was seen, compared with cultures without GNF5837 cotreatment. On the other hand, cucurbitacin-I cotreatment resulted in substantial decrease in in neurite extension length, compared with controls or any other group. Neurite extension lengths were measured with ImageJ. Bar = 800 μm. **(B)**: Neurite extension outgrowth was traced using NIH ImageJ. DRGs were cultured on aligned scaffolds with conditioned media collected from NI- and GM- MiMPCs and MSCs. Results on neurite outgrowth lengths indicate that exposure to NI- and GM- MiMPC and MSC conditioned media improved neurite outgrowth compared with controls, and the addition of Trk-receptor inhibitor (+GNF5837) did not impede length of neurite extension. *, $p < .05$, denotes statistically significant difference compared with both controls. At least 10 axons were measured per group over an $n = 3$. Abbreviations: GM, growth medium; MiMPCs, induced mesenchymal progenitor cells; MSCs, mesenchymal stem cells; NIM, neurotrophic induction medium.

we chose such favorable environments consisting of an aligned nanotopographical surface for DRG cultures to examine the potential advantage of combining MiMPC/MSC conditioned medium with scaffolds on neurite outgrowth. In Figure 6, length measurements showed enhanced DRG axon elongation in conditioned medium cultures compared with controls, although there were no significant differences between the various conditioned medium groups. This result could be due to the fact that NI-treated MiMPCs did not proliferate as well as NI-MSCs. Thus, while MiMPCs are capable of producing more neurotrophins and

cytokines per cell, the overall reduced cell count compared with that of MSCs results in a comparable level of neurotrophins produced per population of cells, and lack of significant difference in axon length between the two groups. Another possibility is that a saturated concentration of neurotrophins has already been reached or exceeded in the experimental system, that is, a "maximum" concentration of neurotrophins and cytokines at which an observable increase in axon length occurs.

All experiments were performed with MiMPCs differentiated from human MSC-derived iPSCs, and the results were compared with those achieved by human MSCs. Sholl analysis on DRGs cultured in conditioned medium on tissue culture plastic, and length measurements taken from DRGs cultured on 2D aligned scaffolds showed enhanced branching and length compared with controls. Our findings show that MiMPCs can provide similar advantages as MSCs, which makes MiMPCs clinically applicable, and can serve as a less invasive and, more importantly, sustainable therapeutic method.

While our findings suggest the potential neurotrophic capabilities of MiMPCs, there are a number of caveats. First, it is noteworthy that MiMPCs are less hardy than MSCs, namely, MiMPCs showed lower viability in the serum-free, neuro-inductive medium. In the literature, induction media treatments are achieved with a 0%–2% serum content [4, 5, 57], while in our investigation, serum content of NIM for MiMPCs was elevated to 5%, which we believe did not significantly compromise production of NTFs. Second, chick embryonic DRGs were used as an in vitro model for functional bioassay of NTFs production by NI-MiMPCs. While this is a well-established system to study neurotrophic effects, it will be necessary to assess NI-MiMPC NTF production and function using mammalian, and preferably in vivo, system as well.

Conclusion

In this study, we have determined that MiMPCs support neurite sprouting and axon elongation through the secretion of neurotrophic factors and are a viable alternative to MSCs for nerve regeneration. Our next work will focus on in vivo studies, designed to determine if combining MiMPCs in a bioscaffold will be beneficial for repairing traumatic sciatic nerve injury in a rat model. As both length and branching pattern were similar upon exposure of DRGs to NI-MiMPCs and GM-MiMPCs in vitro, our in vivo study will use GM-MiMPCs for practicality and ease of cell preparation. Our current research with MiMPCs have focused on differentiation and potential cellular therapy candidates for nerve regeneration, however, in future studies, it may be beneficial to characterize in greater detail the full scope of differences between MiMPCs and MSCs or Schwann cells in terms of secretome and mechanisms behind these differences. Our current experiments did not include Schwann cells for the simple fact that our goal was not to replace the patient's native Schwann cell, but rather, to identify a possible substitute for the MSC, which is by far more ubiquitous in regenerative medicine research, and likeness to the MSC will offer more wide-reaching avenues of future studies. With these studies, we hope to critically examine the applicability of MiMPCs as an alternative cell type to autologous Schwann cells or MSCs to aid the healing of peripheral nerve injuries, particularly those resulting from trauma.

Acknowledgments

We thank Dr. Heidi Zupanc for instructions on DRG isolation, immunofluorescence, and ELISA, Dr. Solvig Diederichs for supplying and instructions on culture of iPSCs, Dr. Jian Tan for isolating and providing control MSCs, and fellow laboratory colleagues for their support and thoughtful comments on this work. This study was supported by the Commonwealth of Pennsylvania Department of Health (SAP 4100050913), and U.S. Department of Defense (W81XWH-10-2-0084, W81XWH-15-1-0600).

Author Contributions

R.M.B., A.X.S., and R.S.T.: manuscript writing, final approval of the manuscript

Disclosure of Potential Conflicts of Interest

The authors indicated no potential conflicts of interests.

Note Added in Proof

This article was published online on 07 December 2017. Minor edits have been made that do not affect data. This notice is included in the online and print versions to indicate that both have been corrected 28 December 2017.

References

1 Fairbairn NG, Meppelink AM, Ng-Glazier J et al. Augmenting peripheral nerve regeneration using stem cells: A review of current opinion. World J Stem Cells 2015;7:11–26.

2 Wolford LM, Stevao ELL. Considerations in nerve repair. Proc (Bayl Univ Med Cent) 2003;16:152–156.

3 Mosahebi A, Fuller P, Wiberg M et al. Effect of allogeneic Schwann cell transplantation on peripheral nerve regeneration. Exp Neurol 2002;173:213–223.

4 Keilhoff G, Stang F, Goihl A et al. Transdifferentiated mesenchymal stem cells as alternative therapy in supporting nerve regeneration and myelination. Cell Mol Neurobiol 2006;26:1233–1250.

5 Jackson WM, Alexander PG, Bulken-Hoover JD et al. Mesenchymal progenitor cells derived from traumatized muscle enhance neurite growth. J Tissue Eng Regen Med 2013;7:443–451.

6 Diederichs S, Tuan RS. Functional comparison of human induced pluripotent stem cell-derived mesenchymal cells and bone marrow-derived mesenchymal stromal cells from the same donor. Stem Cells Dev 2014;23:1594–1610.

7 Nishi R. Autonomic and sensory neuron cultures. In: Marianne B-F, ed. Methods in Cell Biology, Chapter 13. New York: Academic Press, 1996;51:249–263.

8 Albaugh P, Fan Y, Mi Y et al. Discovery of GNF-5837, a selective TRK inhibitor with efficacy in rodent cancer tumor models. ACS Med Chem Lett 2012;3:140–145.

9 Blaskovich MA, Sun J, Cantor A et al. Discovery of JSI-124 (cucurbitacin I), a selective Janus kinase/signal transducer and activator of transcription 3 signaling pathway inhibitor with potent antitumor activity against human and murine cancer cells in mice. Cancer Res 2003;63:1270–1279.

10 Schindelin J, Arganda-Carreras I, Frise E et al. Fiji: An open-source platform for biological image analysis. Nat Methods 2012;9:676. 10.1038/nmeth.2019.

11 Ferreira TA, Blackman AV, Oyrer J et al. Neuronal morphometry directly from bitmap images. Nat Methods 2014;11:982–984.

12 Lin H, Zhang D, Alexander PG et al. Application of visible light-based projection stereolithography for live cell-scaffold fabrication with designed architecture. Biomaterials 2013;34:331–339.

13 Fairbanks BD, Schwartz MP, Bowman CN et al. Photoinitiated polymerization of PEG-diacrylate with lithium phenyl-2,4,6-trimethylbenzoylphosphinate: Polymerization rate and cytocompatibility. Biomaterials 2009; 30:6702–6707.

14 Yang G, Lin H, Rothrauff BB et al. Multilayered polycaprolactone/gelatin fiber-hydrogel composite for tendon tissue engineering. Acta Biomater 2016;35:68–76.

15 Liedtke W, Edelmann W, Bieri PL et al. GFAP is necessary for the integrity of CNS white matter architecture and long-term maintenance of myelination. Neuron 1996;17:607–615.

16 Bentley CA, Lee K-F. p75 is important for axon growth and Schwann cell migration during development. J Neurosci 2000;20: 7706–7715.

17 Abreu RS, Penalva LO, Marcotte EM et al. Global signatures of protein and mRNA expression levels. Mol Biosyst 2009;5:1512–1526.

18 Koussounadis A, Langdon SP, Um IH et al. Relationship between differentially expressed mRNA and mRNA-protein correlations in a xenograft model system. Sci Rep 2015;5:10775.

19 Vogel C, Marcotte EM. Insights into the regulation of protein abundance from proteomic and transcriptomic analyses. Nat Rev Genet 2012;13:227–232.

20 Hirota H, Kiyama H, Kishimoto T et al. Accelerated nerve regeneration in mice by upregulated expression of interleukin (IL) 6 and IL-6 receptor after trauma. J Exp Med 1996;183:2627–2634.

21 Leibinger M, Muller A, Gobrecht P et al. Interleukin-6 contributes to CNS axon regeneration upon inflammatory stimulation. Cell Death Dis 2013;4:e609.

22 Frostick SP, Yin Q, Kemp GJ. Schwann cells, neurotrophic factors, and peripheral nerve regeneration. Microsurgery 1998;18:397–405.

23 McKay HA, Wiberg M, Terenghi G. Exogenous leukaemia inhibitory factor enhances nerve regeneration after late secondary repair using a bioartificial nerve conduit. Br J Plast Surg 2003;56:444–450.

24 Wright MC, Mi R, Connor E et al. Novel roles for osteopontin and clusterin in peripheral motor and sensory axon regeneration. J Neurosci 2014;34:1689–1700.

25 Bampton ETW, Ma CH, Tolkovsky AM et al. Osteonectin is a Schwann cell-secreted factor that promotes retinal ganglion cell survival and process outgrowth. Eur J Neurosci 2005;21:2611–2623.

26 Ma CHE, Palmer A, Taylor JSH. Synergistic effects of osteonectin and NGF in promoting survival and neurite outgrowth of superior cervical ganglion neurons. Brain Res 2009; 1289:1–13.

27 Ma CHE, Bampton ETW, Evans MJ et al. Synergistic effects of osteonectin and brain-derived neurotrophic factor on axotomized retinal ganglion cells neurite outgrowth via the mitogen-activated protein kinase-extracellular signal-regulated kinase1/2 pathways. Neuroscience 2010;165:463–474.

28 Sholl DA. Dendritic organization in the neurons of the visual and motor cortices of the cat. J Anat 1953;87:387–406.

29 Yang P, Wen H, Ou S et al. IL-6 promotes regeneration and functional recovery after cortical spinal tract injury by reactivating intrinsic growth program of neurons and enhancing synapse formation. Exp Neurol 2012;236:19–27.

30 Lin G, Zhang H, Sun F et al. Brain-derived neurotrophic factor promotes nerve regeneration by activating the JAK/STAT pathway in Schwann cells. Transl Androl Urol 2016; 5:167–175.

31 Bella AJ, Lin G, Tantiwongse K et al. Brain-derived neurotrophic factor (BDNF) acts primarily via the JAK/STAT pathway to promote neurite growth in the major pelvic ganglion of the rat: Part I. J Sex Med 2006;3:815–820.

32 Yadav A, Kalita A, Dhillon S et al. JAK/STAT3 pathway is involved in survival of neurons in response to insulin-like growth factor and negatively regulated by suppressor of cytokine signaling-3. J Biol Chem 2005;280: 31830–31840.

33 Elsaeidi F, Bemben MA, Zhao X et al. Jak/Stat signaling stimulates zebrafish optic nerve regeneration and overcomes the inhibitory actions of Socs3 and Sfpq. J. Neurosci 2014;34:2632–2644.

34 Zamani F, Amani-Tehran M, Latifi M et al. The influence of surface nanoroughness of electrospun PLGA nanofibrous scaffold on nerve cell adhesion and proliferation. J Mater Sci Mater Med 2013;24:1551–1560.

35 Brunetti V, Maiorano G, Rizzello L et al. Neurons sense nanoscale roughness with nanometer sensitivity. Proc Natl Acad Sci USA 2010;107:6264–6269.

36 Hoffman-Kim D, Mitchel JA, Bellamkonda RV. Topography, cell response, and nerve regeneration. Annu Rev Biomed Eng 2010;12:203–231.

37 Haase G, Pettmann B, Raoul C et al. Signalling by death receptors in the nervous system. Curr Opin Neurobiol 2008;18:284–291.

38 Bamji SX, Majdan M, Pozniak CD et al. The p75 neurotrophin receptor mediates neuronal apoptosis and is essential for naturally occurring sympathetic neuron death. J Cell Biol 1998;140:911–923.

39 Bai Y, Dergham P, Nedev H et al. Chronic and acute models of retinal neurodegeneration TrkA activity are neuroprotective whereas p75NTR activity is neurotoxic through a paracrine mechanism. J Biol Chem 2010;285: 39392–39400.

40 Delbary-Gossart S, Lee S, Baroni M et al. A novel inhibitor of p75-neurotrophin receptor improves functional outcomes in two models of traumatic brain injury. Brain 2016; 139:1762–1782.

41 Ogai K, Kuwana A, Hisano S et al. Upregulation of leukemia inhibitory factor (LIF) during the early stage of optic nerve regeneration in zebrafish. PLoS One 2014;9: e106010.

42 Rosset EM, Bradshaw AD. SPARC/osteonectin in mineralized tissue. Matrix Biol 2016; 52–54:78–87.

43 Motamed K, Funk SE, Koyama H et al. Inhibition of PDGF-stimulated and matrix-mediated proliferation of human vascular smooth muscle cells by SPARC is independent of changes in cell shape or cyclin-dependent kinase inhibitors. J Cell Biochem 2002;84:759–771.

44 Yost JC, Sage EH. Specific interaction of SPARC with endothelial cells is mediated through a carboxyl-terminal sequence containing a calcium-binding EF hand. J Biol Chem 1993;268:25790–25796.

45 Denhardt DT, Noda M, O'Regan AW et al. Osteopontin as a means to cope with environmental insults: Regulation of inflammation, tissue remodeling, and cell survival. J Clin Invest 2001;107:1055–1061.

46 Hashimoto M, Sun D, Rittling SR et al. Osteopontin-deficient mice exhibit less inflammation, greater tissue damage, and impaired locomotor recovery from spinal cord injury compared with wild-type controls. J Neurosci 2007;27:3603–3611.

47 Dati G, Quattrini A, Bernasconi L et al. Beneficial effects of r-h-CLU on disease severity in different animal models of peripheral neuropathies. J Neuroimmunol 2007;190:8–17.

48 Bonnard A-S, Chan P, Fontaine M. Expression of clusterin and C4 mRNA during rat peripheral nerve regeneration. Immunopharmacology 1997;38:81–86.

49 Liu L, Svensson M, Aldskogius H. Clusterin upregulation following rubrospinal tract lesion in the adult rat. Exp Neurol 1999;157: 69–76.

50 Fitzgerald M, Nairn P, Bartlett CA et al. Metallothionein-IIA promotes neurite growth via the megalin receptor. Exp Brain Res 2007; 183:171–180.

51 Fleming CE, Mar FM, Franquinho F et al. Transthyretin internalization by sensory meurons Is megalin mediated and necessary for Its neuritogenic activity. J Neurosci 2009; 29:3220–3232.

52 Heinrich PC, Behrmann I, Müller-Newen G et al. Interleukin-6-type cytokine signalling through the gp130/Jak/STAT pathway. Biochem J 1998;334:297–314.

53 Günthert U, Birchmeier W. Attempts to Understand Metastasis Formation II: Regulatory Factors. Berlin Heidelberg: Springer, 2012.

54 Boroujeni SM, Mashayekhan S, Vakilian S et al. The synergistic effect of surface topography and sustained release of TGF-β1 on myogenic differentiation of human mesenchymal stem cells. J Biomed Mater Res A 2016; 104:1610–1621.

55 Yim EKF, Pang SW, Leong KW. Synthetic nanostructures inducing differentiation of human mesenchymal stem cells into neuronal lineage. Exp Cell Res 2007;313:1820–1829.

56 Patel S, Kurpinski K, Quigley R et al. Bioactive nanofibers: Synergistic effects of nanotopography and chemical signaling on cell guidance. Nano Lett 2007;7:2122–2128.

57 Sadan O, Shemesh N, Barzilay R et al. Mesenchymal stem cells induced to secrete neurotrophic factors attenuate quinolinic acid toxicity: A potential therapy for Huntington's disease. Exp Neurol 2012;234:417–427.

See www.StemCellsTM.com for supporting information available online.

Biomaterials 203 (2019) 86–95

Contents lists available at ScienceDirect

Biomaterials

journal homepage: www.elsevier.com/locate/biomaterials

Conduits harnessing spatially controlled cell-secreted neurotrophic factors improve peripheral nerve regeneration

Aaron X. Sun[a,b,c,d], Travis A. Prest[d], John R. Fowler[b], Rachel M. Brick[a], Kelsey M. Gloss[a], Xinyu Li[d], Michael DeHart[e], He Shen[a,g], Guang Yang[a,h], Bryan N. Brown[d,f], Peter G. Alexander[a,b,*], Rocky S. Tuan[a,b,d,i,**]

[a] Center for Cellular and Molecular Engineering, Department of Orthopaedic Surgery, University of Pittsburgh School of Medicine, Pittsburgh, PA, USA
[b] Department of Orthopaedic Surgery, University of Pittsburgh School of Medicine, Pittsburgh, PA, USA
[c] Medical Scientist Training Program, University of Pittsburgh School of Medicine, Pittsburgh, PA, USA
[d] Department of Bioengineering, Swanson School of Engineering, University of Pittsburgh, Pittsburgh, PA, USA
[e] Department of Biology, Dietrich School of Arts and Sciences, University of Pittsburgh, Pittsburgh, PA, USA
[f] McGowan Institute for Regenerative Medicine, University of Pittsburgh, Pittsburgh, PA, USA
[g] Key Laboratory of Nano-Bio Interface, Division of Nanobiomedicine, Suzhou Institute of Nano-tech and Nano-bionics, Chinese Academy of Sciences, China
[h] Tissue Engineering & Biomaterials Lab, Fischell Department of Bioengineering, University of Maryland, College Park, MD, USA
[i] Institute for Tissue Engineering and Regenerative Medicine, The Chinese University of Hong Kong, Hong Kong SAR, China

ARTICLE INFO

Keywords:
Mesenchymal stem cells
Peripheral nerve repair
Nerve conduit
Wall encapsulation
Schwann cell distribution

ABSTRACT

An essential structure in nerve regeneration within engineered conduits is the “nerve bridge” initiated by centrally migrating Schwann cells in response to chemokine gradients. Introducing exogenous cells secreting neurotrophic factors aims to augment this repair process, but conventional cell-seeding methods fail to produce a directional chemokine gradient. We report a versatile method to encapsulate cells within conduit walls, allowing for reproducible control of spatial distribution along the conduit. Conduits with stem cells encapsulated within the central third possessed markedly different cell distribution and retention over 6 weeks *in vivo*, compared to standard cell lumen injection. Such a construct promoted Schwann cell migration centrally, and at 16 weeks rats presented with significantly enhanced function and axonal myelination. The method of utilizing a spatially restricted cell secretome departs from traditional homogeneous cell loading, and presents new approaches for studying and maximizing the potential of cell application in peripheral nerve repair.

1. Introduction

Peripheral nerve injury (PNI) affects over 300,000 people each year in the United States and is a significant cause of morbidity and lifelong disability despite surgical intervention [1]. Through a variety of traumatic or disease-based mechanisms, such as high-speed motor vehicle collisions or schwannomas, peripheral nerves function is drastically altered or decreased. Warfighters, in particular, are exposed to higher incidences of PNI due to battlefield injuries, and PNI morbidity leads to reduced military preparedness, early discharge, poor reintegration into civilian life, and has been implicated in higher rates of depression and suicide among these veterans [2,3]. Not only do PNIs cause loss of function and major disability, but they are also a huge economic burden for both the individual as well as society, costing the United States approximately $150 billion annually in healthcare dollars [4].

While there exist innate healing mechanisms for the repair of damaged nerves, complete transection of axons as well as all supporting tissues, termed neurotmesis, is associated with poor outcomes following injury [5]. Currently, the best treatment option for nerve defects is tensionless end-to-end repair given its predictable positive outcomes, but many times this is not an option due to the various conditions that must be met: repair immediately after injury, minimal gap < 2.5 mm in length, good blood supply and soft-tissue coverage, and exact alignment of the opposing ends [6–8]. Alternative options such as autografting and allografting exist, but are limited by donor site morbidity (with a chance for neuroma formation at both sites), availability, and immune

* Corresponding author. Center for Cellular and Molecular Engineering, Department of Orthopaedic Surgery, University of Pittsburgh School of Medicine, Pittsburgh, PA, 15219, USA.
** Corresponding author. Center for Cellular and Molecular Engineering, Department of Orthopaedic Surgery, University of Pittsburgh School of Medicine, Pittsburgh, PA, 15219, USA.
E-mail addresses: pea9@pitt.edu (P.G. Alexander), rst13@pitt.edu, tuanr@cuhk.edu.hk (R.S. Tuan).

https://doi.org/10.1016/j.biomaterials.2019.01.038
Received 23 July 2018; Received in revised form 15 December 2018; Accepted 24 January 2019
Available online 19 February 2019
0142-9612/

rejection, with only a 40–50% success rate for the gold standard of autografting. Another promising regenerative route, the use of a biomaterial nerve conduit, demonstrates potential due to reduced neuroma formation, lack of axonal escape, and lack of donor-site morbidity, but is constrained by range ($\leq$3 cm) and low functional recovery rates [9]. Thus, the ability to provide an efficient and effective method towards bridging the gap in nerve regeneration would be a huge step forward in the care of peripheral nerve injuries.

In the pursuit of an effective nerve conduit, many physical and biological strategies have been employed during fabrication [10–15]. On the physical side, electrospun nanofibers hold great promise due to their ability to be fabricated with aligned arrangements closely resembling native nerve ECM, and they have demonstrated the ability to guide neurite extensions [15–18]. On the biological side, neurotrophic factors (NTFs), such as brain derived neurotrophic factor (BDNF) and vascular endothelial growth factor (VEGF), have been shown to play an important role in facilitating axonal growth, guidance, and survival [19–23]. In addition, chemokine gradients are essential in driving Schwann cell migration into the regenerating nerve bridge and axon elongation [24–33]. Current methods of sustained delivery of growth factors by microparticles, along with other technologies, have demonstrated utility in experimental models of nerve repair, but these technologies have not yet addressed the dynamic time course of growth factor production, the use of anti-inflammatory cytokines, or the capability to supply a multitude of growth factors simultaneously or separately [13,14,34,35].

A potential route toward addressing these issues lies in the use of stem cells. Adult mesenchymal stem cells (MSCs) are multipotent cells that have the ability to differentiate into many lineages, including neural-like lineages [36,37]. Early transplantation experiments involving these stem cells demonstrated that they supported nerve regeneration (originally believed to be due to transdifferentiation to neural lineages but more recently thought to be through production of NTFs), and they have also been shown to possess immunoregulatory functions, which could potentially decrease scar tissue infiltration into conduits and neuroma formation [12,38–40]. Indeed, studies utilizing nerve conduits seeded with MSCs reported both larger axons as well as greater amounts of myelination per axon [12]. Additionally, studies including functional assays generally showed enhanced function compared to non-cellular controls, with some demonstrating function comparable to the gold standard autograft. Along with MSCs, other cell types such as neural stem cells, embryonic stem cells, and Schwann cells have also been applied to successfully support nerve regrowth with efficacies rivaling or exceeding those of MSCs [12].

While cell support demonstrates distinct benefits in conduit-mediated nerve regeneration, cell-seeding protocols typically either involve cell attachment in culture after fabrication, which can be lengthy (clinically undesirable) and potentially result in cell detachment *in vivo*, or injection into the lumen of the conduit, which is susceptible to leakage [12]. In addition, these methods do not allow for precise control of cell seeding number or cellular distribution within the conduit due to the random nature of cell attachment and injection, and the seeded cells are known to migrate out of the conduit, further confounding the dose- and location-dependent effect of the cells. There do exist gel-based systems that allow for encapsulation of cells within gels, which address the cell density challenges and immediate cell seeding, but they have not yet been effectively applied for cell distribution in conduits. Overall, these limitations have led to the inability to effectively produce and harness cell-secreted neurotrophic gradients.

In this study, we aim to overcome these challenges in cell application by allowing for control of spatial distribution and cell density through direct wall-encapsulation of cells during fabrication. We tested the efficacy of this encapsulation system in enhancing peripheral nerve regeneration both *in vitro* and *in vivo* in a rat sciatic transection model. Our *in vivo* results show that spatially restricted cell encapsulation in the implanted engineered conduit leads to improved Schwann cell migration into the nerve bridge and increased functional return compared to controls.

2. Materials and methods

All chemicals were purchased from Sigma Aldrich (St. Louis, MO, USA) unless otherwise specified. All procedures were performed according to the guidelines of the Institutional Animal Care and Use Committee at the University of Pittsburgh (Protocol No. 16036308).

2.1. Fabrication of cell-seeded PCL/GelMA nerve conduits

The composite PCL/GelMA scaffold was produced as previously described [23]. Briefly, a dual-nozzle electrospinning setup with 14.0% w/v PCL (80 kDa) in 2,2,2-trifluoroethanol and 18% methacrylated-gelatin (GelMA) in 95% 2,2,2-triflurorethanol in water was used to produce random and aligned scaffolds. A 2.0 × 5.5 cm sheet of aligned scaffold and a 2.2 × 5.5 cm sheet of random scaffold was cut for each group, and subsequently exposed to UV irradiation for 30 min to sterilize. The aligned scaffold was then overlapped on top of the random scaffold by 2 mm, and approximately 20 μL of photoinitiator solution (8% methacrylated gelatin, 0.3% photoinitiator lithium phenyl-2,4,6-trimethylbenzoylphosphinate (LAP) [41] in HBSS [Gibco, Waltham, MA, USA]) was applied to the overlapped region. This area was then irradiated with a visible light source supplying wavelengths of 395 nm (7202UV395, LED Wholesalers) for 40 s to cure the gelatin and bond the two sheets together. Following this, approximately 300 μL of photointiator solution was used to wet both scaffolds. 50 μL of photoinitator solution was then used to resuspend 6 million cells, which were then pipetted in three vertical stripes 1.2 cm apart and equidistant from the horizontal edges of the scaffold. This completed sheet was then rolled up around a hypodermic needle of 1.5 mm diameter, and subsequently photopolymerized with visible light for 2 min while rotating on the needle. The construct was then removed, and 0.95 cm was removed from each end of the tube followed by cutting the remaining 3.6 cm into three 1.2 cm tubes such that the cell stripes fell into the central third of each conduit (2 million cells/conduit). These wall-encapsulated cellular conduits were then placed in culture medium (10% fetal bovine serum (FBS) [Invitrogen, Carlsbad, CA, USA], 1x PSF [Gibco] in Dulbecco's Minimal Essential Medium (DMEM) [ThermoFisher, Waltham, MA, USA]) until surgical implantation.

2.2. Cytoskeletal fluorescent staining and Calcein-AM live cell staining

Day 8 cell-seeded nerve conduits were carefully unrolled as to not damage the seeded cells, and were washed in PBS, fixed in 4% paraformaldehyde, and incubated with 1% bovine serum albumin (BSA). Subsequently, they were incubated with Alexa Fluor 488 phalloidin (Life Technologies, Carlsbad, CA, USA) for 30 min at room temperature. Lastly, the construct was rinsed with PBS, nuclear counterstained with DAPI (Life Technologies), and imaged using an Olympus inverted microscope (Olympus IX81, Center Valley, PA, USA).

Live/Dead viability/cytotoxicity kit (Invitrogen) was used to visualize live cells via Calcein-AM staining, according to the product manual, following cell-seeded nerve conduit fabrication on Day 0. This construct was imaged using an Olympus SZX16 microscope.

2.3. Culture of DRG-Seeded scaffolds on 2-D cell-seeded PCL/GelMA multilayered constructs

The composite scaffold described above was utilized for the following procedure. A 2.0 × 5.5 cm sheet of aligned scaffold and a 2.2 × 5.5 cm sheet of random scaffold was cut for each group. Approximately 300 μL of photointiator solution was used to wet both scaffolds. Following this, each scaffold was folded lengthwise (along the 5.5 cm side) into halves. The remaining 60 μL of solution was used to

suspend 6 million cells, which was applied to the random and aligned scaffolds before folding, and between the scaffolds before the folded aligned scaffold was placed on top of the random one. The 4-layer construct was then exposed to visible light radiation for 3 min (1.5 min on each side) to photocrosslink the construct. After construction of the completed multilayer scaffold, three cylinders of 12 mm diameter were punched out with a punch biopsy to yield ~2 million cells/scaffold.

DRGs were harvested from day 9 chick embryos using a previously described protocol [42]. A single DRG was placed on the aligned side of each circular scaffold and placed in a 12-well culture plate. The DRG explant constructs were cultured in basal medium (5% FBS, 1x Pen-Strep [ThermoFisher] in Basal Medium Eagle [ThermoFisher]). Medium changes were performed on days 2 and 4 with 2 mL per well in a 12-well plate.

2.4. Immunohistochemistry of DRGs

Cultured DRG explants were rinsed with wash buffer (0.05% Tween 20 in PBS) and fixed in paraformaldehyde for 20 min. After three additional rinses with wash buffer, the constructs were placed in 80 °C 10 mM citric acid with 10% ethanol for 1 h, followed by three washes and subsequent blocking with 5% FBS for 1 h at room temperature or overnight at 4 °C. After equilibration with wash buffer, *anti*-neurofilament heavy polypeptide antibody (Abcam, cat. Ab4680, Cambridge, MA, USA) was added at a 1:10,000 dilution overnight at 4 °C, followed by 2–3 washes, and incubation with secondary antibody (goat anti-chicken AlexaFluor 488 conjugated IgG, Invitrogen) at a dilution of 1:300 for 1 h. The constructs were thoroughly rinsed and then imaged using an Olympus inverted microscope (Olympus IX81) equipped with a motorized stage controlled through MetaMorph (Molecular Devices, San Jose, CA, USA). Resultant mosaic images were stitched using Grid/Collection Stitching (ImageJ, NIH); the 10 longest NEFH-positive neurite extensions were measured from the surface of the original DRG cluster, as previously described [23].

2.5. ECM hydrogel preparation

Peripheral nerve ECM was prepared from sciatic nerves collected from market-weight pigs (Tissue Source; LLC, Lafayette, IN, USA). The tissue was then frozen for at least 16 h at −80 °C. The tissue was quartered longitudinally and cut into sections of < 5 cm. Decellularization was performed as previously described [43]. Enzymatic degradation products were produced from solid ECM scaffold material as previously described [43]. Enzymatic degradation products were aliquoted and lyophilized. Immediately before use, lyophilized degradation products were rehydrated using sterile water. Gelation was then initiated by adjusting the pH to 7.4 and the solution to 0.5 x PBS concentration through the addition of 0.2 N NaOH and 10 x PBS.

2.6. In vivo scaffold implantation

For 1–6 week experiments, nerve conduits for implantation were either cell-free or wall-encapsulated with rat ASCs, which were DiI-labeled with Vibrant CM solution (Invitrogen) according to manufacturer's protocol. The sciatic nerves in Lewis rats were exposed and a 10 mm segment was removed using microscissors. Nerve stumps were sutured 1 mm into each end of the 12 mm conduit (for a gap of 10 mm) using 8-0 nylon suture. Following implantation, DiI labeled rat ASCs (2 million in 10 μL to mimic the number of cells used in the wall-encapsulation groups) were injected into cell-free conduits to represent the cell injection groups, or ECM hydrogel was injected to fill the conduit to represent groups that incorporate hydrogel. A total of n = 6 rats were used for each group for each time point.

2.7. Implant harvesting and immunohistochemical analysis

Implants were harvested at specified experimental time points (either 1, 2, 4, 6, or 16 weeks). The harvested implants were then fixed in 10% buffered formalin phosphate for 2 days at 4 °C, and then processed through a series of solutions: 10% sucrose for 4 h at room temperature, 20% sucrose overnight at 4 °C, and lastly 30% sucrose overnight at 4 °C. After equilibration for 2 h in Optimal Cutting Temperature gel (OCT) (Sakura Finetek USA, Torrance, CA, USA), 3 samples were transversely cut through the middle of the conduit and frozen-embedded in new OCT cut side down, while 3 other samples were embedded longitudinally in fresh OCT. All samples were stored at −80 °C until sectioning. Transverse cryosections with a thickness of 16 μm were collected at every millimeter starting from the center of the conduit, and examined for cell distribution, while the longitudinally embedded samples were sectioned sagittally to assess continuity of nerve growth. See SI text for further details.

2.8. Rat sciatic functional index testing

Rats were placed in the Motorater System (TSE GmbH, Chesterfield, MO, USA) and acclimated for two days prior to testing. Videos were then recorded for rats walking across the length of the Motorater System. Simi Motion 9.2.1 software (Simi Reality Motion Systems GmbH, Unterschleissheim, Germany) was used to measure toe spread distances from acquired videos. SFI measurements from 4 steps were averaged for each rat.

2.9. Statistical analysis

All data were expressed as mean ± standard error of measurement (SEM). Statistical analysis was carried out in Prism 7 (GraphPad, Software, La Jolla, CA, USA). All analyses were performed using ANOVA with Tukey's HSD post-hoc testing unless specified otherwise. One-tailed Mann-Whitney testing was used to determine differences in distributions, and non-linear fitting was used to determine Gaussian and quadratic fitting. One-way ANOVA followed by Fishers LSD post-hoc testing against wall or control was used for Week 6 Schwann and myelin thickness/ratio, respectively. A threshold of $p < 0.05$ was used to determine statistical significance.

3. Results

3.1. Multilayered nanofibrous nerve conduits possess suitable physical properties for in vivo implantation

In order to achieve cell-friendly seeding during fabrication, we employed the combination of electrospun composite nanofibrous mats of co-spun polycaprolactone (PCL) and gelatin methacrylate (GelMA) with both random and aligned fibers for suture retention and neurite guidance, respectively (Fig. 1A**, step 1**). Note: all nerve conduits used in this study utilize both aligned and random fibers as shown in this figure. Gelatin, the denatured form of collagen, is derived from native extracellular matrix, and GelMA has been widely used for the fabrication of hydrogels by virtue of its ability to be photopolymerized as well as its excellent biocompatibility [44]. Despite the hydrophobicity of PCL, the presence of GelMA within the nanofiber mat allowed it to readily incorporate aqueous solutions, which instantly dissolved the GelMA and allowed for immediate seeding of cells onto and between the PCL fibers [45]. Of note, hydration of the composite scaffolds did not change the underlying random *versus* aligned architecture (Fig. S1). Using this technique, we created bonded tubular structures resistant to delamination [45] with cells encapsulated within the walls and separated from the lumen of the conduit by bonding the two layers, applying cells in a GelMA solution (shown here as homogenous but could be in any spatial pattern), and rolling around a hypodermic needle of

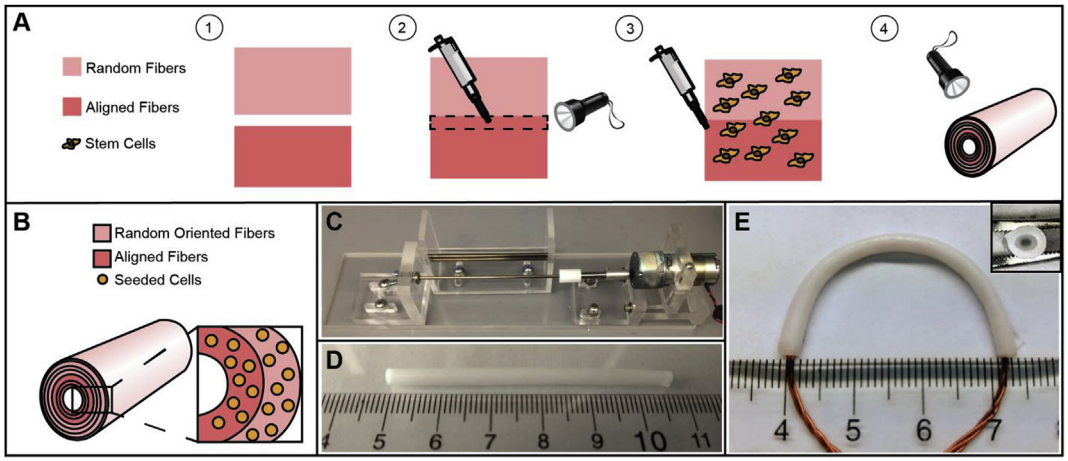

Fig. 1. Construction of nerve conduits with wall-encapsulated cells. (A) Stepwise representation of process. (1) Composite random and aligned PCL/GelMA scaffolds are (2) overlaid and bonded with photointiator solution. (3) The rest of the scaffold is hydrated with photoinitiator solution, and cells are placed on the scaffold (homogeneous seeding is shown here but other seeding approaches are also achievable). (4) The sheet is rolled around a hypodermic needle of desired diameter and cured with visible light to bond layers. **(B)** Schematic of completed conduit – layers are removed in magnified view for clarity. **(C)** Prototype machine used to construct scaffold consisting of a slow-rotating motor, a platform, and hypodermic needle. **(D)** Macroscopic view of 5.5 cm long conduit. **(E)** Flexibility of conduit at 15.8 mm radius of curvature. Inset: conduit retains patency after full compression.

desired diameter (Fig. 1A**, steps 2–4**). The resulting structure was then cured with visible light, to form a multilayered tube with cells localized between every layer (Fig. 1B). Fig. 1C depicts a simple apparatus suitable for construction of this structure (Fig. 1D), with a more complex but user-friendly design in Fig. S2. The conduit was elastic and flexible (Fig. 1E) – shown at a radius of curvature of 15.8 mm, the smallest radius experienced under physiological human conditions at the cubital tunnel [46]– and after full compression of the lumen it retains patency (Fig. 1E**, inset**). In addition, conduits possessed suitable mechanical tensile suture retention strength (far exceeding the necessary 1.7 N [47–49]), and experienced conduit elongation rather than suture pull-through (Fig. S3). Lastly, as expected, the properties of the conduits were consistent with the composition of a faster degrading GelMA component and slower-degrading PCL component, to avoid conduit collapse during the regeneration process (Fig. S4).

3.2. Nerve conduits with concentric wall-encapsulated cells possess topographical cues, biological activity, and significantly enhance dorsal root ganglion (DRG) extension in vitro

Having established the physical suitability of the conduit for surgical manipulation and implantation, we sought to characterize the biological capabilities of this scaffold. In order to determine the effect of nanostructural cues, phalloidin staining was used to visualize the cytoskeletons of the seeded cells (Fig. 2A–D). Fig. 2A depicts the major cell morphologies and their spatial distribution within the nerve conduit. Three distinct cell populations were apparent: cells with randomly oriented processes, elongated aligned cytokeletons, and those with short retracted processes (Fig. 2B–D**, respectively**). These cell morphologies corresponded to three microarchitectures of the biomaterials in the scaffold: random fibers, aligned fibers, and thin hydrogel between the PCL layers. Alignment was also quantified, demonstrating that cell nuclei in random sections of scaffold displayed an average of $-20.45 \pm 48.52^{\circ}$ deviation from vertical as measured from the long axis of the nucleus while aligned sections averaged $-3.23 \pm 18.26^{\circ}$ (Fig. S5). Upon live staining with Calcein AM (Fig. 2E), live cells were observed to exhibit a concentric distribution, further confirmed by visualizing DiI-labeled cells in cross-sections of the construct, showing their continuous concentric distribution between all layers (Fig. 2F and G). Increased metabolic activity was also observed over the course of 28 days of culture, indicating cell proliferation and biomaterial biocompatibility (Fig. S6).

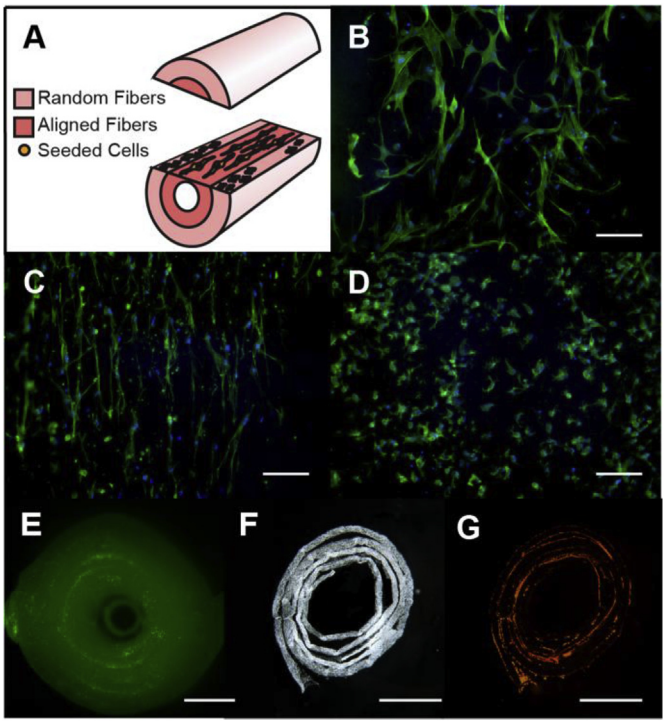

Fig. 2. Cells seeded in conduit respond to topographical cues and are concentrically distributed. (A) Location of aligned and randomly oriented cells in conduit. The following images in **B** and **C** were obtained through random sampling within regions depicted in **A** that correspond to random and aligned nanofibers. **(B)** Cells with randomly oriented processes on random fibers. **(C)** Cells with aligned processes on aligned fibers. **(D)** Cells with short retracted processes in thin hydrogel layer between fiber layers. These were found in gelatinous patches in random locations due to unrolling process, but presumably exist continuously in the thin gelatin layer between nanofibers. **(E)** Live cells are found to be concentrically distributed in conduit by Calcein-AM staining. **(F)** Transverse section of conduit demonstrating close adherence of layers without the use of suture or additional bonding agents. **(G)** DiI-labeled cells are clearly shown to reside between concentric fiber layers of sectioned conduit in **F**. Scale bar: 50 μm (B–D), and 500 μm (E–G). N = 3.

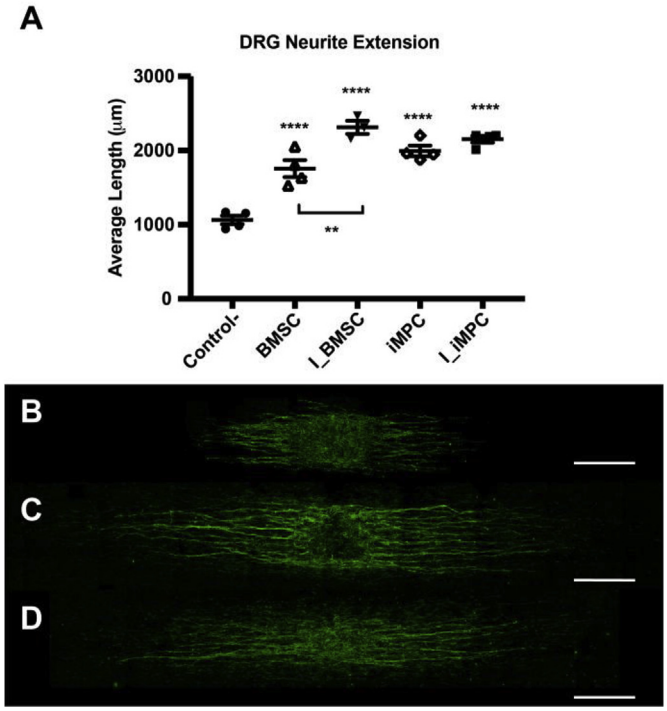

Fig. 3. Wall-encapsulated cells significantly increase DRG neurite extension. (A) Average length of 10 longest DRG neurite extensions when cultured on scaffolds containing various wall-encapsulated cells. Green stain corresponds to Neurofilament Heavy. **(B–D)** Representative images of Control, I_BMSC, and I_iMPC groups, respectively. Control, cell-free multilayer scaffold; BMSC, human bone marrow stem cell; I_, neurotrophically induced; iMPC, mesenchymal progenitor cell derived from iPSCs. **, $p < 0.005$, and ****, $p < 0.0001$, compared to Control. Scale bar: 500 μm. N = 4 per group. (For interpretation of the references to colour in this figure legend, the reader is referred to the Web version of this article.)

In view of the importance of NTFs in nerve regeneration, we were particularly interested in the neurotrophic capabilities of the nerve conduit, particularly the effect of the conduit architecture on NTF production. Our results showed robust gene expression of BDNF and VEGF (two NTFs known to be produced by MSCs in abundance [19,23]) (Fig. S7), and that seeded cells produced neurotrophic factors that permeated throughout the scaffold and were measureable by ELISA (Fig. S8). To assess the effect of the conduit on neurite outgrowth *in vitro*, chick embryonic DRG explants were cultured for 5 days on a 2-dimensional equivalent of the 3-D conduit for easy visualization, and neurite outgrowth was assessed by measuring and averaging the length of the 10 longest neurite extensions measured from surface of the original DRG cluster (Fig. 3). Two different mesenchymal cell sources were used for cell seeding, bone marrow MSCs (BMSCs) and induced mesenchymal progenitor cells (iMPCs). iMPCs were derived from induced pluripotent stem cells (iPS cells), as described previously [23], and were included to demonstrate versatility in terms of cell sourcing and cell incorporation into the nerve conduit using the procedure described here. These two cell types were also exposed to well-defined neurotrophic induction protocols described by our lab and others to optimize neurotrophic gene expression and inductive activity for neural-like differentiation [23]. As seen in Fig. 3A, all groups with seeded cells significantly increased DRG neurite extensions compared to cell-free controls ($p < 0.0001$). In addition, neurotrophically induced BMSCs (I_BMSCs) producing higher levels of BDNF (Fig. S8**)** significantly increased neurite extension length over uninduced BMSCs ($p < 0.005$). Fig. 3B–D depict representative images of control, I_BMSCs, and I_iMPCs. These results correlate well with our previous observation that neurotrophic factors found in the conditioned medium of cultured BMSCs and iMPCs could significantly increase DRG neurite length [23]. Taken together, these findings showed that conduits with wall-encapsulated cells displayed spatially and topographically specific cues and neurotrophic activity, indicated by significant enhancement of DRG neurite extension *in vitro*.

3.3. Cell localization follows different distributions in wall-encapsulation vs injection methods in vivo

Given the effectiveness of the conduit system *in vitro*, we sought to test its *in vivo* characteristics – specifically its ability to control the spatial distribution of seeded cells. In the *in vivo* studies, to minimize xenogenic and allogeneic immune response, we chose to harvest and use adipose stem cells, a readily harvested MSC type, from Lewis rats, which were first analyzed and verified for their differentiation potential and production of growth factors of interest, such as interleukin-6, transforming growth factor-β (TGF-β), BDNF, and VEGF (Fig. S9). The ASCs were DiI-labeled and used to assess the extent of cell migration, first queried *in vitro* upon wall encapsulation within the central third of the length of the nerve conduit. Over the course of two weeks, minimal migration from the center was observed and cells were retained within the walls of the conduit (Fig. S10). Conduits with the same design (DiI labeled ASCs encapsulated within the central third of the conduit) were then implanted allogeneically into Lewis rats in a 1 cm sciatic nerve transection model (Fig. S11), along with another cohort of rats that received cell-free conduits and a lumen injection of DiI labeled ASCs of the same quantity. Over the course of 6 weeks, MSC retention was found to be remarkably different (Fig. 4). Fig. 4A shows representative longitudinal sections of resulting conduits at 1, 2, 4, and 6 weeks. Quantitation of the DiI signal from these sections showed that in the case of wall-encapsulation, ASCs were retained for up to 4 weeks, while with injection the ASCs, cell abundance started to decline after just 1 week (Fig. 4B). Direct comparison for a period of 6 weeks revealed significantly higher intensities at 2 and 4 weeks for wall-encapsulation *versus* injection, with $p < 0.05$ and $p < 0.005$, respectively (Fig. 4C). These findings strongly suggest that cells persisted in wall-encapsulated conduits longer than those introduced via the conventinoal cell injection method.

Since there were significant differences seen at weeks 2 and 4, these time points were assessed in terms of both DiI labeled ASC cell intensity and Schwann cell intensity along the length of the conduit (Fig. 5). Of note, implanted conduits did not elicit a foreign body reaction and they limited fibrous infiltration through the walls of the conduit (Fig. S12). Conduits were serially sectioned transversely 4 mm proximally and distally from their center, stained, and analyzed for Schwann cells and ASCs (Fig. 5A). Fig. 5B demonstrates localization of seeded ASCs relative to migrating Schwann cells in wall-encapsulated conduits, while Fig. 5C portrays those in lumen injected conduits – note the localization of ASCs to walls vs. lumen. Upon examination of ASC intensity along the length of the conduits at Week 4, Fig. 5D and E **top** clearly showed differing distributions. These are significantly different by Mann-Whitney testing ($p = 0.0039$). Upon fitting to either quadratic or Gaussian distributions, wall-encapsulated conduits preferentially fit Gaussian with 84.74% probability and $r^2 = 0.4463$ while injected conduits preferentially fit quadratic with 91.17% probability and $r^2 = 0.3280$ (Fig. 5D and E **bottom**). These profiles described a migration outward from the center of the conduit and migration inward from ends of the conduit, respectively. Correlating these distributions with Schwann cell intensity at 2 weeks, there was a significant trend towards earlier Schwann cell migration into the center of the conduit in the wall-encapsulation group in comparison to the injection group, which showed very limited Schwann migration inwards ($p = 0.0457$, Mann-Whitney)(Fig. 5F). By 4 weeks, Schwann cells appeared to take on a unimodal distribution located near the center of the conduit in wall-encapsulated groups while they were more random in nature in the injection groups (Fig. 5G). Finally, at 6 weeks, complete bridging of

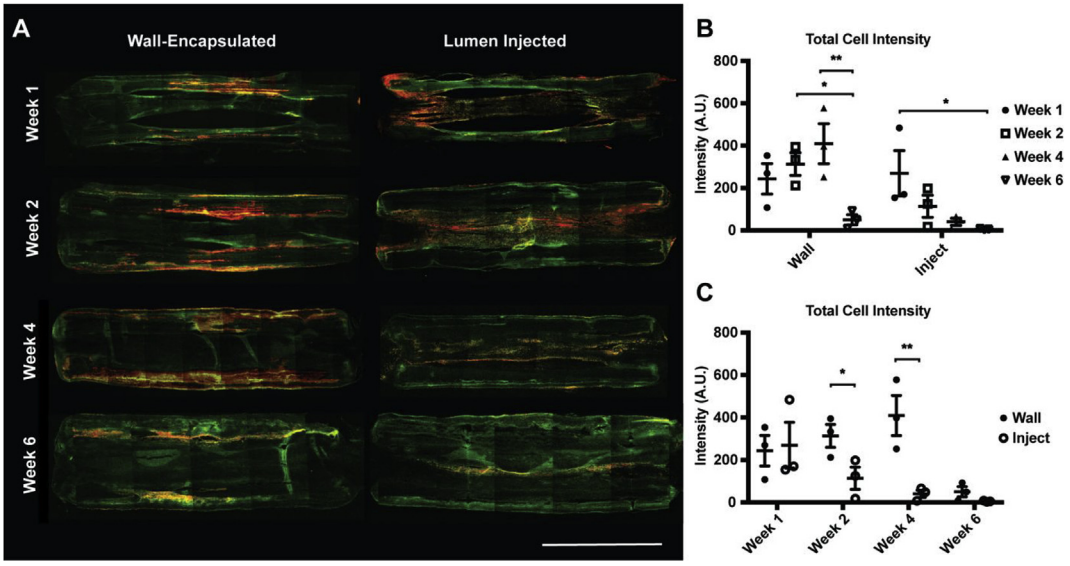

Fig. 4. Cells are retained longer *in vivo* with wall-encapsulation compared to lumen injection. (A) Representative images of DiI labeled cells in conduits at 6 weeks. Red channel is DiI label while green is scaffold autofluorescence. **(B)** Total DiI-labeled cell intensity (A.U., arbitrary units) at 6 weeks for wall-encapsulated *versus* lumen injected cell groups, showing trends within groups. **(C)** Total DiI-labeled cell intensity across 6 weeks comparing between groups at each week. *, $p < 0.05$; **, $p < 0.005$. Scale bar: 5 mm. (For interpretation of the references to colour in this figure legend, the reader is referred to the Web version of this article.)

the nerve conduit with Schwann cells was observed in the wall-encapsulation group (Fig. 6A), and the Schwann cell area in the center of the nerve conduit was significantly higher in the wall-encapsulated group compared to both no-cell control and cell injection (Fig. 6B), suggesting that Schwann cell migration was enhanced in wall-encapsulated groups. N = 3 per group.

3.4. Conduits with wall-encapsulated cells improve peripheral nerve regeneration

To evaluate the significance of the ASC seeding dependent change in Schwann cell distribution, the ability of the different nerve conduits to effect functional recovery in a 10 mm rat sciatic nerve transection model was analyzed. This gap length was chosen due to its common occurrence in literature as a model of critical-sized nerve transection defect [12], but also because we did not want to miss a potential effect in a smaller critical-sized gap before progressing to a larger gap in future studies (such as 15 or 20 mm).

Four groups were tested: conduits with or without wall-encapsulated cells in the central third of the conduit and with or without hydrogel filler. Here, we utilized a hydrogel group to test our conduit system against a commonly applied method of nerve regeneration augmentation (hydrogel lumen filler). In particular, we chose to use a hydrogel filler derived from decellularized peripheral nerve [43]. This hydrogel has also been shown to modulate the Schwann response in nerve regeneration, and we were interested in examining if our cell-encapsulated conduit would synergistically act with this ECM hydrogel by theoretically binding to ECM components within the hydrogel and enhancing neurotrophic factor efficacy.

At 16 weeks post-surgery, the wall-encapsulated cell group (cell) and combination of wall-encapsulated cells with hydrogel (combo) both presented with significantly higher sciatic functional index (SFI) when compared to control ($p < 0.001$) (Fig. 6C). In addition, the cell group also significantly increased SFI compared to the no-cell with hydrogel filler group (hydrogel) ($p < 0.05$). The hydrogel *versus* control and combo *versus* hydrogel comparisons were both at the border of significance ($p = 0.0627$ and $p = 0.0505$, respectively). These results demonstrate that the presence of wall-encapsulated cells greatly enhanced functional outcomes.

Lastly, axon myelination at 16 weeks was also assessed to correlate with functional outcomes (Fig. 7). MSCs have previously been shown to increase myelination when applied in nerve conduits [12]. Fig. 7A depicts representative images of neurofilament, myelin, and DAPI staining while Fig. 7B displays the same images with only the myelin channel for better visualization. The conduit was examined both at the center of the conduit, as well as at approximately 2 mm from the distal end of the transected nerve, given the known distal end of the nerve location of Wallerian degeneration. The cell group was seen to possess thicker axon myelination compared to control ($p < 0.05$)(Fig. 7C and D). The hydrogel group also exhibited increased myelination compared to control ($p < 0.05$)(Fig. 7C and D). The hydrogel group displayed a significantly higher percentage of myelinated axons compared to control ($p < 0.05$)(Fig. 7E). The cell and combo group both had higher average myelination than control, but failed to reach statistical significance, likely due to lack of power ($p = 0.1361$ and $p = 0.0896$, respectively)(Fig. 7E). Overall, nerve conduits with wall-encapsulated cells were observed to significantly enhance functional return and axon myelination in rats 16 weeks post-repair.

4. Discussion

In this study, we have examined the effect of nerve conduits harnessing cell-secreted neurotrophic gradients on the regenerative response of peripheral nerves. To achieve this, a versatile conduit fabrication method capable of incorporating cells in a spatially controlled manner was designed and its biological and physical characteristics were assessed *in vitro* for potential application *in vivo*. Using a 1 cm sciatic nerve transection model in rats, implants with cells wall-encapsulated along the central third of the conduit length were seen to direct a stronger migration of Schwann cells into the center of the conduit compared to their counterparts consisting of lumen-injected cells. This effect resulted in complete bridging of the conduit at 6 weeks by Schwann cells, and a significantly higher area of Schwann cell localization in the center of the conduit compared to both cell-free conduits and conduits with lumen-injected cells. At 16 weeks, rats with these wall-encapsulated cellular conduits presented with significantly increased sciatic functional index and axon myelination over controls. Taken together, these results strongly suggest that the use of spatially

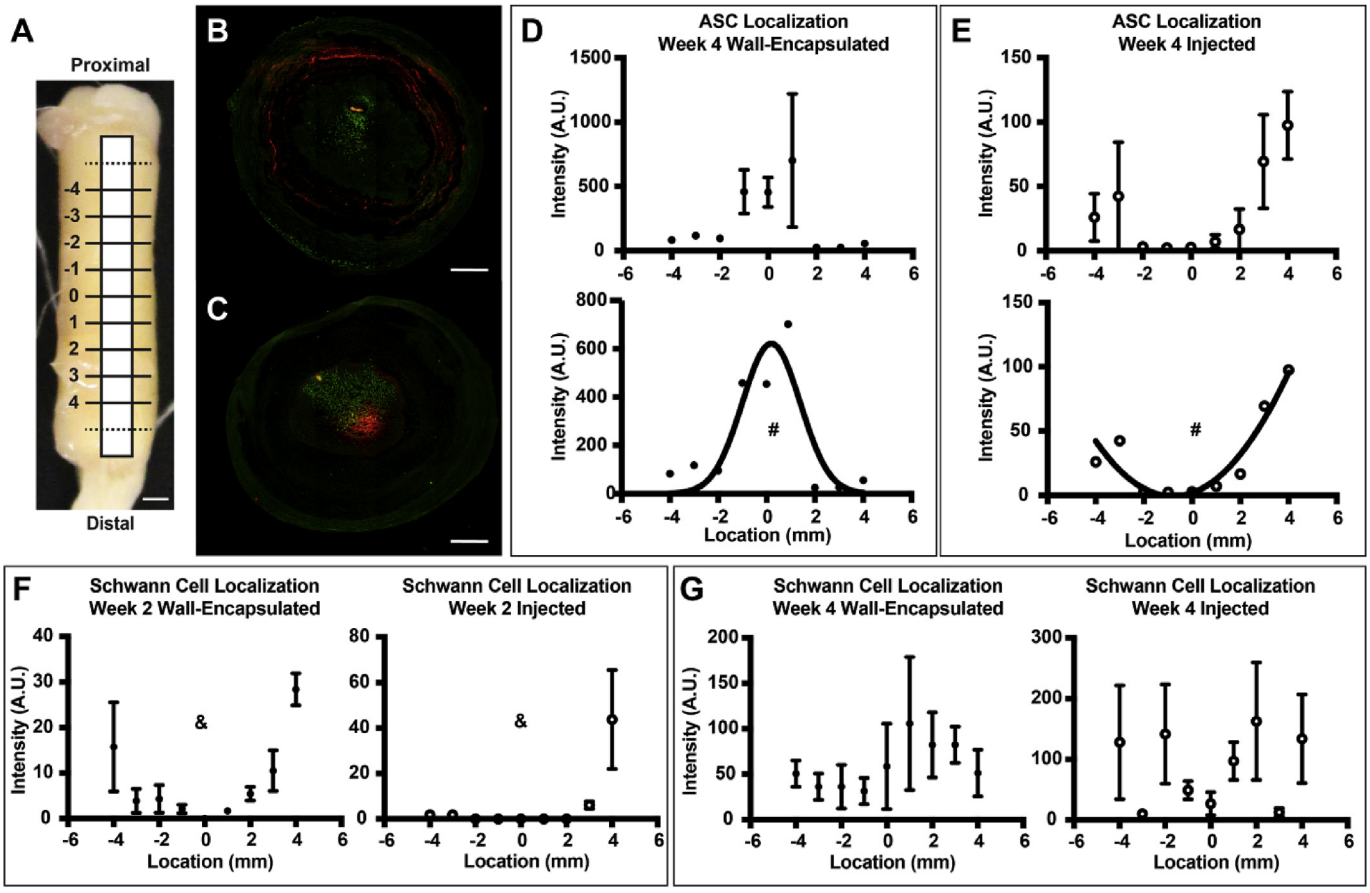

Fig. 5. Conduits with centrally located wall-encapsulated ASCs drive directional Schwann cell migration. (A) Schematic of locations sectioned along explanted nerve conduits (4 mm out from the center proximally and distally) from 1 cm rat sciatic nerve transection model. Scale bar: 1 mm. **(B,C)** Representative micrographs depicting localization of Schwann cells (green) and DiI-labeled (red) wall-encapsulated or lumen-injected ASCs, respectively. Scale bar: 500 μm. **(D,E)** ASC spatial distribution along the length of explanted conduits in wall-encapsulation *versus* lumen injection at 4 weeks. Wall-encapsulated ASCs fit a Gaussian distribution while lumen-injected ASCs fit a quadratic distribution. **(F,G)** Schwann cell localization and distribution along the length of the explanted conduit at two weeks and four weeks, respectively. Schwann cells possess a stronger inward migration at two weeks in wall-encapsulation group, and by four weeks resemble a single peaked distribution near the center of the conduit, as opposed to those in the lumen injection group, which possesses no clear distribution pattern. #, $p < 0.005$ between distributions (Gaussian, fit probability = 84.74% and $r^2 = 0.4463$; Quadratic, fit probability = 91.17% and $r^2 = 0.3280$). &, $p < 0.05$ between distributions. N = 3 per group per timepoint. (For interpretation of the references to colour in this figure legend, the reader is referred to the Web version of this article.)

controlled cell seeding to produce neurotrophic gradients presents a potentially powerful strategy for cell application in improving peripheral nerve regeneration.

Cell incorporation within conduits has been accomplished through a variety of methods [12], but none thus far have allowed for the immediate and controlled incorporation described here (Fig. 1). While electrospun nanofibers have been utilized as conduits with beneficial outcomes, techniques to incorporate cells within these fibers during fabrication are lacking. This is likely due to the fact that nanofibers do not accommodate compressive stress, which makes a cell-friendly fabrication more difficult as thicker conduit walls must be obtained through longer spinning times to avoid conduit collapse *in vivo*. One way around the poor compressive properties is the use of multiple layers of nanofibers to improve conduit stability, as has been described in various studies [11,15,50–52]. However, simply increasing the number of layers and "sandwiching" cells between them is still not suitable for cell seeding because delamination of the layers occurs [45]. The key to the technique described here is in the use of the sacrificial GelMA fiber, which dissolves upon addition of an aqueous solution and allows the solution to permeate between remaining fibers. In this way, after solidifying the aqueous gel component by photocrosslinking, all layers are tightly bonded together and resist delamination. This leads to the cell morphologies and the concentric arrangement of cells observed in the final conduit (Fig. 2). In addition, the gel component grants elasticity to the overall structure, which is lacking in a purely nanofibrous construct (Fig. 1E).

This fabrication strategy was shown to significantly increase DRG neurite extension *in vitro* (Fig. 3). We hypothesize that the increase in length is attributable to paracrine neurotrophic factor secretion as physical contact between the seeded cells and the DRG is lacking. Our results correlate well with reported observations of increased growth using conditioned medium derived from similar cells [23]. Further support is that VEGF and BDNF, two growth factors produced at high levels by these cell types, have been shown to significantly aid axonal extension [19–23]. In addition, there have been many descriptions of neurotrophic factors in the MSC secretome that enhance nerve growth [12,53]. Thus, our observations are in accordance with previous findings, and strongly suggest that wall-encapsulated cells exert their effects through neurotrophic factor secretion rather than other processes such as transdifferentiation [54].

Testing this cell encapsulation system against the standard cell injection method, we found that cells were retained effectively with encapsulation for up to 4 weeks (Fig. 4). We hypothesize that the sudden drop from 4 to 6 weeks is due to loss of the bulk of the GelMA component (Fig. S4), allowing cells to migrate out of the walls of the conduit. On the other hand, the number of cells introduced by injection

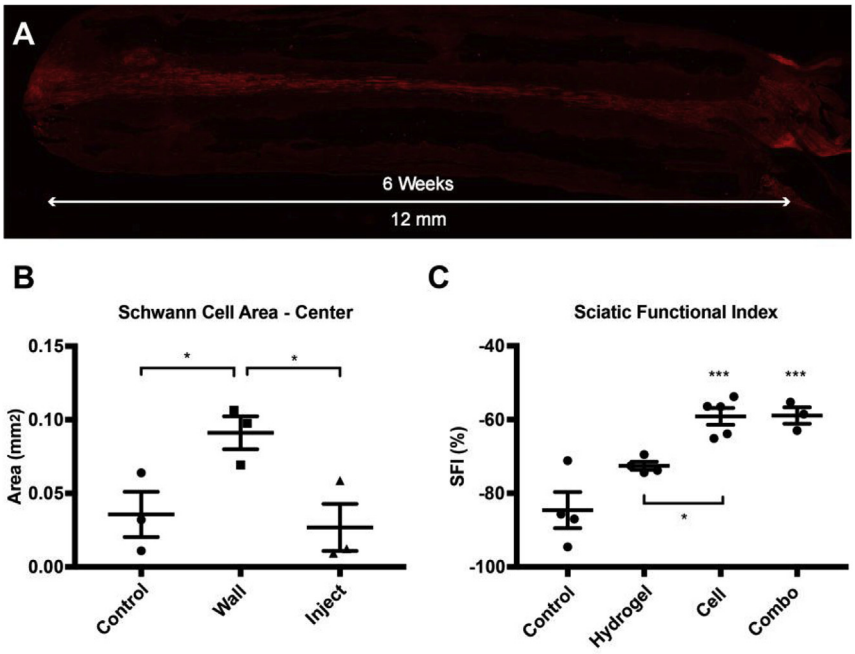

Fig. 6. Conduits with centrally located wall-encapsulated ASCs improve functional return. (A) Image of Schwann cells bridging the nerve conduit with wall-encapsulated ASCs at 6 weeks in a rat 1 cm sciatic nerve transection model. Bar: 1 mm. **(B)** Schwann cell-positive area in cross-section of center of conduits in cell-free control, and wall-encapsulated and lumen injected cell groups. **(C)** Sciatic functional index at 16 weeks for cell-free control (control), nerve conduits with ECM hydrogel lumen filler (hydrogel), nerve conduit with wall-encapsulated cells (cell), or nerve conduit with wall-encapsulated cells plus ECM hydrogel lumen filler groups (combo). *, $p < 0.05$, and ***, $p < 0.001$, compared to Control. $N = 3$ per group figure B. $N = 3–5$ per group figure C (full flexion contractures were unable to be measured in the groups).

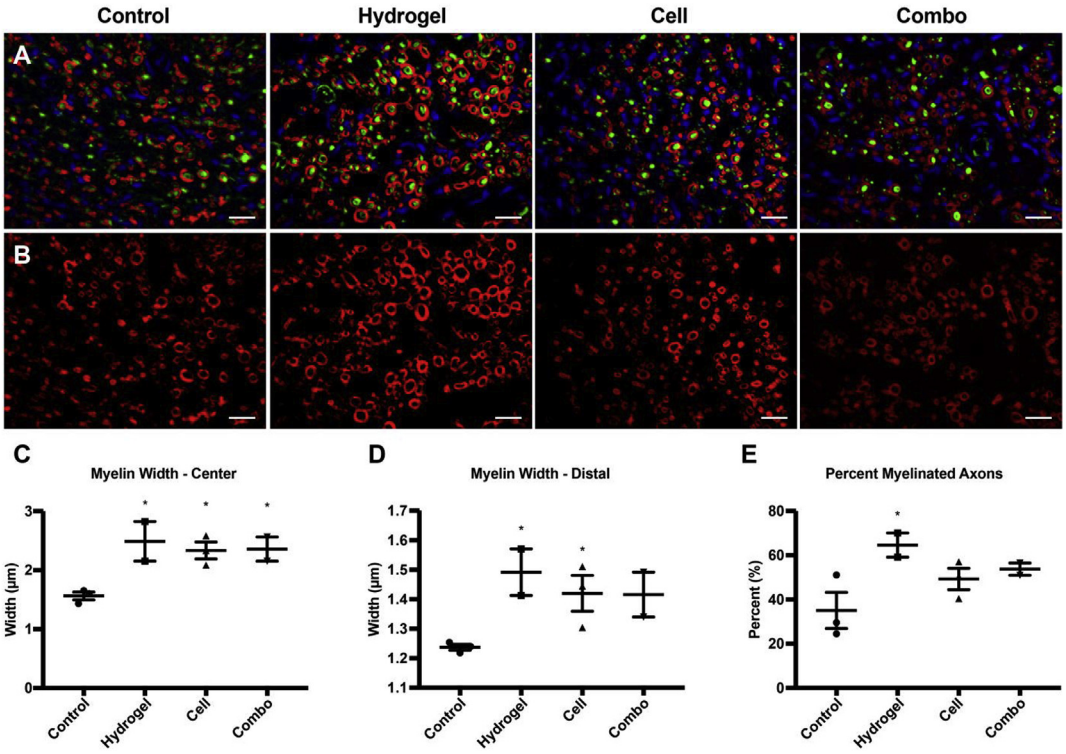

Fig. 7. Conduits with centrally located wall-encapsulated ASCs improve axon myelination. **(A)** Representative images of nuclear, axon, and myelin staining at distal end of conduit for cell-free control (control), nerve conduit with ECM hydrogel lumen filler (hydrogel), nerve conduit with wall-encapsulated cells (cell), or nerve conduit with wall-encapsulated cells plus ECM hydrogel lumen filler groups (combo). Green, NF-160; red, Fluoromyelin; and blue, DAPI. **(B)** Myelin staining isolated from images in **A** for better visualization. **(C)** Myelin width at center of conduit. **(D)** Myelin width at distal end of conduit. **(E)** Percent myelinated axons in distal end of conduit. *, $p < 0.05$, compared to Control. Scale bar: 15 µm. $N = 3$ per group. (For interpretation of the references to colour in this figure legend, the reader is referred to the Web version of this article.)

decreased steadily over the course of 6 weeks, which agrees with previous observations that live injected cells are largely absent in the conduit site [55]. Utilizing cells located in the walls along only the central third of the conduit, we sought to create a biomolecular gradient [33] of cell-secreted NTFs with the highest concentration in the center that decreased towards the ends of the conduit due to diffusion of NTFs (Fig. 5). This method of cell seeding led to a Gaussian distribution pattern instead of the quadratic distribution pattern observed with cell injection (Fig. 5D and E). Note: we recognize that we cannot be certain that DiI label is not being detected in phagocytosing cells, which is a limitation of this study and could potentially obscure the intensity measurements for MSCs. Interestingly, we found that this

localization of cells and the associated, theoretical biomolecular gradient was sufficient to drive Schwann cells into the center of the regenerating nerve bridge as early as 2 weeks (Fig. 5F). Studies utilizing carefully constructed growth factor gradients have also reported either increased axonal extension or increased Schwann cell migration, supporting our hypothesis that cell localization is capable of creating a cell-secreted neurotrophic factor gradient [25–29,32]. By 6 weeks, full bridging of the conduit with Schwann cells is observed (Fig. 6A), with significantly higher Schwann cell-positive area in encapsulation *versus* injection and non-cell seeded controls (Fig. 6B). Surprisingly, implanted ASCs were found to be negative for BDNF, and uninduced ASCs are not known to produce conventional Schwann chemotactic factors like GDNF in appreciable quantity [26,35]. Our observations, however, can be reconciled by the finding that TGF-β, which our implanted ASCs secrete (Fig. S9C), drives Schwann cells into the regenerating nerve bridge during the nerve repair process [24].

At week 16, conduits with wall-encapsulated cells displayed enhanced functional return and axon myelination even in the absence of a lumen filler (Figs. 6C and 7). This increase in myelination is in accordance with observations that injected or seeded MSCs promote axon myelination [12]. As reference, the myelin width of healthy nerve controls in Sprague Dawley and Lewis rats have been reported with some variability between 0.2 and 3.4 μm, with means from 1.46 μm [56] to 1.65 (± 0.04) μm [57]. It is noteworthy that the presence of a hydrogel lumen filler derived from decellularized peripheral nerve did not synergistically add to the capabilities of the cellular conduit. We hypothesize that this is because the hydrogel and cells both act through neurotrophic factor enhancement of nerve regeneration, such that the cell-secretome induced migration of Schwann cells is not further augmented by the NTFs found in the hydrogel (Note: The hydrogel was semi-solid in nature, and was thus unlikely acting as a ready medium for migrating cells).

Among the findings in this study, one aspect we find particularly interesting is the differing Schwann cell distributions at 2 and 4 weeks between wall-encapsulated and injected cells (Fig. 5F and G). Despite the lack of a lumen filler, at both 2 and 4 weeks Schwann cells seem to be making their way to the center of the conduit in the wall-encapsulated groups. However, the distribution of Schwann cells in cell injection groups at 4 weeks shows no clear pattern and seems to be almost random in distribution, with the majority at least 2 mm away from the center. The sudden increase in Schwann density over the course of 2 weeks hints that although seeded-cells can provide directionality to migrating Schwann cells, the limiting factor in this lumen filler-free conduit may be the formation of the fibrin network for the Schwann cells to migrate through [9]. Future studies will assess the capabilities of the wall-encapsulated cellular scaffold with an aligned porous lumen filler to take advantage of the early Schwann cell migration towards the center of the conduit.

We have also shown here that a cell-seeded conduit using polycaprolactone and GelMA can be effective in enhancing the nerve regenerative response. However, this conduit fabrication method is not limited to these particular materials or cells. It is highly versatile, as different nanofibers can be incorporated and different photo-polymerizable aqueous gels can be applied during fabrication as long as a sacrificial nanofiber is present in the composite nanofiber scaffold. This method can be used to modulate various attributes, such as increased permissibility for Schwann cell attachment and migration (i.e. silk fibroin fibers [58]), inclusion of growth factors or microparticles within the gel component for controlled factor release, or incorporation of slower degrading hydrogel component to enhance cell retention.

Lastly, a discussion of the limitations of this study is warranted. The major limitation in our study is the lack of the gold standard autograft group – without it we cannot comment on the merit of this technique compared to the gold standard, only against cell injection methods. Related to this, with the limitation in number of animals we had, we were unable to include cell injection control conduits for 16-week functional assays and instead chose to demonstrate its efficacy given our 6-week results demonstrating stronger Schwann response in wall-encapsulated groups. Both of these avenues will be explored in future studies. Another limitation in our studies involves the neurotrophic gradients and the identity of cells that contribute to it. In this study we did not verify for certain that neurotrophic gradients were found *in vivo*; these gradients were based on theory. Along with this, a thorough characterization of the state of implanted ASCs *in vivo* was not carried out after explantation, nor were infiltrating cells characterized – all points we look to fully address in future studies. Finally, the cells we used here were rat ASCs, whose secretome differs from that of human MSCs, which makes these results difficult to generally apply to use with human MSCs. However, based on our observations in Fig. S9C that they do not secrete certain neurotrophic factors like BDNF that humans MSCs do, we are inclined to believe that there is the potential for human MSCs to have an even greater effect than the one we see in this study.

In designing this conduit fabrication strategy, we sought to harness the neurotrophic capabilities of MSCs by introducing increased control to the process of cell seeding with a versatile conduit fabrication method. Our results demonstrate the efficacy of this method, and we hypothesize that these MSCs enhance regeneration through paracrine factor secretion rather than transdifferentiation. Overall, this method presents a new approach for studying and maximizing the potential of cell application in peripheral nerve repair.

Data availability

The data that support the findings of this study are available from the corresponding authors, P.G.A. and R.S.T., upon reasonable request.

Acknowledgements

This work was funded in part by a research grant from the U.S. Department of Defense (W81XWH-15-1-0600). Aaron X. Sun is a predoctoral trainee supported by NIH T32 EB001026. We would like to acknowledge Harman Ghuman and Dr. Michael Modo for use of their Motorater System, Kim Möller for assistance in photography, Dr. Jian Tan for maintaining the stem cell bank, and Daniel McKeel for design and manufacture of nerve conduit assembly devices. Lastly, we would like to acknowledge Drs. Shinsuke Kihara, Michael Guss, and Hannah Lee for assistance in rat surgeries.

Appendix A. Supplementary data

Supplementary data to this article can be found online at https://doi.org/10.1016/j.biomaterials.2019.01.038.

References

[1] M. Wiberg, G. Terenghi, Will it be possible to produce peripheral nerves? Surg. Technol. Int. 11 (2003) 303–310.
[2] C.B. Novak, D.J. Anastakis, D.E. Beaton, J. Katz, Patient-reported outcome after peripheral nerve injury, J Hand Surg Am 34 (2009) 281–287, https://doi.org/10.1016/j.jhsa.2008.11.017.
[3] C.B. Novak, D.J. Anastakis, D.E. Beaton, J. Katz, Evaluation of pain measurement practices and opinions of peripheral nerve surgeons, Hand (N. Y). 4 (2009) 344–349, https://doi.org/10.1007/s11552-009-9177-8.
[4] J.C. Rivera, G.P. Glebus, M.S. Cho, Disability following combat-sustained nerve injury of the upper limb, Bone Joint Lett. J 96-B (2014) 254–258, https://doi.org/10.1302/0301-620X.96B2.31798.
[5] S. Sunderland, A classification of peripheral nerve injuries producing loss of function, Brain 74 (1951) 491–516 https://doi.org/10.1093/brain/74.4.491.
[6] R. Deumens, A. Bozkurt, M.F. Meek, M.A.E. Marcus, E.A.J. Joosten, J. Weis, G.A. Brook, Repairing injured peripheral nerves: bridging the gap, Prog. Neurobiol. 92 (2010) 245–276, https://doi.org/10.1016/j.pneurobio.2010.10.002.
[7] J.W. Griffin, M. V Hogan, a B. Chhabra, D.N. Deal, Peripheral nerve repair and reconstruction, J Bone Jt. Surg Am. 95 (2013) 2144–2151, https://doi.org/10.2106/jbjs.l.00704.
[8] H.H. Noaman, Surgical treatment of peripheral nerve injury, in: S.M. Rayegani (Ed.), Basic Princ. Peripher. Nerve Disord. 2012, pp. 93–132.

[9] W. Daly, L. Yao, D. Zeugolis, A. Windebank, A. Pandit, A biomaterials approach to peripheral nerve regeneration: bridging the peripheral nerve gap and enhancing functional recovery, J. R. Soc. Interface 9 (2012) 202–221, https://doi.org/10.1098/rsif.2011.0438.

[10] A.D. Widgerow, A.A. Salibian, S. Lalezari, G.R.D. Evans, Neuromodulatory nerve regeneration: adipose tissue-derived stem cells and neurotrophic mediation in peripheral nerve regeneration, J. Neurosci. Res. 91 (2013) 1517–1524, https://doi.org/10.1002/jnr.23284.

[11] A.C. Pinho, A.C. Fonseca, A.C. Serra, J.D. Santos, J.F.J. Coelho, Peripheral nerve regeneration: current status and new strategies using polymeric materials, Adv. Healthc. Mater. 5 (2016) 2732–2744, https://doi.org/10.1002/adhm.201600236.

[12] N.G. Fairbairn, A.M. Meppelink, J. Ng-Glazier, M.A. Randolph, J.M. Winograd, Augmenting peripheral nerve regeneration using stem cells: a review of current opinion, World J. Stem Cell. 7 (2015) 11–26, https://doi.org/10.4252/wjsc.v7.i1.11.

[13] R.D. Price, S.A. Milne, J. Sharkey, N. Matsuoka, Advances in small molecules promoting neurotrophic function, Pharmacol. Ther. 115 (2007) 292–306, https://doi.org/10.1016/j.pharmthera.2007.03.005.

[14] S. Madduri, B. Gander, Growth factor delivery systems and repair strategies for damaged peripheral nerves, J. Contr. Release 161 (2012) 274–282, https://doi.org/10.1016/j.jconrel.2011.11.036.

[15] V. Chiono, C. Tonda-Turo, Trends in the design of nerve guidance channels in peripheral nerve tissue engineering, Prog. Neurobiol. (2015), https://doi.org/10.1016/j.pneurobio.2015.06.001.

[16] E.C. Spivey, Z.Z. Khaing, J.B. Shear, C.E. Schmidt, The fundamental role of subcellular topography in peripheral nerve repair therapies, Biomaterials 33 (2012) 4264–4276, https://doi.org/10.1016/j.biomaterials.2012.02.043.

[17] I.P. Clements, Y. tae Kim, A.W. English, X. Lu, A. Chung, R.V. Bellamkonda, Thin-film enhanced nerve guidance channels for peripheral nerve repair, Biomaterials 30 (2009) 3834–3846, https://doi.org/10.1016/j.biomaterials.2009.04.022.

[18] Y. Kim, V.K. Haftel, S. Kumar, R.V. Bellamkonda, The role of aligned polymer fiber-based constructs in the bridging of long peripheral nerve gaps, Biomaterials 29 (2008) 3117–3127, https://doi.org/10.1016/j.biomaterials.2008.03.042.

[19] H.R.H. Zupanc, P.G. Alexander, R.S. Tuan, Neurotrophic support by traumatized muscle-derived multipotent progenitor cells: role of endothelial cells and Vascular Endothelial Growth Factor-A, Stem Cell Res. Ther. 8 (2017) 226, https://doi.org/10.1186/s13287-017-0665-4.

[20] A.J. Man, G. Kujawski, T.S. Burns, E.N. Miller, F.A. Fierro, J.K. Leach, P. Bannerman, Neurogenic potential of engineered mesenchymal stem cells over-expressing VEGF, Cell. Mol. Bioeng. 9 (2016) 96–106, https://doi.org/10.1007/s12195-015-0425-4.

[21] Y. Cho, J.E. Shin, E.E. Ewan, Y.M. Oh, W. Pita-Thomas, V. Cavalli, Activating injury-responsive genes with hypoxia enhances axon regeneration through neuronal HIF-1α, Neuron 88 (2015) 720–734, https://doi.org/10.1016/j.neuron.2015.09.050.

[22] I. Allodi, E. Udina, X. Navarro, Specificity of peripheral nerve regeneration: interactions at the axon level, Prog. Neurobiol. 98 (2012) 16–37, https://doi.org/10.1016/j.pneurobio.2012.05.005.

[23] R.M. Brick, A.X. Sun, R.S. Tuan, Neurotrophically induced mesenchymal progenitor cells derived from induced pluripotent stem cells enhance neuritogenesis via neurotrophin and cytokine production, Stem Cells Transl. Med. 7 (2018) 45–58, https://doi.org/10.1002/sctm.17-0108.

[24] M.P. Clements, E. Byrne, L.F. Camarillo Guerrero, A.L. Cattin, L. Zakka, A. Ashraf, J.J. Burden, S. Khadayate, A.C. Lloyd, S. Marguerat, S. Parrinello, The wound microenvironment reprograms Schwann cells to invasive mesenchymal-like cells to drive peripheral nerve regeneration, Neuron 96 (2017) 98–114, https://doi.org/10.1016/j.neuron.2017.09.008 e7.

[25] Y.C. Chang, M.H. Chen, S.Y. Liao, H.C. Wu, C.H. Kuan, J.S. Sun, T.W. Wang, Multichanneled nerve guidance conduit with spatial gradients of neurotrophic factors and oriented nanotopography for repairing the peripheral nervous system, ACS Appl. Mater. Interfaces 9 (2017) 37623–37636, https://doi.org/10.1021/acsami.7b12567.

[26] Y.C. Lin, M. Ramadan, M. Hronik-Tupaj, D.L. Kaplan, B.J. Philips, W. Sivak, J.P. Rubin, K.G. Marra, Spatially controlled delivery of neurotrophic factors in silk fibroin-based nerve conduits for peripheral nerve repair, Ann, Plast. Surg. 67 (2011) 147–155, https://doi.org/10.1097/SAP.0b013e3182240346.

[27] M.C. Dodla, R.V. Bellamkonda, Differences between the effect of anisotropic and isotropic laminin and nerve growth factor presenting scaffolds on nerve regeneration across long peripheral nerve gaps, Biomaterials 29 (2008) 33–46, https://doi.org/10.1016/j.biomaterials.2007.08.045.

[28] L.M.Y. Yu, F.D. Miller, M.S. Shoichet, The use of immobilized neurotrophins to support neuron survival and guide nerve fiber growth in compartmentalized chambers, Biomaterials 31 (2010) 6987–6999, https://doi.org/10.1016/j.biomaterials.2010.05.070.

[29] K. Moore, M. Macsween, M. Shoichet, Immobilized concentration gradients of neurotrophic factors guide neurite outgrowth of primary neurons in macroporous scaffolds, Tissue Eng. 12 (2006) 267–278, https://doi.org/10.1089/ten.2006.12.267.

[30] D. Mortimer, T. Fothergill, Z. Pujic, L.J. Richards, G.J. Goodhill, Growth cone chemotaxis, Trends Neurosci. 31 (2008) 90–98, https://doi.org/10.1016/j.tins.2007.11.008.

[31] B.J. Dickson, Molecular mechanisms of axon guidance, Science 298 (2002) 1959–1964, https://doi.org/10.1126/science.1072165.

[32] S. Tang, J. Zhu, Y. Xu, A.P. Xiang, M.H. Jiang, D. Quan, The effects of gradients of nerve growth factor immobilized PCLA scaffolds on neurite outgrowth invitro and peripheral nerve regeneration in rats, Biomaterials 34 (2013) 7086–7096, https://doi.org/10.1016/j.biomaterials.2013.05.080.

[33] T.M. Keenan, A. Folch, Biomolecular gradients in cell culture systems, Lab Chip 8 (2008) 34–57, https://doi.org/10.1039/B711887B.

[34] L.E. Kokai, D. Bourbeau, D. Weber, J. McAtee, K.G. Marra, Sustained growth factor delivery promotes axonal regeneration in long gap peripheral nerve repair, Tissue Eng. Part A. 17 (2011) 1263–1275, https://doi.org/10.1089/ten.tea.2010.0507.

[35] L.E. Kokai, A.M. Ghaznavi, K.G. Marra, Incorporation of double-walled microspheres into polymer nerve guides for the sustained delivery of glial cell line-derived neurotrophic factor, Biomaterials 31 (2010) 2313–2322, https://doi.org/10.1016/j.biomaterials.2009.11.075.

[36] M.F. Pittenger, Multilineage potential of adult human mesenchymal stem cells, Science 284 (1999) 143–147, https://doi.org/10.1126/science.284.5411.143 80.

[37] S. Suon, H. Jin, Transient differentiation of adult human bone marrow cells into neuron-like cells in culture: development of morphological and biochemical traits is mediated by different molecular mechanisms, Dev. 13 (2004) 625–635 http://online.liebertpub.com/doi/abs/10.1089/scd.2004.13.625.

[38] L.Y. Santiago, J. Clavijo-Alvarez, C. Brayfield, J.P. Rubin, K.G. Marra, Delivery of adipose-derived precursor cells for peripheral nerve repair, Cell Transplant. 18 (2009) 145–158, https://doi.org/10.3727/096368909788341289.

[39] W.M. Jackson, L.J. Nesti, R.S. Tuan, Concise review: clinical translation of wound healing therapies based on mesenchymal stem cells, Stem Cells Transl. Med. 1 (2012) 44–50, https://doi.org/10.5966/sctm.2011-0024.

[40] C.E. Petrie Aronin, R.S. Tuan, Therapeutic potential of the immunomodulatory activities of adult mesenchymal stem cells, Birth Defects Res. Part C Embryo Today - Rev. 90 (2010) 67–74, https://doi.org/10.1002/bdrc.20174.

[41] B.D. Fairbanks, M.P. Schwartz, C.N. Bowman, K.S. Anseth, Photoinitiated polymerization of PEG-diacrylate with lithium phenyl-2,4,6-trimethylbenzoylphosphinate: polymerization rate and cytocompatibility, Biomaterials 30 (2009) 6702–6707, https://doi.org/10.1016/j.biomaterials.2009.08.055.

[42] R. Nishi, Autonomic and sensory neuron cultures, Methods Cell Biol. 51 (1996) 249–263 http://www.ncbi.nlm.nih.gov/pubmed/8722480.

[43] T.A. Prest, E. Yeager, S.T. LoPresti, E. Zygelyte, M.J. Martin, L. Dong, A. Gibson, O.O. Olutoye, B.N. Brown, J. Cheetham, Nerve-specific, xenogeneic extracellular matrix hydrogel promotes recovery following peripheral nerve injury, J. Biomed. Mater. Res. 106 (2018) 450–459, https://doi.org/10.1002/jbm.a.36235.

[44] K. Yue, G. Trujillo-de Santiago, M.M. Alvarez, A. Tamayol, N. Annabi, A. Khademhosseini, Synthesis, properties, and biomedical applications of gelatin methacryloyl (GelMA) hydrogels, Biomaterials 73 (2015) 254–271, https://doi.org/10.1016/j.biomaterials.2015.08.045.

[45] G. Yang, H. Lin, B.B. Rothrauff, S. Yu, R.S. Tuan, Multilayered polycaprolactone/gelatin fiber-hydrogel composite for tendon tissue engineering, Acta Biomater. 35 (2016) 68–76, https://doi.org/10.1016/j.actbio.2016.03.004.

[46] J. James, L.G. Sutton, F.W. Werner, N. Basu, M.A. Allison, A.K. Palmer, Morphology of the cubital tunnel: an anatomical and biomechanical study with implications for treatment of ulnar nerve compression, J. Hand Surg. Am. 36 (2011) 1988–1995, https://doi.org/10.1016/j.jhsa.2011.09.014.

[47] G.H. Borschel, K.F. Kia, W.M. Kuzon, R.G. Dennis, Mechanical properties of acellular peripheral nerve, J. Surg. Res. 114 (2003) 133–139, https://doi.org/10.1016/S0022-4804(03)00255-5.

[48] R.T. Tran, P. Thevenot, Y. Zhang, D. Gyawali, L. Tang, J. Yang, Scaffold sheet design strategy for soft tissue engineering, Materials 3 (2010) 1375–1389, https://doi.org/10.3390/ma3021375.

[49] T. Huynh, G. Abraham, J. Murray, K. Brockbank, P.O. Hagen, S. Sullivan, Remodeling of an acellular collagen graff into a physiologically responsive neovessel, Nat. Biotechnol. 17 (1999) 1083–1086, https://doi.org/10.1038/15062.

[50] E.M. Jeffries, Y. Wang, Incorporation of parallel electrospun fibers for improved topographical guidance in 3D nerve guides, Biofabrication 5 (2013), https://doi.org/10.1088/1758-5082/5/3/035015.

[51] J.I. Kim, T.I. Hwang, L.E. Aguilar, C.H. Park, C.S. Kim, A controlled design of aligned and random nanofibers for 3D Bi-functionalized nerve conduits fabricated via a novel electrospinning set-up, Sci. Rep. 6 (2016), https://doi.org/10.1038/srep23761.

[52] F. Hu, X. Zhang, H. Liu, P. Xu, Doulathunnisa, G. Teng, Z. Xiao, Neuronally differentiated adipose-derived stem cells and aligned PHBV nanofiber nerve scaffolds promote sciatic nerve regeneration, Biochem. Biophys. Res. Commun. 489 (2017) 171–178, https://doi.org/10.1016/j.bbrc.2017.05.119.

[53] Y. Sowa, T. Imura, T. Numajiri, K. Nishino, S. Fushiki, Adipose-derived stem cells produce factors enhancing peripheral nerve regeneration: influence of age and anatomic site of origin, Stem Cell. Dev. 21 (2012) 1852–1862, https://doi.org/10.1089/scd.2011.0403.

[54] Y. Sowa, T. Kishida, T. Imura, T. Numajiri, K. Nishino, Y. Tabata, O. Mazda, Adipose-derived stem cells promote peripheral nerve regeneration in vivo without differentiation into schwann-like lineage, Plast. Reconstr. Surg. 137 (2016) 318e–330e, https://doi.org/10.1097/01.prs.0000475762.86580.36.

[55] P. Erba, C. Mantovani, D.F. Kalbermatten, G. Pierer, G. Terenghi, P.J. Kingham, Regeneration potential and survival of transplanted undifferentiated adipose tissue-derived stem cells in peripheral nerve conduits, J. Plast. Reconstr. Aesthetic Surg. 63 (2010), https://doi.org/10.1016/j.bjps.2010.08.013.

[56] A. Kilic, G. Konopka, Y. Akelina, R. Regalbuto, P. Tang, Ipsilateral, cabled sural nerve for a. sciatic nerve defect: an experimental model in the rat, J. Neurosci. Methods 197 (2011) 137–142, https://doi.org/10.1016/j.jneumeth.2011.02.006.

[57] L.P. Cartarozzi, A.B. Spejo, R.S. Ferreira Jr., B. Barraviera, E. Duek, J.L. Carvalho, A.M. Goes, A.L. Oliveira, Mesenchymal stem cells engrafted in a fibrin scaffold stimulate Schwann cell reactivity and axonal regeneration following sciatic nerve tubulization, Brain Res. Bull. 112 (2015) 14–24, https://doi.org/10.1016/j.brainresbull.2015.01.005.

[58] D. Jao, X. Mou, X. Hu, Tissue regeneration: a silk road, J. Funct. Biomater. 7 (2016) 22, https://doi.org/10.3390/jfb7030022.